2006

Cd(II)-, Pb(II)- AND Hg(II)-2-AMINOETHANETHIOLATES

Mohan Singh Bharara
University of Kentucky, mohan8sk@gmail.com

ABSTRACT OF DISSERTATION

Mohan Singh Bharara

The Graduate School
University of Kentucky
2006

Cd(II)-, Pb(II)- AND Hg(II)-2-AMINOETHANETHIOLATES

ABSTRACT OF DISSERTATION

A dissertation submitted in partial fulfillment of the requirement for the degree of Doctor of Philosophy in the College of Arts and Science at The University of Kentucky

By

Mohan Singh Bharara

Lexington, Kentucky

Director: Dr. David A. Atwood, Professor of Chemistry

Lexington, Kentucky

2006

ABSTRACT OF DISSERTATION

Cd(II)-, Pb(II)- and Hg(II)-2-Aminoethanethiolates

This theses presents the synthesis and characterization of Cd(II)-, Pb(II)- and Hg(II)-aminoethanethiolates in aqueous media. 2-Aminoethanethiolate, a versatile sulfur and nitrogen (S/N) based ligand was used due to its resemblance to the naturally occurring amino acid, cysteine. The work is presented in four major parts: first, background information on the versatile structural chemistry of Cd, Pb and Hg-thiolates with S/N containing ligands; second, synthesis and characterization of Cd(II) with 2-aminoethanethiolates; third, synthesis and characterization and structural chemistry of Pb(II) with 2-aminoethanethiolates; and fourth, synthesis and characterization of Hg(II)-2-aminoethanethiolates in solution- and solid-state with emphasis on the mechanistic pathways for the formation of clusters.

The compounds reported here are synthesized by direct addition of the metal salts and the ligand in deionized water. For Cd(II)-thiolates, insoluble products (**77** - **80** and **82** - **84**) due to the formation of oligomers and polymers were obtained. In Pb(II)-thiolates (**85** - **89**), the structural chemistry is variable due to the extensive array of coordination environments Pb can acquire. This can be related to the stoichiometry of the reaction as well as the reaction conditions. The structural trends in Cd(II)- and Pb(II)-thiolates are not observed in the Hg(II)-thiolates. Rather the halide influences the formation of molecular as well as non-molecular structures. Systematic pathways for the formation of the compounds based on a variety of commonly observed structural 'building blocks' are presented. For Cl, Br derivatives, a four-coordinate intermediate, $[Hg(SR)_2X_2]$ (**88** - **96**) and for I derivatives three-coordinate intermediates, $[HgI(SR)_2]$ and $[HgI_2(SR)]$ (**97** - **100**) can be considered as building units. The compounds were characterized with IR/Raman, NMR, MS, Uv-Vis and X-ray crystallography.

KEYWORDS: Hg(II), Cd(II), Pb(II), S/N ligand, thiolates

Cd(II)-, Pb(II)- AND Hg(II)-2-AMINOETHANETHIOLATES

By

Mohan Singh Bharara

Dr. David A. Atwood

(Director of Dissertation)

Dr. Mark S. Meier

(Director of Graduate Studies)

RULES FOR THE USE OF DISSERTATION

Unpublished dissertations submitted for the Doctor's degree and deposited in the University of Kentucky Library are as a rule open for inspection, but are to be used only with due regard to the rights of the authors. Biblio-graphical references may be noted, but quotations or summaries of parts may be published only with the permission of the author, and with the usual scholarly acknowledgments.

Extensive copying or publication of the dissertation in whole or in part also requires the consent of the Dean of The Graduate School of the University of Kentucky.

DISSERTATION

Mohan Singh Bharara

The Graduate School

University of Kentucky

2006

Cd(II)-, Pb(II)- AND Hg(II)-2-AMINOETHANETHIOLATES

DISSERTATION

A dissertation submitted in partial fulfillment of the requirement for the degree of Doctor of Philosophy in the College of Arts and Science at The University of Kentucky

By

Mohan Singh Bharara

Lexington, Kentucky

Director: Dr. David A. Atwood, Professor of Chemistry

Lexington, Kentucky

2006

Acknowledgement

I would like to acknowledge and thank people that have given me guidance and knowledge to make this dissertation possible. I would like to thank my advisor, Dr David A. Atwood, for his help, guidance and support during this time. I want to thank my committee members, Dr Jack Selegue, Dr. Edward Demoll, Dr Mark Meier and Dr Christopher J. Matocha for their input and motivation during graduate school career. I want to specially thank Sean Parkin for his teaching, training and all the help with X-ray diffraction and John Layton for all his help with the NMR equipment. I want to thank the entire Atwood group for their support and help in the lab. Thanks to all the chemistry department office staff for their help.

Above all I want to thank my parents for their support. I want to thank God for his grace and faithfulness throughout my life.

Table of Content

List of Schemes

List of Figure

Chapter 1

Introduction and Background

The organothiolate anion (RS^-) is a fundamental ligand type that can be classified as a pseudohalide and compared to ligands such as Cl^-, Br^- and I^-, due to the one-electron oxidation reaction.

$$RS^- \rightleftharpoons 1/2\ RSSR + e^-$$

The substituent 'R' can be controlled and adjusted for steric and electronic control of ligation ability. Metal-thiolates have been known since the beginning of coordination chemistry. However, in the last few decades interest in the study of these compounds has ensued as a result of the following factors.[1-7]

1. The toxic effect of soft heavy metals such as Cd, Hg and Pb. The intermediate compounds and ultimate binding sites of these elements and thiol groups.

2. The presence of thiolate donors in the coordination sphere of metal ions in active sites of metalloproteins.[8] For example, Fe^{2+} in peptide deformylase,[9] Co^{2+} in the active site of nitrile hydratase,[10] [NiFe]-hydrogenase,[11] and metallothioneins containing Zn, Hg, Cd, Cu.[12]

3. In the application of certain metal-thiolates in medicine, such as Au(I)-thiolates for the treatment of arthritis and triphenylphosphinegold(I) compounds as antitumor agents.[8,13] Recently technetium- and rhenium-thiolates have gained importance in medical radiotherapeutic applications.[14]

4. Metal-thiolates are known to be involved in radioactive protective efficacy and protection against alkylating reagents. These metal complexes contribute to a greater

capacity to scavenge the superoxide radicals produced on exposure to ionizing radiation.[15,16]

5. Use of volatile molecular metal-thiolates as starting materials in chemical vapor deposition (CVD). This requires the use of low molecular weight thiolates, which sublime at low pressure and temperature.[17-19]

Apart from these applications, metal-thiolates are interesting from a structural point of view, since they are known to adopt geometries of variable nuclearities with great structural complexity. This is due to the ease of formation of metal-thiolate bridges. Diversity in both the structural and physicochemical properties is observed for these sulfur-bridged compounds. The structural motifs were thought to be governed by two factors, coordination mode and geometry.[20] However, an understanding of their structural chemistry has been hampered by their low solubility due to the formation of insoluble oligomers and polymers. The tendency toward polymerization can be modulated by manipulation of the group attached to the sulfur atom. In general an increase in the size of the 'R' group is associated with lower degrees of polymerization. However, in the case of metal ions with an $nd^{10}(n-1)s^2$ configuration the structural chemistry is variable. These complicating factors have yet to be adressed in any study of the biological activity of these elements.

This chapter provides background information on the diverse structural chemistry of Cd(II)-, Pb(II)- and Hg(II)-thiolates. In the compounds discussed henceforth the metal (Cd, Pb and Hg) is attached to sulfur and/or nitrogen atoms and in some cases oxygen and halides. The examples selected are those deemed to be of most relevance to the biological binding of the metals. The goal was to determine how these elements are

bound in living systems. The hypothesis was that simple two-coordinate compounds, merely fulfilling the divalent oxidation state of the element, were too simplistic to be used as model systems. It was anticipated that much more complicated bonding arrangement could be obtained when thiols were combined with these elements.

1.1 Cadmium(II)-thiolates

Cadmium (Cd) is a soft, blue-white, malleable, lustrous metal or a grayish-white powder and common in nature as greenokite (CdS). It is used for electroplating, galvanization, and production of pigments, batteries and in several industrial processes.[21] It is one of the 20 most toxic elements, which when released into the environment in sufficient, but low, amounts present a risk to human health.[22] It is more efficiently absorbed from the lungs than from the gastrointestinal tract and is transported in blood by red blood cells and high-molecular weight proteins and accumulates in the kidney and liver.[23] Chronic Cd exposure leads to renal toxicity characterized by tubular proteinuria and dietary intake is implicated in osteomalacia and osteoporosis.[24] At the cellular level, Cd toxicity includes nuclear condensation, dilation of endoplasmic reticulum, followed by mitochondrial swelling.[25]

The presence of Cd in metallothionein (MT), a cysteine-rich low molecular weight protein, has increased the interest in its thiolate coordination chemistry. Most studies have focused on the interaction of Cd with amino acids.[26] The Cd(II)-thiolates are generally synthesized by combination of the metal salt and ligand in common organic solvents. An electrochemical synthetic methodology is often used for heterocyclic

thiones,[27] as well as mixed compounds such as bipyridine (bipy), phenanthroline (phen) and pyridine (py). In the case of simple thiols, salt metathesis is generally used.[28]

1.1.1 Mononuclear Compounds

The coordination number observed in mononuclear Cd(II)-thiolates containing both S and N with halide and/or counter anion is either four or six (Figure 1.1). [Cd(2-methyl, 8-quinolinethiol)$_2$] (**1**) is one of the few structurally characterized mononuclear tetracoordinate Cd compounds with an S/N ligand.[29] The geometry around Cd can be best described as distorted tetrahedral with two strong Cd-S and two weak Cd-N bonds with distortion observed in the S-Cd-S and S-Cd-N angles (Table A1).

The coordination around Cd in [Cd(HAmhexim)$_2$X$_2$] (Amhexim = 2-pyridineformamide-3-hexamethyleneiminylthiosemicarbazone and X = Cl (**2**), Br (**3**) and I (**4**))[30] and [Cd(HAmpip)X$_2$]·DMSO (HAmpip = 2-pyridineformamide-3-piperidyl-thiosemicarbazone) (X = Cl (**5**), Br (**6**) and I (**7**)) consists of S, N and halide atoms.[31] Compounds **2** - **4** and **5** - **7** are isostructural with distortion towards a trigonal bipyramidal geometry. The Cd-N$_{imine}$ is shorter than Cd-N$_{py}$ and in accord with distances observed in metal complexes with heterocyclic thiosemicarbazones.[32] The Cd-X distances are different with the largest difference observed in **4**, most probably due to the steric influence of I. However, significant differences in Cd-X bonds in **7** are not observed despite being isostructural to **4**. These compounds exhibit extensive intermolecular hydrogen bonding involving amine, water molecule and halogen from neighboring molecule. The angle between thiosemicarbazone and pyridine ring decreases with the size of halogen atom (**4** to **2** and **7** to **5**), presumably due to the greater steric

effect of I. The mean plane deviation of the thiosemicarbazone unit is significantly larger than that observed in [M(HAmpip)X_2] (M = Fe^{3+}, $Co^{2+/3+}$, Cu^{2+}, Zn^{2+} and X = Cl, Br and I).[33] The NH--S interactions observed in **7** are not observed in **4**, which may be due to the stronger Cd-I bond and the least deviation of the thiosemicarbazone unit.

In contrast to **2** - **7**, the Cd coordination in [Cd(Amhexim)$_2$] (**8**) consists of only S and N.[30] The geometry around Cd in **8** is approximately octahedral with the two ligands in a meridional arrangement. The Cd-S and Cd-N distances are variable but in the range observed in **2** - **7**. The distortion in the octahedral geometry is indicated by the N-Cd-N angle of 152.0º compared to 169.6º observed in the related compound, [Ni(Amhexim)$_2$].[33] The planarity of the ligand and the angles involved in chelation are mainly responsible for the distortion from perfect octahedral geometry.

In the distorted octahedral geometry around Cd in [Cd(pymS)$_2$(phen)] (**9**) (pymS = pyridine-2-thiol),[34] the S atoms are present in *cis* positions, whereas similar structures with Ru, Sn, Os, Ni and Zn have *trans* S atoms.[35,36] The Cd-S distances are close to those found in compounds containing CdS_5 and CdS_4 environments.[37,38] These distances are however, much smaller than mononuclear Cd(II)-thiolates with additional N-donor ligands.[39] The Cd-N distances are considerably longer than those found in tetrahedral as well as octahedral Cd(II)-thiolates.[39]

In $[Cd(C_7H_4NS_2)_3]^-$,[40] the Cd is surrounded by ligands in an octahedral fashion with exocyclic Cd-S and Cd-N bonds. The small chelate angle associated with the N-C-S unit leads to a smaller distortion from trigonal prismatic toward octahedral geometry (25.8º). The Cd-S distances are longer than those observed in **9**.

In contrast to **8** - **10**, the octahedral coordination around Cd in $[Cd(bmppa)(ClO_4)](ClO_4)\cdot 1.5MeOH$ (**11**) (bmppa = N-bis-2-(methylthio)ethyl-N-(6-pivaloylamido-2-pyridylmethyl)amine)[41] is completed by ClO_4^-. The amide O and one O atom from ClO_4^- occupy adjacent coordination positions yielding a distorted trigonal prismatic geometry. The strain associated with the angle O3-Cd-O2 (76.9º) is minimized by the distortion of the planarity of the amide chelate.

The compound, $[Cd(6\text{-mercaptopurine})_4Cl_2]$ (**12**)[42] contains one isolated, distorted-octahedral $[Cd(6\text{-mercaptopurine})_2Cl_2]$ unit, which is similar to that of **1** with two additional Cl and two non-coordinating 6-mercaptopurine units. The Cd-Cl distances (2.719 Å) are longer than those observed in **2** and **5** (avg 2.475 Å). In addition to NH--Cl bonds, weak NH--S interactions between coordinating and non-coordinating molecules are also observed.

1.1.2 Dinuclear Compounds

In $[Cd_2(3\text{-trimethylsilyl-pyridine-2-thiolate})_4]$ (**13**), the dimer possesses a crystallographic center of symmetry (Figure 1.2).[43] The Cd atoms are pentacoordinate in a distorted trigonal bipyramidal geometry, where the bridging ligand acts as a $[N\text{-}(\mu\text{-}S)_2]$ five-electron donor. The two Cd and two S bridging atoms are coplanar, with two longer and two shorter Cd-S bonds. The distortion around Cd is due to the steric constraints, where the angles (S1-Cd-N1, 62.06º and S2-Cd-N2, 64.84º) are more acute than 90º. The Cd-S distances are variable and depend on their position at either bridging or terminal sites. In contrast, the Cd-N distances are slightly longer than those observed in octahedral Cd(II)-thiolates with additional N donor ligands (Table A2).

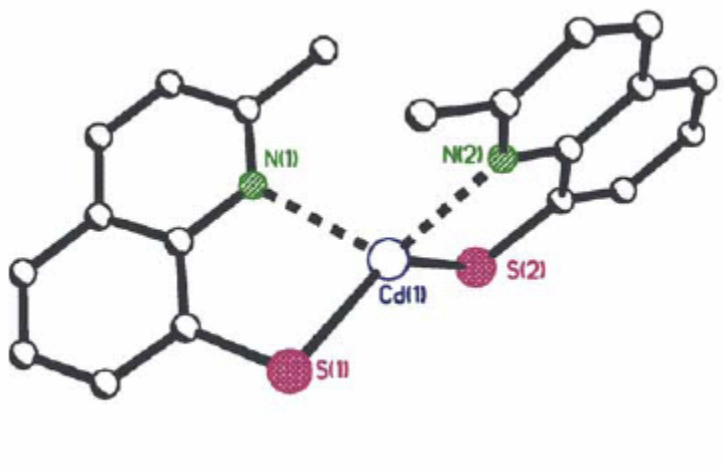

(**1**)

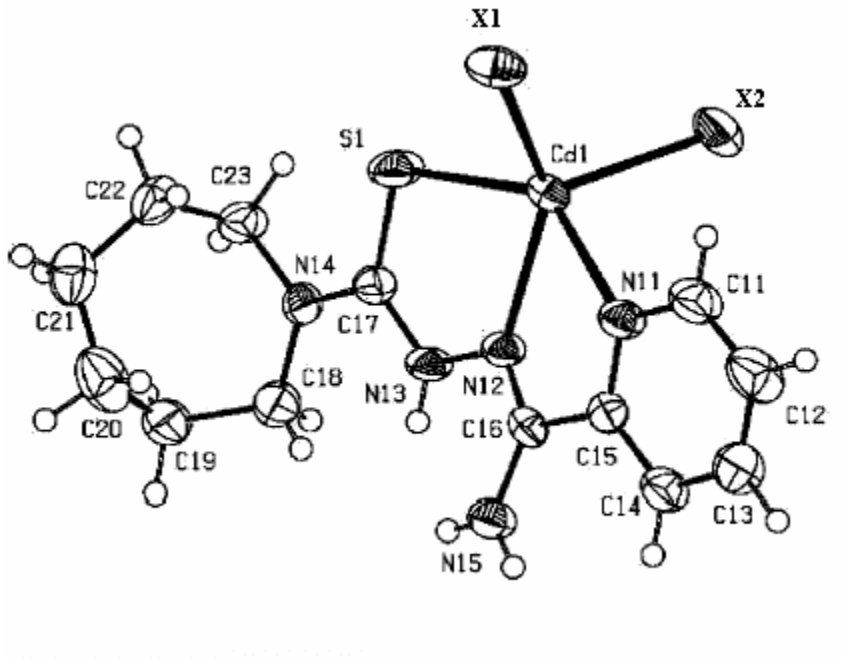

(**2** (X = Cl), **3** (X = Br), **4** (X = I))

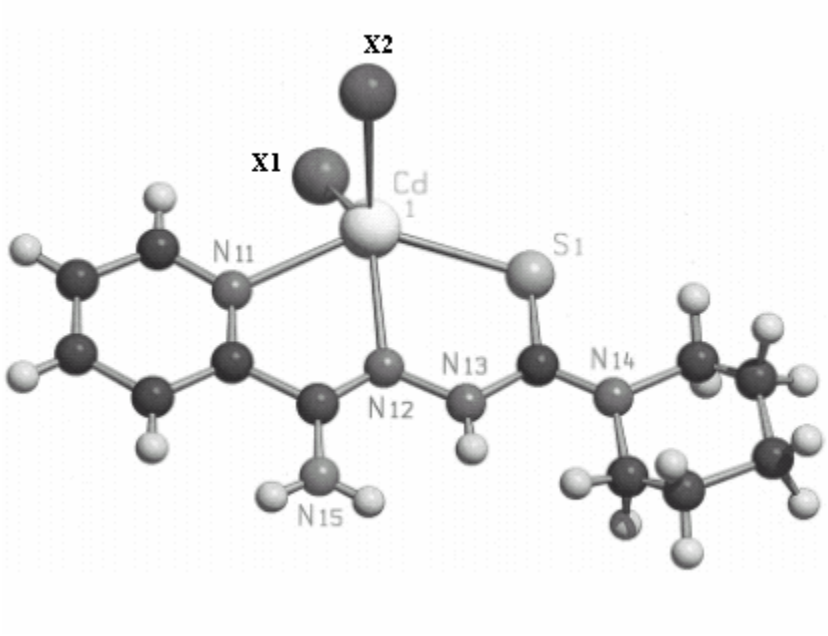

(**5** (X = Cl), **6** (X = Br), **7** (X = I))

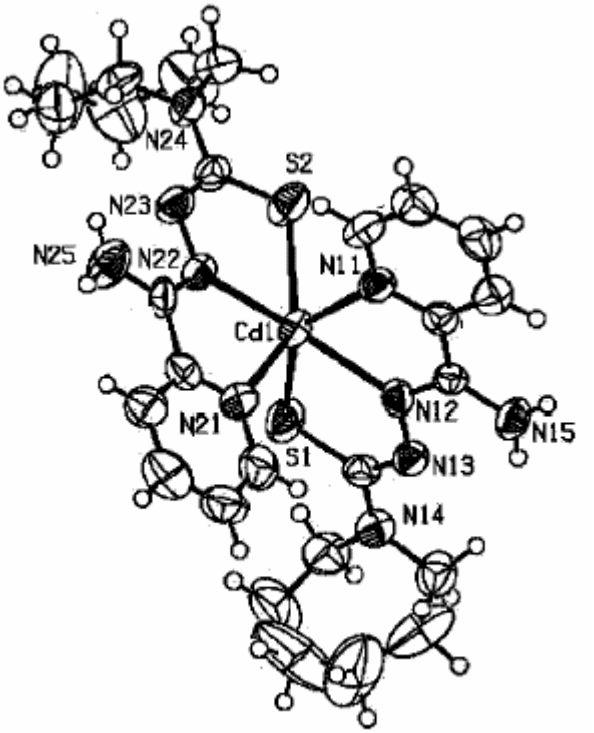

(**8**)

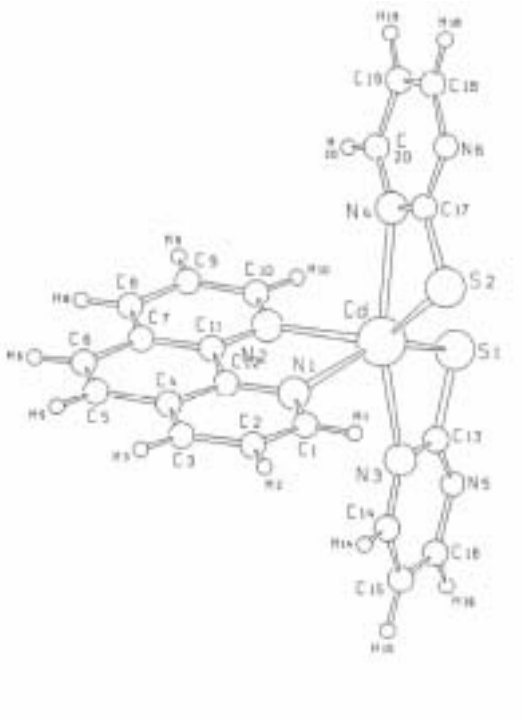

(**9**)

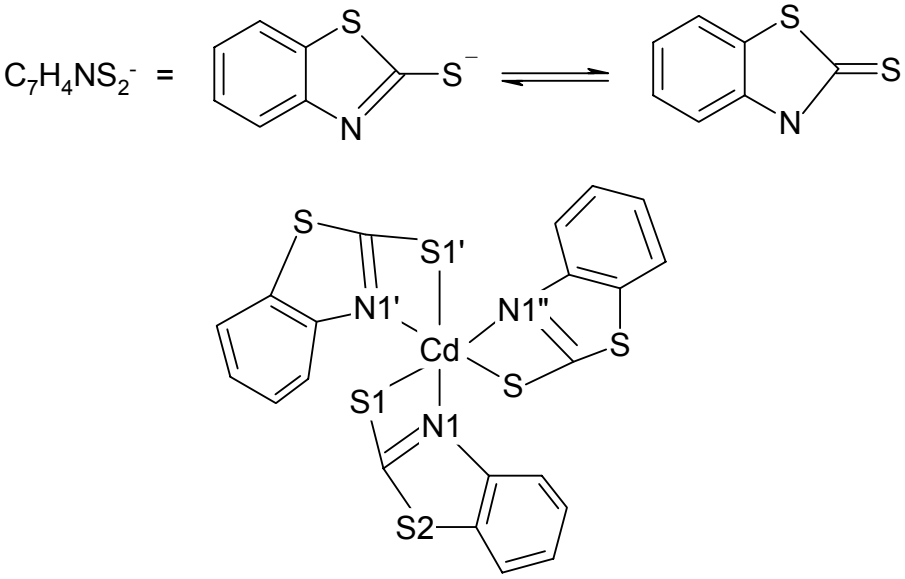

(**10**)

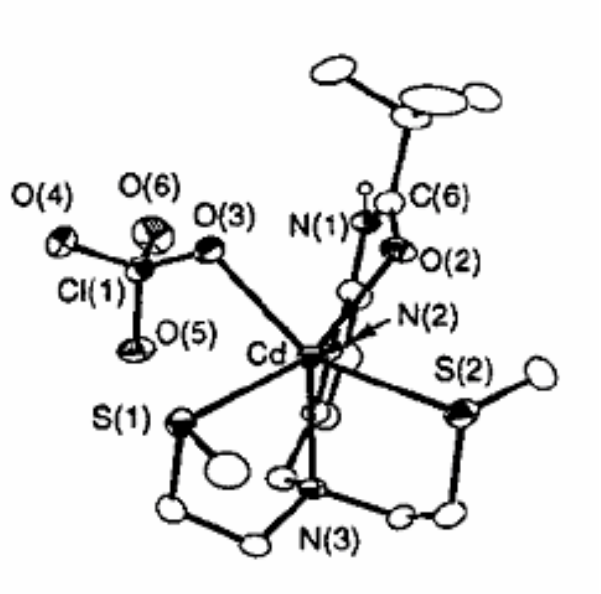

(**11**)

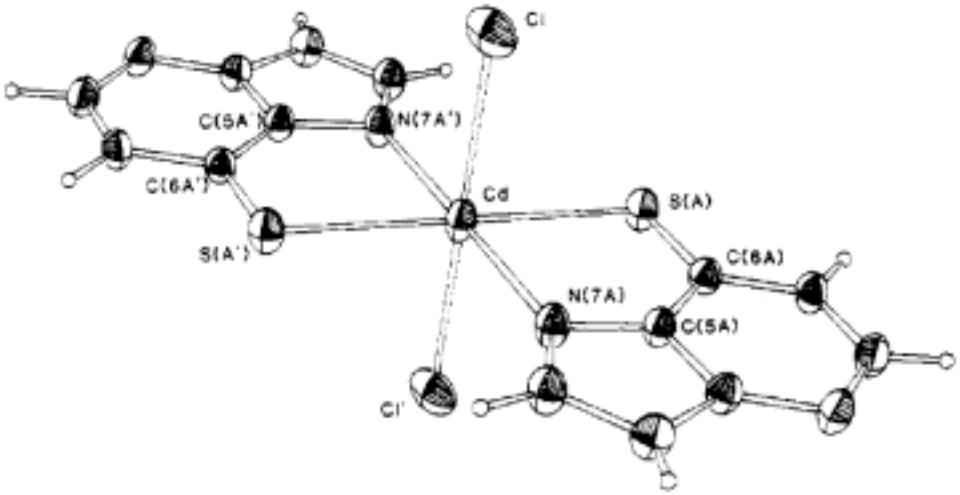

(**12**)

Figure 1.1. Structures of selected mononuclear Cd(II)-thiolates.

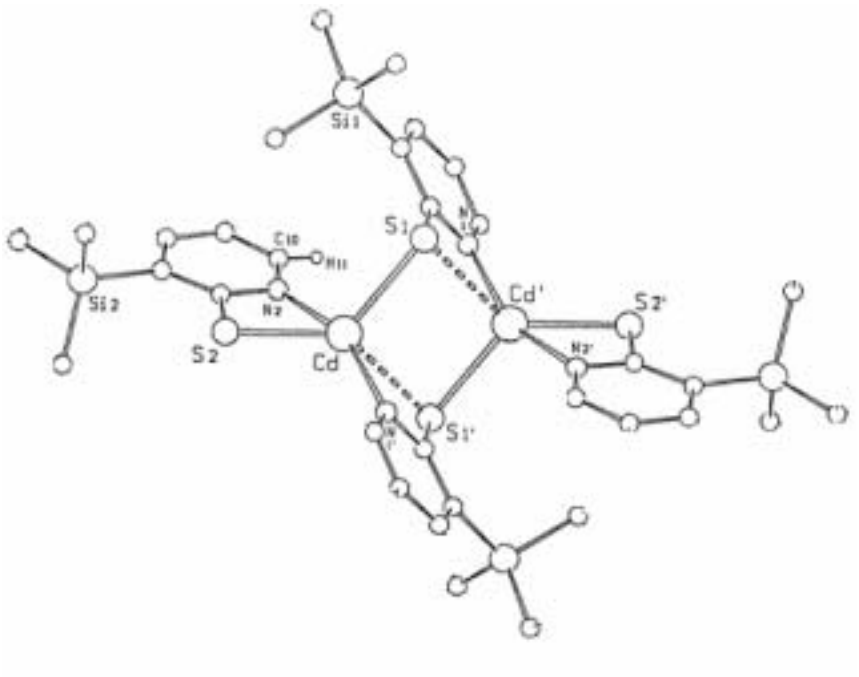

Figure 1.2. Structure of [Cd_2(3-trimethylsilyl-pyridine-2-thiolate)$_4$] (**13)**.[43]

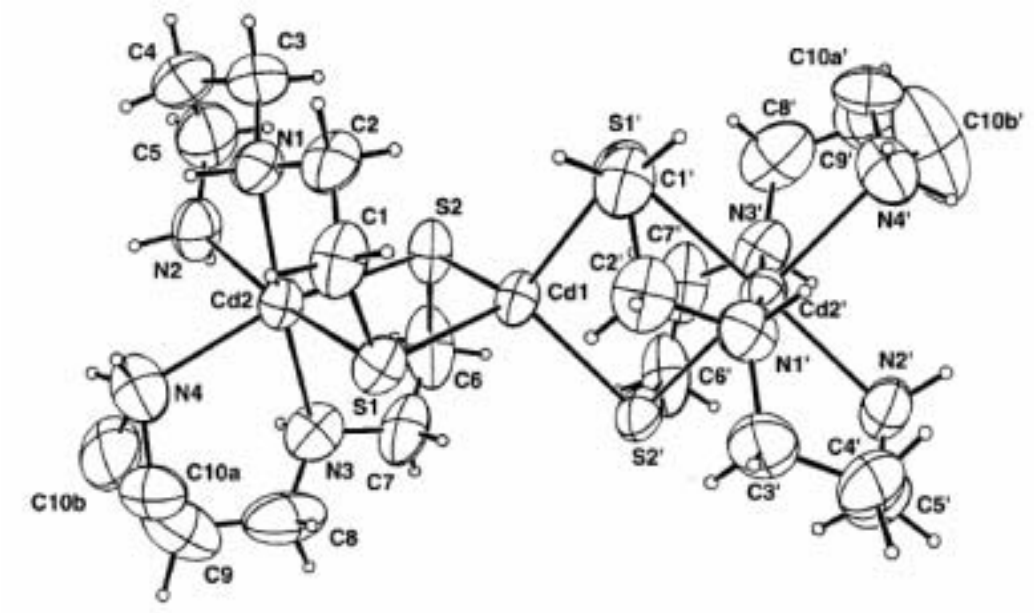

Figure 1.3. Isostructural **14** and **15** (which differ in the counteranion)**.** The counter ions and solvent molecules are not shown for clarity.

1.1.3 Trinuclear Compounds

The trinuclear compounds, $[Cd\{Cd(L)_2\}_2](ClO_4)_2{\cdot}CH_3CON(CH_3)_2$ (**14**) and $[Cd\{Cd(L)_2\}_2]Cl_2{\cdot}2CH_3OH$ (**15**) (L = 2-[(3-aminopropyl)amino]ethanethiol) are similar with the presence of two types of Cd atoms (Figure 1.3).[44] The geometry around the central Cd (Cd_c) is distorted tetrahedral, whereas the terminal Cd (Cd_t) acquires a distorted octahedral geometry. The Cd_c-S distances (2.533 - 2.538 Å) and angles S-Cd_c-S (99.2 - 116°) are comparable to Cd(II)-thiolates with a CdS_4 unit (2.450 - 2.635 Å).[45,46] The Cd_t-S distances (2.695 - 2.706 Å) are longer than the Cd_c-S (2.533 - 2.538 Å) distances but fall within the range observed for octahedral Cd(II)-thiolates (2.461 - 2.717 Å).[47] The Cd_t-N distances are within the limit observed for Cd(II)-thiolates containing an additional N donor ligand (2.35 - 2.55 Å).[47]

1.1.4 Tetranuclear Compounds

In $[Cd\{SC(CH_3)_2CH_2NH_2\}_2CdCl_2]_2{\cdot}2H_2O$ (**16**), $[Cd\{SCH_2CH_2N(CH_3)_2\}CdBr_2]_2$ (**17**) and $[Cd_4\{SCH_2CH_2N(CH_3)_2\}_4Cl_4]$ (**18**) a tetranuclear unit is observed with variable geometry around the Cd atoms (Figure 1.4, Table A3).[48,49]

Two independent types of Cd atoms are observed in **16** - **18** with one of the Cd bound by an S/N chelate. The Cl in **16** bridges both octahedral and tetrahedral Cd atom. In **17**, a distorted tetrahedral geometry is observed around two independent Cd atoms, namely CdS_2N_2 and CdS_2Br_2. In **18**, one of the Cd atom is octahedrally coordinated to two bridging S, Cl and two terminal N atoms, whereas the second Cd is bonded to two S and an S/N chelate to yield a highly distorted CdS_3N coordination environment. However, weak interactions involving Cl in **18** give rise to a distorted trigonal-

bipyramidal geometry around Cd. It is also observed that the Cl derivative of **17** reacts with excess of thiolate ligand to form **18**.

1.1.5 Hexanuclear Compounds

The hexanuclear [{Cd(dmpymt)$_2$}$_6$] (dmpymt = 4,6-dimethylpyrimidine-2-thione) (**19**) consists of a non-regular hexagon of six Cd atoms (Figure 1.5).[50] Each Cd is coordinated to two N and four bridging S atoms to acquire a distorted octahedral geometry. The ligand acts as a [N(μ-S)$_2$] five-electron donor unit similar to that observed in **13**.

The Cd-S distances in the ring are variable (2.638 - 2.761 Å) but in accord with six-coordinate Cd(II)-thiolates containing Cd_2S_2 unit (2.543 - 2.649 Å and 2.809 - 3.129 Å).[51] The Cd-N distances (2.360 and 2.380 Å) are similar to Cd(II)-thiolates containing an additional N donor ligand such as [$CdCl_2(py)_2$] (2.350 Å).[52] The cavity in **19** is large enough to accommodate small molecules such as acetonitrile, carbon monoxide and molecular iodine.

1.1.6 Polynuclear Compounds

The thiolate form of 6-mercaptopurine (MP) with Cd(II) forms a compound that is polymeric [Cd(MP$^-$)$_2$]$_n$·nH_2O (**20**), whereas the thione (HMP) forms **12**.[42] Mercaptobenzothiazole (bzSH) and pyridine-1-thiol (pySH) with cadmium acetate form polymeric [Cd(bzS)$_2$]$_n$ (**21**) and [Cd(pyS)$_2$]$_n$ (**22**), respectively.[53] The latter compounds due to their high volatility sublime at reduced pressure to yield pure CdS in CVD.

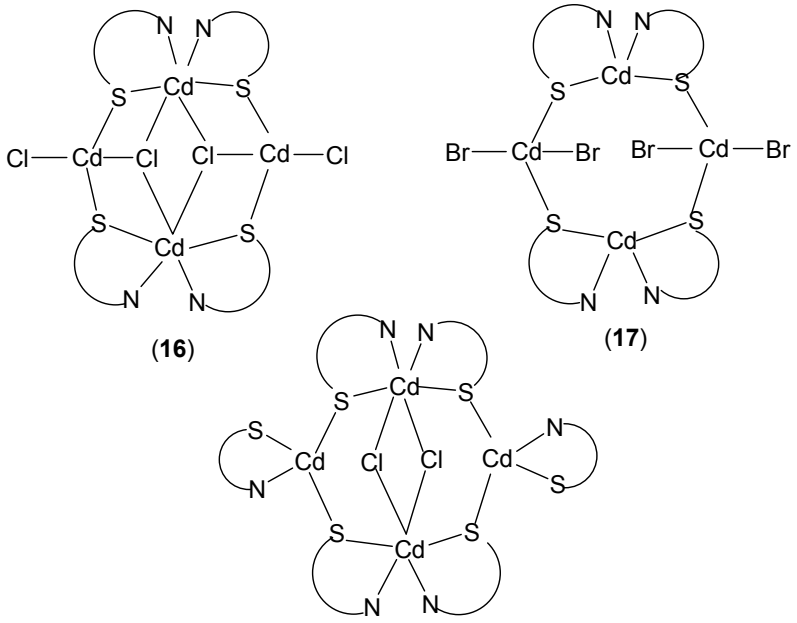

Figure 1.4. Diagram depicting structures in **16 - 18** (S/N = $SC(CH_3)_2CH_2NH_2$ (**16**); $SCH_2CH_2N(CH_3)_2$ (**17** and **18**)).

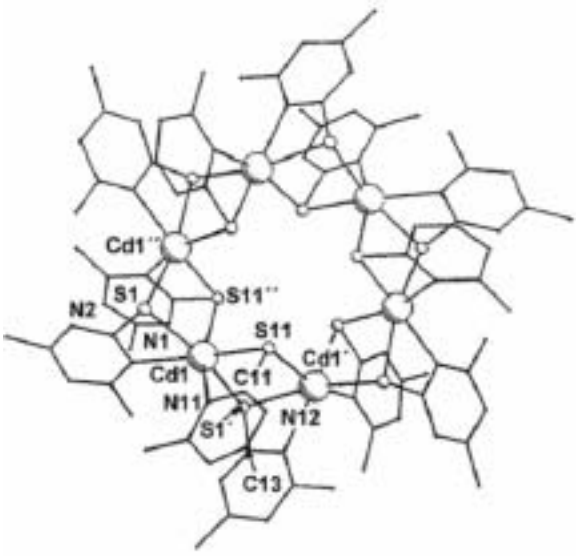

Figure 1.5. Structure of [{Cd(4,6-dimethylpyrimidine-2-thione)$_2$}$_6$] (**19**).[50]

In contrast to the direct addition of Cd salts and thiol as done for **20** - **22**, the electrochemical oxidation of Cd in a solution of 4-methyl-6-trifluoromethylpyrimidine-2-thione ($MeCF_3$-pymSH) in acetonitrile yields polymeric $[Cd(MeCF_3\text{-pymS})_2]_n$ (**23**).[54] The common feature observed in **20** - **23** is a six-coordinate Cd, which is attached to both S and N atoms along with a bridging thiolate to yield polymeric structures (Figure 1.6, Table A4). In **20**, the N atoms in the CdS_4N_2 environment are in *trans* positions, whereas in **21** - **23** the N atoms are in *cis* positions.

The octahedral Cd in $[Cd\{pen\}]\cdot H_2O$ (pen = penicillamine) (**24**) is coordinated to S, N and O atoms.[55] However, each pen molecule is attached to four different Cd atoms to form a polymeric chain (Figure 1.7). Some of the Cd atoms are involved in a five-member chelate ring with S and N atoms, while other atoms are part of a six-member chelate ring with S and O atoms. The S atoms as well as one of the O atoms act as a bridge, while the other O atoms are attached to the central Cd.

The aberrant feature observed in polymeric $[Cd(SMC)_2]$ (SMC = S-methyl-L-cysteinato) (**25**) is the absence of a direct Cd-S contact.[56] The geometry around Cd is octahedral with N and O atoms (Figure 1.7). Two O atoms belonging to the neighboring molecule complete the coordination around Cd.

In polymeric $[Cd(SCH_2CH(NH_3)COO)_2]$ (**26**), a direct Cd-N contact is not observed as indicated by ^{113}Cd CP/MAS NMR.[57] The octahedral Cd is attached to only S and O atoms to form a highly amorphous polymeric compound (Figure 1.7).

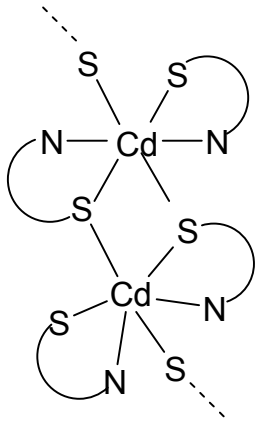

Figure 1.6. Repeating unit observed in **20** - **23** (S/N = 6-mercaptopurine (**20**), mercaptobenzothiazle (**21**), pyridine-1-thiol (**22**) and 4-methyl-6-trifluoromethylpyrimidine-2-thione (**23**)).

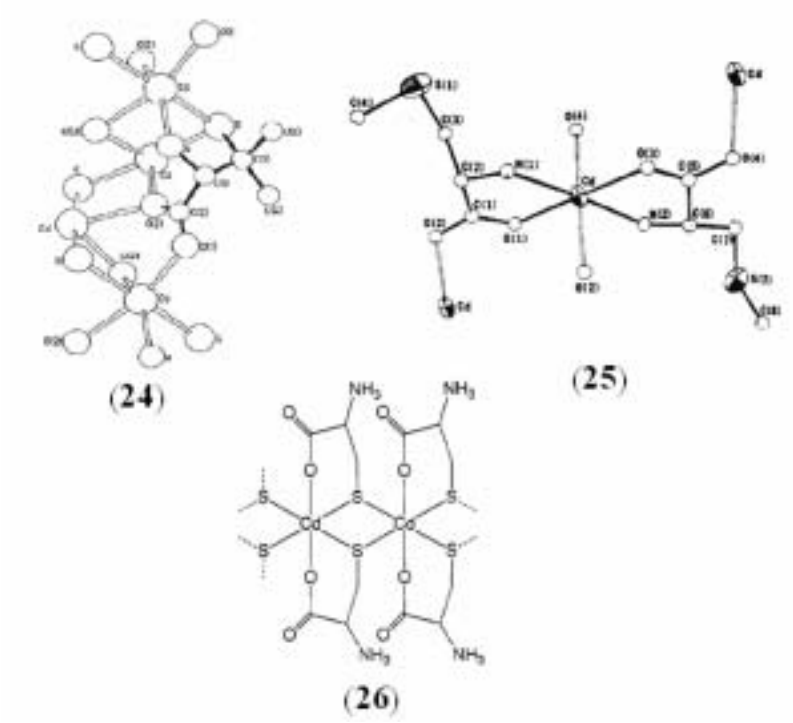

Figure 1.7. Structure of [Cd{penicillamine}]$_n$·(**24**),[55] [Cd(S-methyl-L-cysteinato)$_2$] (**25**)[56] and proposed structure of [Cd(SCH$_2$CH(NH$_3$)COO)$_2$] (**26**).[57]

1.2 Lead(II)-thiolates

Lead (Pb), the most widely distributed of the toxic elements, enters the environment by escaping during smelting of its sulfide ore, Galena (PbS), as well as through use in batteries, pipes and conduit, solder and pewter, and especially the addition of tetraethyl lead to gasoline. Lead, like other soft metals, binds to and inactivates SH- containing substrates such as dihydrolipopyl transacetylase and consequently inhibits heme biosynthesis. The hypothesis put forward is that the lead toxicity arises because it targets calcium and zinc binding sites in proteins. Such enzymes contain a zinc-binding site with a mixture of histidine, cysteine, and carboxylate residues. The yeast and mammalian forms of ALAD (aminolevulinic acid dehydratase) contains a unique catalytic zinc-binding site with three cysteine (Cys) residues. Lead prefers the Cys_3 site in the ALAD because this constitutes a tight binding site for lead. This is supported by recent model compounds studies.[58] Due to the lone pair and empty p-orbitals, Pb has a potentially extensive array of coordination geometries; however due to compounds solubility problems, the structural data are often limited.

1.2.1 Mononuclear Compounds

Two-and three-coordinate Pb(II)-thiolates include compounds such as, $[Pb(S_2N_2)]$ (**27**) and $[Pb(S_2N_2)(NH_3)]$ (**28**),[59] in which the geometry is similar except for the presence of a weakly bonded ammonium ion in **28** (Figure 1.8). The Pb is attached to S and N in **27** and S and two N atoms in **28** with the chelate angle around Pb close to 75º. In **28**, the NH_3 group is present at an axial position almost perpendicular to the plane containing the

S/N chelate. In **28**, the Pb-S bond is longer and Pb-N bond is shorter compared to the corresponding bonds in **27**.

The geometry around four-coordinate Pb in $[Pb(SCH_2CH_2NH_2)_2]$ (**29**)[60] and $[Pb(3\text{-}CF_3\text{-}PyS)_2]$ (**30**) (3-CF_3-PyS = 3-(trifluoromethyl)pyridine-2-thione)[61] is pseudo-trigonal bipyramidal with distortion toward square pyramidal geometry in the latter. The source of the distortion is the small angle associated with the chelate and the lone pair present on Pb. The S-Pb-S and N-Pb-N angles are in the range, 86 - 149º, which are significantly different from the ideal value of 90º. The Pb-S distances in **29** are much shorter than those observed in **27**, **28** and **30**. One of the Pb-N distances in **30** is significantly shorter than the other one but close to that observed in **29** as well as Pb(II)-thiolates with an additional pyridine ligand (Table A5).[62]

In $[Pb(Ishexim)_2]$ (Ishexim = isatin-3-hexamethyleneiminylthiosemicarbazone) (**31**)[63], the Pb is four-coordinate with S and N atoms. However, including the additional weak interactions with oxygen atoms the geometry is closer to distorted trigonal bipyramidal with the lone pair in the apical position (Figure 1.9).

In $[Pb(H_2DAPTsz\text{-}Me)]$ (**32**)[64] (H_2DAPTsz-Me = bis(4-N-methylthiosemicarbazone)-2,6-diacetylpyridine) the geometry around the Pb atom is distorted pentagonal with a sixth position occupied by the lone-pair (Figure 1.11). However, for five-coordinate Pb(II)-thiolates the geometry around Pb can also be hemidirected trigonal-bipyramidal (Figure 1.10b) and hemidirected square-pyramidal (Figure 1.10c) in contrast to an "umbrella-like" distorted geometry observed in **32** (Figure 1.10a).[65]

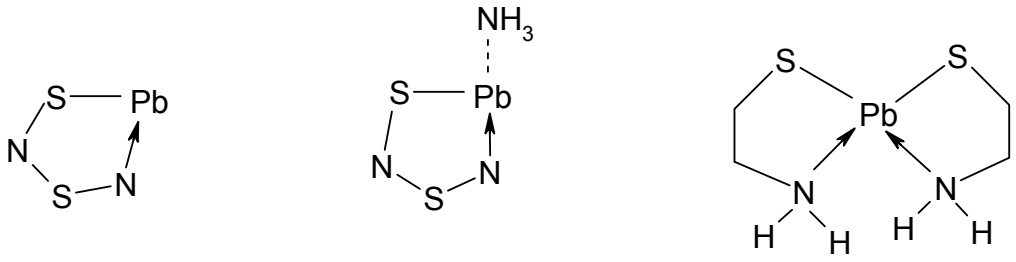

(**27**) (**28**) (**29**)

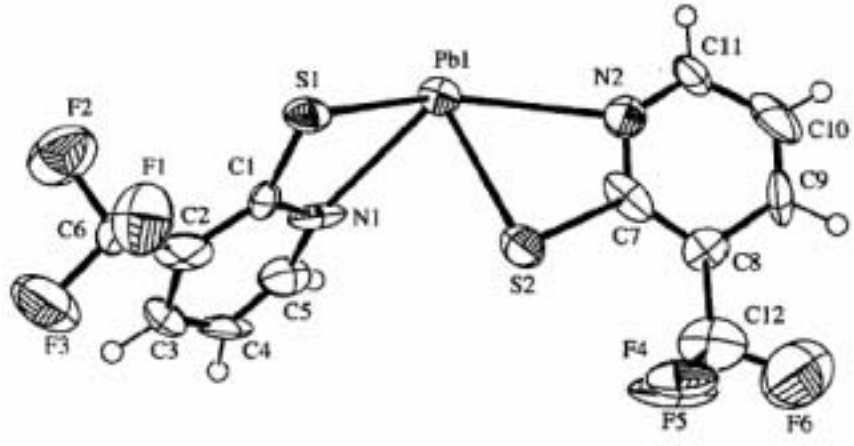

(**30**)

Figure 1.8. Structural formula of **27** - **29** and molecular structure of **30**.

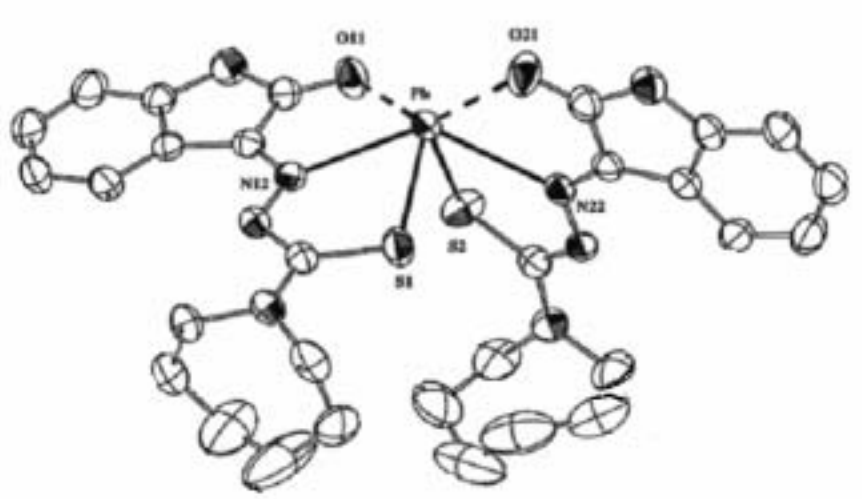

Figure 1.9. Structure of [Pb(isatin-3-hexamethyleneiminylthiosemicarbazone)$_2$] (**31**).[63]

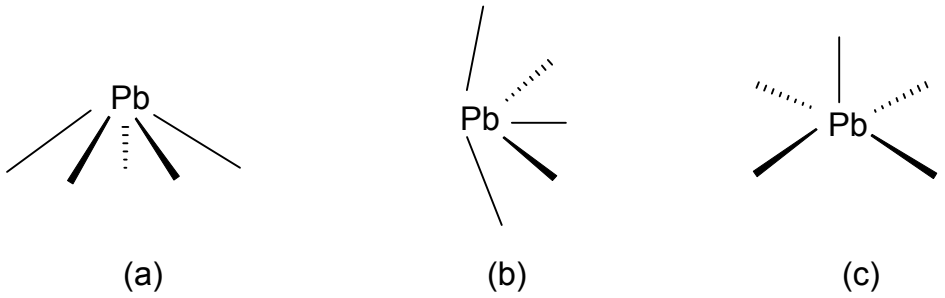

Figure 1.10. Geometries observed in five-coordinate Pb(II)-compounds.

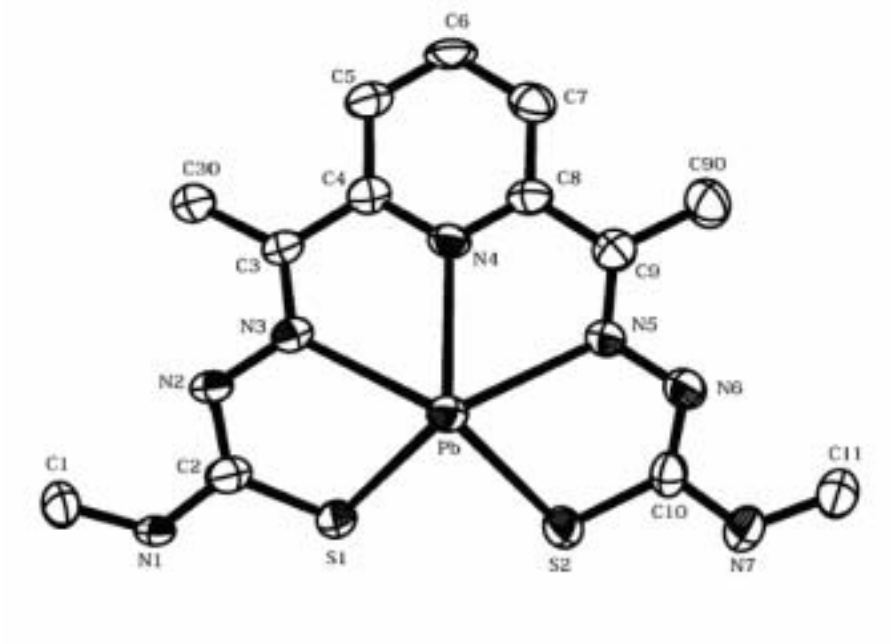

Figure 1.11. Structure of [Pb(bis(4-N-methylthiosemicarbazone)-2,6-diacetylpyridine)] (**32**).[64]

The Pb-N distances in **31** and **32** are similar but the Pb-S distances vary with slightly longer distances observed in **32** (Table A6). These distances are notably longer than those found in monomeric Pb(II)-thiolates containing a thiosemicarbazone ligand.[64] These distances are also outside the range (2.37 - 2.56 Å) proposed for Pb(II)-thiolates with a stereochemically active lone pair and coordination number less than eight.[66]

The environment around Pb in $[PbPh_2Cl_2(HSTSC)_2]$ (HSTSC = salicylaldehyde thiosemicarbazone) (**33**), $[PbPh_2Cl(PyTSC)]$ (PyTSC = pyridine-2-carbaldehyde thiosemicarbazone) (**34**), and $[PbPh_2Cl(AcPyTSC)]$ (AcPyTSC = 2-acetylpyridine thiosemicarbazone) (**35**),[67] is variable despite having similar ligands. For instance Pb is coordinated to two S and two Cl atoms in **33** (Figure 1.12), one S, one N, one Cl, a weakly bonded N in **34** and one S, one Cl and two N atoms in **35** beside two phenyl groups attached to Pb in all the cases.

The geometry around Pb in these compounds is distorted pentagonal bipyramidal including weak interactions involving S, N and Cl atoms. Despite the similarity of the HSTSC, HPyTSC and HAcPyTSC ligands the interaction with the $[Ph_2PbCl]^+$ ion is different. In **33**, the N atoms of the ligands are not interacting with the Pb atoms in contrast to the Pb-N bond observed in **34** and **35.** The Pb-S distance in **34** (2.582 Å) is much shorter than those observed in **33** and **35** (avg 2.700 Å).

In the Pb-penicillamine adduct, $[Pb(SC(CH_3)_2CH(NH_2)COO]$ (**36**),[68] the Pb is surrounded by S, N and O atoms. Without including the weak interactions the geometry around the Pb can be considered as distorted tetrahedral with S, N and O from ligand. But the presence of weak interactions and lone pair provides distorted pentagonal bipyramidal geometry around Pb (Figure 1.13).

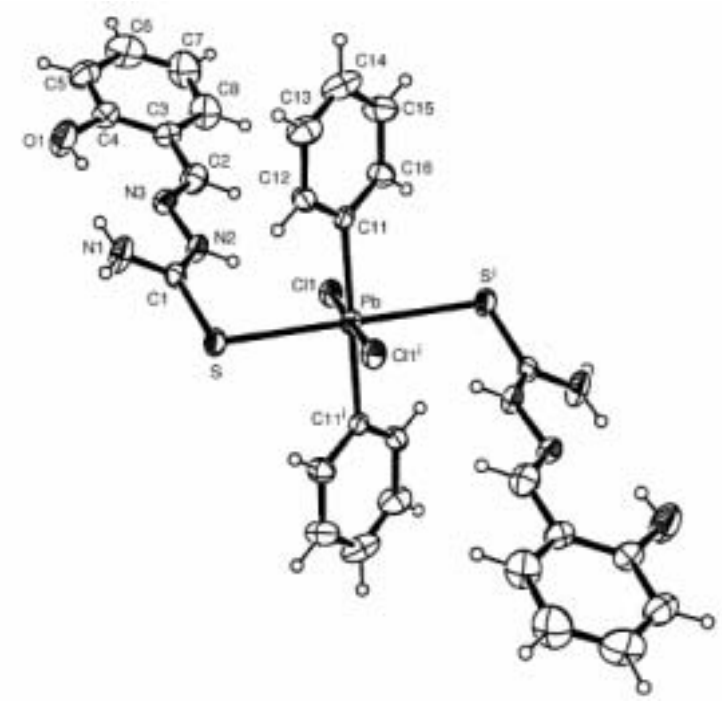
C6
C7
C5
C8
C3
O1
C4
C2
N3
N2
N1
C1
S
C14
C13
C15
C12
C16
C11
Cl1
Pb
S'
Cl1'
C11'

(**33**)

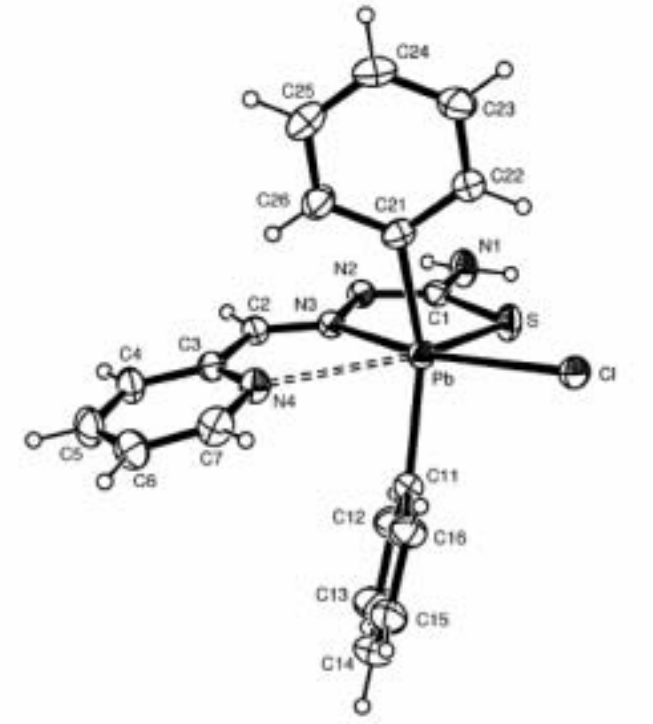
C24
C25
C23
C22
C26
C21
N1
N2
C2
N3
C1
S
C3
C4
Pb
Cl
N4
C5
C7
C6
C11
C12
C16
C13
C15
C14

(**34**)

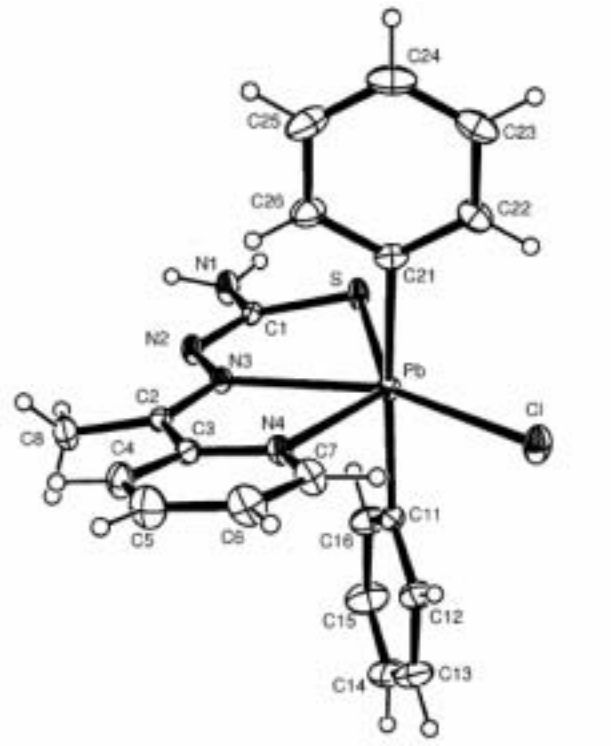

(**35**)

Figure 1.12. Molecular structures of **33**, **34** and **35**.

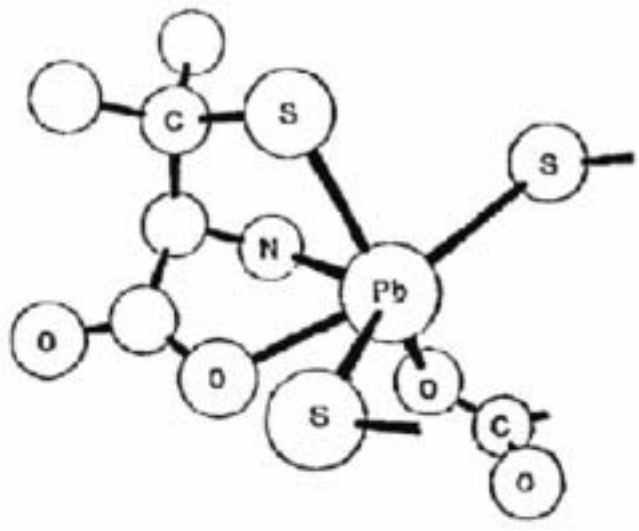

Figure 1.13. Structure of [Pb(SC(CH_3)$_2$CH(NH_2)COO] (**36**).[68]

In **35** and **36**, the Pb is shown to interact with the S atoms of different molecules with a distance much longer than usually observed. The Pb-N distances in **34** and **35** are variable with a greater difference observed in the former due to the presence of weak Pb-N interactions. These distances are longer compared to the corresponding distances observed in **36**. In **34**, the distortion from an ideal geometry is most probably due to the strong Pb-S and small chelate angles. The selected bond angles and distances are summarized in Table A7.

The Pb compounds with macromolecules containing N_3S_2 (L^1), N_2S_2 (L^2) and N_2S_2O (L^3) units form $[Pb(L^1)(MeOH)(H_2O)]^+$ (**37**),[69] $[Pb(L^2)_2]^{2+}$ (**38**) and $(Pb(L^3)]^{2+}$ (**39**)[70], respectively. The coordination number around Pb ranges from seven to nine including weak interaction with counter anion and solvent molecules (Figure 1.14, Table A8). These compounds have been synthesized by direct addition of Pb(II) salts and the corresponding ligands in water or in common organic solvents. In **37**, the Pb is surrounded by three N and two S atoms in equatorial position and solvent molecules (water and methanol) in axial position. The geometry around Pb can be best described as *nido*-hexagonal bipyramidal. The Pb-N distances are in agreement with the corresponding distances observed in Pb(II) compounds with imine and pyridine ligands.[71] The Pb-S distances are close to the estimated sum of the Shannon ionic radius of Pb (1.29 Å) and van der Waals radius of S (1.85 Å)[72] and also in accord with distances found in Pb(II)-thiolates with macrocyclic ligands such as $[Pb(C_{18}H_{20}N_4S_2)(O_2CMe)(PF_6)]PF_6$ ($C_{18}H_{20}N_4S_2$ = 18-membered mixed donor macromolecule).[73]

The intramolecular Pb---N interactions (3.260 Å) are longer than those observed in Pb(II) compounds with mixed donor macromolecules.[73] Moreover, the tilt observed in

the pyridyl ring is not consistent with a Pb---N interaction. The non-linear O-Pb-O angle (142º) is due to the localization of a stereochemically active lone pair of electrons.

In **38**, the Pb atom is sandwiched between two ligands with covalent contact with N and S in addition to two weak Pb-S contacts. The Pb-S distances are in the upper limit of the range observed in **37** as well as in Pb(II)-thioethers.[74] The overall [4N + 4S] coordination and Pb-N contacts are typical of those observed for Pb(II) compounds with imine and pyridine ligands.[71,75,76] On passage from L^2 to L^3, **39** is obtained in which the coordination around Pb is completed by two N, two S and one O atom from the ligand as well as four O atoms from ClO_4^- and CH_3NO_2. The Pb-S as well as Pb-N distances are comparable to those observed in **36** and **37** but the Pb-O_{ligand} is shorter than the Pb-O bond associated with ClO_4^- and $MeNO_2$. These distances are, however, much longer than those expected for Pb(II) compounds with O-donating counteranions.[74]

1.2.2 Dinuclear Compounds

Dinuclear Pb(II)-thiolates with S/N ligands are rare but the weak interactions involving counter anions and solvent molecules can generate structures such as $[Pb(L^4)][ClO_4]_2 \cdot 1/2H_2O$ (**40**) (L^4 = N_2S_3 containing macrocyle) (Figure 1.15).[70] This is, however, in contrast to $[\{PbPh_2Cl(HPyTSC\}_2][PbPh_2Cl_3(MeOH)]_2$ (**41**), where the individual molecules are held together through terminal Cl atoms (Figure 1.16).[67]

In **40**, two perchlorate ions and a water molecule bridge two $[PbL^4]^{2+}$ units to form a dinuclear species and each Pb in both units further interact with O atoms from the perchlorate ion to acquire a nine-coordinate geometry.

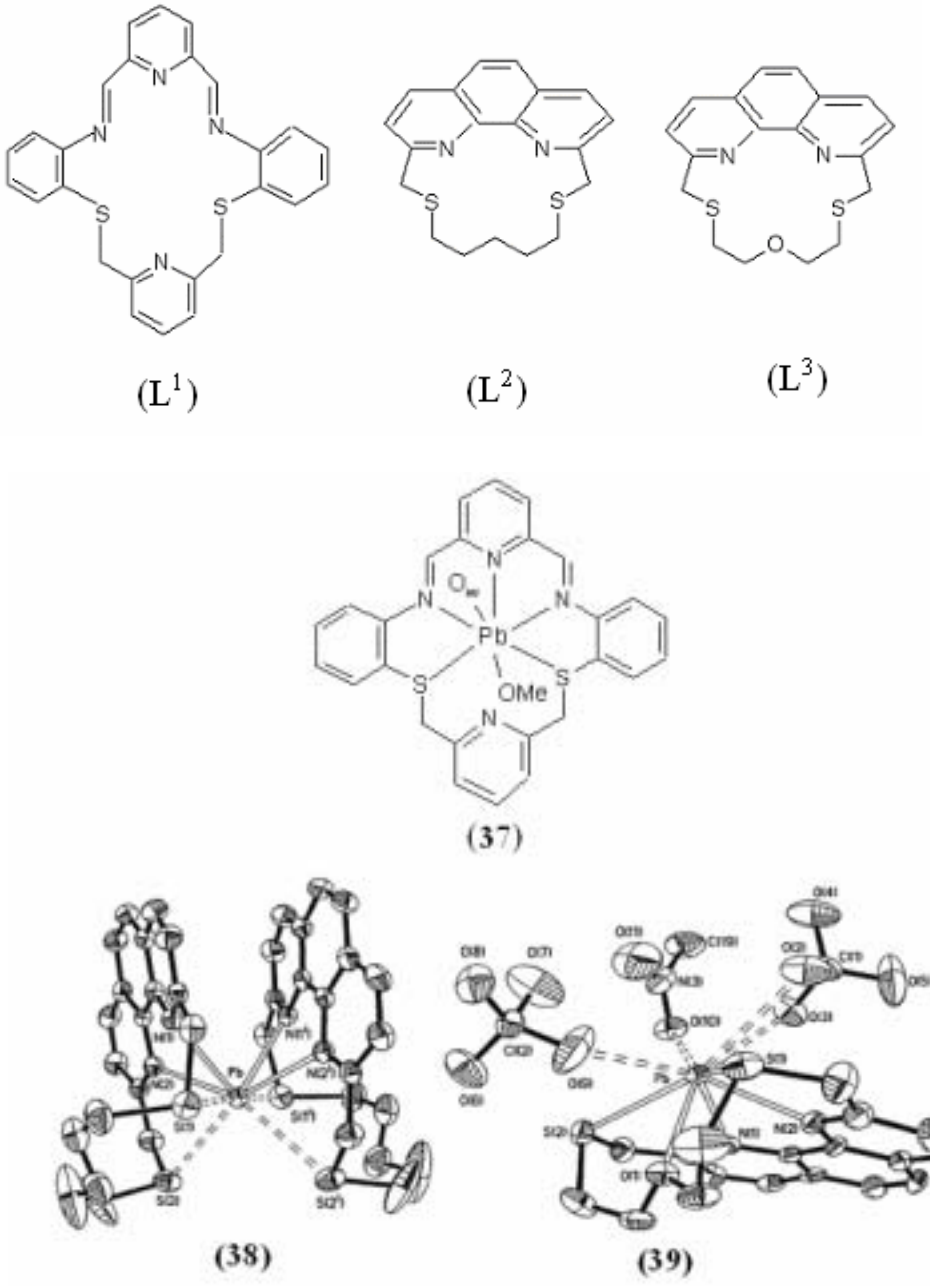

Figure 1.14. Structure of macromolecules L^1, L^2 and L^3. Molecular geometry of **37** and structures of **38** and **39**.

The Pb-S and Pb-N distances are comparable to those observed in **38** and **39** and compounds containing Pb-$S_{thioether}$ bonds.[74] However, the Pb-O distances involving perchlorate ion and water molecule are rather long (2.852 - 3.105 Å) compared to those found for O-donating counteranions coordinating to Pb(II). These distances are also longer than the estimated sum of the Shannon ionic radii of nine-coordinate Pb(II) and oxygen (2.85 Å).[77] The Pb in the dimer is shifted 0.920 Å toward the O-donor manifold of the perchlorate ions and the water molecules from the mean plane defined by N(1), N(2), S(1) and S(2), which is similar to that observed in Pb compound with macrocycle ligand containing N atoms.[78]

The formation of a dimer in **41** gives rise to a doubly charged dinuclear cation $[\{PbPh_2Cl(HPyTSC)\}_2]^{2+}$ with hepta-coordination around Pb. Hence, the geometry around Pb can be considered as distorted pentagonal bipyramidal with phenyl groups in the axial positions. The cationic centers are linked together through Cl (Pb-Cl = 2.911 Å). The Pb is octahedral in the counter anion $[PbPh_2Cl_3(MeOH)]^-$, which is most probably generated from $[PbPhCl_3]^-$. The OH--Cl hydrogen bonding keeps the counter anion together, while hydrogen bonding involving N, O and Cl atms connect the dimeric cation together to form a two-dimensional network.

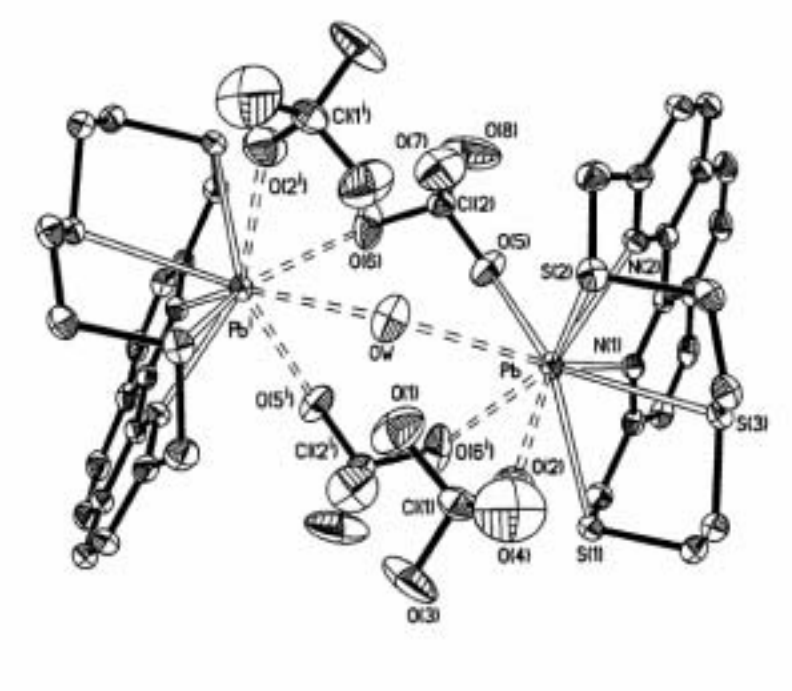

Figure 1.15. Dimer of **40** with solvent molecules acting as bridging atoms.[70]

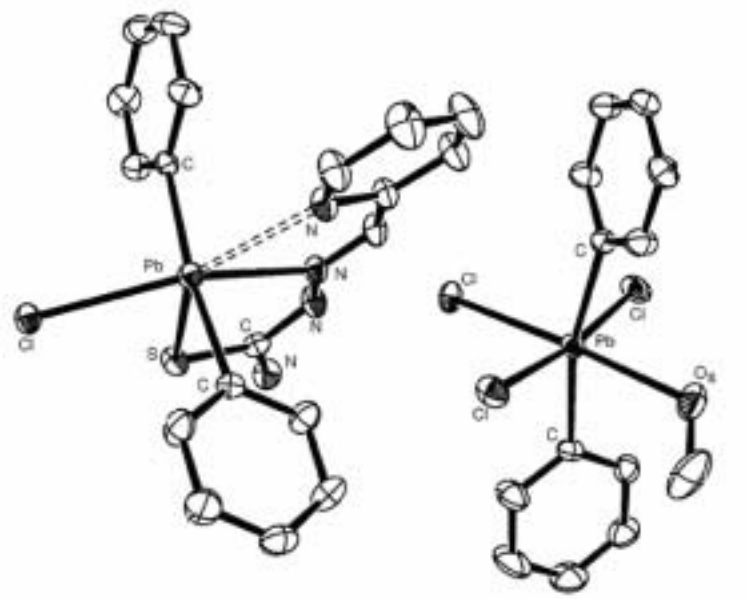

Figure 1.16. Structure of **41** showing $[PbPh_2Cl(HPyTSC)_2]^+$ and $[PbPh_2Cl_3(MeOH)]^-$ units.[67]

1.2.3 Trinuclear Compounds

The geometry around Pb in trinuclear $[\{PbCl(SCH_2CH_2NH_2)\}_2\{Pb(SCH_2CH_2NH_2)_2\}]$ (**42**) and $[Pb_3(2\text{-}SC_5H_3N\text{-}3\text{-}SiMe_3)_6]$ (**43**) is variable as two independent Pb centers are observed.[60,79] The Pb is coordinated to S and Cl with weak Pb-N interactions in **42** (Figure 1.17), whereas strong Pb-S and Pb-N contacts are observed in **43** (Figure 1.18). The molecules in **42** are held together through weak Pb---S and NH---Cl bonding. The Pb1A with the stereochemically active lone pair exhibits a distorted pseudo-octahedral geometry. On the other hand, Pb1B, which is coordinated by S (covalent) and N (dative) acquires a distorted pseudo trigonal bipyramidal configuration. The distances involved in weak Pb-S---Pb-S contacts (3.036 Å) are shorter than those observed in $\{4\text{-}t\text{Bu-}2,6\text{-}[P(O)(OEt)_2]_2C_6H_2PbSPh\}$ (3.295 Å) indicating strong interactions.[80]

Compound **43** consists of a discrete trinuclear species with irregular geometries associated with Pb due to the stereochemically active lone pair. The Pb1 exhibits trigonal pyramidal, whereas Pb2 exhibits a square pyramidal, geometry. The Pb1-N distance (2.810 Å) is longer than Pb2-N (2.510 Å) but within the sum of van der Waals radii of Pb and N atoms (3.550 Å).[72] Secondary interactions with S atoms produce a distorted eight-coordinate geometry around Pb2. The bond angles and distances for **40** - **43** are summarized in Table A9.

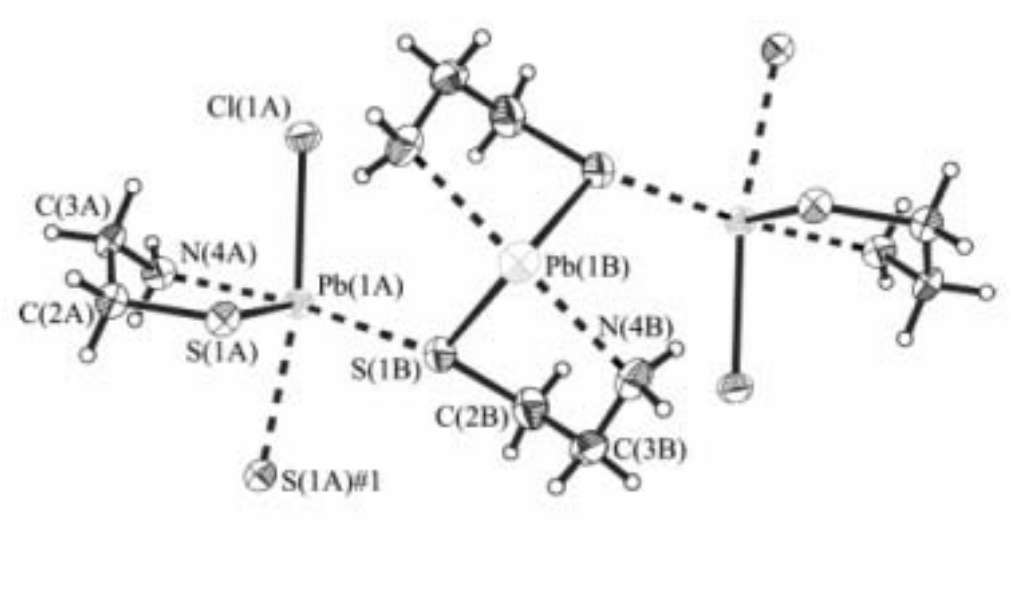

Figure 1.17. Molecular structure of [{$PbCl_2(SCH_2CH_2NH_2)$}{$Pb(SCH_2CH_2NH_2)$}] (**42**) with weak Pb---S contacts.[60]

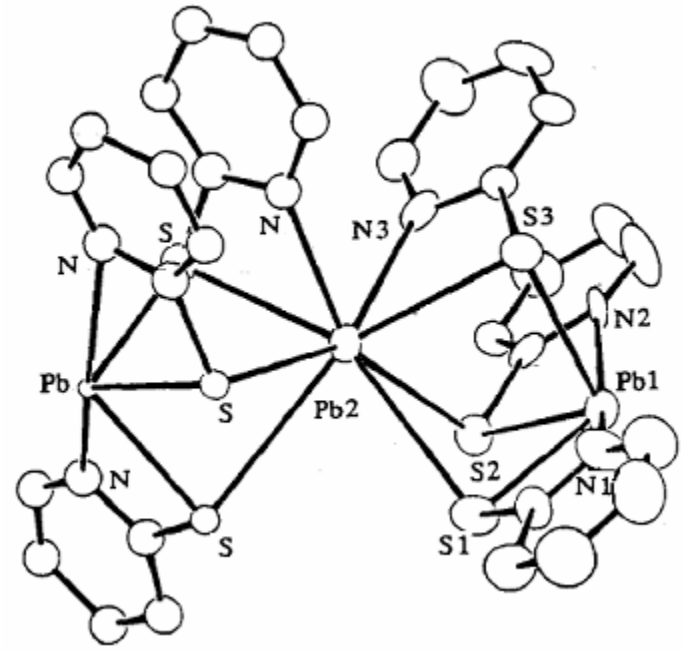

Figure 1.18. Structure of [$Pb_3(2\text{-}SC_5H_3N\text{-}3\text{-}SiMe_3)_6$] (**43**). The -$SiMe_3$ groups are not shown for clarity.[79]

1.3 Mercury(II)-thiolates

Mercury is one of the most toxic elements in the periodic table. In the lab it is used for making instruments like thermometers, barometers, diffusion pumps, etc. The most important and primary source of low-level mercury exposure is dental amalgams and the consumption of fish. Other sources include production of chlorine, paper and pulp, fungicides/seed preservatives, paints, combustion of fossil fuels and mining. The organic mercury compounds are more dangerous and toxic than the inorganic salts. For example, methylmercury ($HgMe^{+}$) is readily absorbed through the skin due to its lipophilic nature. The lipophilic methylmercury compounds easily penetrate nerves and bind to cysteine on acetycholine receptors, resulting in neurological dysfunction and in extreme cases, death. Inside the cell Hg^{2+} and $MeHg^{+}$ form covalent bonds with sulfhydryl residues of the proteins and inhibit the polymerization of tubulin, depolymerization of microtubules, and in animals it results in brain lesions related to Alzheimer's Disease.[81,82] Natural methylation by microorganisms is a major contributor to the biological cycling of mercury in the environment. Mercuric ion, released from mercury ore such as HgS or from other sources, is methylated to methyl mercury species that can be absorbed into the organism or eventually converted to volatile dimethylmercury. Photodegradation in water or the atmosphere removes the alkyl groups and returns the Hg as the inorganic ion.

The interaction of Hg with thiolate sulfur is thermodynamically favored and stability is achieved by the formation of a number of structures of equal energy with varying geometry around the Hg atom.[83] In homoleptic Hg(II)-thiolates, Hg adopts discrete molecular ($[Hg_x(SR)_y]$) (x = 1 - 5 and y = 2 - 8) as well as polymeric ($[Hg(SR)_2]_\infty$

and $[Hg_2(SR)_3]^+_\infty$) structures(R = alkyl or aryl groups).[84-87] On the other hand, the heteroleptic thiolates (containing both monodentate thiol and halide) are generally non-molecular polymeric compounds containing one-dimensional ($[Hg(SR)Cl]_\infty$ and [Hg(S-Steroid)Br]$_\infty$) or two-dimensional ($[Hg(SMe)X]_\infty$ (X = Cl or Br) and $[Hg(SPr^i)Cl]_\infty$) units.[88-90] However, discrete molecular structures of higher nuclearity are also observed, including $(Ph_4P)[(\mu\text{-}SEt)_5(\mu\text{-}Br)(HgBr)_4]$, $(Et_4N)_2[(\mu\text{-}I)(\mu\text{-}SPr^n)(HgI_2)_2]$, $(Bu^n{}_4N)_2[Hg_4(SR)_6X_4]$ (R = SEt and SPr^i), $[Hg_4\{S(CH_2)_2NMe_2\}_4X_4]$ and $[Hg_7(SC_6H_{11})_{12}X_2]$ (X = Cl, Br or I).[91] In this chapter, the heteroleptic Hg(II)-thiolates with S/N containing ligands are discussed according to the nuclearity.

1.3.1 Mononuclear Compounds

The geometries in mononuclear Hg(II)-thiolates range from linear to square pyramidal with coordination number two to five (Figure 1.19, Table A10).

The two-coordinate molecular compounds are rare but include $[Hg\{SCH_2CH(NH_3)COO\}\{SCH_2CH(NH_3)COOH]^+$ (**44**),[92] $[Hg(SC_5H_9NH(CH_3))_2]^{2+}$ (**45**),[93] $[Hg(4\text{-}SC_6H_4NH_2)_2]$ (**46**),[94] and $[Hg(bztzS)_2]$ (bztzS = benzo-1,3-thiazoline-2-thione) (**47**).[95] The molecular framework is similar in these compounds with Hg linearly coordinated to two S atoms and in some cases there are weak interaction with counter anions or solvent molecules. The Hg-S distances are similar and in the range 2.329 - 2.361 Å, which is comparable to those observed in homoleptic $[Hg(SR)_2]$ compounds (avg 2.339 Å).[96] The S-Hg-S angles are linear (170.0 - 178.0º) with the greatest distortion observed in **44**. This may be due to the presence of a Cl anion in close proximity to the Hg center, something not observed in **45 - 47**. In contrast, the presence of additional weak

Hg---S (3.190 Å) interactions in **45** increases the coordination number from two to five providing a square-pyramidal geometry.

Three-coordinate mercury thiolates are not very common, restricted to the compounds $[Hg(S\text{-}^tBu)_3]^-$ and $[Hg(SC_6H_5)_3]^-$.[97] On the other hand, three-coordinate heteroleptic thiolates include $[HgI_2(bzimtH_2)]$ (**48**)[98] ($bzimtH_2$ = benzo-1, 3-imidazole-2-thione) and $[HgI_2(imtH_2)]$ (**49**) ($imtH_2$ = 1,3-imidazole-2-thione), where the Hg is coordinated to two I and one S atom.[99] The formation of a three-coordinate Hg is most probably due to the steric effects of the I atom, as with Cl and Br higher coordination numbers are usually observed. The geometry around Hg in **48** and **49** is distorted trigonal with the I atoms involved in bridging with neighboring molecules.

The centrosymmetric dimers formed by Hg---I interactions are close to the sum of van der Waals radii of Hg and I (1.55 + 2.13 Å) acquiring a [3 + 1] coordination around Hg.[100] The distortion in the trigonal geometry is evident by the large bond angles of 112.9º and 134.6º (S-Hg-I1) accompanied by short Hg-I bonds. The intermolecular hydrogen bonding seem to be dependent on the ligand. In **48** the larger $bzimtH_2$ allows shorter Hg---I contacts as a result of NH---I bonding, whereas in **49** only NH---S distances are observed. The more extended π-delocalized ring in **48** compared to **49** might be responsible for a stronger Hg---I contact as it enables a better π-stacking assembly of the ligand molecules.

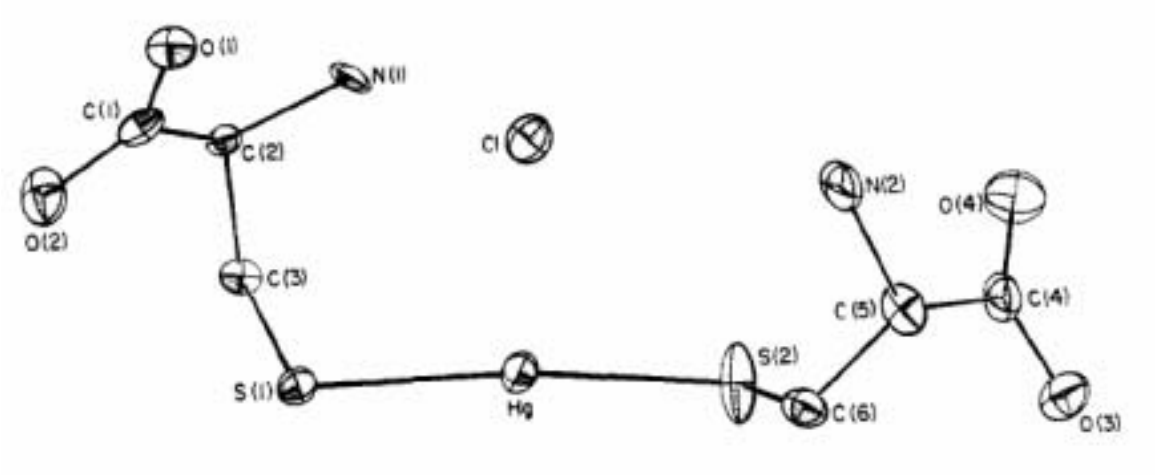
O(1)
N(1)
C(1)
C(2)
Cl
O(2)
C(3)
N(2)
O(4)
C(5)
C(4)
S(2)
S(1)
Hg
C(6)
O(3)

(**44**)

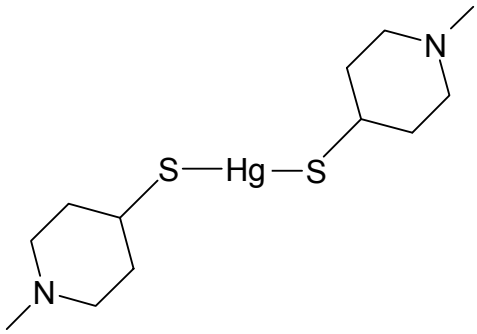
N
S—Hg—S
N

(**45**)

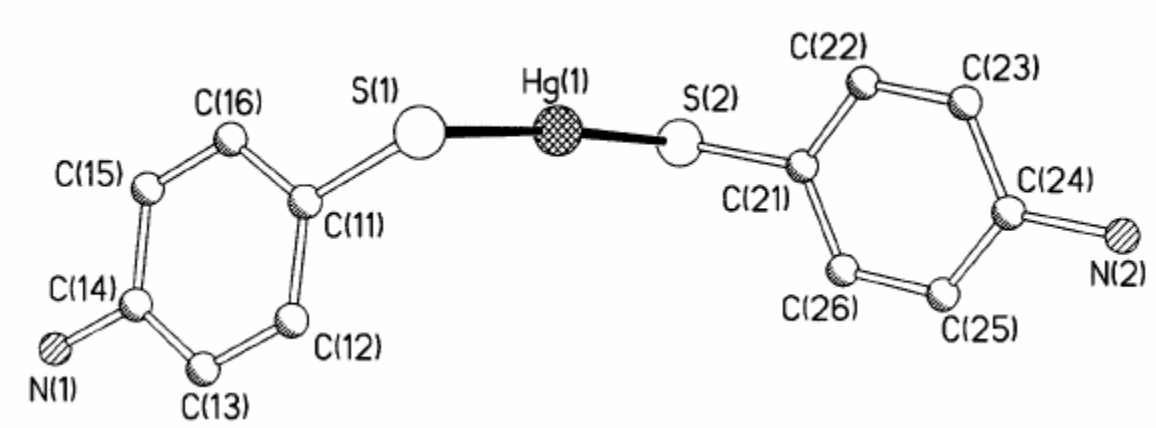
C(22)
C(23)
C(16)
S(1)
Hg(1)
S(2)
C(15)
C(21)
C(24)
C(11)
N(2)
C(14)
C(26)
C(25)
C(12)
N(1)
C(13)

(**46**)

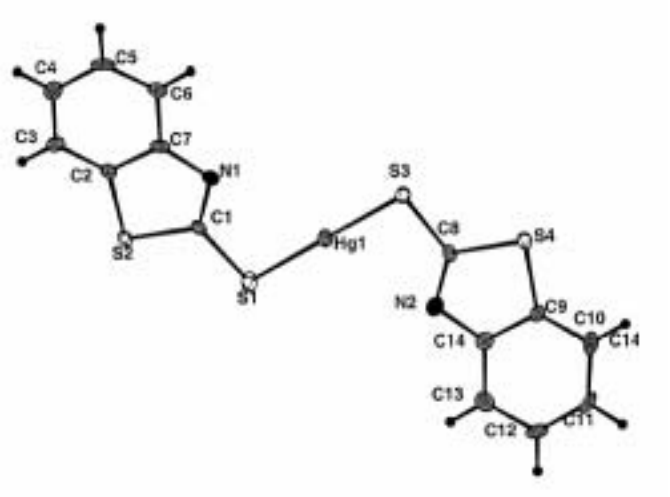
C4
C5
C6
C3
C7
N1
C2
C1
S2
S1
Hg1
S3
C8
S4
N2
C9
C10
C14
C14
C13
C12
C11

(**47**)

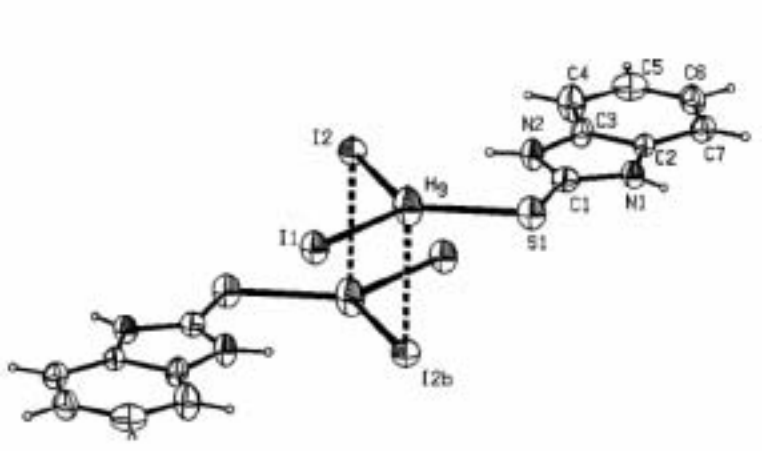
C4
C5
C6
N2
C3
C2
C7
I2
Hg
C1
N1
I1
S1
I2b

(**48**)

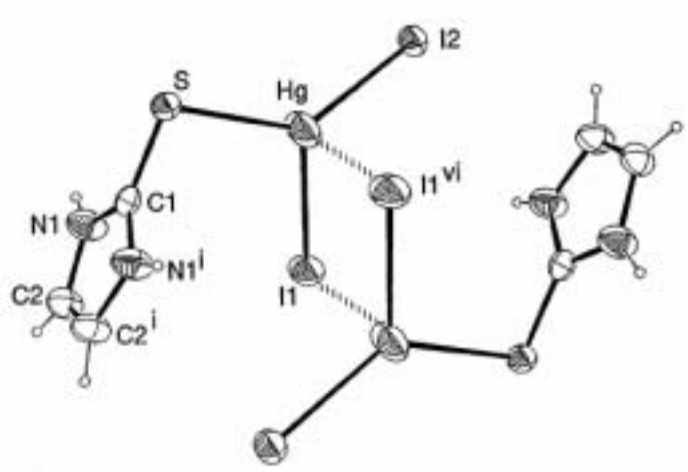
I2
S
Hg
I1vi
C1
N1
N1i
C2
I1
C2i

(**49**)

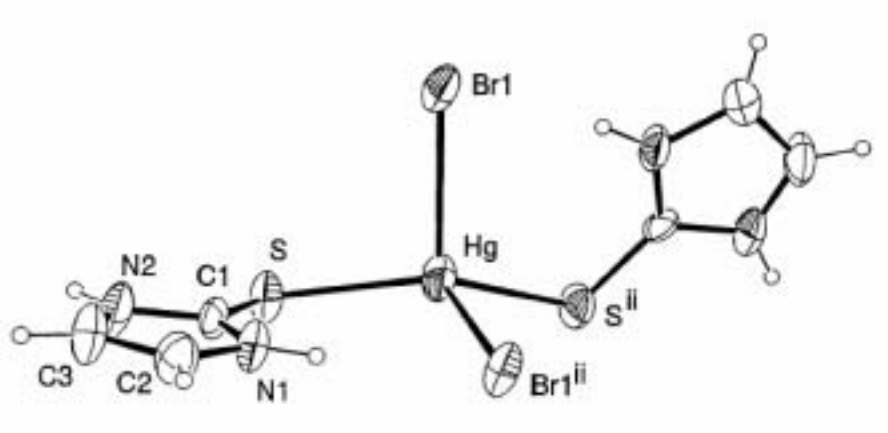
Br1
Hg
S
N2
C1
C3
C2
N1
S^ii
Br1^ii

(**50**)

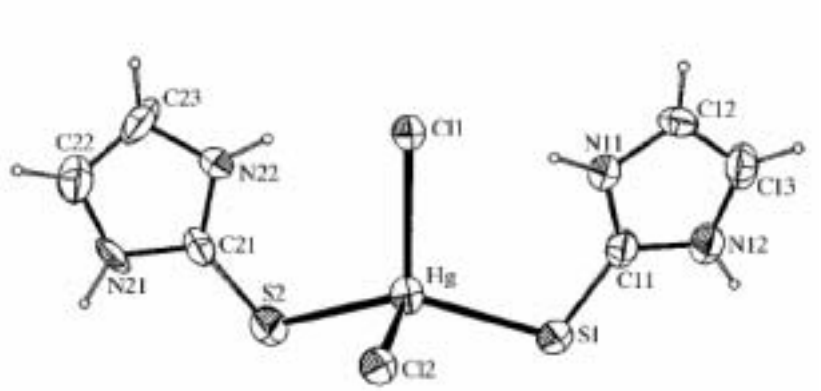
C23
C22
N22
C21
N21
S2
Cl1
Hg
Cl2
S1
C12
N11
C13
N12
C11

(**51**)

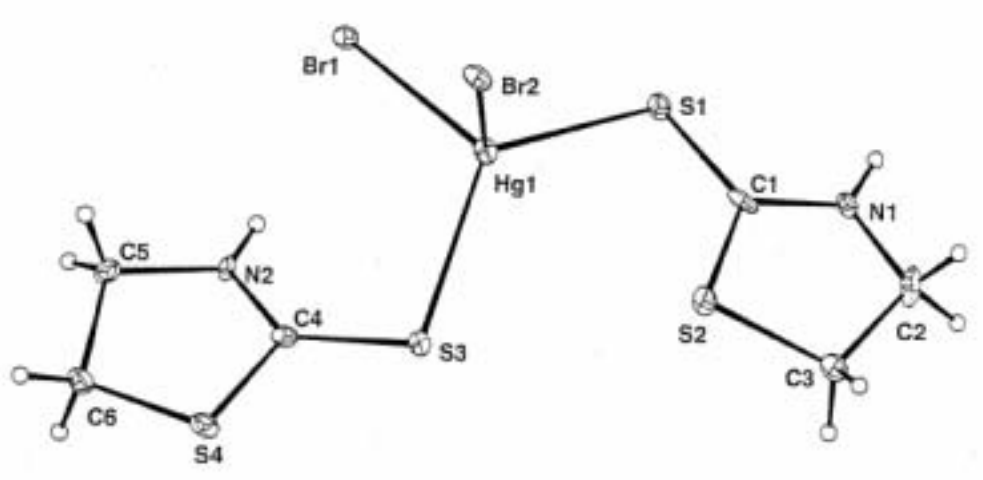
Br1
Br2
S1
Hg1
C1
N1
C5
N2
C4
S3
S2
C2
C3
C6
S4

(**52**)

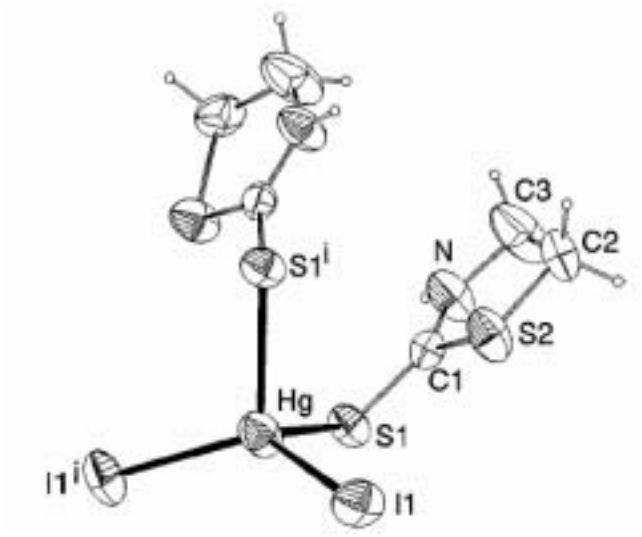
C3
C2
N
S1i
S2
C1
Hg
S1
I1i
I1

(**53**)

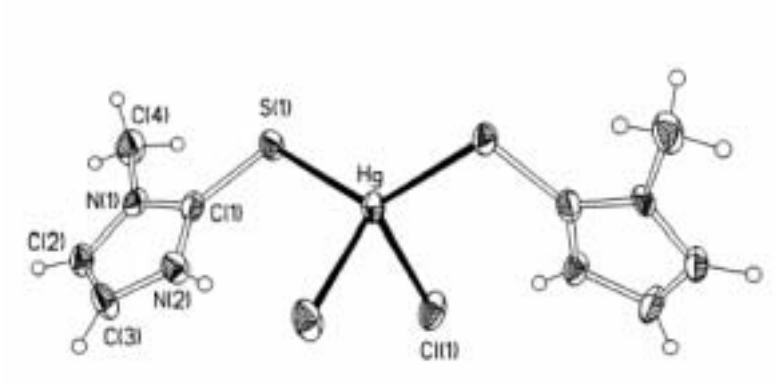
C(4)
S(1)
Hg
N(1)
C(1)
C(2)
N(2)
C(3)
Cl(1)

(**54**)

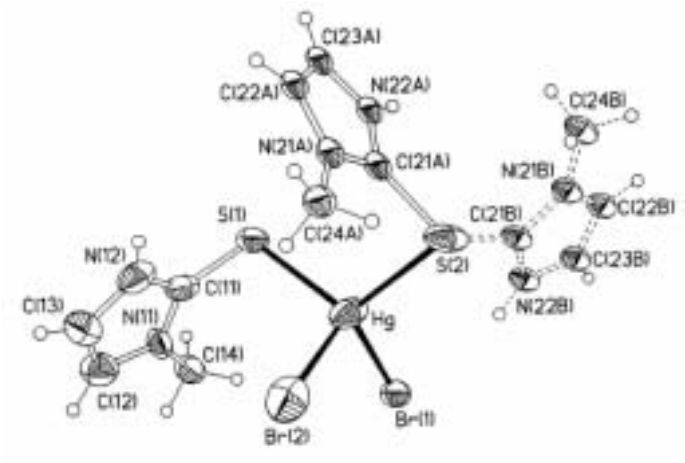
C(23A)
C(22A)
N(22A)
C(24B)
N(21A)
C(21A)
N(21B)
C(22B)
S(1)
C(24A)
C(21B)
N(12)
C(11)
S(2)
C(23B)
C(13)
N(11)
Hg
N(22B)
C(14)
C(12)
Br(2)
Br(1)

(**55**)

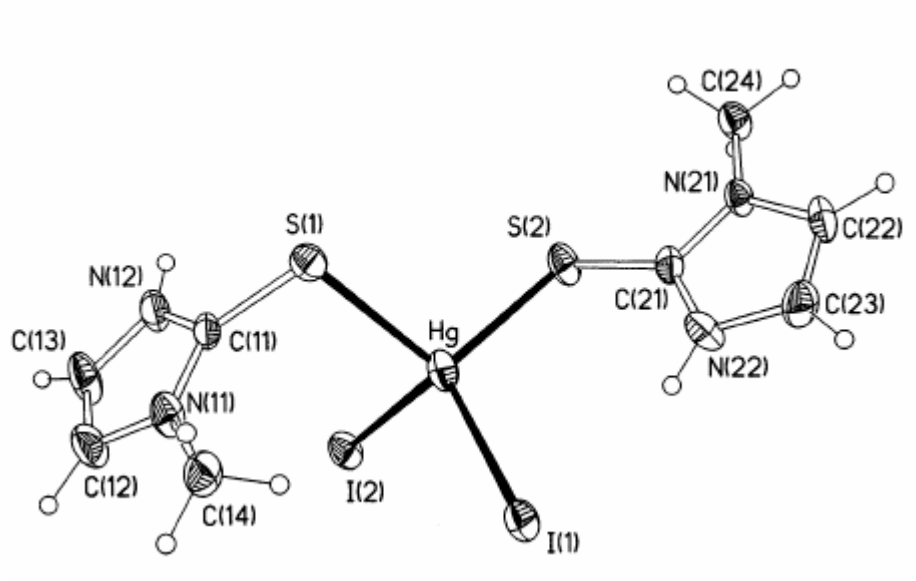

(**56**)

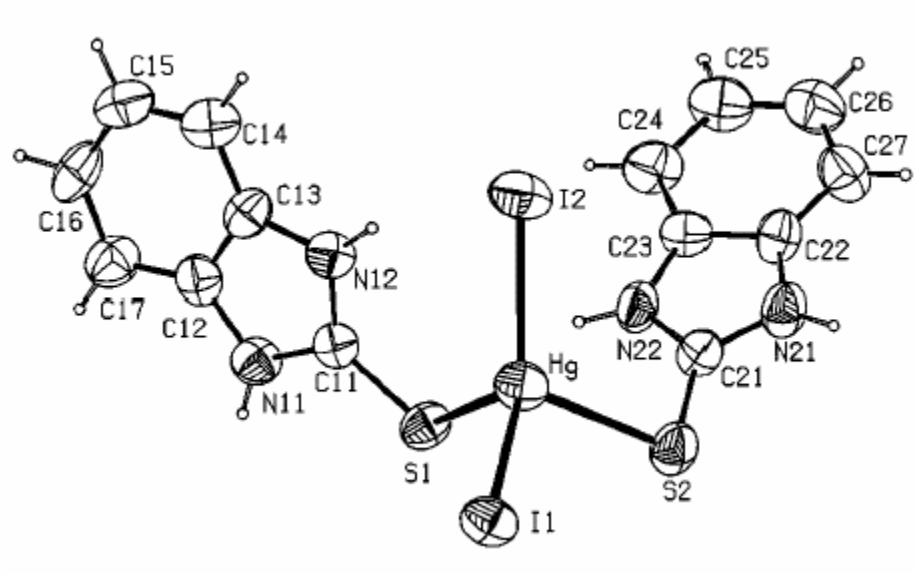

(**57**)

Figure 1.19. Molecular geometry of **45** and molecular structures of **44**, **46 - 57**.

In $[HgX_2(imtH_2)_2]$ (X = Br (**50**) and Cl (**51**)),[99] $[HgX_2(tzdtH)_2]$ (tzdtH = thiazolidine-2-thione) (X = Br (**52**) and I (**53**)),[95] $[HgX_2(meimdSH)_2]$ (meimdSH = 1-methyl-imidazoline-2(3H)-thione) (X = Cl (**54**), Br (**55**) and I (**56**)][101] and $[HgI_2(bzimtH_2)_2]$ (**57**),[98] the geometry around the four-coordinate Hg is distorted tetrahedral with the coordination sphere consisting of two thiolate S and two halide atoms.

The Hg-S and Hg-X distances in **50** are symmetrical but variable in **51**, which is most probably due to inter- and intra-molecular interactions. However, with Br in **50**, the presence of weak interactions does not affect the geometry around Hg. The Hg-S distances (avg 2.453 Å) are shorter than the sum of the covalent radii of S and tetrahedral Hg (2.520 Å) indicating stronger bonds.[72] The Hg-X distances are longer than the sum of covalent radii of tetrahedral Hg, Br and Cl atoms, indicating weaker bonding. The longer Hg-X and shorter Hg-S distances are followed by smaller bond angles associated with X and broader angles associated with S atoms. The deformation of the angles and shorter Hg-S bonds can be related to the weaker Hg-X bonds.

The Hg-S distances in **53** and **56** (avg 2.609 Å) are longer than those observed in **52**, **54** and **55** (avg 2.495 Å), which is most probably due to the presence of the Hg-I bond. The Hg-S distances in **54** - **56** show a regular incremental shortening from Cl to I. The Hg-X distances as well as X-Hg-X angles increase as the covalent radius of the halide increases despite the strong Hg-S contact. Another influence on the Hg-S and Hg-X bonds is the involvement of the donor atoms in hydrogen bonding.

In **57**, the Hg-S distances are slightly longer (avg 2.626 Å) and Hg-I are shorter (avg 2.710 Å) than usually observed for four-coordinate Hg(II)-thiolates. The tetrahedral

environment is distorted with angles in the range 88.0º to 124º and the largest angle is observed for the strong I atoms. The distinct feature observed in **57** compared to **56** is the presence of an N-H---S contact, which might be responsible for a longer Hg-S bond.

In five-coordinate Hg compounds, the Hg is bonded to S, N and Cl as shown in figure 1.20. The electroneutrality of $[HgCl\{N(CH_2CH_2SCH(CH_3)_2\}_3]_2^+$ (**58**) cation is completed by additional Hg_2Cl_6 anions, which is comprised of two $HgCl_4$ tetrahedra sharing a common edge.[102] The terminal (2.379 Å) and bridging (2.622 Å) Hg-Cl distances in the anion are in agreement with those found in the literature (2.367 - 2.390 Å and 2.624 - 2.641 Å respectively).[103] In the cation, the Hg is surrounded by S and N atoms with the geometry intermediate between trigonal bipyramidal and tetrahedral. The extent of distortion is similar to those observed for organomercury compounds containing tris(2-diphenylphosphinoethyl)amine (Me_6tren)[104] and tris(2-dimethylaminoethyl)amine (np_3) ligands.[105] The Hg-S distances are variable and slightly longer (2.612 Å) than those observed for four-coordinate complexes. The Hg-N distance (2.626 Å) is significantly longer than the corresponding distance observed in $[(Me_6tren)HgPh]^+$ (2.270 Å) and shorter than that observed in $[(np_3)HgMe]^+$ (3.500 Å).[105]

In contrast to **58**, the Hg in $[Hg(tptp)Cl]\cdot CH_2Cl_2$ (**59**) (tptp = tetraphenyl-21-thiaporphyrin) [106] is surrounded by three N, one S and one Cl atom to acquire a distorted bipyramidal geometry. The bonding pattern is similar to those observed for Fe(II), Ni(II) and Cu(II) with the same ligand.[107] The Hg-S distance (2.801 Å) implies a covalent bond, which is intermediate between that observed in **58** and $[Hg_5(Et_2dithiocarbamate)_8]^+$ (2.922 Å),[108] $[Hg_2(S_2CNEt_2)_4]$ (2.965 Å),[109] $[Hg\{(i\text{-}C_3H_7O)_2PS_2\}_2]$ (2.885 Å).[110]

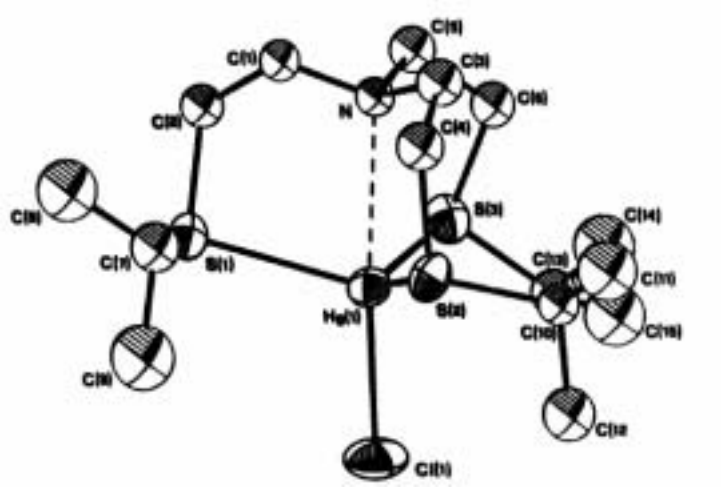

(**58**)

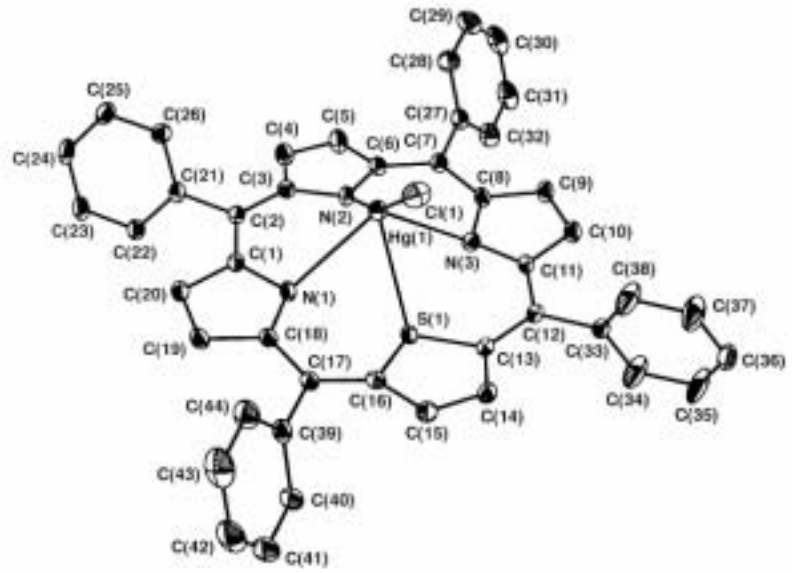

(**59**)

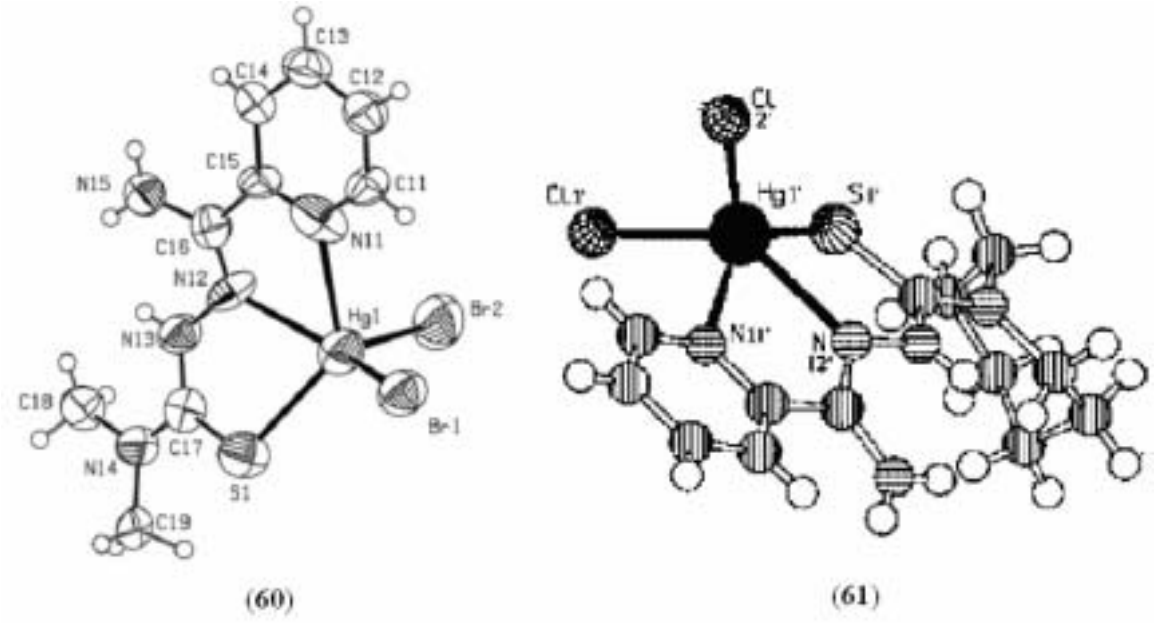

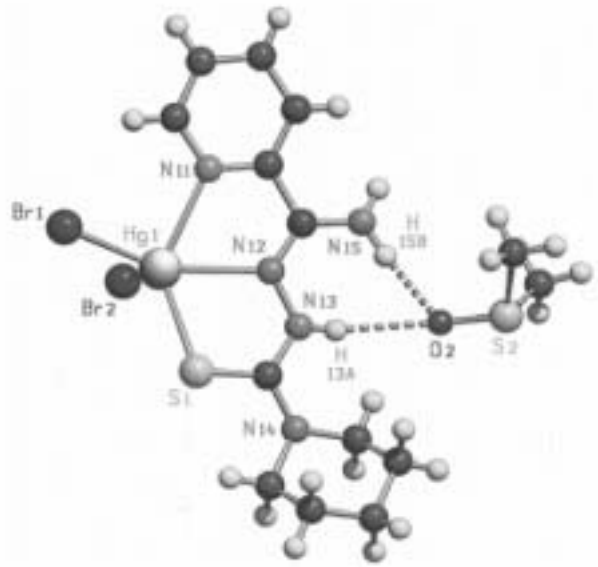

Figure 1.20. Molecular structures of **58 - 62** with five-coordinate Hg(II).

One of the nitrogen atoms is strongly bonded to Hg as indicated by the smaller Hg-N distance of 2.104 Å compared to the other Hg-N distances (avg 2.632 Å). These latter distances can be best described as secondary contacts to provide an effective [3 + 2] coordination sphere.

The coordination sphere around Hg in $[Hg(HAm4DM)Br_2]\cdot DMSO$ (**60**) (HAm4DM = 2-pyridineformamide N(4)-dimethylthiosemicarbazone),[111] $[Hg(HAmhexim)Cl_2]\cdot DMSO$ (**61**),[30] and $[Hg(Ampip)Br_2]\cdot DMSO$ (**62**)[31] consists of one S, two N, and two halide atoms (Figure 1.20). The geometry around Hg in **60** is square pyramidal and a distorted tetragonal pyramidal geometry in **61** and **62**. The Hg-S distance is smallest in **62** (2.506 Å) compared to those observed in **60** (2.578 Å) and **61** (2.522 Å). The Hg-N distances in **62** are similar (avg 2.463 Å) but variable in **60** and **61** (avg 2.412 and 2.528 Å). The difference in terminal Hg-Br distances in **60** is much smaller than those in **62**, but comparable to the terminal Hg-Br distance reported in the literature (2.470 - 2.650 Å).[112,113] Due to the difference in Hg donor bond distances the N-Hg-S angle in **60** (128º) is different from that observed in **62** (135º). The hydrogen bonding involving the DMSO molecule in all the cases is similar except for the presence of short NH--S contacts observed in **62**. Also, in **60** one of the amine hydrogens interacts with the oxygen of a single DMSO molecule but the amine hydrogen in **61** interacts with two molecules of DMSO.

1.3.2 Dinuclear Compounds

The dinuclear Hg(II)-thiolates such as $[HgX_2(tzdSH)]_2$ (X = Br (**63**) and I (**64**)) (tzdSH = 1,3-thiazolidine-2-thione)[114] and $[HgBr_2(meimz2SH)]_2$ (meimz2SH = 1-

methylimidazoline-2(3H)-thione) (**65**) are similar but not isostructural (Figure 1.21, Table A11).[115]

The irregular tetrahedral geometry around Hg is composed of thione S, one terminal halide and one bridging halide atom. The Hg-S distances in **65** (2.407 Å) are smaller compared to those of **63** (2.435 Å) and **64** (2.510 Å) but in agreement with the sum of covalent radii of tetrahedral Hg and S atoms (2.520 Å).[72] The trend in the Hg-S bond distances decreasing from Br to I is also observed in $\{HgX_2[SCHN(CH_3)_2]_2\}$ (X = Cl, Br and I).[116] The terminal Hg-X distances are much shorter than the bridging Hg-X distances with the least difference observed in **64**. The largest angle around Hg is S-Hg-X_{ter}, which is smaller in **64** compared to **63** and **65** indicating a more distorted tetrahedral geometry around Hg. In **64** the weak Hg-Br interaction as well as large S-Hg-Br angle involving terminal Br atom gives rise to a characteristic five coordinate trigonal bipyramidal geometry around Hg. Such Hg-Br interactions are not observed in **63** despite having a similar structure. Weak hydrogen bonding is also observed in **63** and **65** involving N, halide and S atoms. In **64**, the short Hg-I contacts give rise to longer N---I distances (3.900 Å), which are too long to be considered as hydrogen bonding.

The dinuclear compounds $[Hg(Am4DM)X]_2$ (X = Cl (**66**) and Br(**67**)) are isostructural with pentacoordinate Hg surrounded by X, two N, one S atom of thiosemicarbazone and one more S from a neighboring molecule (Figure 1.21, Table 1.11).[111] The geometry around Hg in **66** and **67** is close to square pyramidal. The Hg-S and Hg-N distances are variable in both compounds with the longer Hg-S present in the five-membered ring and the shorter ones in the four-membered ring. The angles involving the Am4DM ligand are very similar with a small difference in the mean plane

angles between pyridine ring and thiosemicarbazide. However, the donor atoms defining the geometry around Hg deviate considerably from coplanarity.

The compound $[Hg(C_4H_4N_2S)(C_4H_3N_2S)]_2[HgBr_4]$ (**68**) consists of a complex cation and $[HgBr_4]^{2-}$ anion (Figure 1.22).[117] The Hg atom in the cation is coordinated to S atoms in a linear fashion and weakly coordinated to N and Br atoms (effective coordination = [2 + 4]). The secondary contacts are responsible for elongated Hg-S distances (2.357 Å), which are longer than the sum of covalent radii of two-coordinate Hg and S atoms (2.340 Å).[72] The deviation in the S-Hg-S angle from linearity is related to the presence of secondary contacts as observed in four coordinate **50** and **51**.[99] One of the two ligands in the cation is protonated and is responsible for NH---N hydrogen bonding to obtain an infinite chain.

1.3.3 Tetranuclear Compounds

The only known reported tetranuclear Hg-thiolate involving both S and N covalent bonding is $[Hg_4\{SCH_2CH_2N(CH_3)_2\}_4Cl_4]$ (**69**), where two independent Hg atoms are observed.[49] Hg1 is coordinated to 2S and 2N atoms, whereas Hg2 is attached to 2S and 2Cl atoms, both in a distorted tetrahedral geometry (Figure 1.23). The Hg1-S distances (avg 2.414 Å) are symmetrical, however some difference is observed in the Hg1-N distances (2.464 and 2.506 Å). The bridging Hg-S distances (2.487 and 2.504 Å) are also variable but in agreement with the bridging distances observed in $[Hg_4(S\text{-}^tBu)_4(Py)_2Cl_4]$ (avg 2.469 Å).[118]

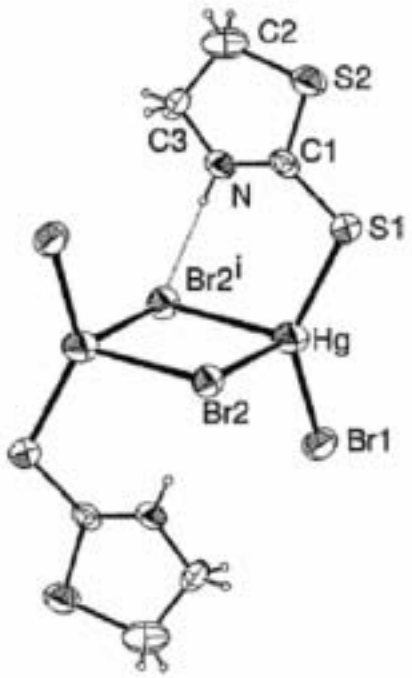
C2
S2
C3
C1
N
S1
Br2i
Hg
Br2
Br1

(63)

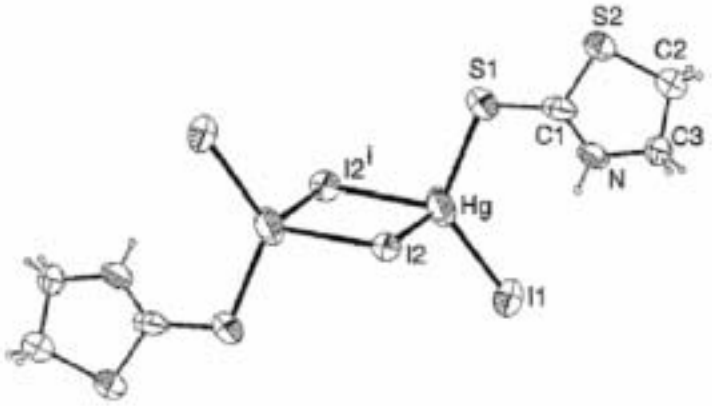
S2
C2
S1
C1
C3
N
I2i
Hg
I2
I1

(64)

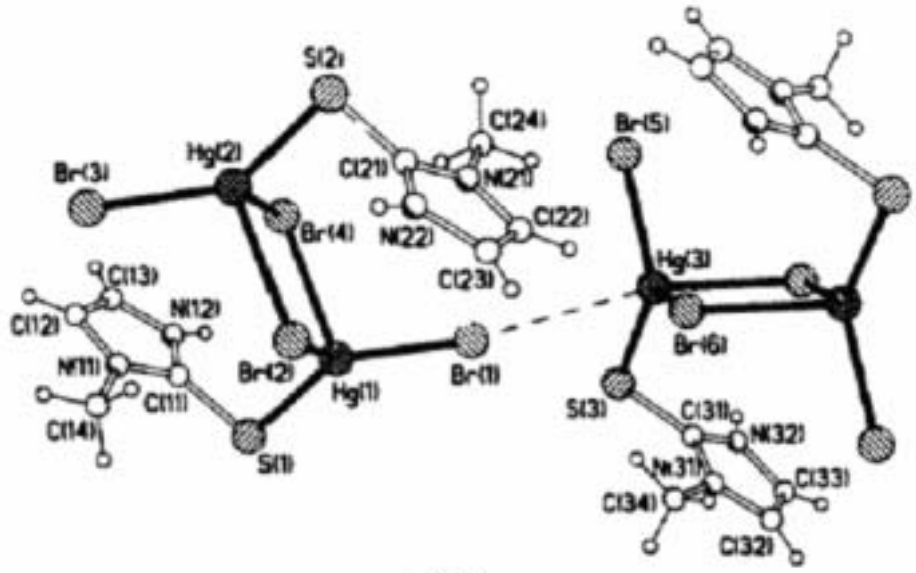
S(2)
C(24)
Br(5)
Hg(2)
Br(3)
C(21)
N(21)
Br(4)
N(22)
C(22)
C(23)
Hg(3)
C(13)
N(12)
C(12)
Br(6)
N(11)
Br(2)
Hg(1)
Br(1)
C(11)
S(3)
C(31)
C(14)
N(32)
S(1)
N(31)
C(33)
C(34)
C(32)

(65)

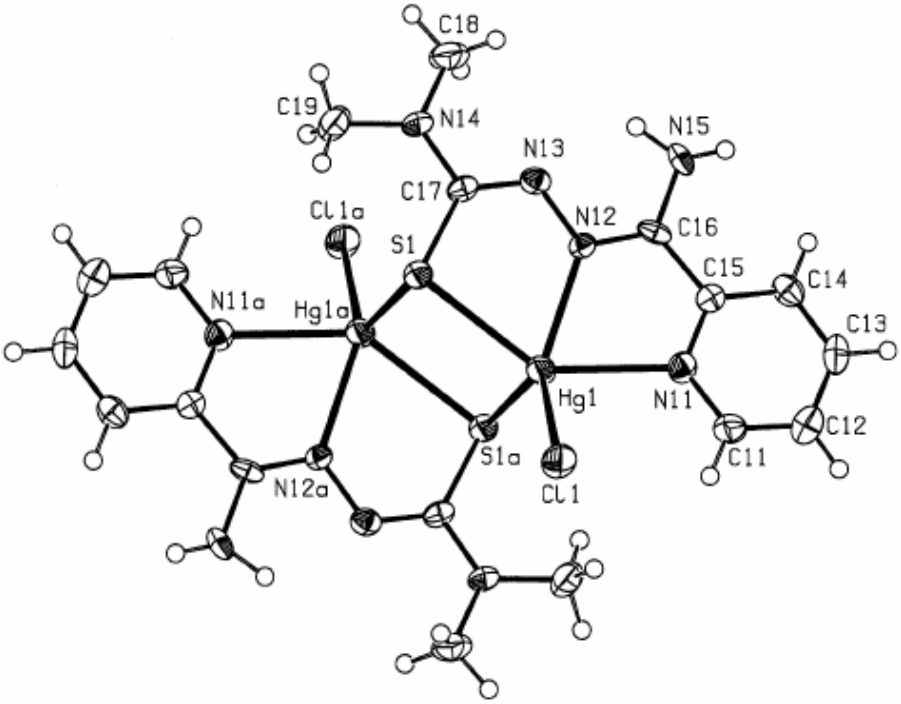

(**66**)

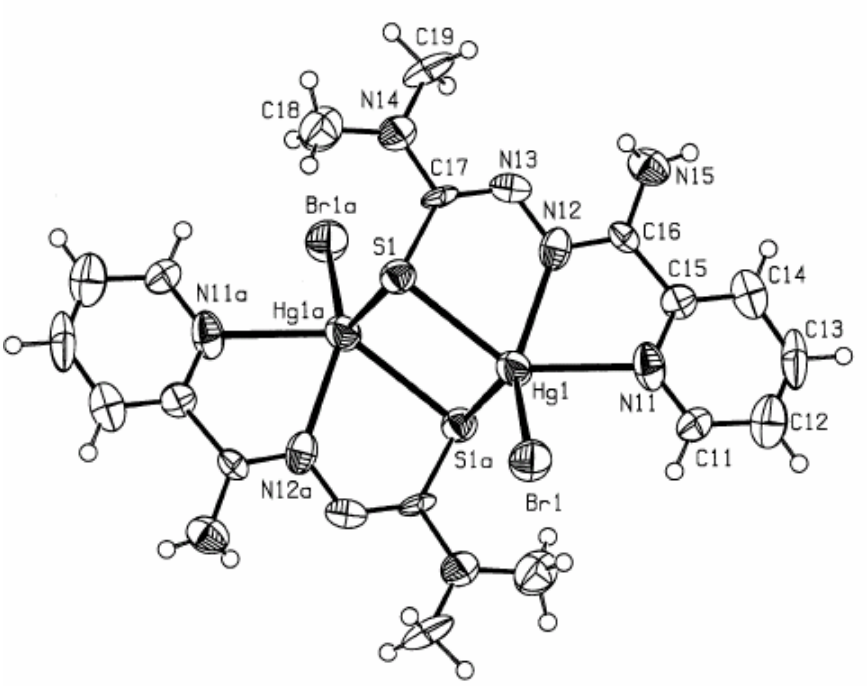

(**67**)

Figure 1.21. Molecular structures of **63 - 67**.

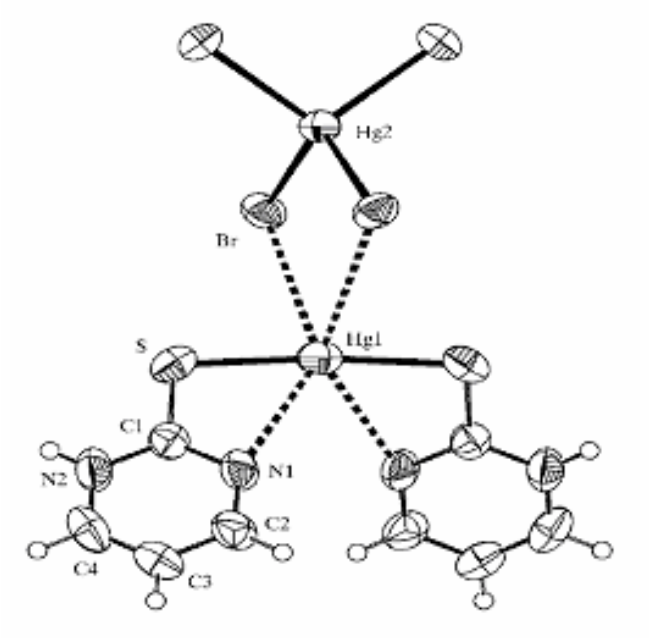

Figure 1.22. Structure of $[Hg(C_4H_4N_2S)(C_4H_3N_2S)]_2[HgBr_4]$ (**68**).[117]

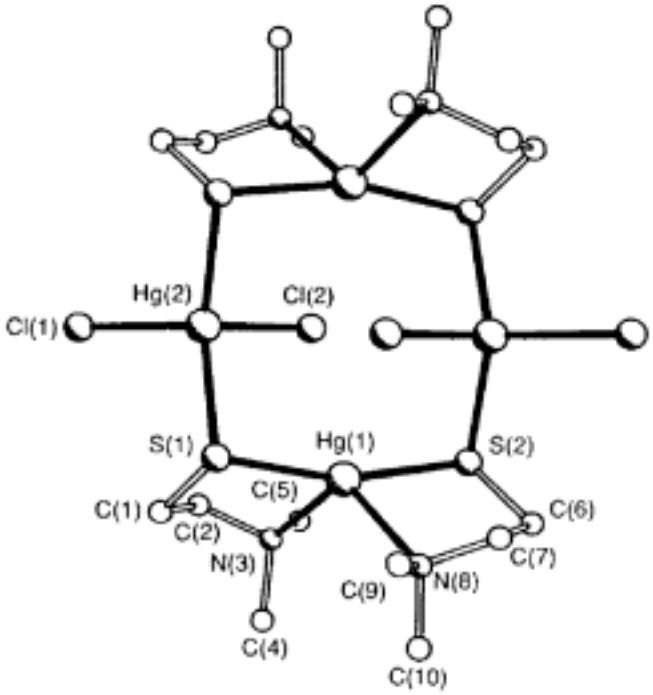

Figure 1.23. View of $[Hg_4\{S(CH_2)_2N(CH_3)_2\}_4Cl_4]$ (**69**).[49]

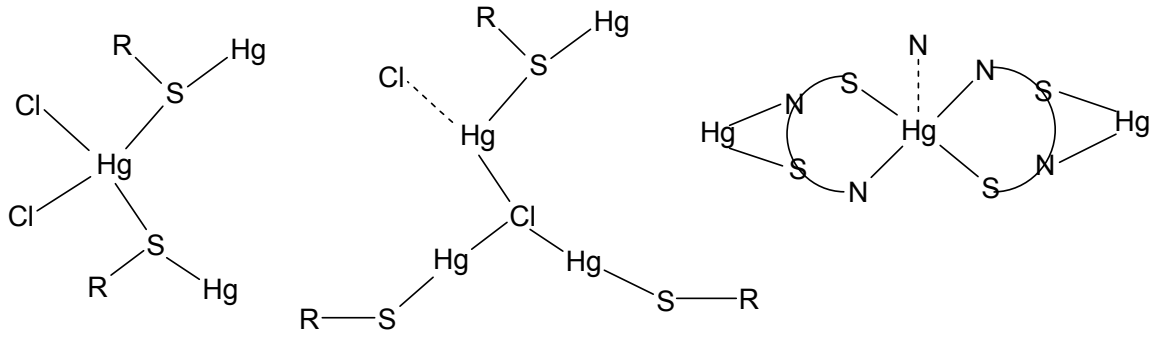

(**70**) (**71**, **72**) (**73**, **74**)

Figure 1.24. Repeating units observed in **70** - **74**, where SR = L-cysteine (**70**), D-penicillamine (**71**), 3-dimethylamino-1-propanethiol (**72**), 1-methyl-1,3-imidazole-2-thione (**73**) and 4,6-dimethylpyrimidine-2-thiolate (**74**).

The terminal Hg-Cl distances (2.506 and 2.648 Å) are smaller than those observed in $[Hg_4(S\text{-}^tBu)_4(picoline)_2Cl_4]$ (2.755 Å) indicating a stronger bond. The distortion around Hg1 is evident with the chelate angles associated with S-Hg-N (81 and 83º), whereas the smallest angles around Hg2 are Cl-Hg-S (105 and 101º).

1.3.4 Polynuclear Compounds

The 1:1 reaction of Hg(II) with simple thiols usually forms polymeric structures, where the structure consists of $(\text{-Hg-S-})_n$ chains and occasionally through bridging halide or acetate. The general polymeric formula can be presented as $[Hg(SR)L_x]_n$ (X = 1 - 3 and L = acetate, halide and/or pyridine base). For instance simple thiols such as L-cysteine, D-penicillamine, 3-dimethylamino-1-propanethiol yield polymeric $[HgCl_2(L\text{-}Cys)_2]$ (**70**),[92] $2[(\mu_3\text{-}Cl)\{HgSC(CH_3)_2CH(NH_3)COO\}_3]\cdot(\mu_2\text{-}Cl)\cdot 2(H_3O)\cdot(H_2O\cdot Cl)_3$ (**71**)[119] and $[HgCl_2\{\mu\text{-}S(CH_2)_3NH(CH_3)_2\}]$ (**72**), respectively (Table A12).[88] However, larger ligands yield unusual structures (Figure 1.24) as observed in $[Hg(meimt)_2]_n$ (**73**) (meimt = 1-methyl-1,3-imidazole-2-thione) [99] and [Hg(4,6-dimethylpyrimidine-2-thiolate)] (**74**).[120]

Bridging Hg-S and Hg-Cl in **70** and **72** and weak Hg-N contacts in **73** and **74** are responsible for the polymeric structure. The repeating unit of **72** is unusual as it contains a triply bridged Cl joining the individual units together. The Hg-S distances in **70** and **72** are similar but longer than those in **71**. The short Hg-S and Hg-Cl distances in the latter might be due to the presence of the triply bridged Cl with overall coordination around Hg as [2 + 1]. The geometry around Hg in **70** - **72** is distorted tetrahedral, where the distortion around Hg, well evident in the S-Hg-S angle can be related to the number of

secondary contacts. In contrast to **70** - **72**, the polymeric chain in **73** is connected through both S and N atoms giving rise to $[Hg(S/N)]_n$ repeating units. The Hg is coordinated to two S atoms with the Hg-S distances intermediate between linear and tetrahedral Hg-thiolates. This might be due to the presence of longer Hg-N contacts. These distances are, however, comparable to Hg-thiolates with additional N donor ligands such as $[Hg(terpy)_2]^{2+}$ (avg Hg-N = 2.270 - 2.530 Å) (terpy = 2,2':6',2'-terpyridine).[121]

In **74**, the repeating unit consists of Hg attached to pyrimidinethiol in a linear fashion (169º) with equidistant S atoms from Hg (2.330 Å). However, the presence of a weak Hg-N bond from pyrimidinethiol and one of the ring N atoms give rise to a distorted trigonal pyramidal geometry. The N atoms are present in equatorial positions and S atoms in apical positions. The Hg-N distances are longer than those observed in **73** as well as the sum of covalent radii of the atoms involved (2.310 Å).[72] These distances are somewhat shorter than the van der Waals radii of Hg and N (3.230 Å).[72] Of the two ligands, one behaves as a bidentate chelate with S and N atoms and the other as a tridentate chelate with S and two azomethine N atoms. Hence, the whole structure consists of alternate bidentate and tridentate ligands around Hg.

1.4 Conclusion

In Cd(II)-thiolates containing S/N ligands the coordination number around mononuclear compounds (**1** - **12**) is variable (4 to 6). The Cd is either distorted tetrahedral or distorted octahedral with a coordination environment consisting of S, N, halides and counter anions. The Cd-S distances increase with the increase of coordination number around Cd. This trend is not observed for the Cd-N distances. The Cd-X distances are variable with the largest difference observed in the I derivatives (**4** and **7**). The distortion around Cd is mainly due to the presence of chelate angles as well as the planarity of the backbone. Bridging thiolates as well as halides in a few cases (**16** and **18**) are mainly responsible for the formation of polynuclear structures. It was observed that excess thiol reacts with **17** to form **18.** This observation could not be made in the Hg derivatives.

In contrast to Cd(II)-thiolates, the Pb geometry in Pb(II)-thiolates is variable with coordination numbers ranging from two (**27**) to nine (**39**). This is due to the presence of a lone pair and empty p-orbitals on Pb. The Pb environment consists of S, N, halides and weak interactions with the counter anions. The Pb-S distances are variable depending on the coordination number. In some cases (**31** and **32**) Pb-N distances are almost similar. Bridging S and halides are responsible for the formation of polynuclear compounds, although weak Pb---S and Pb---N interactions are also observed in **42**. It was reported that for simple S/N ligands, the final product depends on the stoichiometry of the reactants as well as the reaction conditions. For instance, a similar reaction yielded mononuclear **29** as well as trinuclear **42**. The compounds with weak Pb---S interactions are shown to dissociate partially in solution to Pb(II) and thiol ligand.

The diversity in the structural chemistry is more profound in the Hg(II)-thiolates. This is due to the ease of formation of bridging thiolate S and halide in Hg compared to either Cd or Pb. Mononuclear Hg(II)-thiolates are rare, however, steric effects due to the bulky backbone on the thiols are responsible for the formation of such compounds (**44** - **47**). The geometry around Hg in mononuclear thiolates is distorted tetrahedral with coordination environments consisting of S, N and halide atoms. However, depending on the ligand environment five-coordinate Hg can also be observed as in **58** - **62**. In **58**, due to the presence of weak Hg---N the effective coordination around Hg can be considered as 5 [3 + 2].

Bridging halides as well as thiolates are responsible for the formation of polynuclear compounds (**63** - **73**), however additional Hg-N interactions in **74** instead of Hg-X is responsible for the polynuclear structure. Compound **69** is the only reported tetranuclear heteroleptic Hg(II)-thiolate, where two independent Hg centers are observed. This might be due to the presence of a more simple S/N ligand. The Hg-S distances in heteroleptic thiolates increases with the increase in coordination number around Hg as well as with the increase in the size of halide. The Hg-X distances as well as X-Hg-X angles increase as the covalent radius of the halide increases. The distortion around four-coordinate Hg increases with the increase in the size of halide (**50** - **57**).

Weak intermolecular interactions involving S, N and counter anions are observed in Cd(II)-, Pb(II)- and Hg(II)-thiolates containing S/N ligands. These are mostly responsible for the formation of three-dimensional networks.

Chapter 2

Cadmium(II)-2-Aminoethanethiolates

2.1 Overview

Cadmium has been used as a substitute for zinc in metalloproteins as well as in model compounds to study the spectroscopic features of zinc centers because zinc is spectroscopically silent.[122] In addition, the presence of Cd in biological metallothioneins has increased the interest in its coordination chemistry. However, the insolubility of Cd(II)-thiolates ($[Cd(SR)_2]_n$) in common solvents has limited their study. However, Cd(II)-thiolates with an additional donor atom including N and O are much more soluble and they also can be used as models for $[Zn(S\text{-}cys)_2(His)_2]$ sites in zinc-finger proteins.[123] Similar studies have been conducted with naturally occurring amino acids (cysteine, glycine, serine, histidine, ornithine, aspartate and glutamate) or biological model ligands such as 2-aminoethanethiol (AET).[26]

This chapter will discuss the reactions of Cd(II) salts with AET in various stoichiometries and the resulting compounds will be characterized with IR/Raman, solution NMR and X-ray crystallography.

2.2 Synthesis and Characterization

2-aminoethanethiol hydrochloride (AET·HCl) and CdX_2 (X = Cl, Br, I, acetate, NO_3) were combined in various stoichiometric amounts in deionized (DI) water to obtain white precipitates of **75** - **84** in quantitative yields (Scheme 2.1). The melting temperatures of **75** - **84** are in the range 150 - 260 ºC, however compounds **76**, **79** and **80** decompose without melting.

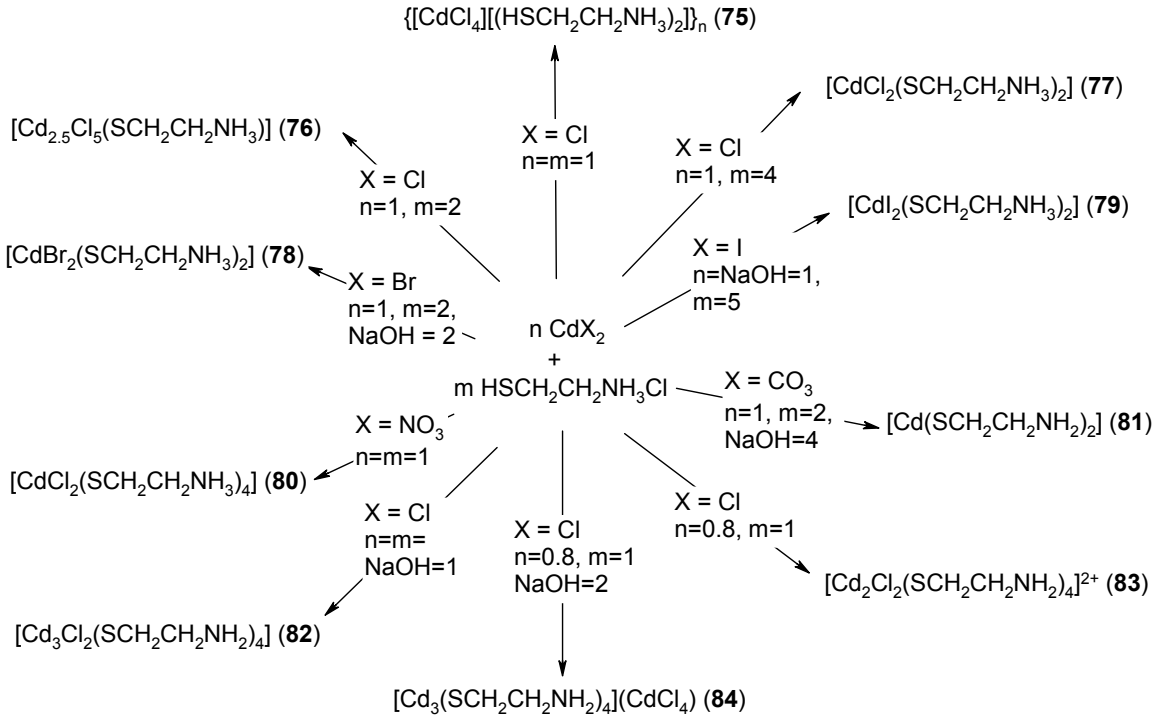

Scheme 2.1. Synthesis of compounds **75** - **84**. In **83**, HCl from AET·HCl was removed using equivalent amount of NaOH prior to the addition of $CdCl_2$.

2.2.1 Spectroscopy

In the ^{1}H and ^{13}C NMR spectra of this series of compounds, a significant shift is observed for the methylene protons and the C atom of the CH_2 groups attached to S in **78** - **84**. Compared to the spectra of the free ligand these shifts indicate the presence of a direct Cd-S contact. Despite similar reaction conditions a Cd-S bond is not observed in **75**, which is most probably due to the presence of excess Cl anions. Similarly, no significant shifts in the CH_2 protons and C attached to N in **75** - **80** and **84** indicate the presence of an ammonium group (Table 2.1).

In the IR spectrum the absence of a -SH peak around 2500 - 2550 cm^{-1} in **76** - **84** confirms covalent Cd-S bonds. In **75** - **80** and **84**, peaks at 3200 - 3300 cm^{-1} (symmetric stretching) indicate an ammonium group. The N-H scissoring and wagging modes for all the compounds is observed around 1500 - 1650 and 660 - 900 cm^{-1}, respectively. In the Raman spectrum, the Cd-S stretch for **76** - **84** is observed between 150 - 190 cm^{-1}. For **81** - **83**, peaks observed around 340 cm^{-1} can be assigned to the Cd-N bonds. In **75** - **84**, except **78**, **79** and **81,** the stretches at ≈ 220 cm^{-1} can be assigned to the Cd-Cl bond. In **78** and **79** the peaks due to Cd-Br and Cd-I are observed at much lower wavelength (180 and 140 cm^{-1}, respectively) due to the presence of the heavier halide atoms. These values are comparable to those reported in the literature for homo- and heteroleptic Cd(II)-thiolates.[124-127] In the ^{113}Cd NMR spectra of **75** a broad peak for six- coordinate Cd is observed at 285 ppm compared to external 0.1 M $Cd(NO_3)_2$.[128] Suitable peaks in the ^{113}Cd spectra for **76** - **81** could not be obtained employing similar experimental conditions. However, in **82** - **84**, a broad peaks are observed between 450 - 520 ppm, which are comparable to Cd(II)-thiolates containing S/N chelate.[129]

Table. 2.1. ^{1}H and ^{13}C NMR shifts (in ppm) for AET·HCl in D_2O and **75** - **84** in d_6-DMSO.

	^{1}H			^{13}C	
Compound	SCH_2	NCH_2	NH_2/NH_3*	C-S	C-N
AET·HCl	2.99	2.69	-	22.2	42.8
75	2.95	2.69	7.71	21.3	41.8
76	3.14	2.69	7.75	33.9	43.1
77	2.74	2.63	-	27.7	42.9
78	2.74	2.66	-	28.0	42.7
79	2.74	2.66	-	29.0	42.5
80	2.92	2.67	-	24.6	43.2
81	3.01	2.73	-	28.2	44.02
82	2.85	2.73	-	28.1	42.9
83	2.97	2.73	-	28.2	42.7
84	2.90	2.69	-	24.4	43.2

*NH_2/NH_3 peaks are not observed in the ^{1}H spectrum of most of the compounds.

Based on the stoichiometry of the reactants and spectral data the following structures are proposed for **75**, **77** - **80** and **82** - **84** (Figure 2.1). In most of the cases the Cd is hexacoordinate with halide and thiolate ligands. In the presence of excess Cl^- and no base in the solution (OH^-), coordination around Cd is completed by only Cl atoms as observed in **75**. This is also evident from the absence of Cd-S and Cd-N peaks in the Raman spectrum along with no significant shifts observed in NMR. However, in the presence of base but in the absence of a Cd-N bond, the coordination around Cd is completed by thiolate ligand and halide atoms. In **84**, due to the presence of excess base in the solution a Cd-Cl bond is not likely. However, a peak due to Cd-Cl in Raman spectrum can possibly be attributed to a $[CdCl_4]^{2-}$ unit. A similar structure to that of **84** has been proposed earlier, however only magnetic properties were studied.[130] The additional Cd-N bond in **81**, **82** - **84** can be attributed to the use of excess base in the reaction.

2.2.2 Crystal Structures

The crystals for **75**, **76** and **81** were obtained either from supernatant cooled to 4 °C or by recrystallization of the precipitates from hot water. The crystal structure of **75** could not be resolved due to the disorder present in the AET groups. All the attempts to crystallize **77** - **80** and **82** - **84** failed, despite the use of a variety of solvents such as water, ethanol, dimethyl sulfoxide, and pyridine as well as mixtures of different solvents. Compound **76** has three-dimensional connectivity indicative of a solid-state material but it is nevertheless soluble in common solvents, which qualifies it as a "molecular solid".[131]

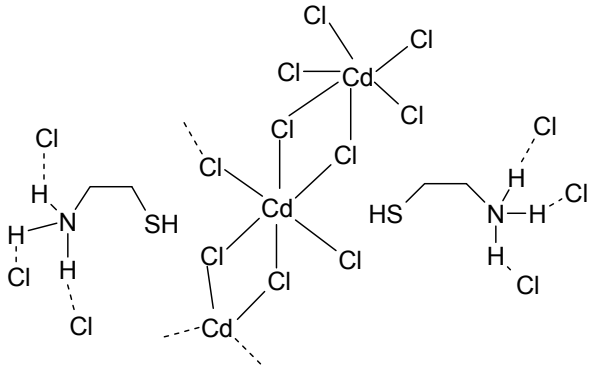

(**75**)

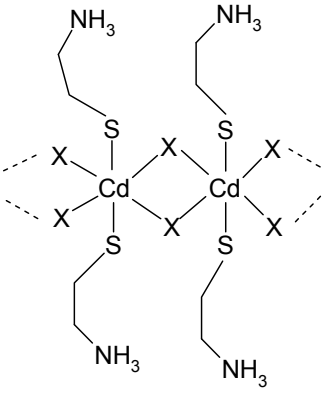

77 (X = Cl), **78** (X = Br), **79** (X = I)

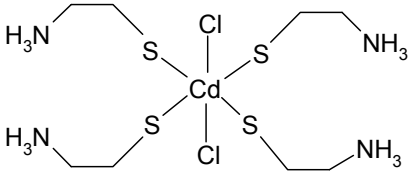

(**80**)

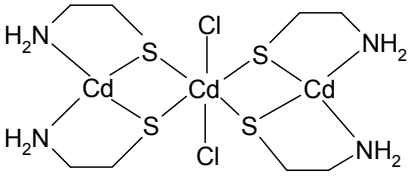

(**82**)

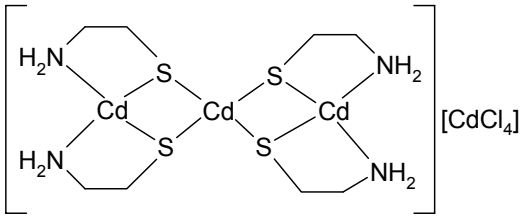

(**83**)

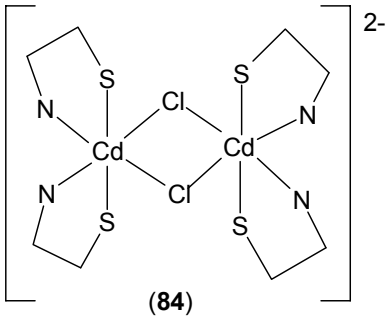

(**84**)

Figure 2.1. The proposed structures of **75**, **77** - **80** and **82** - **84**.

The structure contains layers of repeating (Cd(Cl)SR) units perpendicular to each other (Figure 2.2, Table A13) and comprised of alternate opposite open cores of hexacoordinate Cd with Cl and S present at the corners.

A similar polymeric chain with hexacoordinate Cd atoms is also observed in $[Cd_2(5\text{-}CF_3\text{-}pyS)_4(DMF)]_n$, where the coordination is completed by S, N of the ligand and the solvent, DMF.[132] However, in **76** the coordination around Cd is completed by S and Cl atoms to achieve an octahedral geometry. A repeating pattern is observed in the units consisting of $[Cd(S_2Cl_4)]$, $[Cd(SCl_5)]$, $[Cd(S_2Cl_4)]$ and so on. One of the Cd atoms is coordinated to two S and four Cl with two bridging Cl atoms. However, the second Cd is bonded to one S and five Cl atoms with one terminal Cl atom. The Cd-S distances are variable in the different units with similar distances observed associated with first and third Cd atoms (avg 2.498 Å). On the other hand, the Cd-S distance associated with the second Cd is longer (2.601 Å). These distances are in accord with those reported for similar polymeric Cd(II)-thiolates (**20** - **23**).[133]

Variations in the Cd-Cl distances are also observed for terminal and bridging Cl atoms. The $Cd\text{-}Cl_{ter}$ distances are shorter (avg 2.808 Å) compared to the $Cd\text{-}Cl_{br}$ distances (avg 2.920 Å). These distances are in contrast to the terminal and bridging Cd-Cl distances observed in $[Cd_2Cl_4(C_{14}H_{23}N_4OPS)_2]$ ($Cd\text{-}Cl_{br}$ = 2.644 and $Cd\text{-}Cl_{ter}$ = 2.387 Å).[134]

The S-Cd-S angles in **76** are almost linear (avg 178º) due to the presence of a regular structure, in contrast to the corresponding angle observed in $[CdBr_2(C_5H_{13}NS)]$ (126.9º).[133] The octahedral geometry around Cd consists of linear and perpendicular Cl-Cd-Cl angles (167 - 180º and 90º). In $[Cd_2Cl_4(C_{14}H_{23}N_4OPS)_2]$, the distortion around Cd

is evident with Cl-Cd-Cl angles ranging from 89 - 112º.[134] The amine units are oriented away from the core with an N1-C2-C1 angle of 112º, which will reduce any steric interactions. These groups are, however, involved in intermolecular hydrogen bonding with Cl from adjacent units. Similar interactions have been observed for Cd(II)-thiolates containing S/N ligands, where the ammonium groups are involved in intermolecular hydrogen-bonding with halide from adjacent molecules.[133]

Compound **81** consists of discrete $[Cd(SCH_2CH_2NH_2)_2]$ molecules (Figure 2.3, Table A14) that are linked through intermolecular hydrogen bonds. The Cd is pentacoordinate, bonded to three S and two N atoms in a distorted square pyramidal geometry. The absence of halide attached to the Cd could be attributed to the presence of excess base in solution. In the dimeric unit the two Cd atoms are related by a center of inversion. One of the ligands acts as a terminal chelating unit, while the other chelate is also involved in bridging. The Cd_2S_2 core is nearly planar with average internal angles close to 90º. The Cd-S distances vary from 2.492 – 2.735 Å for axial and equatorial chelates as well as for the central core. These distances are, however, comparable to similar S-bridged Cd(II)-thiolates (2.537-2.713 Å) as well as those containing an S/N chelate (2.466- 2.673 Å).[133-135] The Cd-N distances are variable in the four- (2.308 Å) and five-membered rings (2.436 Å) but comparable to corresponding distances in similar compounds.[134-137] The Cd-S1 distance is larger than Cd-S2 whereas Cd-N1 is smaller than Cd-N2 implying stronger Cd-S bonding in the axial position. This trend is also observed in $[Cd(3\text{-}CF_3\text{-}pyS)_2(DMF)_2]$ containing distorted octahedral Cd.[132]

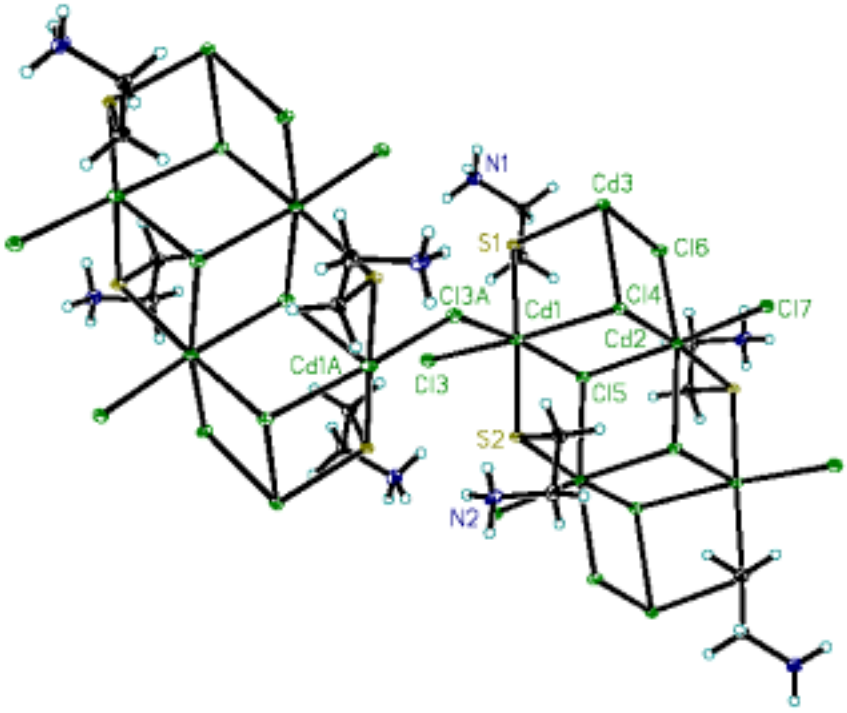

Figure 2.2. View of **76** with 50 % thermal ellipsoids.

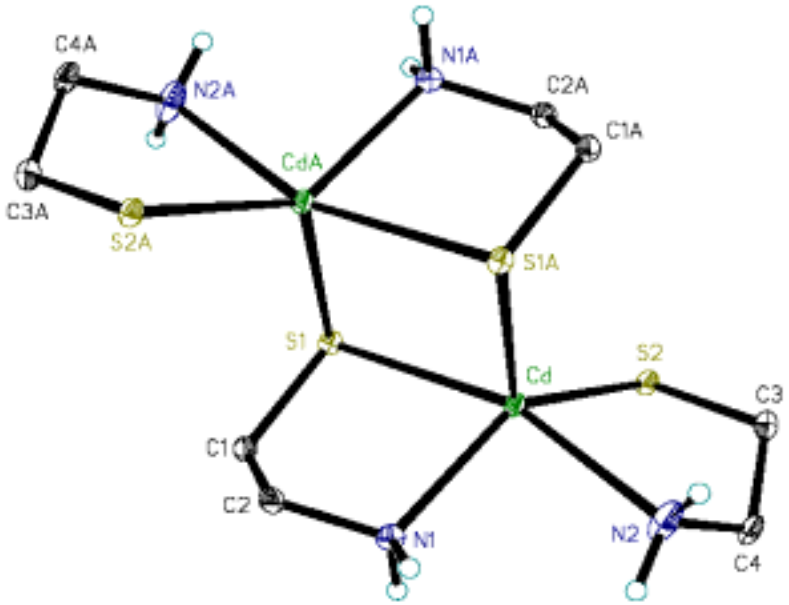

Figure 2.3. Molecular structure of **81**.

The aminoethanethiol units in axial and equatorial positions are neither perpendicular nor parallel to each other (N(1)-Cd-S(1)', 101.8 and C(1)-S(1)-Cd(1)', 102.9º). This deformity is due to the interaction of the S and N atoms with the amine hydrogens from adjacent units.

2.3 Experimental Section

All the reactions were carried out at room temperature in deionized water. The reagents $CdCl_2$, $CdBr_2$, CdI_2, $CdCO_3$, $Cd(NO_3)_2$ (J. T. Baker) and 2-aminoethanethiol hydrochloride (TCI America) were used as received. The NMR (^1H and ^{13}C) data were obtained with JEOL-GSX-400 and 270 instruments operating at 199.17 and 399.78 MHz using d^6-DMSO and D_2O as solvent, with tetramethylsilane as the reference. ^{113}Cd NMR spectra of 0.5 - 0.1M **82** - **84** in d_6-DMSO were collected at 25 ºC on a varian INOV 400 MHz instrument with 4-nucleus Autoswitchable 5mm Probe and referenced to external 0.1 M $Cd(NO_3)_2$ at zero ppm.[128] IR data were recorded as KBr pellets on a Matheson Instrument 2020 Galaxy Series spectrometer and are reported in cm^{-1}. Raman spectra were obtained on a Nicolet FT-Raman 906 Spectrometer ESP between 100 - 800 cm^{-1} in the Center for Applied Energy Research at the University of Kentucky. Mass Spectral data were obtained from the University of Kentucky Mass Spectrometry Facility. X-ray data for **75, 76** and **81** were collected on a Nonius Kappa-CCD unit using Mo-Kα radiation from colorless regular shaped crystals.

Synthesis of $\{[CdCl_4][(HSCH_2CH_2NH_3)_2]\}_n$ (75): Cadmium (II) chloride (2.28 g, 10.0 mmol) was stirred in deionized water (50.0 mL) and to this AET·HCl (1.14 g, 10.0 mmol)

dissolved in DI water (20.0 mL) was added. The resulting mixture was stirred for 3 days. A white amorphous precipitate was isolatec by filteration and washed with water and methanol and dried. The filtrate was reduced in volume and allowed to stand in the refrigerator at 4 ºC, causing needle shaped colorless crystals to form. Yield (crystal + precipitate): 3.10 g (75.0 %). Mp: 262 - 264 ºC. ^{1}H NMR (d_6-DMSO, 200 MHz, ppm): δ 2.69 (t, 2H, CH_2N), δ 2.95 (t, 2H, CH_2S), δ 3.17 (s, 1H, SH), δ 7.71 (b, 3H, NH_3). ^{13}C NMR (d_6-DMSO, 200 MHz, ppm): δ 21.3 (CH_2S), δ 41.8 (CH_2N). IR (KBr, ν/cm^{-1}): 461, 659 (C-S), 1235 (C-N, stretching), 1265, 1324, 1471 (S-CH_2), 1568 (-NH_2 and N-H, bending), 2885 - 3007 (symmetric NH_3^+ stretch), 3141 (NH_3^+). HRMS (EI, positive): 415 $(M)^+$, 410 $(M - CH_3)^+$, 355 $([CdCl_6][CH_2NH_3])^+$, 327 $(CdCl_6)^+$, 289 $(CdCl_5)^+$, 251 $(CdCl_4)^+$, 149 $(CdCl)^+$, 77 $(SCH_2CH_2NH_3)^+$.

Synthesis of $[Cd_{2.5}Cl_5(SCH_2CH_2NH_3)]$ (76): Cadmium (II) chloride (1.14 g, 5.00 mmol) was added to a stirring solution of AET·HCl (1.14 g, 10.0 mmol) in deionized water (20.0 mL) and the resulting mixture was stirred over 3 days. The resulting solution was reduced in volume and allowed to stand in the refrigerator at 4 ºC, which formed cubic shaped colorless crystals. Yield: 0.290 g (10.0 %). Mp: 222 - 224 ºC (dec). ^{1}H NMR (d_6-DMSO, 200 MHz, ppm): δ 2.69 (t, 2H, CH_2N), δ 3.14 (t, 2H, CH_2S), δ 7.75 (s, 3H, NH_3). ^{13}C NMR (d_6-DMSO, 200 MHz, ppm): δ 33.9 (CH_2S), δ 43.1 (CH_2N). IR (KBr, ν/cm^{-1}): 657 (C-S), 1230 (C-N, stretching), 1258, 1320, 1376, 1427 (S-CH_2), 1491, 1561, 1583 (-NH_2 and N-H, bending), 2361, 2938, 3130 (NH_3^+), 3450 (R-NH_2, stretching). HRMS (EI, positive): 247 $(M + 2)^+$, 171 $(M - SCH_2CH_2NH_2)^+$, 92 $(M - 2(SCH_2CH_2NH_2)^+$, 77

$(SCH_2CH_2NH_3)^+$. Anal. Calcd for $C_4H_{14}N_2S_2Cl_5Cd_{2.5}$: C, 7.84; H, 2.30; N, 4.57; S, 10.47. Found: C, 7.65; H, 2.20; N, 4.55; S, 10.43

Synthesis of $[CdCl_2(SCH_2CH_2NH_3)_2]$ (77): AET·HCl (1.14 g, 10.0 mmol) and sodium hydroxide (0.400 g, 10.0 mmol) was dissolved in DI water (40.0 mL) and to this cadmium (II) chloride (1.14 g, 5.00 mmol) dissolved in water (20.0 mL) was added and stirred for 2 days. The resulting white precipitate was filtered, washed with water and methanol and dried. Yield (precipitate): 0.600 g (75.0 %). Mp: 166 - 168 ºC. ^{1}H NMR (d_6-DMSO, 200 MHz, ppm): δ 2.63 (t, 2H, CH_2N), δ 2.74 (t, 2H, CH_2S). ^{13}C NMR (d_6-DMSO, 200 MHz, ppm): δ 27.7 (CH_2S), δ 42.9 (CH_2N). IR/Raman (ν/cm^{-1}): 189 (Cd-S), 220 (Cd-Cl), 466, 668 (C-S), 1234 (C-N), 1285, 1467, 1581 (NH_2, scissoring), 2882 - 2981 (symmetric NH_3^+ stretch), 3227 (NH_2, symmetric stretch). HRMS (EI, positive): 406 $(CdCl_4(SCH_2CH_2NH_3)_2)^+$, 369 (406 - Cl)$^+$, 301 (406 - 3Cl)$^+$, 267 $(Cd(SCH_2CH_2NH_3)_2)^+$, 232 $((Cd(SCH_2CH_2)_2)^+$, 206 $(Cd(SCH_2)_2)^+$, 189 $(Cd(SCH_2CH_2NH_3))^+$, 146 $(CdCl)^+$, 77 $(SCH_2CH_2NH_3)^+$.

Synthesis of $[CdBr_2(SCH_2CH_2NH_3)_2]$ (78): AET·HCl (1.14 g, 10.0 mmol) and sodium hydroxide (0.400 g, 10.0 mmol) was dissolved in DI water (40.0 mL) and to this cadmium (II) bromide (1.72 g, 5.00 mmol) dissolved in water (20.0 mL) was added and stirred for 2 days. The resulting white precipitate was filtered and washed with water and methanol and dried. Yield (precipitate): 1.80 g (84.0 %). Mp: 160 - 162 ºC. ^{1}H NMR (d_6-DMSO, 200 MHz, ppm): δ 2.66 (t, 2H, CH_2N), δ 2.74 (t, 2H, CH_2S). ^{13}C NMR (d_6-DMSO, 200 MHz, ppm): δ 28.0 (CH_2S), δ 42.7 (CH_2N). IR/Raman (KBr, ν/cm^{-1}): 189

(Cd-S or Cd-Br), 466, 655 (C-S), 1229 (C-N), 1579 (NH_2, scissoring), 2873 - 2968 (symmetric NH_3^+ stretch), 3249 (NH_2, stretching). HRMS (EI, positive): 969 $(M + 3)^+$, 901 $(M - 4NH_3)^+$, 873 $(901 - 2CH_2)^+$, 845 $(901 - 4CH_2)^+$, 789 $(Cd_3S_4Br_4)^+$, 269 $(CdBr(SCH_2CH_2NH_3))^+$, 190 $((Cd(SCH_2CH_2NH_3))^+$, 77 $(SCH_2CH_2NH_3)^+$.

Synthesis of $[CdI_2(SCH_2CH_2NH_3)_2]$ (79): AET·HCl (1.14 g, 10.0 mmol) dissolved in DI water (40.0 mL) along with sodium hydroxide (0.400 g, 10.0 mmol) and cadmium (II) iodide (1.83 g, 5.00 mmol) was added and the resulting mixture was stirred for 2 days. The white precipitate was filtered, washed with water and methanol and dried. Yield (precipitate): 1.90 g (73.0 %). Mp: 256 - 258 ºC (dec). ^{1}H NMR (d_6-DMSO, 200 MHz, ppm): δ 2.66 (t, 2H, CH_2N), δ 2.74 (t, 2H, CH_2S). ^{13}C NMR (d_6-DMSO, 200 MHz, ppm): δ 29.0 (CH_2S), δ 42.5 (CH_2N). IR/Raman (KBr, ν/cm^{-1}): 103 (Cd-I), 142 (Cd-S), 358, 457, 660 (C-S), 1221 (C-N), 1376, 1570 (NH_2, scissoring), 2856 - 2964 (symmetric NH_3^+ stretch), 3322 (NH_2, stretching). MS (EI, positive): 646 $(Cd_3(SCH_2CH_2NH_3)_4)^+$, 577 $(M/2)^+$, 567 $(Cd_3S_4C_7H_{18})^+$, 552 $(567 - CH_3)^+$, 537 $(567 - 2CH_3)^+$, 522 $(567 - 3CH_3)^+$, 507 $(567 - 4CH_3)^+$, 492 $(567 - 5CH_3)^+$, 462 $(567 - 7CH_3)^+$, 465 $(Cd_3S_4)^+$, 353 $(465 - Cd)^+$, 240 $(CdS_4)^+$, 129 $(353 - 2Cd)^+$, 77 $(SCH_2CH_2NH_3)^+$.

Synthesis of $[CdCl_2(SCH_2CH_2NH_3)_4]$ (80): AET·HCl (1.14 g, 10.0 mmol) was dissolved in DI water (50.0 mL) and to this cadmium (II) nitrate (3.08 g, 10.0 mmol) was added and the resulting solution was stirred for 2 days. The resulting solution was evaporated at room temperature to obtain white precipitate. Yield (precipitate): 2.40 g (49.0 %). Mp: 250 - 252 ºC (dec without melting). ^{1}H NMR (d_6-DMSO, 200 MHz, ppm):

δ 2.69 (t, 2H, CH_2N), δ 2.90 (t, 2H, CH_2S). ^{13}C NMR (d_6-DMSO, 200 MHz, ppm): δ 24.4 (CH_2S), δ 43.2 (CH_2N). IR/Raman (KBr, ν/cm^{-1}): 116, 185 (Cd-S), 409 (Cd-S-C), 746 (C-S), 1048, 1259 (C-N), 1145, 1580 (NH_2, scissoring), 2942 - 2977 (NH_2). HRMS (EI, positive): 495 $(M + 3)^+$, 457 $(CdCl(SCH_2CH_2NH_3)_4))^+$, 420 $(Cd(SCH_2CH_2NH_3)_4))^+$, 416 $(Cd(SCH_2CH_2NH_3)_4 - 4)^+$, 371 $(416 - CH_2CH_2NH_3)^+$, 327 $(416 - 2CH_2CH_2NH_3)^+$, 281 $(416 - 3CH_2CH_2NH_3)^+$, 241 $(CdS_4)^+$, 77 $(SCH_2CH_2NH_3)^+$.

Synthesis of $[Cd(SCH_2CH_2NH_2)_2]$ (81): To a stirring solution of AET·HCl (1.14 g, 10.0 mmol) in DI water (20.0 mL), sodium hydroxide (0.800 g, 20.0 mmol) was added followed by addition of cadmium carbonate (0.860 g, 5.00 mmol). The resulting mixture was stirred overnight and then filtered to isolate a white precipitate. The X-ray quality colorless crystals were obtained from the supernatant at 4 ºC. Crystalline yield: 0.620 g (47.0 %). Mp: 172 - 174 ºC. ^1H NMR (D_2O, 200 MHz, ppm): δ 2.73 (t, 2H, CH_2N), δ 3.01 (t, 2H, CH_2S). ^{13}C NMR (D_2O, 200 MHz, ppm): δ 28.29 (CH_2S), δ 44.02 (CH_2N). IR (KBr, ν/cm^{-1}): 622-661 (C-S), 1051, 1064, 1120, 1214, 1228 (C-N, stretching), 1423 (S-CH_2), 1580 (-NH_2 and N-H, bending), 3551 (R-NH_2, stretching). HRMS (EI, positive): 266 $(M + 2)^+$, 190 $(M–SCH_2CH_2NH_2)^+$, 114 $(M–2(SCH_2CH_2NH_2))^+$, 76 $(SCH_2CH_2NH_2)^+$. Anal. Calcd for $C_4H_{12}N_2S_2Cd$: C, 18.15; H, 4.57; N, 10.58; S, 24.23. Found: C, 18.00; H, 4.62; N, 10.51; S, 24.05.

Synthesis of $[Cd_3Cl_2(SCH_2CH_2NH_2)_4]$ (82): AET·HCl (1.14 g, 10.0 mmol) and sodium hydroxide (0.400 g, 10.0 mmol) were dissolved in DI water (40.0 mL) and to this cadmium (II) chloride (2.28 g, 10.0 mmol) dissolved in water (20 mL) was added and

stirred for 2 days. The white precipitate obtained was filtered and washed with water and methanol and dried. Yield (precipitate): 1.39 g (20.0 %). Mp: 258 - 260 ºC. ^{1}H NMR (d_6-DMSO, 200 MHz, ppm): δ 2.74 (t, 2H, CH_2N), δ 2.97 (t, 2H, CH_2S), δ 7.45 (s, 2H, NH_2). ^{13}C NMR (d_6-DMSO, 200 MHz, ppm): δ 24.3 (CH_2S), δ 42.8 (CH_2N). IR/Raman (KBr, ν/cm^{-1}): 464, 659 (C-S), 878, 1085, 1262 (C-N, stretching), 1319, 1430, 1469 (S-CH_2), 1557, 1595 (-NH_2 and N-H, bending), 2930, 3129, 3440 (R-NH_2, stretching). HRMS (EI, positive): 641 $(Cd_3(SCH_2CH_2NH_2)_4))^+$, 356 $(M/2)^+$, 300 $(CdCl(SCH_2CH_2NH_2)_2)^+$, 264 $(Cd(SCH_2CH_2NH_2)_2)^+$, 188 $(Cd(SCH_2CH_2NH_2))^+$, 149 $(CdCl)^+$, 78 $(SCH_2CH_2NH_2 + 2)^+$.

Synthesis of $[Cd_3(SCH_2CH_2NH_2)_4](CdCl_4)$ (83): AET·HCl (1.14 g, 10.0 mmol) was dissolved in methanol (20.0 mL) along with sodium hydroxide (0.800 g, 20.0 mmol) and stirred for few hours. The resulting precipitate of NaCl was filtered and the clear solution was evaporated under vacuum to obtain AET. The resulting AET was dissolved in DI water (20.0 mL) and to this cadmium (II) chloride (1.83 g, 8.00 mmol) was added and the resulting mixture was stirred for 2 days. Yield (precipitate): 2.75 g (39.0 %). Mp: 182 - 184 ºC. ^{1}H NMR (d_6-DMSO, 200 MHz, ppm): δ 2.73 (b, 2H, CH_2N), δ 2.97 (b, 2H, CH_2S). ^{13}C NMR (d_6-DMSO, 200 MHz, ppm): δ 28.2 (CH_2S), δ 42.7 (CH_2N). IR/Raman (KBr, ν/cm^{-1}): 120, 189 (Cd-S), 220 (Cd-Cl), 345 (Cd-N), 466, 664, 832 (C-S), 1083, 1238 (C-N), 1290, 1406, 1462 (NH_2, scissoring), 2929 (NH_2), 3257, 3340 (NH_2, stretching). HRMS (EI, positive): 410 $(Cd_2S(SCH_2CH_2NH_2)_2)^+$, 345 $(Cd_2(SCH_2CH_2)_2)^+$, 288 $(Cd_2S_2)^+$, 265 $(Cd(SCH_2CH_2NH_2))^+$, 255 $(CdCl_4)^+$, 224 $(CdCl(SCH_2CH_2NH_2))^+$, 188 $(Cd(SCH_2CH_2NH_2))^+$, 144 $(CdS)^+$, 77 $(SCH_2CH_2NH_2)^+$.

Synthesis of $Na_2[Cd_2Cl_2(SCH_2CH_2NH_2)_4]$ (84): AET·HCl (1.14 g, 10.0 mmol) and sodium hydroxide (0.800 g, 20.0 mmol) was dissolved in DI water and to this cadmium (II) chloride (1.83 g, 8 mmol) was added and stirred for 2 days. The resulting white precipitate was filtered and washed with water and methanol and dried. The white precipitate obtained was filtered and washed with water and methanol and dried. Yield (precipitate): 2.20 g (43.0 %). Mp: 192 - 194 ºC. ^{1}H NMR (d_6-DMSO, 200 MHz, ppm): δ 2.73 (b, 2H, CH_2N), δ 2.85 (b, 2H, CH_2S). ^{13}C NMR (d_6-DMSO, 200 MHz, ppm): δ 28.1 (CH_2S), δ 42.9 (CH_2N). IR/Raman (KBr, ν/cm^{-1}): 181 (Cd-S), 220 (Cd-Cl), 345 (Cd-N), 461, 664 (C-S), 1091, 1238 (C-N, stretching), 1285, 1415, 1471, 2934 (NH_2), 3444 (NH_2, stretching). HRMS (EI, positive): 480 $(Cd_2Cl_2S(SCH_2CH_2NH_2)_2))^+$, 296 $(CdS(SCH_2CH_2NH_2)_2))^+$, 255 $(CdCl(SCH_2CH_2NH_2))^+$, 226 $(CdSCl(SCH2))^+$, 204 $(CdS(SCH_2CH_2))^+$, 181 $(CdSCl)^+$, 172 $(Cd(SCH_2CH_2))^+$, 154 $(Cd(SCH_2))^+$, 76 $(SCH_2CH_2NH_2)^+$.

2.4 Conclusion

Novel Cd(II)-thiolates have been synthesized and characterized with NMR, IR/Raman and X-ray crystallography for **76** and **81**. Although the reactions have been carried out following similar procedures, the compounds obtained present different stoichiometries and variable geometries. However, the structural chemistry of Cd can be predicted according to the reaction conditions. For instance, a Cd-S bond is observed in all cases except **75**. The absence of Cd-S in **75** can be attributed to excess Cl^-. The Cd is hexa-coordinated surrounded with six Cl atoms, which are further involved in bridging with other Cd atoms to form a three-dimensional network. Compound **76** is closely related to **75**, where two Cl are replaced with thiol groups. The network in **76** is further extended with intermolecular hydrogen bonding involving ammonium groups and Cl atoms. A Cd-N bond is observed in the compounds when the base/Cd^{2+} ratio is greater than 2. Compounds **81** and **84** are dinuclear with both bridging S and Cl atoms. Compounds **82** and **83** are trinuclear with the central Cd attached to four S and two Cl atoms.

In **20** and **23** bridging thiolates are responsible for the polymeric structure as observed in **76**, and the bridging halides are also responsible for three-dimensional network. The coordination environment around Cd in **76** consisting of S and halide is regular compared to those around Cd observed in **20** - **23,** where S and N atoms are observed. The five-membered S/N chelate is not observed in **76** in contrast to **20** - **23** due to the presence of ammonium groups. However a S/N coordination mode is observed in **81**, where the Cd atoms are four- and five-coordinate in contrast to that observed in **13**, where the Cd atoms are five-coordinate with bridging thiolates. The Cd-S distances in the

S/N chelate in **81** and **13** are similar, however, the bridging distances in **81** are much longer. The Cd-N distances in the five-membered chelate are variable in **81** but in accordance with those observed in **13**.

The ligands cysteine and pencillamine, which are structurally similar to AET employ N, O as well as S to complete the six coordinate environment around Cd. In the Cd-AET adduct (**76**), in contrast the coordination environment around Cd consists of S and halide atoms.

Since AET is related structurally with cysteine and pencillamine, the complexes of Cd(II) with AET may be relevant to further studies of Cd containing metallothioneins as well as in the development of treatments for heavy metal poisoning. D-pencillamine, a potential chelator for Cd^{2+}, instead of excretion cause mobilization and re-distribution of the metal ion to other tissues.[138] Hence, formation of insoluble Cd(II)-AET compounds in aqueous media might be relevant to the lower mobility of Cd^{2+} ions in the biological systems.

Chapter 3

Lead(II)-2-Aminoethanethiolates

3.1 Overview

In the last few years there has been a resurgence in the coordination chemistry of heavy p-block elements due to their extensive Lewis acid properties and their potential use as solid-state materials.[139-142] Lead (Pb) has attracted particular attention, due to its versatility in adopting varying coordination geometries in compounds.[143,144] The interesting property of lead(II) arises due to its nature to bind well with both hard and soft donor atoms and in forming compounds that are different from those conventionally expected.

Homoleptic organolead(II)-thiolates containing Pb-C bonds are unstable and disproportionate to $R_3Pb\text{-}PbR_3$ and elemental Pb unless attached to bulky ligands.[145] Lead(II)-thiolates, on the other hand, are stable with respect to disproportionation and hydrolysis but are typically insoluble in non-coordinating solvents. This prevents the isolation of crystalline materials and hence limits an understanding of the structures present. Ligands containing both S and N donor have a significant advantage over the conventional thiolate ligands, due to the formation of stable and soluble compounds. However, only a few lead thiolates with both S and N coordination have been reported.[146-148] This is in contrast with the vast amount of literature available for the zinc analogue.[149] To address this limitation on the chemistry of Pb, and to gain insight into the biological activity of the element this chapter will present synthesis, characterization and structural study of lead(II)-2-aminoethanethiolates.

3.2 Synthesis and Characterization

The combination of Pb(acetate)$_2$·3H$_2$O, AET·HCl and NaOH in 1:2:2 ratio in DI water yielded a tetranuclear compound consisting of [$Pb_2Cl(SCH_2CH_2NH_2)_3$] (**85**).[150] A similar reaction with Pb(NO_3)$_2$·5H$_2$O yielded [$Pb_2(SCH_2CH_2NH_2)_3$](NO_3)$_{0.67}$(Cl)$_{0.33}$ (**86**),[150] which is similar to **85**. In contrast to **86**, combination of an equivalent amount of Pb(NO_3)$_2$·5H$_2$O, 2 AET·HCl and NaOH in water yielded a two-dimensional polymeric structure with the repeating unit consisting of [$PbCl(SCH_2CH_2NH_3)$](NO_3) (**87**).[151] The colorless to light yellow crystals of **85 - 87** were obtained from filtrate as well as from the recrystallization of the precipitate in DI water. Similar reactions with variable amounts of Pb(II) salt, AET and NaOH in alcohol are shown to yield discrete molecular structures.[60] Hence, it can be argued that the nature of the product can be manipulated by the nature of the solvent as well as the stoichiometry of the reactants (Table A15). The syntheses are summarized in scheme 3.1.

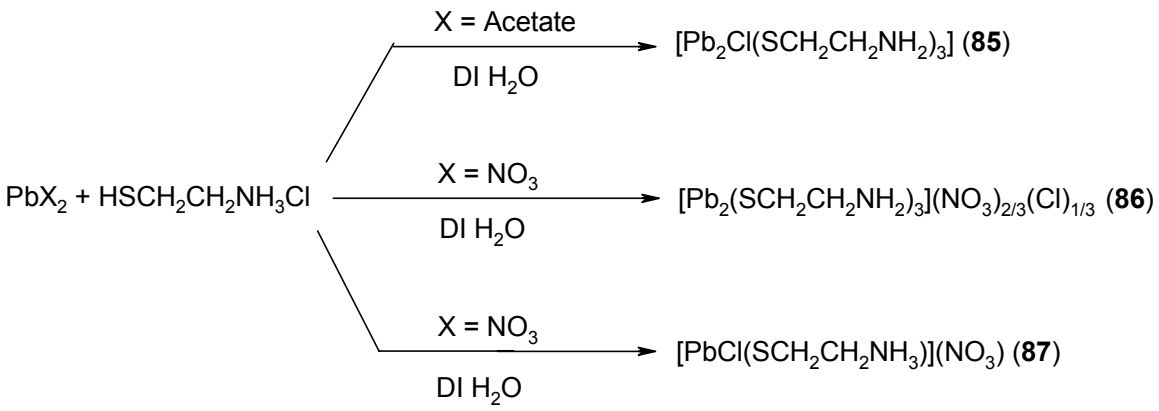

Scheme 3.1. Synthesis of Pb(II)-2-aminoethanethiolates.[60,150,151]

3.2.1 Spectroscopy

In the ^{1}H NMR spectra of **85** - **87**, single peaks were observed for the CH_2N and CH_2S groups, which are consistent with the symmetrical nature of the compounds in solution. Despite similar structures, a profound shift in the CH_2S peaks is observed in **86** compared to that observed in **85**. The corresponding peaks for **87** fall within the range observed for **85** and **86**. In the ^{13}C NMR, the presence of a Pb-S contact in **85** - **87** is evident by the deshielded C attached to S (25 - 29 ppm). Similarly, deshielding observed for C attached to N in **85** and **86** indicate the presence of a Pb-N contact. On the other hand, the nominal shift of CN observed in **87** is indicative of the absence of Pb-N contact (Table A16).

In the IR spectra, the absence of a peak at 2500 cm^{-1} for the -SH group confirms a direct Pb-S contact. This is also evident by the C-S and S-CH_2 stretches, which are shifted to lower frequencies compared to the free ligand. The peaks at 2938-3130, 1561-1583 cm^{-1} and no change in the C-N stretching in **87** indicates a free ammonium group. On the other hand, the presence of NH_2 stretching and bending modes at higher frequencies in **85** and **86** indicate a Pb-N contact.

In the Uv-Vis spectra for **85** - **87** in water the λ_{max} is observed at around 260 nm, which is due to an S → Pb LMCT (ligand to metal charge transfer) and fall in the range usually observed for Pb(II)-thiolates (250 - 400 nm) indicating retention of the geometry around Pb.[152] However, for **88** and **89**, the λ_{max} at 201 nm due to unligated Pb(II) indicated dissociation of the compounds under experimental condition.[60]

3.2.2 Crystal Structures

In **85**, two independent Pb centers are observed, namely, PbS_2N_2 and $PbClS_3N$ (Figure 3.1, Table A17). The presence of an open coordination site suggests the presence of stereochemically active lone pair. The geometry around four- and five-coordinate Pb can be considered as distorted tetrahedral and trigonal bipyramidal, respectively. The five-coordinate Pb forms a planar four-membered Pb_2S_2 ring with average internal angles close to 90º. The Pb-S distances observed around the five-coordinate Pb (2.737 and 2.897 Å) are slightly longer than the corresponding distances observed around the four-coordinate Pb (2.673 and 2.713 Å). On the other hand, the Pb-N distance around the four-coordinate Pb (2.629 Å) is slightly longer than that observed around the five-coordinate Pb (2.613 Å). This trend in Pb-S and Pb-N distances observed is probably to achieve an overall stability. The unsymmetrical Pb-S distances in the Pb_2S_2 core (2.737 and 3.053 Å) relieve the strain caused by the four-membered ring. This also indicates the presence of a stereochemically active lone pair.[153] Similar unsymmetrical distances are also observed around four-coordinate Pb. The bridging Pb-S distance (2.897 Å) connecting PbS_2N_2 and $PbClS_3N$ sub-units is in agreement with the corresponding distances observed in Pb(II)-thiolates containing bridging S atoms (2.671 - 2.960 Å).[153,154] The Pb-N distances are also comparable to four- and five-coordinate Pb(II)-thiolates with S/N chelates (2.436-2.532 Å).

The PbS_2N_2 moiety is attached to the Pb_2S_2 core in a linear fashion with an S-Pb-S angle close to 165.0º, which is comparable to similar angles observed in $[Pb(SCH_2CH_2OH)](NO_3)$ (162.7º)[155] and $[Pb(SPh)_2]$ (158.9º).[154] The deformation around Pb is most probably due to the presence of intermolecular hydrogen bonding. The Cl

from the $PbClS_3N$ unit is weakly bonded to the $-NH_2$ group of the PbS_2N_2 unit. On the other hand, the NH from the five-membered ring attached to the Pb_2S_2 core is involved in hydrogen bonding with the S atom of a PbS_2N_2 unit from a second molecule. Hence, the intermolecular hydrogen bonding is responsible for the stacking of the molecules. This stacking, however, with weak Pb---S interactions parallel to each other is also observed in $[Pb(SPh)_2]$.[154]

Compound **86** is isostructural to **85**, except for the presence of Cl attached to a Pb in the Pb_2S_2 core. The overall structure reveals two independent Pb centers, namely, PbS_2N_2 and PbS_3N. The geometry around Pb can be best described as distorted tetrahedral. The open coordination site suggests the presence of a stereochemically lone pair on Pb (Figure 3.2, Table A18).

The Pb-S distance in the PbS_2N_2 unit (2.713 Å) is shorter than the corresponding distance observed in the PbS_3N unit (2.704 and 2.893 Å). Similar to **85**, unsymmetrical Pb-S distances (2.704 and 3.085 Å) are observed in the Pb_2S_2 core indicating the presence of a stereochemically active lone pair. The presence of extensive hydrogen bonding in **86** might explain the higher thermal stability compared to **85**. This might be due to the presence of NO_3^-, which supplies more hydrogen bonding contacts than a single Cl ion. The $-NH_2$ hydrogens are also weakly bonded to S and Cl atoms of another unit similar to those observed in **85**.

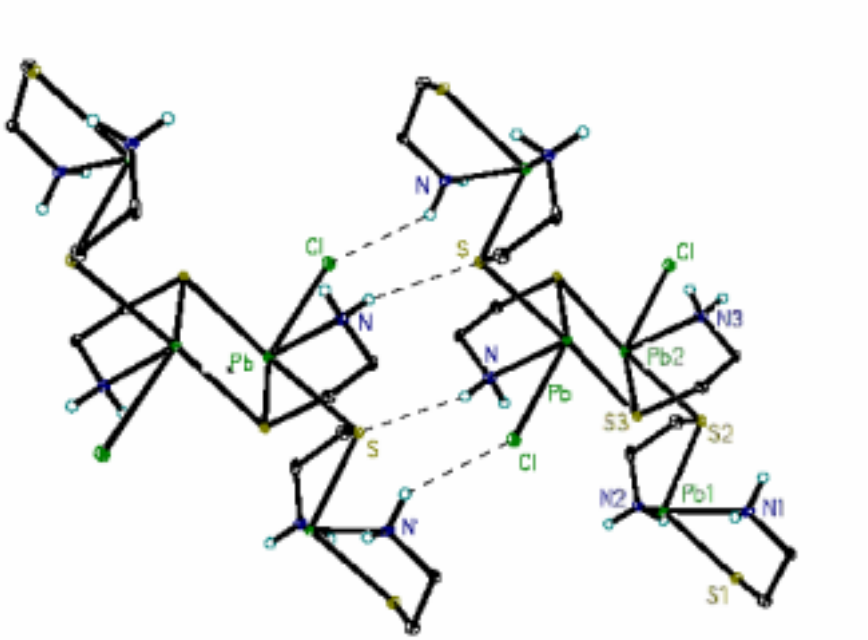

Figure 3.1. View of **85** showing inter-molecular hydrogen bonding with dotted lines.

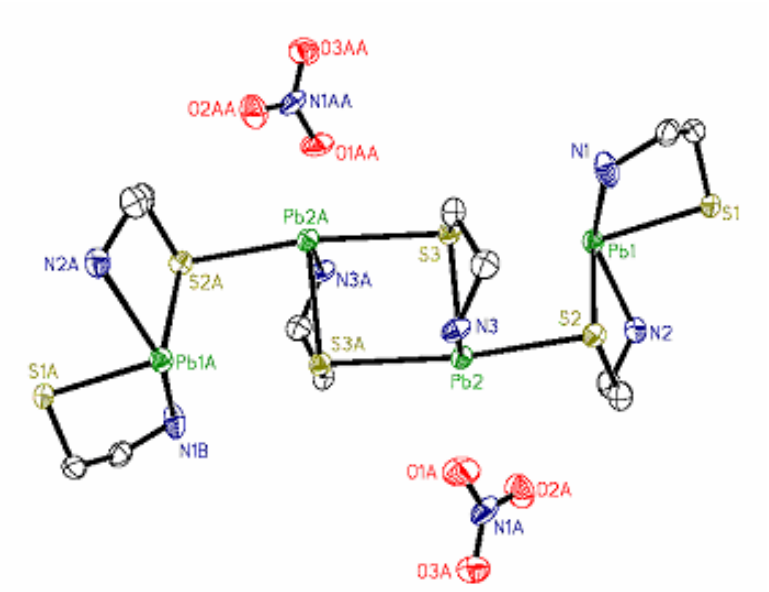

Figure 3.2. Molecular structure of **86** with 50% thermal ellipsoids**.** The counter anions 0.66 NO_3^- and 0.33 Cl^- are present at the same position.

In **87**, the Pb atoms are tetracoordinate with two bridging S and two bridging Cl atoms (Figure 3.3, Table A19). However, taking into account weak interactions with NO_3, two independent Pb are observed, namely, PbS_2Cl_2 (CN = 4) and $PbS_2Cl_2O_2$ (CN = 6). The absence of a Pb-N bond as seen in **85**, **86**, **29** and **42** can be attributed to the presence of an ammonium group. The angle spanning Cl-Pb-Cl is linear, 170º - 173º, while the Cl-Pb-S angles range from 81º to 90º providing a "see-saw" structure. The presence of an open coordination site indicates the presence of a stereochemically active lone pair on Pb.

The strain in the four membered Pb_2S_2 ring is evident in the S-Pb-S angle of 84º, which is comparable to those observed in **85** and **86** (83º - 87º).[150] The Pb---Pb distance observed in the Pb_2S_2 core (4.145 Å) is slightly longer than the sum of van der Waals radii of two Pb(II) atoms (4.0 Å)[156] but falls in the range observed for Pb(II)-thiolates containing a Pb_2S_2 core (3.994 - 4.612 Å).[153,157] In contrast, the S---S distances in the Pb_2S_2 core (3.371 Å) are much smaller than the sum of covalent radii of two S atoms (3.700 Å)[158] but in the range observed in similar Pb(II)-thiolates (3.103 - 3.836 Å).[159,160] The closest possible homonuclear interactions between the chains are through the open face with Pb---Pb (4.320 Å) and Cl---Cl interactions (3.952), which are comparable to those observed in polymeric Pb(II)-thiolates.[145]

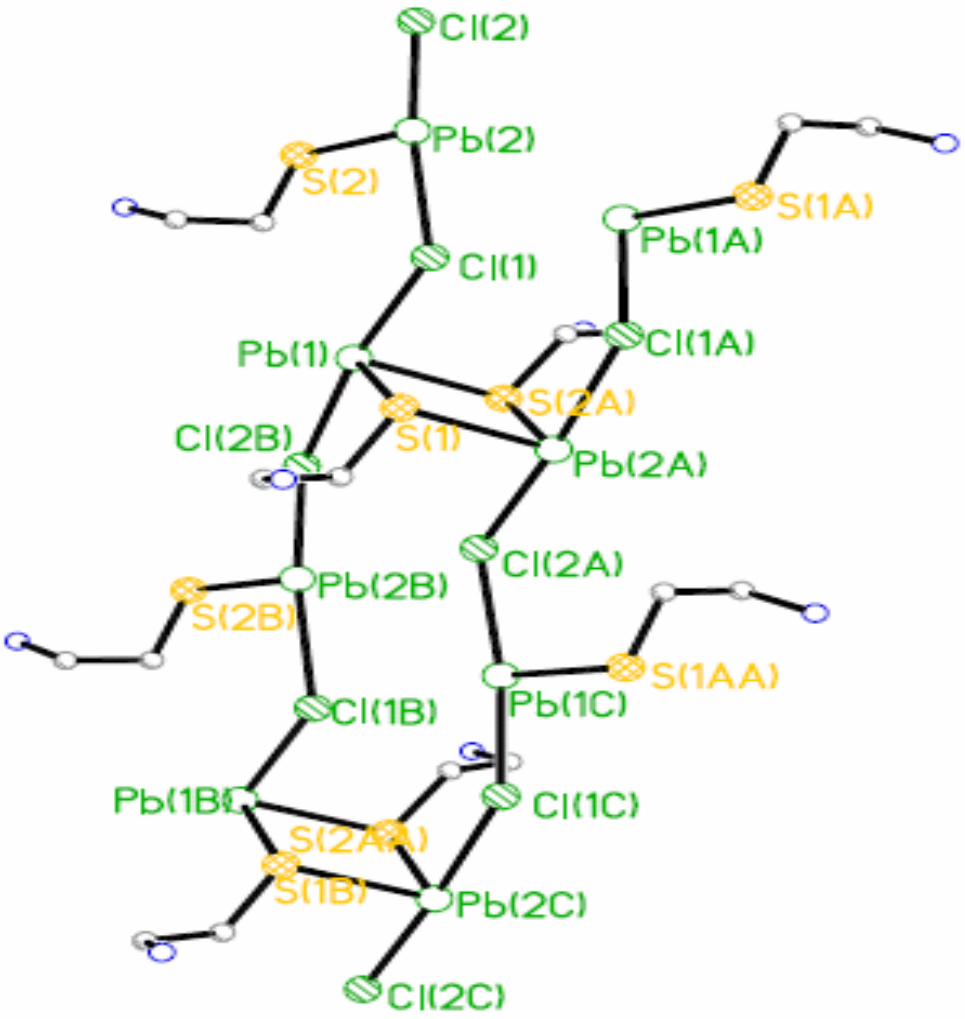

Figure 3.3. View of **87** along the 'c' axis with 50 % thermal ellipsoids. Additional Pb-S bonds, nitrate ions and hydrogen atoms are not shown.

The presence of an unsymmetrical Pb-S distances (2.734 and 2.841 Å) may relieve the strain caused by the four-membered Pb_2S_2 ring,[161] which also suggests that the lone pair on Pb is stereochemically active.[153] These distances are, however much larger than the corresponding distances observed for tetracoordinate Pb in **85, 86** and **29** (2.63 - 2.71 Å). This observation is in contrast to the fact that exchange of N with Cl (**29** and **42**) as an additional donor atom leads to the formation of stronger Pb-S bonds.[60] The Pb-Cl distances (2.784 and 3.034 Å) fall between those observed for tetracoordinate Pb (2.791 Å in **85** and **86**) and pentacoordinate Pb (3.082 Å in **29**). Hence, the two-dimensional network is formed of PbS_2Cl_2 repeating units along with the individual chains linked to each other by the Pb_2S_2 core. This might be a reason for the stability of the compound in solution, in contrast to polymeric Pb(II)-thiolates, where the chains are usually held together through weak Pb---S/N contacts.[60] However, polymeric chains connected through the ligand are also known, for example $\{[HB(pz)_3]Pb(\mu\text{-}NCS)\}_n$ (HB(pz) = pyrazolyl borate).[162] The $-CH_2CH_2NH_3$ groups in the core are present above and below the Pb_2S_2 plane and further involved in hydrogen bonding with bridging Cl and nitrate.

The two-dimensional network in **87** is extended to a three-dimensional framework by intermolecular hydrogen bonding involving NH_3, NO_3^- and Cl. The NH---Cl distance of 3.311 Å is much smaller than those observed in **85** and **86** (3.403 - 3.571 Å) indicating a stronger interaction. The nitrate ions are present within the chains and weakly bonded to the amine groups with distances in the range 2.884 - 3.009 Å and are smaller than those observed in **85** and **86** (2.9 - 3.2 Å). The Pb2---O(nitrate) distances (2.867 and 3.187 Å) are within the range observed for similar interaction of Pb with nitrate or perchlorate (2.58 - 3.20 Å).[70]

3.3 Experimental Section

All the reactions were carried out at room temperature in deionized water. The reagents $PbCl_2$, $Pb(NO_3)_2$ (J. T. Baker) and 2-aminoethanethiol hydrochloride (TCI America) were used as received. The NMR (^1H and ^{13}C) data were obtained with JEOL-GSX-400 and 270 instruments operating at 199.17 and 399.78 MHz using d^6-DMSO and D_2O as solvent, with tetramethylsilane as the reference. IR data were recorded as KBr pellets on a Matheson Instrument 2020 Galaxy Series spectrometer and are reported in cm^{-1}. Raman spectra were obtained on a Nicolet FT-Raman 906 Spectrometer ESP between 100 - 800 cm^{-1} in the Center for Applied Energy Research at the University of Kentucky. Mass Spectral data were obtained from the University of Kentucky Mass Spectrometry Facility. X-ray quality crystals were obtained from supernatant at either room temperature or at 4 ºC. X-ray data for **85** - **87** were collected on a Nonius Kappa-CCD unit using Mo-Kα radiation from colorless regular shaped crystals.

Synthesis of $[Pb_2Cl(SCH_2CH_2NH_2)_3]$ (85): To a stirring solution of AET·HCl (1.14 g, 10 mmol) in DI water (20.0 mL), sodium hydroxide (0.800 g, 20.0 mmol) was added followed by addition of lead acetate trihydrate (1.90 g, 5.00 mmol), followed by stirring for one day. The solution was filtered to remove yellow precipitate and the filtrate was allowed to stand for 3 days in the refrigerator at 4 ºC, during which time pale yellow needle shaped crystals formed. Yield (crystals): 0.640 g (19.0 %). Mp: 120 - 122 ºC. ^1H NMR (D_2O, 200 MHz, ppm): δ 2.85 (t, 2H, CH_2N), δ 3.02 (t, 2H, CH_2S). ^{13}C NMR (D_2O, 200 MHz, ppm): δ 29.1 (CH_2S), 48.5 (CH_2N). IR (KBr, ν/cm^{-1}): 668 - 657 (C-S), 1032, 1065, 1105, 1219 (C-N, stretching), 1417 (S-CH_2), 1596 (-NH_2 and N-H, bending),

3463 (R-NH_2, stretching). HRMS (EI, positive): 359 $(Pb(SCH_2CH_2NH_2)_2)^+$, 282 $(Pb(SCH_2CH_2NH_2))^+$, 76 $(SCH_2CH_2NH_2)^+$ Anal. Calcd for $C_6H_{18}N_3S_3ClPb_2$: C, 10.6; H, 2.67; N, 6.20. Found: C, 10.2; H, 2.48; N, 5.87.

Synthesis of $[Pb_2(SCH_2CH_2NH_2)_3](NO_3)_{0.67}(Cl)_{0.33}$ (86): Sodium hydroxide (20.0 mmol, 0.800 g) was added to a stirring solution of AET·HCl (10.0 mmol, 1.14 g) in DI water (20.0 mL) followed by the addition of lead nitrate (1.66 g, 5.00 mmol), followed by stirring for one day. The resulting solution was filtered to remove white precipitate and the filtrate was allowed to stand for 10 days in the refrigerator at 4 ºC, during which time colorless crystals were formed. Yield (crystals): 0.410 g (24.0 %). Mp: 132 - 134 ºC. ^{1}H NMR (d_6-DMSO, 200 MHz, ppm): δ 2.74 (t, 2H, CH_2N), δ 3.20 (t, 2H CH_2S). ^{13}C NMR (d_6-DMSO, 200 MHz, ppm): δ 30.0 (CH_2S), δ 49.3 (CH_2N). IR (KBr, ν/cm^{-1}): 628 - 706 (C-S), 1046 - 1221 (C-N, stretching), 1430 (S-CH_2), 1593 (-NH_2 and N-H, bending), 3448 (R-NH_2, stretching). HRMS (EI, positive): 359 $(Pb(SCH_2CH_2NH_2)_2)^+$, 282 $(Pb(SCH_2CH_2NH_2))^+$, 76 $(SCH_2CH_2NH_2)^+$Anal. Calcd for $C_6H_{18}N_{3.67}S_3O_{2.02}Cl_{0.33}Pb_2$: C, 10.3; H, 2.61; N, 7.38. Found: C, 10.3; H, 2.57; N, 7.36.

Synthesis of $[PbCl(SCH_2CH_2NH_3)](NO_3)$ (87): To a stirring solution of AET·HCl (10.0 mmol, 1.14 g), sodium hydroxide (10.0 mmol, 0.400 g) was added in 30 mL of DI water and stirred for few minutes. To the clear solution lead nitrate (10.0 mmol, 3.31 g) was added and stirred for 24 hours. The resulting precipitate was washed with cold DI water and methanol and dried well. The filtrate was evaporated to yield light yellow needle shaped crystals. The same crystals were also obtained from the recrystallization of the

precipitate from hot water. Yield(crystals + precipitate): 3.50 g (81.0 %). Mp: 188 - 190ºC. ^{1}H NMR(d_6-DMSO, 200 MHz, ppm): 3.06 (m, 4H, CH_2CH_2) and 7.36 (br, 3H, NH_3). ^{13}C NMR (d_6-DMSO, 200 MHz, ppm): 25.1 (CS) and 44.6 (CN). IR (KBr, ν/cm^{-1}): 357, 656, 819, 881, 1033, 1091, 1335, 1390, 1475, 1596, 3137. HRMS (EI, positive): 427 (M^+, 2), (M-2Cl$^+$, 2). Anal. Cald for [PbCl($SCH_2CH_2NH_3$)](NO_3): C, 6.29; H, 1.84; N, 7.37. Found: C, 6.28; H, 1.80; N, 7.36.

3.4 Conclusion

Compounds **85** and **86** are the first structurally characterized tetranuclear Pb(II)-thiolates containing an S/N ligand. The solubility of 2-aminoethanethiol and its compounds has facilitated the preparation and structural study of soluble Lewis acid-base adducts **85**, **86** and **87**. The structures of **85** and **86** are based on a simple bonding model for Pb(II)-thiolates, in which the amine nitrogen donates electron density to the empty p-orbitals of Pb. In the absence of a bridging Cl atom (**86** and **87**) molecular compounds are observed. A three-dimensional network is acquired due to the formation of intermolecular hydrogen bonding involving amine groups and counter anions. In contrast, the bridging Cl in **87** yields a one-dimensional network, which is extended to a two-dimensional network with bridging S atoms. It is interesting to note that weak Pb--S as well as Pb---N interactions in Pb(II)-thiolates are responsible for the formation of polymeric structures, which are either unstable in solution[60] or insoluble in non-coordinating solvents.[145] In contrast to **85** - **87**, similar reactions in alcohol (**29**, **42**) in the presence of excess base yielded molecular compounds with intramolecular Pb---S interactions. These compounds are shown to partially dissociate in solution, in contrast to robust **85** - **87**. The Pb-S distances for the four-coordinate Pb in **85** and **86** are variable compared to those observed around **29** and **30**. The average Pb-N distances in the five-membered chelate in **85** and **86** are shorter than those observed in **29** and **30**.

Chapter 4

Mercury(II)-2-Aminoethanethiolates

4.1 Overview

Mercury-thiolate chemistry has attracted much attention in the last few decades due to the presence of sulfur compounds in the biological cycling of the element.[164] The well-documented toxicity is due to the interaction of mercury with sulfur, present in biomolecules as cysteine[92] and methionine.[165] In particular, the organomercury(II) compounds have stimulated much attention due to their ability to cause irreversible damage to the central nervous system.[166] The inorganic form of mercury, if ingested by organisms, is easily transformed into organic species by alkylation making it more soluble in water as well as more lipophilic thereby increasing its toxicity.[167]

Mercury(II)-thiolates can be divided into two categories according to the donor atoms: a) homoleptic thiolates (Hg bonded to only S atoms) and b) heteroleptic thiolates (Hg bonded to halide, N or O along with an S atom). Homoleptic mercury(II)-thiolates can be mononuclear ($Hg(SR)_n$, n = 2 - 4); dinuclear ($Hg_2(SR)_n$, n = 3, 6); trinuclear ($Hg_3(SR)_4$); tetranuclear ($Hg_4(SR)_6$); pentanuclear ($Hg_5(SR)_8$) and polynuclear ($[Hg(SR)]_n$).[12,83,87,168,169] On the other hand, the heteroleptic mercury(II)-thiolates are generally polymeric such as $[Hg(SR)Cl_2]_\infty$, $[Hg(S\text{-steroid})Br]_\infty$, $[Hg(SMe)X]_\infty$ (X = Cl or Br) and $[Hg(SPr^i)Cl]_\infty$). However, heteroleptic compounds of higher nuclearity are also known such as tetranuclear $(Ph_4P)[(\mu\text{-}SEt)_5(\mu\text{-}Br)(HgBr)_4]$, $(Bu^n{}_4N)_2[Hg_4(SR)_6X_4)$ (R = SEt, SPr^i) and heptanuclear $[Hg_7(SC_6H_{11})_{12}X_2]$, where X = Cl, Br or I[89-91,170,171] The common feature observed in the heteroleptic mercury(II)-thiolates is that the geometry around the Hg(II) center is affected by the size of the halide.

The interaction of Hg with thiolate S atoms is thermodynamically favorable and the stability of the compounds may be achieved by the formation of a number of different structures of equal or similar energy. The ease of deformation of $[Hg(SR)_x]$-type compounds is due to the low energy barrier separating different species, which leads to a complicated solution chemistry.[172,173] The structural diversity found generally in metal-thiolates is exemplified dramatically in the unusual coordination chemistry of mercury(II)-thiolates. Aminothiols with protected or quaternized groups are of greater synthetic and spectroscopic utility by comparison to conventional monodentate thiols as the metal compounds are generally more soluble. Thus, structural and solution equilibria studies can be achieved.

This chapter summarizes compounds of Hg(II) salts with AET·HCl and their structural studies along with proposed mechanisms for the formation of compounds of higher nuclearity. The mechanistic pathways are topochemical and therefore incorporate the known structural chemistry of Hg(II)-thiolates reported in the literature.

4.2 Compounds of AET with $HgCl_2$

4.2.1 Synthesis and Characterization

The combination of $HgCl_2$ (or Hg_2Cl_2) with AET·HCl in DI water at room temperature yielded $[Hg(SCH_2CH_2NH_3)_2]Cl_2$ **(88)**, $[Hg_6Cl_8(SCH_2CH_2NH_3)_8]Cl_4$ **(89),** $[Hg_3Cl_5(SCH_2CH_2NH_3)_3]Cl$ **(90)** and $[Hg_2Cl_2(SCH_2CH_2NH_2)(H_2O)]$ **(91)** with variable nuclearites.[174-176] However, a similar reaction at 0 ºC yielded only a tetranuclear cyclic compound, $[Hg_4Cl_6(SCH_2CH_2NH_3)_4]Cl_2$ **(93)**.[177] In contrast, combination of the neutral ligand with $HgCl_2$ in methanol yielded a mononuclear four-coordinate compound,

$[Hg(SCH_2CH_2NH_2)_2]$ **(92)**.[126] The structures obtained apparently depended on the stoichiometry of the reaction, time and temperature (Table A20). X-ray quality crystals were mostly obtained from the supernatant at either room temperature or cooled to 4 ºC.

4.2.2 Spectroscopy

In the ^{1}H and ^{13}C NMR spectra, a significant shift is observed for the methylene protons and C atoms of the CH_2 groups attached to S in **88** - **92** (Table A21) compared to the free ligand, indicating the presence of an Hg-S bond. The protons due to the NH_2/NH_3^+ groups are observed as a broad peak in the range 6.0 - 8.0 ppm for **89** - **91**. A significant shift in the C attached to the NH_2 group is not observed in **91** despite an Hg-N bond, compared to **92**.

The ^{199}Hg solution NMR of compound **88** suggests the presence of a four-coordinate $[Hg(SR)_2Cl_2]$ compound in solution. The peak at -618 ppm relative to 1M $HgCl_2$ in DMSO (as external reference) is in the range reported for four-coordinate Hg(II)-thiolates (0 - -800 ppm).[169] In **89**, despite the presence of three independent Hg centers only one single peak at -678 ppm indicating a four-coordinate Hg center is observed. This might be due to the dissociation of the cluster to a simple $[Hg(SR)_2Cl_2]$ compound. No suitable peaks for **90** and **91** could be observed despite their high solubility in DMSO, which can be attributed to the rapid exchange occurring in solution.

In the IR spectrum the absence of an -SH peak around 2500 - 2550 cm^{-1} in **88** - **92** confirms the presence of covalent Hg-S bonds. In **88** - **90**, peaks at 3200 - 3300 cm^{-1} (symmetric stretching) indicate protonated amine groups. The N-H scissoring and wagging modes for all the compounds were observed around 1500 - 1650 and 660 - 900

cm^{-1}, respectively. A red shift in the C-S stretch around 600 cm^{-1} for **88 - 92** compared to the free ligand (750 cm^{-1}) also indicates interaction between the thiolate S atom and Hg.

In the Raman spectrum (Table A22), the symmetric and asymmetric stretch for Hg-S in **88 - 92** are observed around 280 and 340 cm^{-1}, which are comparable to those reported in the literature (252 - 337 cm^{-1}). The stretch due to Hg-Cl in **89 - 91** is observed around 230 cm^{-1}, which is also comparable to the literature values.[88,116]

In the UV-Vis spectrum the λ_{max} due to the S → Hg LMCT for **88 - 91** is observed around 270 nm, which indicates the presence of four-coordinate Hg in solution. However in **88**, despite a linear geometry in the solid-state, the geometry around Hg in solution is more like distorted tetrahedral due to the presence of two Cl ions in close proximity. Low-energy LMCT bands in the wavelength range 280 - 310 nm are characteristic of distorted tetrahedral complexes containing Hg-S bonds as observed in $[Hg(SR)_2]$ (R = ethyl and isopropyl),[178] Hg-plastocyanin[179] and two types of metallothionein.[180-182]

4.2.3 Crystal Structures of 88 - 92

The geometry around **88** is essential linear with S-Hg-S close to 170° (Figure 4.1). The deviation from linearity is due to a weak interaction with the Cl ions. A similar deviation is also observed in **44 - 46** (154 - 170°).[92-94] The Hg-S distances (avg 2.33 Å) are comparable to two-coordinate Hg(II)-thiolates.[92-95]

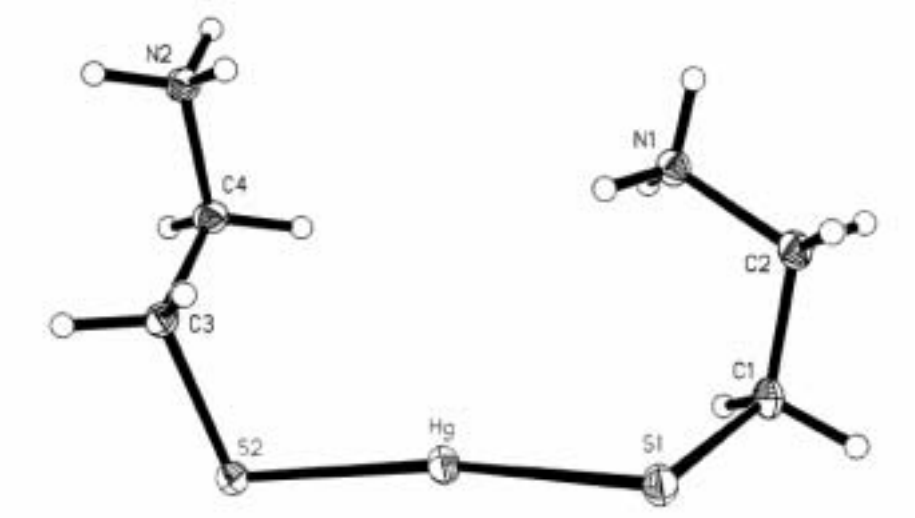

Figure 4.1. ORTEP view of the dication of **88** without Cl ions.

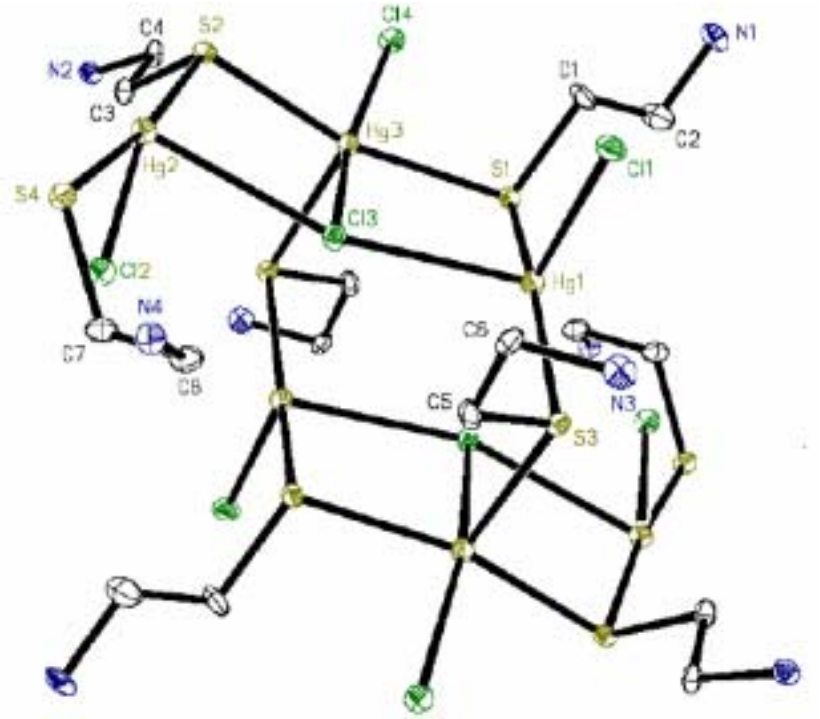

Figure 4.2. Molecular structure of **89** with 50% thermal ellipsoids. The counter anions and hydrogen atoms are omitted for clarity.

A unique feature that has been identified in **88**, in contrast to similar Hg(II)-thiolates, such as **44** is the presence of short S---H contacts.[183]. The S---N distance is 3.26 Å implying a short hydrogen bond distance of ~ 2.20 Å. This type of contact, although rare, has been found to be important in the structures of ferredoxins.[184,185]

The cationic cluster of **89** can be considered to be formed by linking two equivalent trinuclear species $[Hg_3Cl_4(SCH_2CH_2NH_3)_4]^{2+}$ with two bridging thiolate S atoms (Figure 4.2, Table A23). In the molecule two independent Hg (H1, Hg2 (four-coordinate) and Hg3 (five-coordinate)), Cl (bridging and terminal) and bridging S atoms (inter- and intra unit) are observed. The geometry around Hg1 and Hg2 can be best described as distorted tetrahedral and around Hg3 as distorted square pyramidal. The Hg-S distances are variable and in the range, 2.339 - 2.631 Å. The Hg1-S and Hg2-S bond distances are nearly equal (avg 2.399 Å) except for Hg3-S4 (2.339 Å), where S4 is not a bridging atom. These distances are found on the upper range of the distances observed for two-coordinate Hg(II)-thiolates with additional secondary contacts (2.316 - 2.395 Å)[93,96,186,187] but slightly shorter than the corresponding distances observed in four-coordinate Hg(II)-thiolates (2.410 - 2.606 Å).[89,90,118,188] The Hg3-S1 and Hg3-S2 distances (avg 2.509 Å) are much longer than the Hg-S distances associated with Hg1 and Hg2. The bridging thiolate distance between trinuclear units (2.631 Å) is longer than the bridging Hg-S distances observed within the units. These distances are comparable to bridging Hg-S distances observed in molecular $[Hg_2(SMe)]^{2+}$ (avg 2.667 Å),[84] $[Ph_4P][Hg_3(SCH_2C_6H_4CH_2S)_4]\cdot 6MeOH$ (avg 2.708 Å),[86] and polymeric $[Hg(S\text{-}^tBu)_2]_n$ (avg 2.625 Å) and $[Hg_2(SCH_2CH_2S)_3]_n$ (avg 2.72 Å).[85]

The three Hg atoms in each fragment are arranged around the triply bridged chloride at similar distances (avg 2.924 Å). The trinuclear fragment $[Hg_3Cl_4(SCH_2CH_2NH_3)_4]^{2+}$ can be compared to **71**, where a triply bridged Cl is also observed.[119] The Hg1-Cl1 (2.730 Å) and Hg2-Cl2 (3.106 Å) distances are different despite similar environments. The Hg-Cl distance to triply bridged chloride in **89** is much longer than the corresponding distances observed in **71** (2.370 Å). The significantly longer distance may be due to the formation of a four-membered ring, Hg_2SCl, involving bridging S and Cl atoms. In **71**, the trinuclear units are held together through moderately strong chloride bridges forming a three-dimensional network, in contrast to **89**, where the units are held together through bridging S atoms.

The Hg environment is distorted with primary S-Hg-S angles ranging from 171.8º - 158.0º, much more linear compared to those associated with tetrahedral Hg with a Cl_2S_2 environment as in **51** (130.8º),[189] and **70** (112.5º and 130.2º).[92] The largest bond angles are associated with the sulfur and the more narrow angles are associated with the triply bridged chlorides (S1-Hg1-Cl3, S2-Hg2-Cl3 and S1-Hg3-Cl3, ≈ 88º). The distortion around Hg can be attributed to the vibronic coupling mechanisms leading to d-orbital contribution, which give rise to deformation or a "plasticity" effect for tetrahedrally coordinated Hg(II) with sulfur donor ligands.[190]

It is interesting to observe that despite the variation in the distances and the angles, each Hg atom is bonded to two sulfurs and two chlorides (with the exception of long S contact to Hg3). The $Cl_{triply\ bridged}$-Hg-S angles in **89** (89º – 98º) are much more acute than the corresponding angles in **71** (167.2º) due to the involvement of bridged S atoms.

The geometry defined by 3Hg, 2S and one Cl atom (Cl3) is planar with Hg1-Cl3-Hg2 and S1-Hg3-S2 close to 160º. The terminal $-CH_2CH_2NH_3^+$ groups are involved in intermolecular hydrogen bonding.

The repeating unit in **90** is $[Hg_3Cl_5(SCH_2CH_2NH_3)]^+$ with a highly distorted geometry around the Hg atoms (Figure 4.3, Table A24). Three independent Hg atoms are observed, namely HgS_2Cl, HgS_3Cl and $HgSCl_3$. Hg3 is unique as it is bonded to only one S atom, despite the tendency of Hg(II) to maximize bonding with thiolate S atoms. The geometry around Hg1 and Hg3 can be best described as distorted tetrahedral and around Hg2 as slightly distorted 'T' shaped. The Hg-S distances within a unit (avg 2.442 Å) are comparable to those observed for four-coordinate polynuclear Hg(II)-thiolates.[169]

The Hg-S distance connecting trinuclear units is larger (2.794 Å) than the corresponding Hg-S distances observed within the trinuclear unit (avg 2.442 Å). The average Hg-Cl distance around Hg1 and Hg2 (2.743 Å) is longer than the terminal Hg-Cl distance observed in similar Hg(II)-thiolates (2.37 - 2.642 Å) indicative of weaker Hg-Cl bonding.[89,189,191] The Hg-Cl distances around Hg3 are variable and in the range 2.434 - 2.707 Å. The longer distance may be attributed to the groups involved in intermolecular hydrogen bonding. In contrast, the long Hg1-Cl1 bond is not involved in any kind of secondary interaction, which may be attributed to the fact that Hg1 is three-coordinate compared to four-coordinate Hg2 and Hg3.

The smallest and largest bond angles around the Hg atoms are 167º, 85.0º (Hg1), 149º, 90.0º (Hg2) and 142º, 93.0º (Hg3). The more obtuse angles are associated with S compared to bonding with Cl atoms in the order S-Hg-S > S-Hg-Cl > Cl-Hg-Cl.

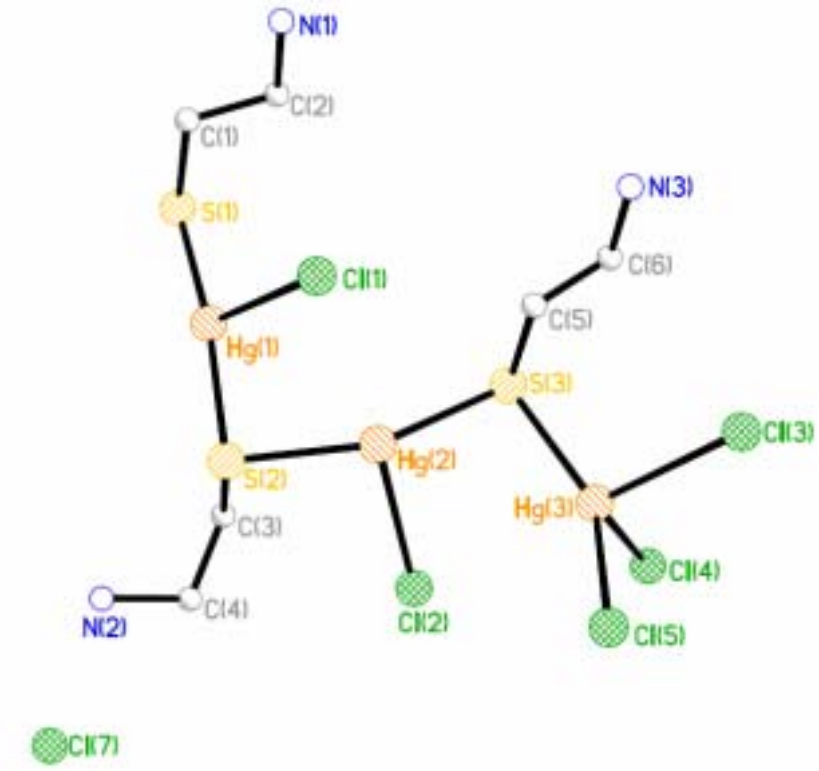

Figure 4.3. The trinuclear repeating unit of **90**. The additional Hg-S contacts are not shown for clarity.

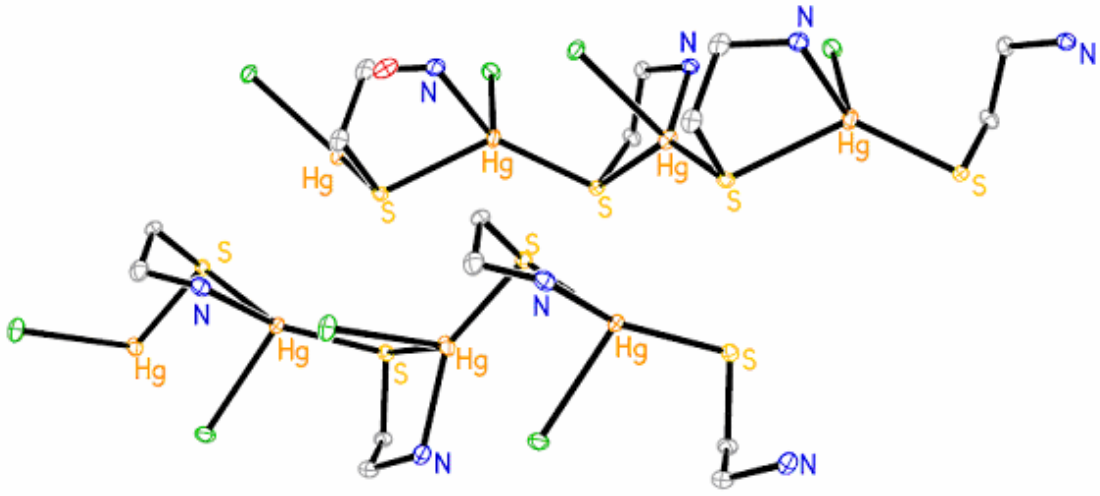

Figure 4.4. Polymeric structure of **91** with 50 % thermal ellipsoids. The hydrogen atoms are not shown for clarity.

The effective angular distortion of S-Hg-S is directly related to the presence of secondary contacts and asymmetric primary coordination. This is evident in the presence of a linear angle around Hg1 (S-Hg-S = 167º) compared to Hg2 (S-Hg-S = 149º). The Hg1 environment is quite unusual as compounds with $[Hg(SR)_2Cl]^+$ moieties are not known. However it can be compared to **71**, where the Cl is not bonded directly but present as chloride in close proximity (S-Hg-S = 169.8º and Hg-Cl = 3.232 Å).[92] The T-shaped geometry around Hg1 is common for three-coordinate Hg as observed in $[HgXL_2]$ (X = I; L = N,N,N',N'-tetraethylthiuram disulfide.[192,193] The S-Hg-Cl angles around Hg3 are more linear compared to the almost perpendicular S-Hg-Cl angles around Hg1 and Hg2. Hg1, however, acts as a linear Hg(II)-bis-thiolate due to the absence of weak interactions associated with the Cl atom.

In the one-dimensional chain the $HgSCl_3$ moieties are present on the opposite side of the chain. The ammonium groups are pointing away from the plane containing Hg, S and Cl to avoid steric interactions. All the Cl atoms, except Cl1, are involved in intermolecular hydrogen bonding with the ammonium group of a second chain to acquire a three dimensional structure. The NH---Cl distances (avg 3.222 Å) are slightly longer than those observed in Hg(II)-thiolates with N and Cl atoms (avg 3.150 Å[88] and 3.160 Å[189]) but comparable to those observed in free ligand (avg 3.200 Å).[174]

The geometry around Hg in the repeating unit of **91** $[HgCl(SCH_2CH_2NH_2)(H_2O)_2]$, is distorted tetrahedral with the coordination sphere consisting of S, N and Cl atoms (Figure 4.4, Table A25). The repeating units are attached through bridging S in a unidirectional fashion. However, intermolecular hydrogen

bonding involving an NH_2 group, Cl and water molecules generate a three-dimensional structure.

The five-membered rings are neither parallel nor perpendicular to each other (N-Hg-S-C torsion angle ≈ 100º). This distortion might be due to the hydrogen bonding of amine with Cl from an alternate chain and to avoid any kind of steric interaction among the five-membered rings. In the chelate ring the average Hg-S (2.652 Å) distance is much longer and the Hg-N distance (2.268 Å) is much shorter than the corresponding distances observed in other Hg(II)-thiolates with S/N chelates (avg 2.400 Å).[49,99] These distances are indicative of weaker Hg-S and stronger Hg-N bonds. The chelate Hg-S distance (2.652 Å) is much longer than the bridging Hg-S bond (2.423 Å), which is in contrast to the observations made in **69**, where the S/N chelating Hg-S distances are shorter than non-chelating Hg-S distances (2.414 and 2.495 Å, respectively).[49] The Hg-N distances are shorter than those observed in Hg(II)-thiolates with additional N donor ligands (2.390 - 2.480 Å).[111] The bridging Hg-S distances (avg 2.408 Å) present between repeating units are slightly shorter than the bridging distances observed in **90**, which can be attributed to a larger Hg-S bond present in the chelate. The terminal Hg-Cl distances are variable with Hg1-Cl1, 2.719 Å, Hg2-Cl2, 2.717 Å and Hg3-Cl3, 2.630 Å. The contribution of Cl in intermolecular hydrogen bonding makes the Hg-Cl length slightly elongated, which is found in the upper limit range (2.310 - 2.830 Å) observed in Hg(II)-thiolates with terminal Cl atoms.[88,106,191]

In **92**, the coordination around Hg consists of S and N atoms (Figure 4.5) with a nearly linear S-Hg-S (161º) arrangement and narrow N-Hg-N angles (93º).[126] The linear S-Hg-S indicates the tendency of Hg to maximize the bonding with S atoms rather than N

atoms. Additionally, a weak Hg---S contact is also observed leading to the formation of a dimer. The dimers are further connected by intermolecular hydrogen bonding. The Hg-S (avg 2.360 Å) and Hg-N distances (avg 2.590 Å) are in accordance with four-coordinate Hg(II)-thiolates.[169]

A similar reaction used for the synthesis of **88** at 0 ºC yielded a polynuclear compound, $[Hg_4Cl_4(SCH_2CH_2NH_3)_4]$ (**93**) (Figure 4.6). The core structure is shown to consist of repeating tetranuclear units, which are connected with bridging Cl atoms to form a one-dimensional polymeric chain. Two independent Hg centers are observed, namely, HgS_2Cl_4 and HgS_2Cl_2, with distorted octahedral and tetrahedral geometry, respectively.

The Hg-S distances in the HgS_2Cl_4 unit (avg 2.368 Å) are close to those observed for two-coordinate rather than six-coordinate Hg(II)-thiolates. Similarly the S-Hg-S angles (avg 173º) are comparable to those observed in **88.** On the other hand, the Hg-S distances in the HgS_2Cl_2 units (2.524 Å) are comparable to tetrahedral Hg(II)-thiolates. The Hg-Cl distances in the Hg_2Cl_2 unit (2.953 Å) are much longer than those present in the HgS_2Cl_2 units (avg 2.549 Å).

4.2.4 Mechanistic pathway for the formation of 88 - 93

The formation of Hg(II)-bis-thiolate, **88** can be considered to occur through a stepwise process with the formation of a four-coordinate intermediate in solution (Scheme 4.1). The Hg-Cl distances of 3.120 and 3.470 Å in **88** clearly indicate chlorides as essentially ionic.

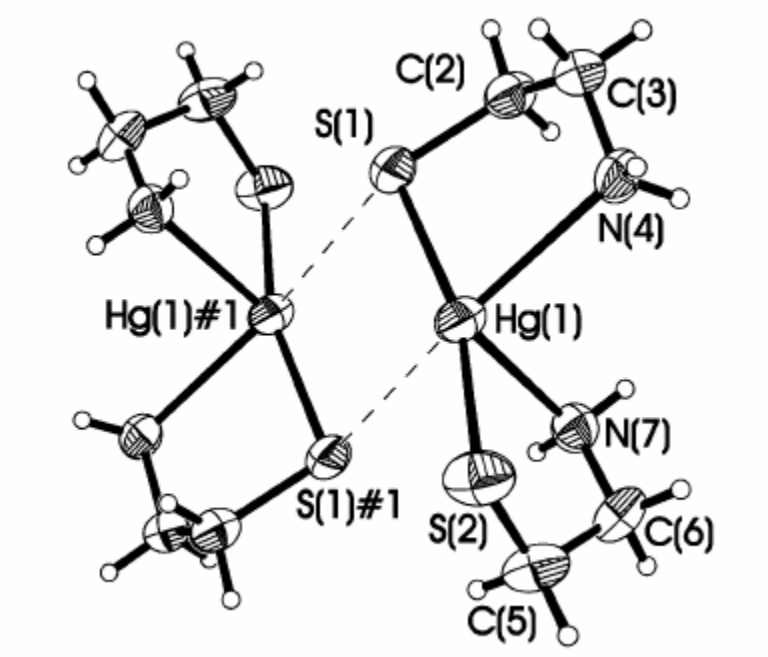

Figure 4.5. Dimer of **92** with weak Hg---S contacts shown with dotted lines.[126]

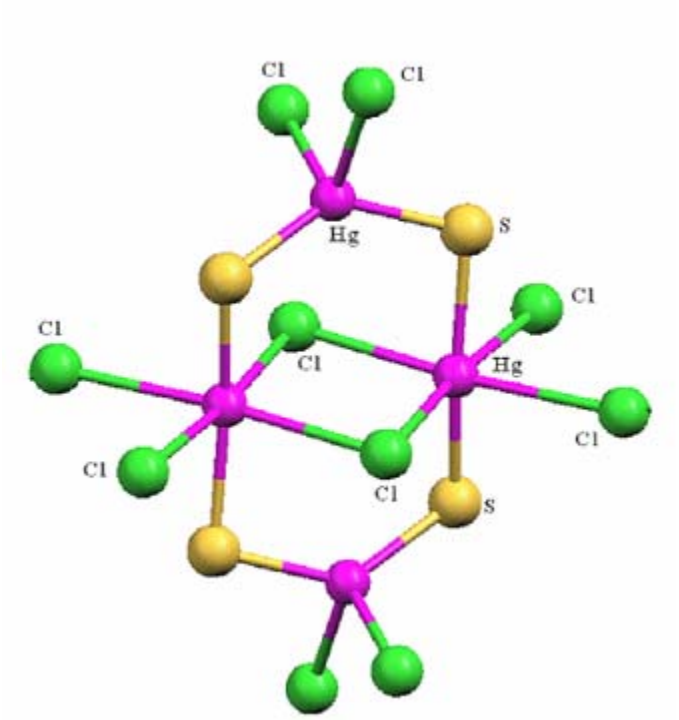

Figure 4.6. Repeating unit observed in **93** drawn with Mercury.[194] The disordered -$CH_2CH_2NH_3$ groups are not shown for clarity.

As indicated by the bond angles and the distances it can be easily concluded that the pathway for the formation of **93** involves **88** and free $HgCl_2$ (Scheme 4.1). The presence of free $HgCl_2$ in the solution can be attributed to its low solubility at 0ºC. In the solution free $HgCl_2$ add across **88** to from a dinuclear species, which in turn dimerize to form the tetranuclear unit of **93**.

The formation of **89** and **90** can be considered to proceed through a three-coordinate intermediate $[HgCl(SCH_2CH_2NH_3)_2]^+$, which could exist in solution in equilibrium with **88** (Scheme 4.2). There are no reports for formation of such an intermediate; however, compounds of general formula, ClHgSR (R = benzyl, neopentyl and isopropyl) have been reported.[87] For **89** a free $HgCl_2$ interacts with the three-coordinate intermediate to form a dinuclear species, $[Hg_2Cl_3(SCH_2CH_2NH_3)_2]^-$, which in turn interacts with another three-coordinate intermediate to form the trinuclear unit. This trinuclear unit dimerizes with a bridging thiolate to form the hexanuclear unit of **89**.

In **90**, the three-coordinate intermediate dimerizes through a bridging thiolate to form the dinuclear unit, $[Hg_2Cl_2((SCH_2CH_2NH_3)_4]^{2+}$. The free $HgCl_2$ then reacts with a terminal thiolate atom to form the trinuclear unit, $[Hg_3Cl_4(SCH_2CH_2NH_3)_4]^{2-}$. The fourth coordination around this Hg unit is further completed by the addition of a free Cl^- ion. This pathway is implicit in the Hg-Cl distances of 2.430 and 2.540 Å in the $HgSCl_3$ unit.

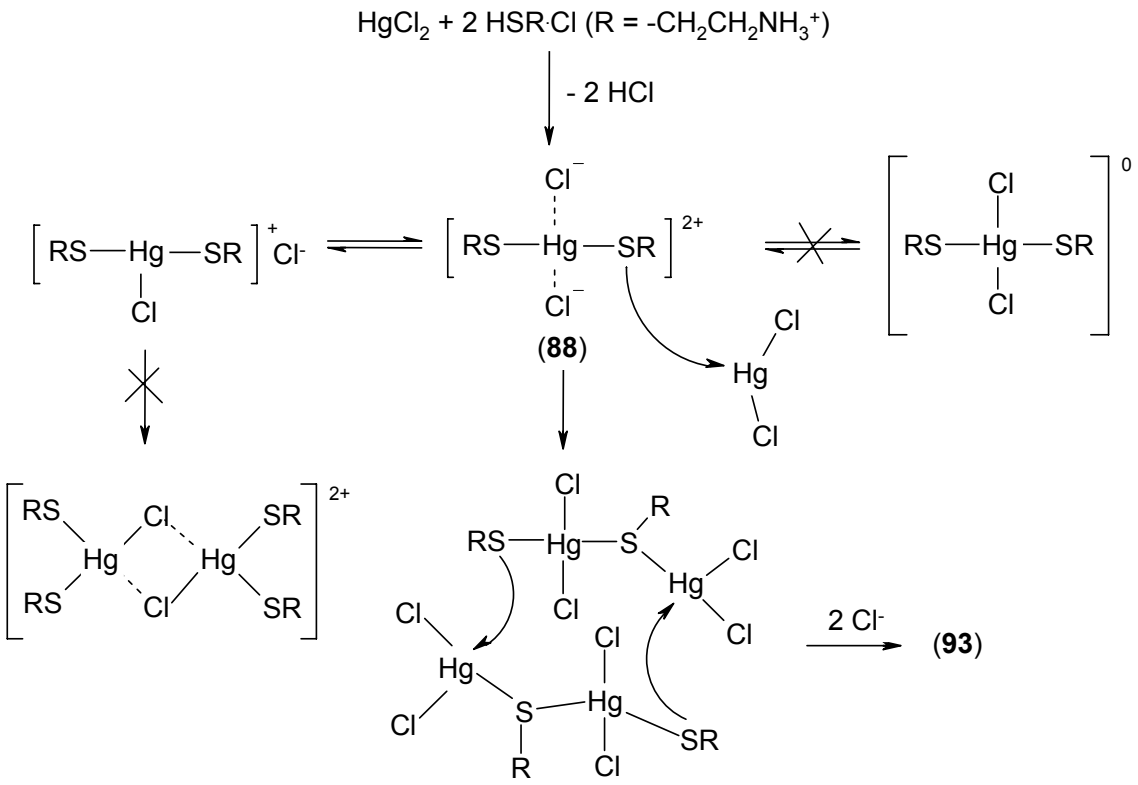

Scheme 4.1. Formation of **88** and **93** where R = $-CH_2CH_2NH_3^+$.

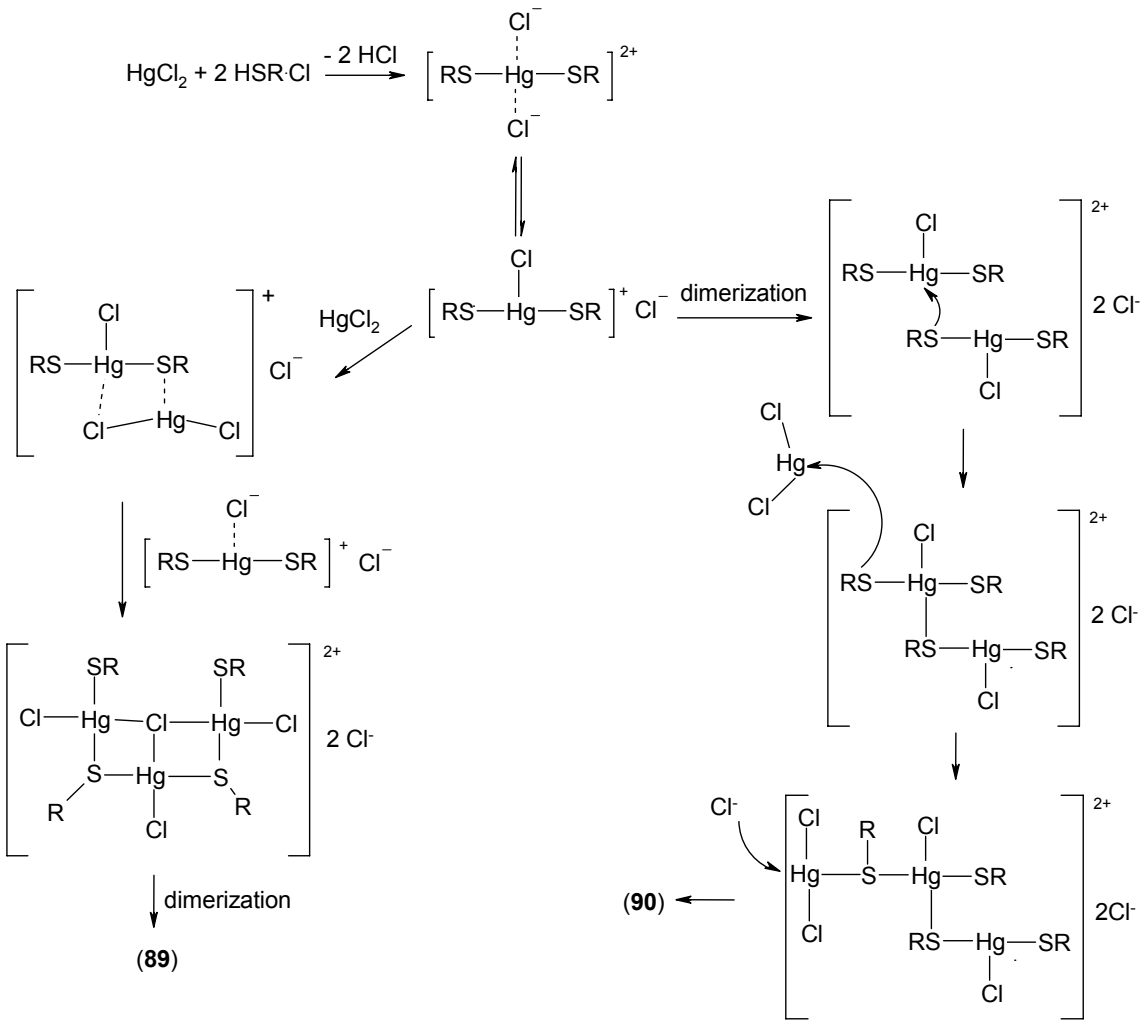

Scheme 4.2. Formation of **89** and **90** from the three-coordinate intermediate. (R = -$CH_2CH_2NH_3^+$).

In the presence of a base (NaOH) the formation of an additional Hg-N bond is observed in **91** and **92**. The formation of four-coordinate Hg in **91** and **92** happens through the initial formation of the three-coordinate intermediate, $[HgCl(SCH_2CH_2NH_2)]$. The fourth coordination around Hg in **91** is completed by bonding to the thiolate present on another three-coordinate intermediate (Scheme 4.3). The fourth coordination around Hg, however, can be completed by formation of $[HgCl_2(SCH_2CH_2NH_2)]^-$ or by dimerization to form $\{[HgCl(SCH_2CH_2NH_2)]\}_2$. Such intermediate have not been isolated but reported to exist in solution.[195-197] Formation of an additional Hg-S bond prevails over the formation of an additional Hg-Cl bond to minimize the energy. However, in **92**, the stability around $[HgCl(SCH_2CH_2NH_2)]^+$ is achieved by the additional S/N chelate to form a four-coordinate compound, $[HgCl(SCH_2CH_2NH_2)_2]$ (Scheme 4.4).

4.3 Compounds of AET with $HgBr_2$

4.3.1 Synthesis and Characterization

The 1:2 combination of $HgBr_2$ and AET·HCl and AET in DI water yielded nona-nuclear $[Hg_9Br_{15}(SCH_2CH_2NH_3)_9]^{3+}$ (**94**) and tetranuclear $\{[HgBr_4][(NH_3CH_2CH_2S\text{-})_2]\}$ (**95**), respectively.[175,198] However, a bis-thiolate, $[Hg(SCH_2CH_2NH_3)_2](Cl/Br)_2$ (**96**), which is isostructural to **88** can be obtained if the reaction is conducted for a shorter time. The compounds are obtained as white precipitates in quantitative yields. X-ray quality colorless crystals for **94** were obtained from supernatant at 4 ºC, while for **95** and **96** the crystals were obtained from slow evaporation of the supernatant at room temperature.

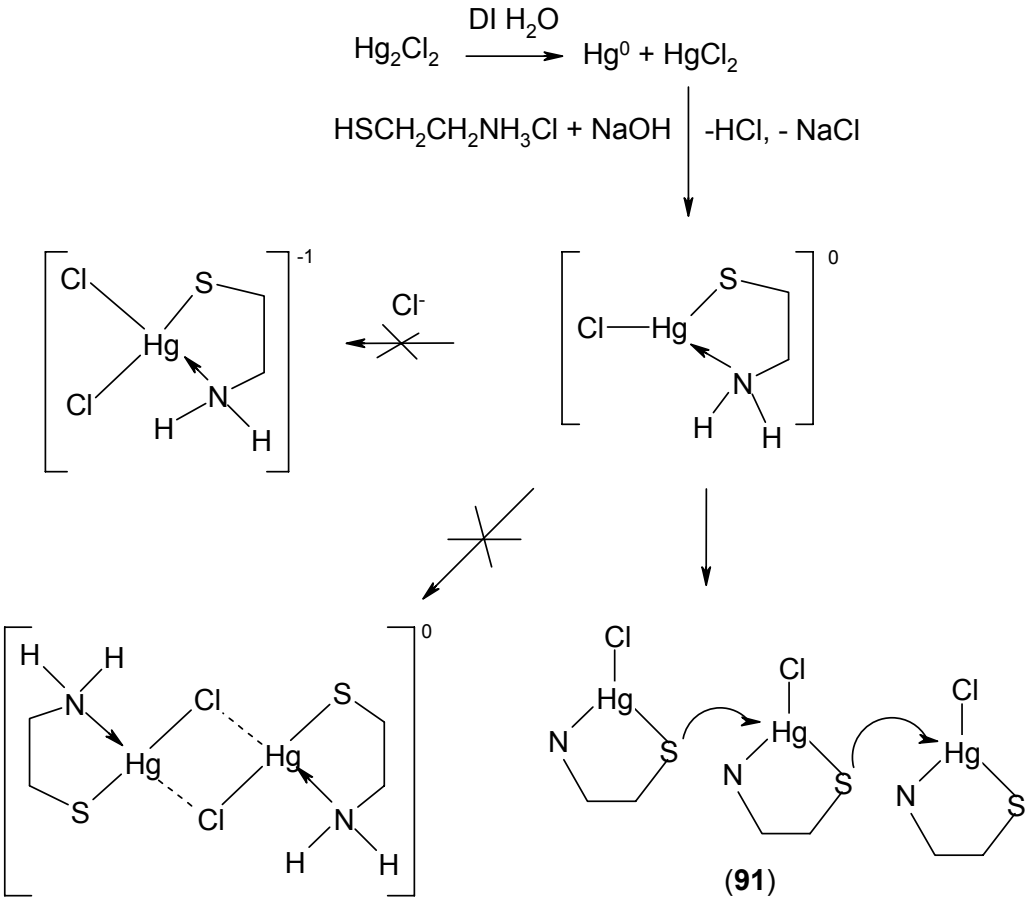

Scheme 4.3. Proposed mechanism for the formation of **91**.

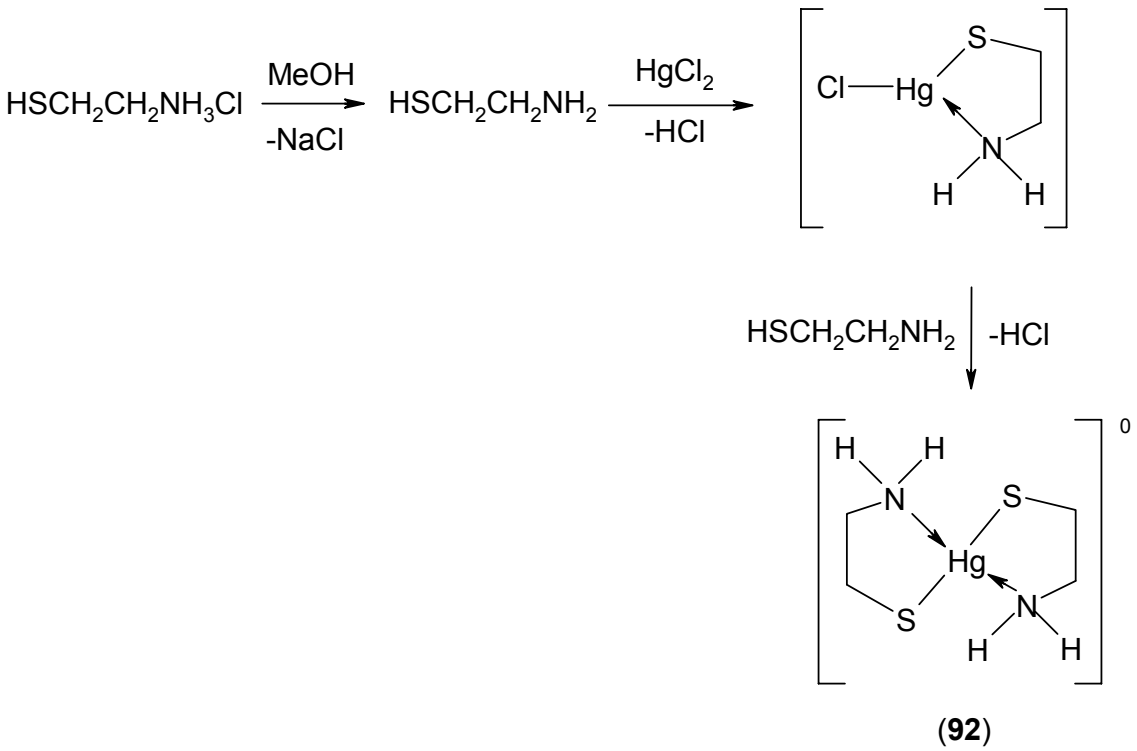

(**92**)

Scheme 4.4. Proposed mechanism for the formation of **92**.

4.3.2 Spectroscopy

In the ^{1}H NMR for **94**, the CH_2S and CH_2N peaks are observed at 3.0 and 3.14 ppm, respectively. In the ^{13}C NMR, the corresponding peaks are observed at 25.9 and 43.0 ppm, respectively. In **95**, shifts from the free ligand are not observed indicating the absence of Hg-S and Hg-N bonds.

A suitable peak in the ^{199}Hg solution NMR of **94** could not be obtained, which is most probably due to the presence of five independent (three- and four-coordinate) Hg centers.

In the IR and Raman, the absence of a peak at 2500 cm^{-1} indicates the absence of an -SH group. The characteristic peaks at 3400 cm^{-1} are indicative of the NH_3^+ group. The symmetric and asymmetric stretches for Hg-S in **94** are observed at 288 and 339 cm^{-1}, respectively. The stretch due to a terminal Hg-Br bond in both **94** and **95** could be assigned to the peaks at 190 cm^{-1}. Similar peaks have been observed in anionic $[Hg_2Br_6]^{2-}$ (150 cm^{-1}).[199]

The λ_{max} due to the S → Hg LMCT for **94** is observed around 270 nm indicating a tetrahedral geometry around the Hg center. Similar transitions due to tetrahedral Hg are observed in **88 - 91**.

4.3.3 Crystal Structures

The compound **94** (Figure 4.7, Table A26) is the only known nonanuclear heteroleptic Hg(II)-thiolate. The molecule can be considered as composed of three trinuclear $[Hg_3Br_5(SCH_2CH_2NH_3)_3]^+$ units with bridging S and Br atoms. In the molecule four different types of environment are observed around the Hg atoms, namely $HgSBr_3$,

HgS_2Br_2, $HgSBr_3$ and HgS_2Br. Within a unit, three independent Hg atoms are observed. The Hg atoms are three- and four-coordinate with bridging S and either bridging or terminal Br atoms. The Hg-S distances observed (2.424 - 2.488 Å) within a unit are close to the range observed for similar four-coordinate Hg(II)- thiolates (2.360 - 2.420 Å, 2.480 – 2.610 Å).[91,171] The bridging Hg-S distances (Hg2-S1B and S1-Hg2B = 2.811 Å) between the units are much longer than the corresponding Hg-S distances within the unit. The Hg3-S distances are slightly longer than the distances observed in Hg(II)-thiolates with an $HgSBr_3$ moiety such as $[HgBr_2(tzdtH)]_2$ (2.435 Å).[114] This is due to the presence of a bridging rather than a terminal thiolate. The terminal Hg-Br distances (2.559 – 2.790 Å) are close to the range found in the literature (2.470 – 2.650 Å).[112,113] The bridging Hg-Br distances (avg 3.004 Å) are also close to the literature values (2.730 – 2.900 Å).[171] A variation is commonly found for terminal and bridging Hg-Br distances of thiolate-bridged compounds of Hg(II).[200] The Hg-Br-Hg bridge is symmetrical (3.073 Å), which is in contrast to the fact that unsymmetrical Hg-Br-Hg bridges are more frequently observed.[201-203] The weak Hg-S_{br} (between units) and normal Hg-Br_{br} distances suggest that Br plays a more important role than S in holding three different units together.

The greatest deviation from an ideal tetrahedral geometry is observed in the angles S1-Hg1-S2, 172º and S2-Hg1-Br2, 85.0º. The relatively weaker secondary contacts around Hg are responsible for an almost linear S-Hg-S angle (168º). The broader angles observed are bonded to S atoms and the more narrow angles are associated with bridging Br. The Hg atoms in a unit are arranged in a zigzag pattern similar to that observed in **70**.[92] If seen along the 'b' axis it is observed that the Hg atoms in unit one and unit three are on top of each other and the second unit is arranged in a spiral fashion

with bridging thiolate and bromide atoms. Such a bonding pattern has not been observed previously. For example, in clusters such as $[Ag_9(SCH_2CH_2S)_6]^{3-}$ the Ag atoms are arranged in a tetragonal prism of eight Ag, centered by a ninth Ag atom.[204]

The structure of **95** revealed a diammonium disulfide along with $[HgBr_4]^{2-}$ as the counter anion (Figure 4.8, Table A27). The absence of Hg-S or Hg-N bonds is remarkable, as similar reaction conditions are shown to yield Hg(II)-thiolates such as **92** and **100**. However, similar adducts have been reported in the literature, for example; {$[HgI_4][tab]$} (tab = 4-trimethyl-ammoniumphenyl disulfide).[205] This compound was obtained from organic solvents, in contrast to **95**, which was obtained from aqueous media. The geometry around Hg is distorted tetrahedral with the Br atoms involved in intermolecular hydrogen bonding with the ammonium groups from the disulfide unit.

4.3.4 Mechanistic Pathway for the formation of 94

Compound **94** is composed of three equivalent trinuclear units. The formation of an individual unit can be thought to proceed through rearrangement of a two-coordinate intermediate ($[HgBr(SCH_2CH_2NH_3)]^+$), three-coordinate intermediate $[HgBr(SCH_2CH_2NH_3)_2]^+$] and free $HgBr_2$ present in the solution (Scheme 4.5). The free Br^- in solution further adds across an $[HgSBr_2]$ unit to form $[HgSBr_3]$, with a four-coordinate Hg, similar to that observed in **90**. The individual trinuclear units organize further through with weak Hg-S and Hg-Br interactions to form the nonanuclear cluster (**94**).

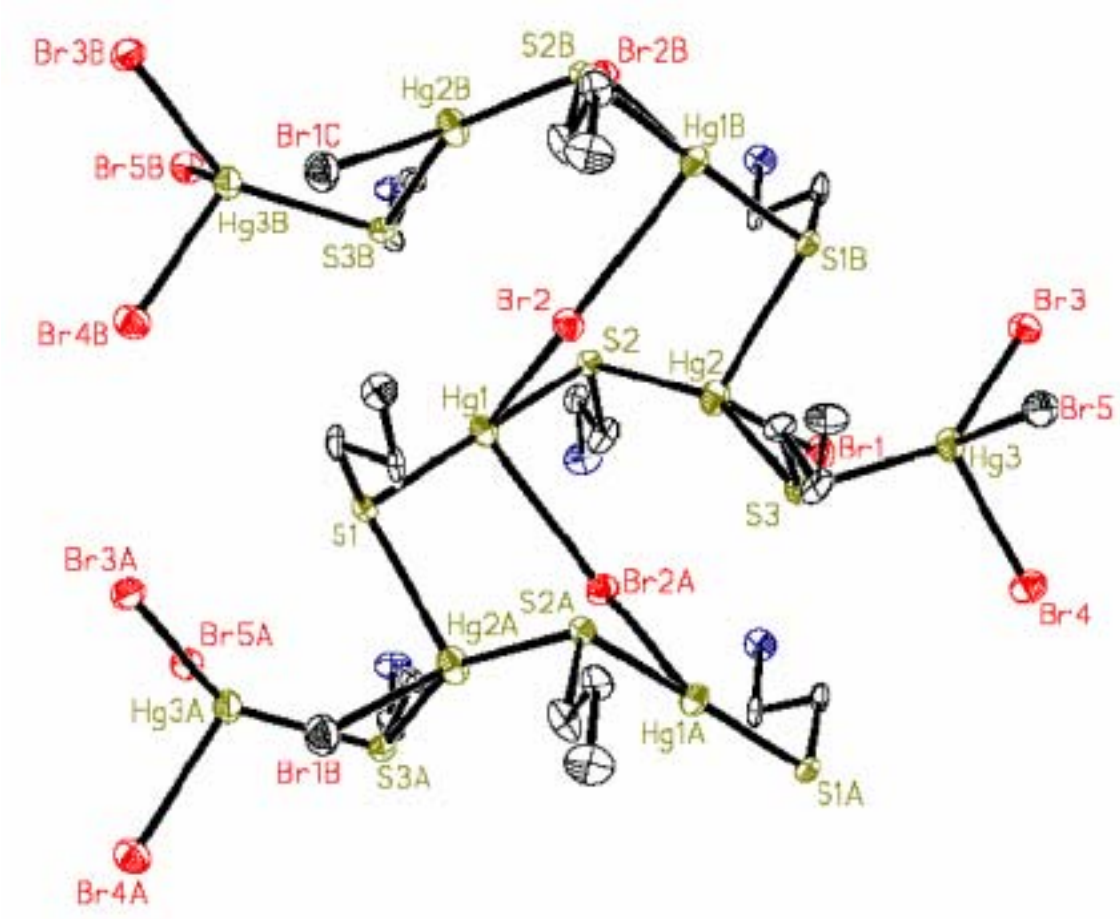

Figure 4.7. Molecular structure of **94** with 50 % probability thermal ellipsoids. The hydrogen atoms and counter anions are omitted for clarity.

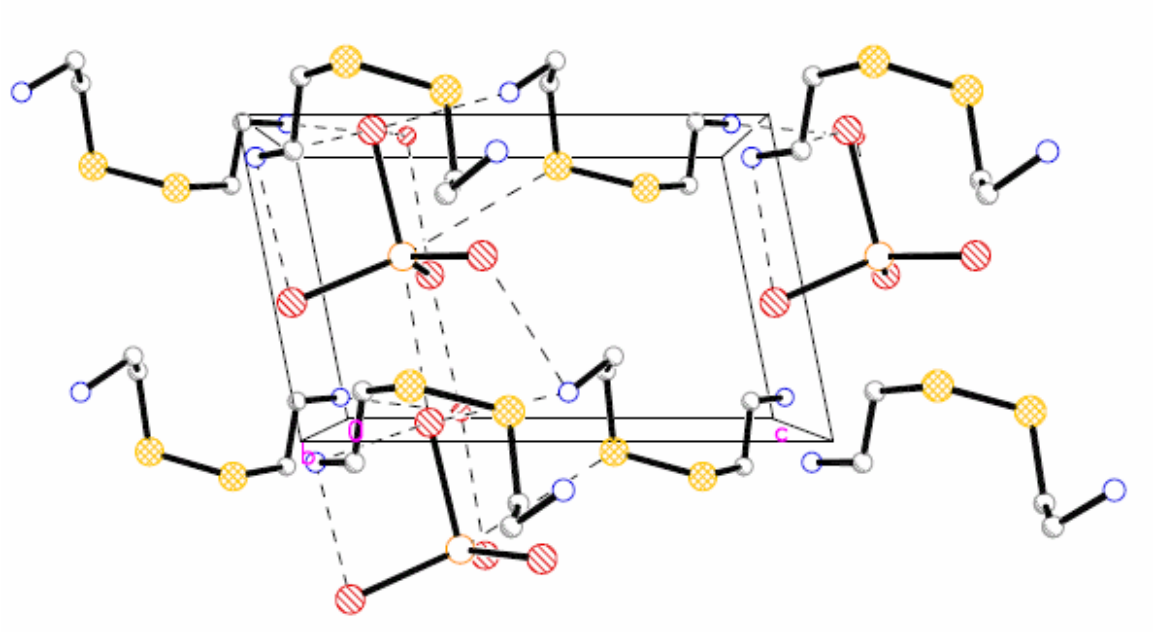

Figure 4.8. View of **95** with intermolecular hydrogen bonding shown with dotted lines.

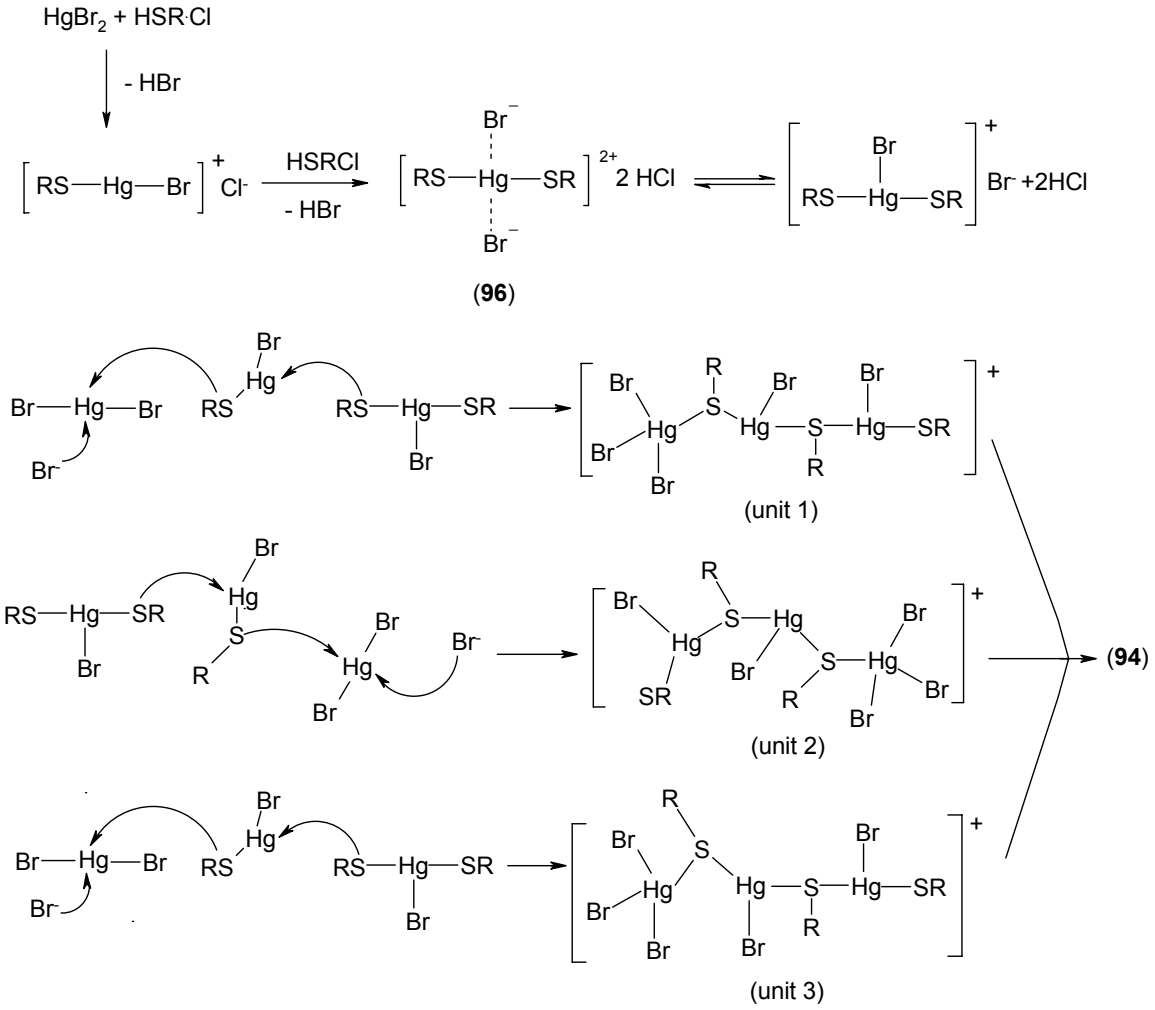

Scheme 4.5. Proposed pathway for the formation of **94** through **96**, where R = -$CH_2CH_2NH_3^+$.

4.4 Compounds of AET with HgI_2

4.4.1 Synthesis and Characterization

Combination of AET·HCl and HgI_2 in a 2:1 ratio yielded the linear bis-thiolate $[Hg(SCH_2CH_2NH_3)_2]I_2$ (**97**), which is isostructural to **88** and **96**. However, a similar reaction, if stirred for a longer time yielded polynuclear $[Hg_4I_8(SCH_2CH_2NH_3)_2]_n \cdot nH_2O$ (**98**). In the presence of an equivalent amount of base (OH^-) a cyclic molecular structure, $[Hg_4I_4(SCH_2CH_2NH_2)_4]$ (**99**) is obtained.[206] The same reaction used in the formation of **99** with neutral ligand yielded a compound with a cyclic structure $[Hg_4I_6(SCH_2CH_2NH_2)_2(SCH_2CH_2NH_3)_2]$ (**100**), when a four-coordinate compound similar to **92** was expected.[198] This is most probably due to the higher polarity of water compared to alcohol, where ligand exchange and rearrangement is much faster. The reactions are summarized in scheme 4.6.

4.4.2 Spectroscopy

The ^1H NMR spectra of **98** - **100** show a significant downfield shift in the methylene protons attached to sulfur (Table A28) from that of free ligand (2.69 ppm). These shifts are, however, slightly upfield compared to those observed for **97** (3.27 ppm). In **99** and **100**, the shift observed for the methylene protons adjacent to nitrogen (~ 2.96 ppm) is comparable to that observed in **91** (2.97 ppm) and **92** (2.92 ppm),[126] indicating an Hg-N contact.

In the ^{13}C spectra a downfield shift is observed for C-S in comparison to that of 2-aminoethanethiol (22.2 ppm). The C-N peaks, however, do not show profound shifts from that observed for free ligand (42.8 ppm for 2-aminoethanethiol).

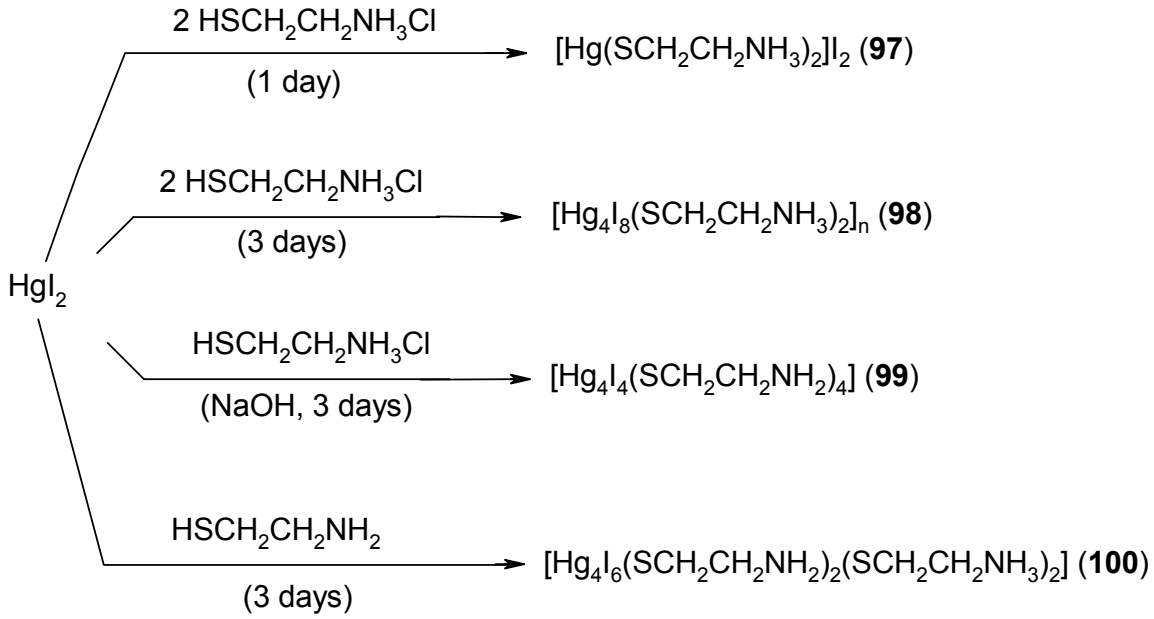

Scheme 4.6. Synthesis of **97** - **100**.

This observation is in contrast to the presence of the Hg-N bond observed in **99** and **100**. It can be concluded that in the presence of an additional Hg-I bond, the shielding of carbon attached to nitrogen is negligible, something not observed in **92** (46.1 ppm), where a significant shift is observed despite a weaker Hg-N bond.[126]

A suitable peak in the ^{199}Hg solution NMR for **98** could not be observed due to the presence of three independent Hg centers and shielding due to I atoms. However, in **99** a broad peak at -642 ppm indicates the presence of four-coordinate Hg. The broadening of the signal supports the presence of an Hg-N bond since coupling between N and Hg could be responsible for such broadening. Similar broadening has been observed for amine-mercuric chloride complexes[207] as well as in **92** (-659 ppm in d_6-DMSO).[126] The ^{199}Hg NMR for **100** shows two distinct peaks at - 2983 and - 1928 ppm, which could be assigned to HgI_2S_2 and HgISN coordination environments, respectively. The shielding present in the first peak is most probably due to the presence of two Hg-I bonds. Despite a similar [$HgIS_2N$] environment as of **99**, a broad peak around -660 ppm is not observed in **100** indicating absence of an Hg-N bond. This could be due to the equilibrium between four-coordinate [$HgIS_2N$] and three-coordinate [$HgIS_2$] units in the solution.

In the IR spectra a significant change in the C-S stretch (≈ 629 - 675 cm^{-1}) is observed compared to the free ligand (757 cm^{-1}). This might be due to the slight difference in the C-S distance compared to the free ligand as evident from the X-ray studies. In **97** and **98**, the band at 2962 cm^{-1} can be assigned to a symmetric NH_3^+ stretch. Also peaks at 1468 and 1594 cm^{-1} can be assigned to symmetric deformation and degenerate deformation modes, respectively, for the -NH_3^+ group. In **99** and **100**, peaks

around 3000 - 3448 cm^{-1} can be assigned to antisymmetric as well as symmetric NH_2 stretches, which are characteristic of primary amines.

In the Raman spectra of **99** and **100** the symmetric and asymmetric frequencies for Hg-S are observed around 260 and 341 cm^{-1}, respectively. In **98**, the corresponding peaks are observed around 287 and 340 cm^{-1} and are in the range observed for a distorted tetrahedral Hg environment. In **99** and **100**, the peak at ~ 490 cm^{-1} can be assigned to the Hg-N stretch, which is in the range observed for Hg-thiolates with Hg-N bonding (400 - 700 cm^{-1}).[208] The terminal Hg-I frequencies can be assigned to the peaks around 125 and 135 cm^{-1}, respectively, and are in accord with the terminal Hg-I frequencies reported in the literature.[95,116,209] The peak at 106 cm^{-1} can be assigned to the bridging Hg-I stretch, which is comparable to the peak observed in $[Hg_2I_6]^{2-}$.[210]

4.4.3 Crystal Structures

The tetranuclear repeating unit in **98,** $[Hg_4I_8(SCH_2CH_2NH_3)_2]$,·connected through bridging S atoms to form a one-dimensional polymeric chain, consists of three independent Hg centers, namely HgI_3S, HgI_2S_2 and HgI_4 (Figure 4.9, Table A29). Hg1 and Hg2 are are bonded to one bridging S, one terminal I, and two bridging I atoms, Hg2 is bonded to two bridging S and I atoms and Hg4 is attached to two bridging and two terminal I atoms. The geometry around the Hg atoms can be best described as distorted tetrahedral, which is indicated by angles ranging from 141º to 89º. The smallest deviation is observed in the HgI_4 moiety followed by the HgI_3S unit, which suggests the tendency of Hg to maximize bonding with S (S-Hg-S = 133º in HgS_2I_2 moiety). The Hg-I_{br}-Hg angles observed (avg 86.7º) are in the range found for $Hg_2I_6^{2-}$ (83.8 - 88.0º).[211] The Hg-S

distances in the tetranuclear unit as well as between the repeating units (avg 2.478 Å) are in accord with other polymeric heteroleptic Hg-thiolates (avg 2.450 Å). [85,212] The Hg-I distances are variable depending on their presence at terminal (avg 2.687 Å) or bridging (avg 2.953 Å) positions but in agreement with corresponding distances observed in Hg-thiolates with both terminal and bridging Hg-I bonding such as $[HgI_2(tzdtH)]_2$ (2.669 Å (ter) and 3.059 Å (br)) and $[Hg_2I_5(SC_3H_7)]^{2+}$ (2.723 Å (ter) and 2.994 Å (br)).[211]

Compound **99** is a centrosymmetric tetranuclear molecule with an eight-membered ring consisting of alternate Hg and S atoms. The four metal centers have similar coordination environments consisting of S, N and a terminal I atom (Figure 4.10, Table A30). The octagonal ring is non-planar with the I atoms attached to Hg and present on the opposite sides of the mean plane. However, the geometry defined by the four Hg atoms can be considered as square planar with S atoms present above and below the plane. The sets of equivalent $[HgI(SCH_2CH_2NH_2)]$ units are connected through bridging S atoms. The geometry around HgS_2Cl_2 is distorted tetrahedral, whereas around HgS_2N_2 it is approximately octahedral including the secondary interactions with Cl or Br ions.

The geometry around the Hg atom is distorted tetrahedral with the smallest angles observed in the five-membered ring (N-Hg-S ≈ 82º) and largest angles associated with the thiolate S atoms (S-Hg-S' ≈123º). The Hg1-S1 distance (2.518 Å) associated with the five membered S/N chelate is longer than the bridging Hg1-S2 distance (2.476 Å). The Hg1-S1 distance is similar to the sum of the covalent radii of tetrahedral Hg and S atoms (2.52 Å),[213] whereas Hg2-S1 is much smaller. Asymmetric distances are quite common for Hg-thiolates, where formation of a longer bond is compensated by the presence of another shorter Hg-S bond to achieve overall electronic stability.[214] The Hg-N distances

are variable (2.371 Å and 2.404 Å) but in accord with the corresponding distances observed in Hg(II)-thiolates with an additional N donor ligand such as in $[HgO_2CCH_2(RS)(L)]$ (R = Me, Et, and L = C_6H_7N and C_5H_5N) (avg Hg-N 2.48 Å). [89,118]

In **100**, two independent Hg centers, namely, HgS_2I_2 and HgS_2NI are observed (Figure 4.11, Table A31). The geometry around Hg can be best described as distorted tetrahedral with the smallest angle observed in the five-membered chelate (83º) and largest angle in S-Hg-S (136º).

Similar trends have been observed for **99**. The average Hg-S distance of 2.485 Å is smaller than that observed in **99** as well as in tetrahedral Hg(II)-thiolates (2.505 - 2.606 Å). Similarly, average Hg-I distances (2.827 Å) are slightly longer than those observed in **99** (avg 2.758 Å).

However, the Hg-N distances (avg 2.391 Å) are in agreement with those observed in **99** (2.387 Å) but smaller than those reported for Hg(II)-thiolates with an additional N donor ligand (avg 2.480 Å).[89,118] The trend in Hg-S and Hg-I distances compared to **99** is in agreement that longer Hg-I are compensated by shorter Hg-S to achieve overall stability.

The $-CH_2CH_2NH_2/NH_3^+$ groups are opposite to each other with respect to the plane formed by four Hg atoms to avoid steric interactions. Similarly the HgI_2 units are also present above and below the plane. The amine/ammonium groups are involved in intermolecular hydrogen bonding to form a three-dimensional network.

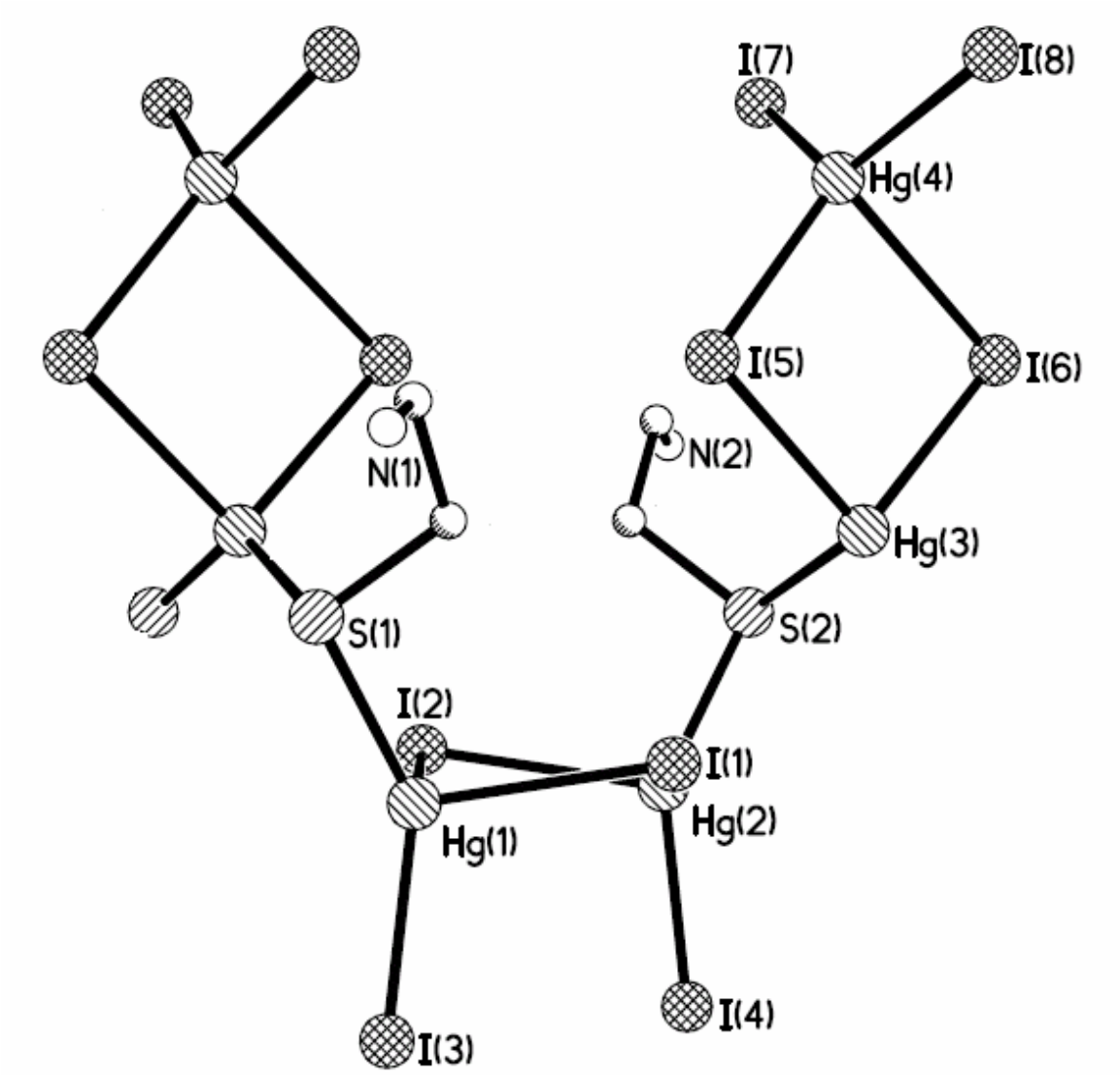

Figure 4.9. The repeating unit of **98**. The bridging Hg-S bonds are not shown for clarity.

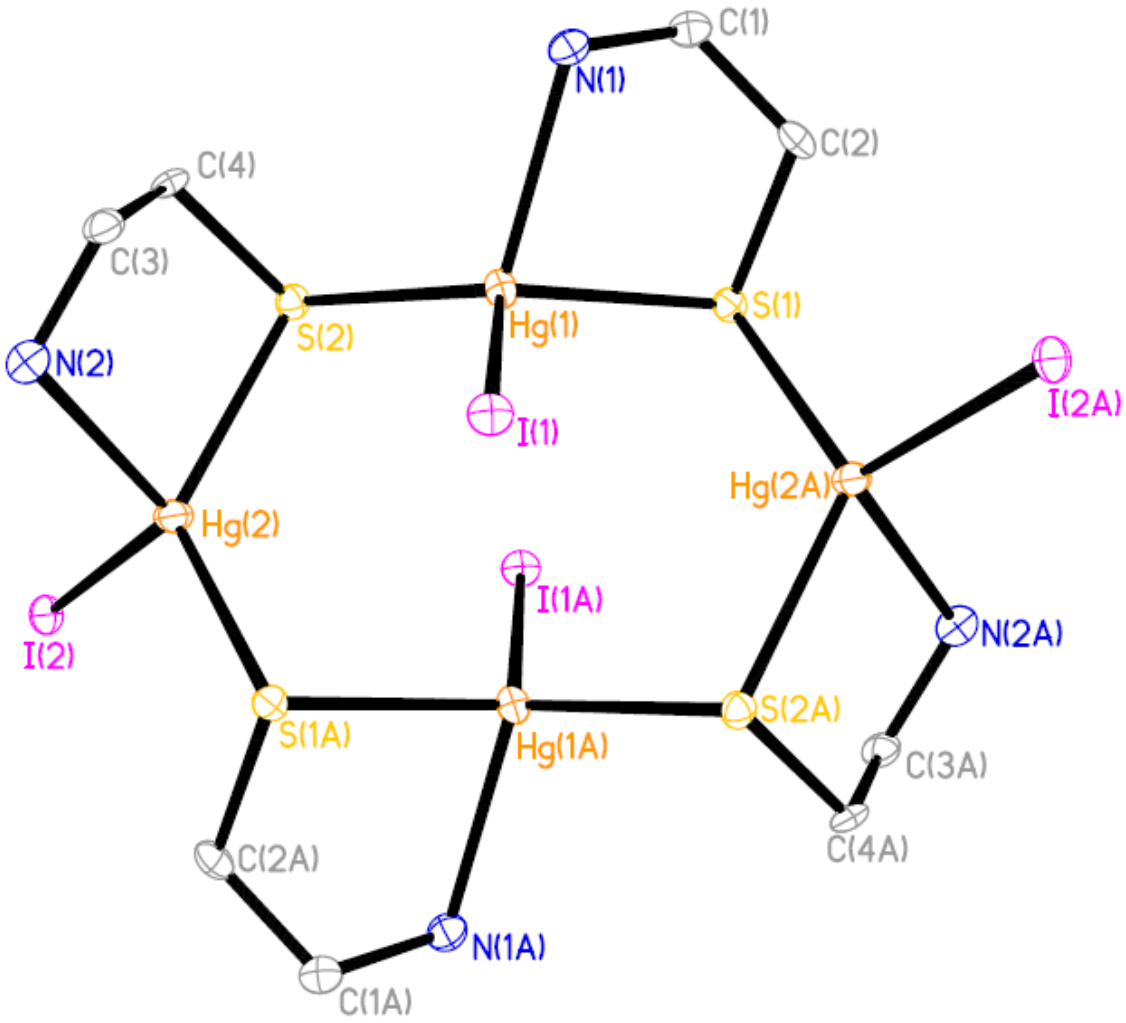

Figure 4.10. View of **99** with 50% thermal ellipsoids and hydrogen atoms omitted for clarity.

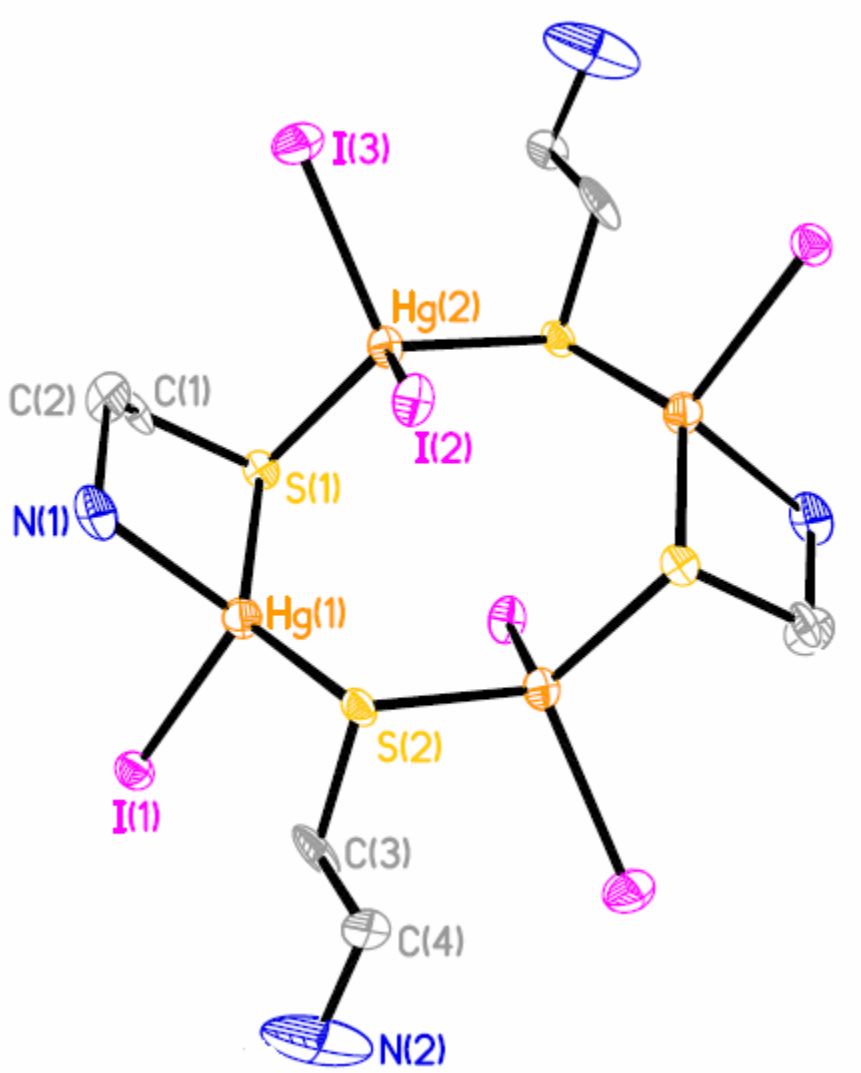

Figure 4.11. View of **100** with 50 % thermal ellipsoids. Solvent molecules and hydrogen atoms are not shown for clarity.

4.4.4 Mechanistic pathway for the formation of 98 - 100

Based on two distinct $Hg_2S_2I_4$ moieties and common features observed for HgI_2-thiolates a general mechanism for the formation of **98** can be proposed (Scheme 4.7). The reaction proceeds through the formation of a three-coordinate intermediate, $[HgI_2(SCH_2CH_2NH_3)]$. This three-coordinate unit is common for Hg(II)-thiolates containing I atoms such as tzdtH[114] and $imtH_2$)[99]. The intermediate can either dimerize to form $[Hg_2I_4(SCH_2CH_2NH_3)_2]$ or react with free HgI_2 to form $[Hg_2I_4(SCH_2CH_2NH_3)]$. One of the thiolates from unit $[Hg_2I_4(SCH_2CH_2NH_3)_2]$ adds across $[Hg_2I_4(SCH_2CH_2NH_3)]$ to yield **98**. The three-coordinate intermediate and the dinuclear species could be isolated from less polar solvents, where the rate of ligand exchange is much slower.

For the formation of **99** and **100**, two different three-coordinate intermediates, namely $[HgI_2(SCH_2CH_2NH_3)]$ and $[HgI(SCH_2CH_2NH_2)]$ can be considered as building units (Scheme 4.8). These structural units have been reported for several Hg(II)-thiolates including **48** and **49**.[98,99] The formation of $[HgI_2(SCH_2CH_2NH_3)]$ is most probably due to the partial solubility of HgI_2 in water, which otherwise in alcohol would have yielded $[Hg(SCH_2CH_2NH_2)_2]$. The stability around the three-coordinate Hg(II) intermediate is achieved by formation of bridging Hg-S with a thiolate from another unit. These units further oligomerize to form the cyclic tetranuclear unit of **99**. The choice of formation of $[HgI(\mu\text{-}SCH_2CH_2NH_2)(SCH_2CH_2NH_2)]$ over $[HgI_2(SCH_2CH_2NH_2)]$ in **99** is most probably due to the preference of Hg for S over I (bond energies 217.1 and 34.69 kJ/mol, respectively). This is also evident from the X-ray structure, where the Hg-S distance between two $[HgI(SCH_2CH_2NH_2)]$ units is stronger compared to that in the five-

membered ring. However, in case of **100**, another three-coordinate intermediate, namely $[HgI_2(SCH_2CH_2NH_3)]$ comes in contact with $[HgI(SCH_2CH_2NH_2)]$ to form a dimer, which oligomerize to form tetranuclear unit of **100**.

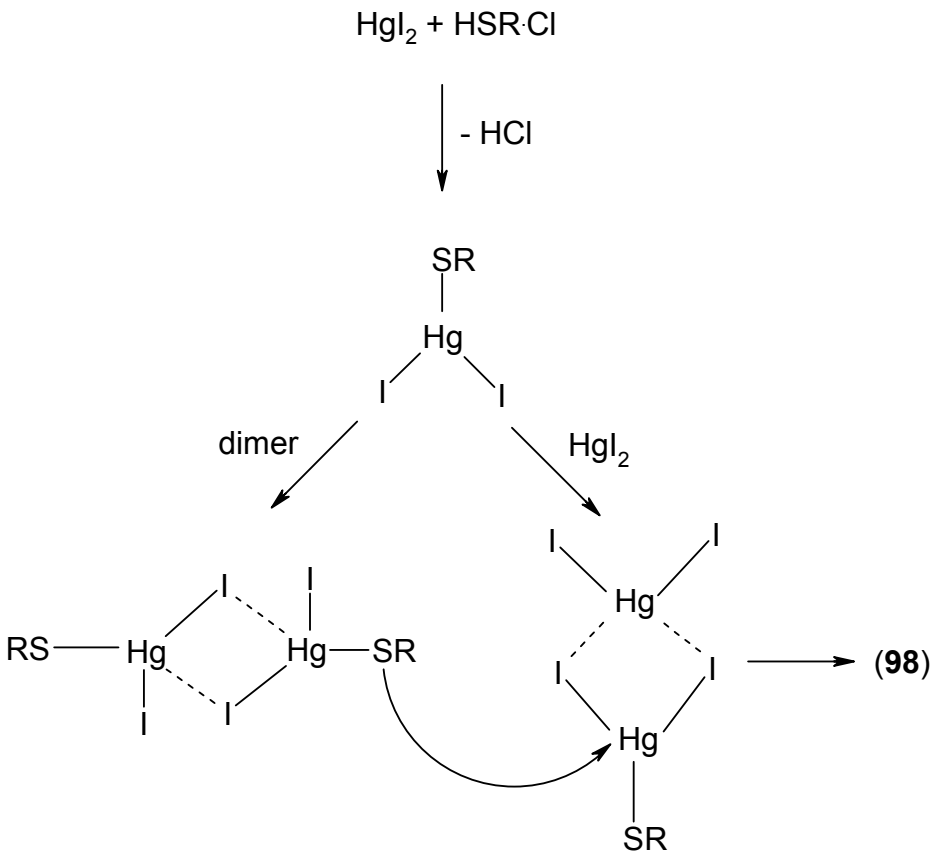

Scheme 4.7. Proposed mechanism for the formation of **98**, where R = $-CH_2CH_2NH_3^+$.

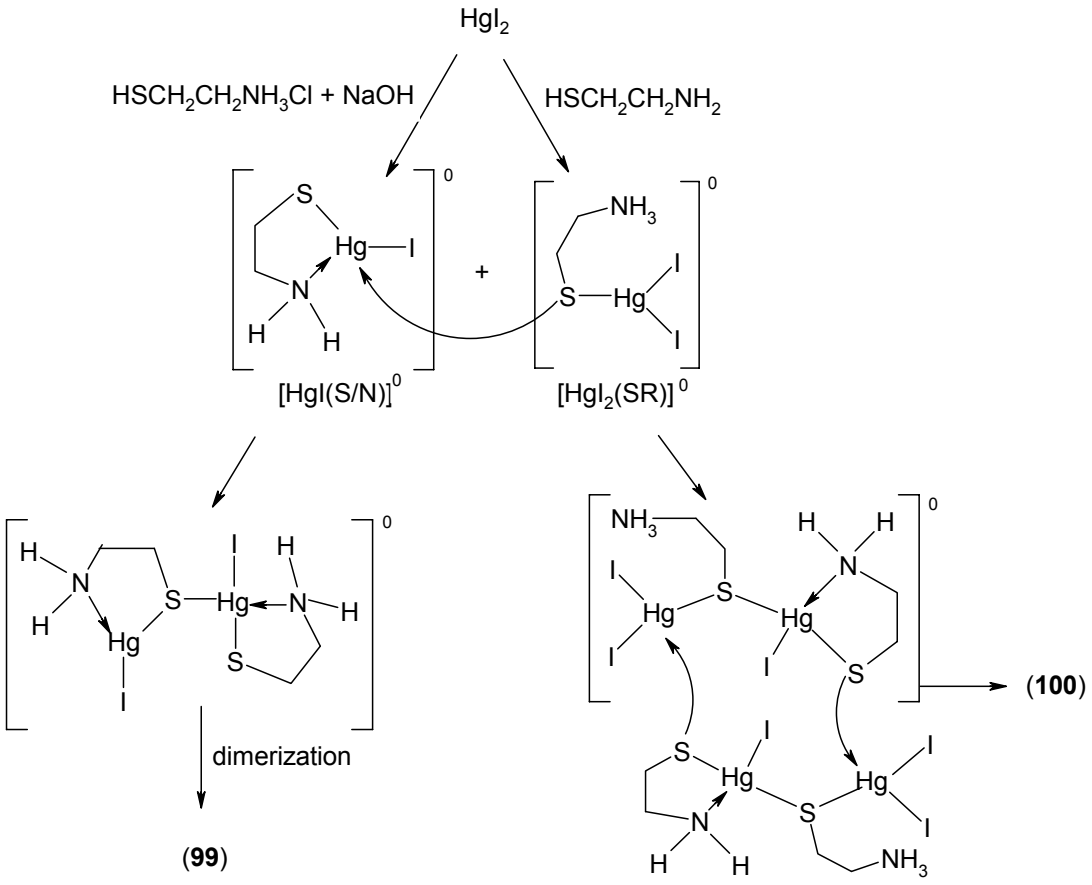

Scheme 4.8. Proposed mechanism for the formation of compounds **99** and **100**.

4.5 Experimental Section

General Procedure. The reactions were carried out at room temperature in a mixture of DI water and methanol under nitrogen. The reagents 2-aminoethanethiol hydrochloride (TCI America) and HgX_2 (X = Cl, Br and I) (Alfa Aesar) were used as received. ^{1}H and ^{13}C NMR data were obtained with JEOL-GSX-400 and 270 instruments operating at 199.17 MHz using d_6-DMSO as solvent. The $^{199}Hg\{^{1}H\}$ NMR spectrum in d_6-DMSO were collected at 25 ºC on a Varian INOV 400 MHz instrument with 4-Nucleus Autoswitchable 5mm Probe and referenced to 1M $HgCl_2$ in DMSO at -1500 ppm as external reference[207,215] and checked against external 0.1M $Hg(ClO_4)_2$ in D_2O (-2250 ppm).[216] The IR data was recorded as KBr pellets on a Mattson Galaxy 5200 FT-IR instrument between 400 - 4000 cm^{-1}. Mass Spectral data were obtained from the University of Kentucky Mass Spectrometry Facility. Raman spectra were obtained on a Nicolet FT-Raman 906 Spectrometer ESP between 100 - 800 cm^{-1} in Center for Applied Energy Research at the University of Kentucky Facility. The UV-Vis studies were conducted on an Agilent HP 8453 instrument by using 0.05 mM solutions in deionized water.

X-ray Crystallography. Crystals of compounds **88** to **100** were obtained from the supernatant at 4 ºC or by recrystallization of the resulting precipitate from hot water. X-ray diffraction data of **100** and **88 - 99** were collected at 90 K on a Bruker-Nonius X8 Proteum diffractometer unit using Cu-Kα radiation and Nonius Kappa CCD diffractometer unit using Mo-Kα radiation, respectively from regular shaped crystals mounted in Paratone-N oil on glass fibers. Initial cell parameters were obtained using

DENZO[217] from 1º frames and were refined *via* a least-square scheme using all data-collection frames (SCALEPACK).[217] The structures were solved by direct methods (SHELXL97)[218] and completed by difference Fourier methods (SHELXL97).[218] Refinement was performed against F^2 by weighted full-matrix least-square and empirical absorption correction (SADABS)[218] were applied. Hydrogen atoms were placed at calculated positions using suitable riding models with isotropic displacement parameters derived from their carrier atoms. Non-hydrogen atoms were refined with anisotropic displacement parameters. Atomic scattering factors were taken from the International Tables for Crystallography Volume C.[219]

Synthesis of $[Hg(SCH_2CH_2NH_3)_2](Cl)_2$ (88): To a stirring solution of AET·HCl (1.14 g, 10.0 mmol) in DI water (15.0 mL) was added mercury(II) chloride (1.36 g, 5.00 mmol) and stirred overnight at room temperature. The resulting solution was allowed to stand for 2 weeks at 4 C during which time colorless cubic crystals formed in high yield. Yield: 1.72 g (81.0 %); Mp: 218 – 220 C (dec.). ^{1}H NMR (D_2O, 400 MHz): δ 3.23 (t, 2H, CH_2N), 3.27 (t, 2H, CH_2S). ^{13}C NMR (D_2O, 100 MHz): δ 25.2 (CH_2S), 43.3 (CH_2N). IR (KBr; ν/cm^{-1}): 3445w, 2991s, 2904s, 2720w, 2606w, 2532w, 2410w, 1604s, 1566s, 1491s, 1477s, 1420w, 1405m, 1366w, 1315m, 1264s, 1249m, 1134m, 1094m, 1077m, 1034m, 1015w, 933s, 882m, 802w, 787m, 724w, 653w, 453w. Anal. Calc. for $C_4H_{14}Cl_2HgN_2S_2$: C, 11.2; H, 3.32; N, 6.58; S, 15.1. Found: C, 11.3; H, 3.25; N, 6.70; S, 15.0.

Synthesis of $[Hg_6Cl_8(SCH_2CH_2NH_3)_8)]Cl_4{\cdot}4H_2O$ (89): To a stirring solution of AET·HCl (2.28 g, 20.0 mmol) in DI water (40.0 mL) was added mercury(II) chloride (2.70 g, 10.0 mmol) and the resulting solution was stirred for 3 days at room temperature. The solution was then allowed to stand for 2 weeks in the refrigerator at 4 ºC, during which time colorless cubic crystals formed. Crystalline yield: 3.46 gm (60.0 %); Mp: 204 - 206 ºC. ^{1}H NMR (DMSO, 200MHz, ppm): δ 3.00 (t, 2H, CH_2N), δ 3.14 (t, 2H, CH_2S) and δ 7.91 (s, 3H, NH_3). ^{13}C NMR (DMSO, 200 MHz, ppm): δ 25.9 (CH_2S), δ 43.0 (CH_2N). IR/Raman (KBr, ν/cm^{-1}): 3448, 3058, 2991, 2906, 1604, 1566, 1477, 1404, 1365, 1313, 1263, 932, 881, 786, 724, 712, 691, 502, 340, 298, 285, 272, 263, 251, 234, 221, 178, 133. MS (EI, +ve): 356, $[Hg(SCH_2CH_2NH_3)_2 + 1]^+$; 389, $[HgCl(SCH_2CH_2NH_3)_2 - 1]^+$; 313, $[HgCl(SCH_2CH_2NH_3)]^+$. Anal. calcd for $[Hg_6Cl_8(SCH_2CH_2NH_3)_8)]Cl_4{\cdot}4H_2O$: C, 8.28; H, 2.78; N, 4.83. Found: C, 8.20; H, 2.63; N, 4.79.

Synthesis of $[\{Hg_3Cl_5(SCH_2CH_2NH_3)_3\}Cl]_n$,(90): To a stirring solution of AET·HCl (1.14 g, 10.0 mmol) in DI water (50 mL) was added mercurous(I) chloride (1.80 g, 5.00 mmol). The resulting solution was stirred at room temperature for 3 days to obtain clear solution. The elemental mercury was removed and the filtrate was partially evaporated to obtain colorless crystals. Yield: 2.01 gm, 77.0 % and Hg^0 (0.480 gm, ≈ 50.0 %). Mp: 204 - 206 ºC. ^{1}H NMR (DMSO, 200 MHz, ppm): 2.94 (t, 2H, CH_2N), 3.08 (t, 2H, CH_2S) and 6.33 (br, 3H, NH_3). ^{13}C NMR (DMSO, 200 MHz, ppm): 26.7 (CH_2S), 42.8 (CH_2N). IR/Raman (KBr, ν/cm^{-1}): 3444, 2966, 1603, 1467, 1366, 1285, 1029, 807, 763, 686, 629, 621, 559, 477, 391, 351, 269, 225, 215, 189. MS (EI, +ve): 390,

($[HgCl(SCH_2CH_2NH_3)_2]^+$, 5%); 309, ($[Hg(SCH_2CH_2NH_3)_2]^+$, 10%); 277, ($[Hg(SCH_2CH_2NH_3)]^+$, 12%); 200, ([Hg]º, 25%); 77, ($[SCH_2CH_2NH_3]^+$,25%). Anal. calcd for $C_6H_{21}C1_6Hg_3N_3S_3$: C, 6.89; H, 2.02; N, 4.01. Found: C, 6.82; H, 1.99; N, 3.98.

Synthesis of $[\{Hg_2Cl_2(SCH_2CH_2NH_2)\}_nH_2O]_n$, (91): To a stirring solution of AET·HCl (1.14 g, 10.0 mmol) and NaOH (0.040 g, 10.0 mmol) in DI water (50 mL) was added mercurous(I) chloride (3.60 g, 10.0 mmol). The resulting solution was stirred for 3 days at room temperature to obtain clear solution. The elemental mercury was removed and the filtrate was partially evaporated to obtain colorless crystals. Yield: 3.61 gm, 78.0 % and Hg^0 (0.980 gm, ≈ 50.0 %). Mp: 221 - 223 ºC (decompose without melting). ^{1}H NMR (DMSO, 200 MHz, ppm): 2.97 - 3.09 (m, 4H, CH_2N and CH_2S) and 8.13 (s, 2H, NH_2). ^{13}C NMR (DMSO, 200 MHz, ppm): 25.6 (CH_2S), 42.9 (CH_2N). IR/Raman (KBr, ν/cm^{-1}): 3452, 2966, 2827, 1603, 1386, 1262, 1102, 1021, 807, 757, 675, 627, 584, 467, 398, 345, 299, 248, 226, 190. MS (EI, +ve): 624, ($[HgCl(SCH_2CH_2NH_2)]_2^+$, 3%); 388, ($[HgCl(SCH_2CH_2NH_2)_2]^+$,4%); 200, ([Hg]º, 26%); 76, ($[SCH_2CH_2NH_2]^+$, 75%). Anal. calcd for $C_6H_{22}Cl_{13}Hg_3N_3S_3O_3$ requires: C, 7.05; H, 2.28; N, 4.32. Found: C, 7.02; H, 2.21; N, 4.26.

Synthesis of $[Hg_4Cl_6(SCH_2CH_2NH_3)_4]Cl_2$ (93): AET·HCl (1.14 g, 10.0 mmol) in deaerated DI water (30 mL) was added to a stirring solution of mercury(II) chloride (5.00 mmol, 1.80 g) in an ice bath. The resulting solution was stirred overnight in ice bath. The resulting turbid solution was filtered and kept at 4 ºC for crystallization. Colorless

crystals were obtained in less than 5 % yield, hence could not be characterized using spectroscopic techniques.

Synthesis of $[Hg_9Br_{15}(SCH_2CH_2NH_3)_9](Cl_{0.8}{\cdot}Br_{0.2})_3$ (94): To a stirring solution of AET·HCl (1.14 g, 10.0 mmol) in deionized water (20 mL) was added mercury(II) bromide (1.80 g, 5.00 mmol) to obtain a white precipitate. The precipitate was removed and dried and the filtrate was allowed to stand for 2 weeks at 4 ºC, during which time colorless crystals formed. Yield (crystals): 2.68 gm (42.0 %). Mp: 154 - 156 ºC. ^{1}H NMR (DMSO, 200 MHz, ppm): δ 2.95 (t, 2H, CH_2N), δ 3.15 (t, 2H, CH_2S) and δ 7.70 (s, 3H, NH_3). ^{13}C NMR (DMSO, 200 MHz, ppm): δ 27.1 (CH_2S), δ 42.8 (CH_2N). IR/Raman (KBr, ν/cm^{-1}): 3433, 3005, 2893, 1576, 1502, 1475, 1455, 1378, 1316, 1272, 1126, 1069, 1009, 933, 764, 752, 717, 604, 454, 339, 288, 268, 221, 196, 174, 150. MS (EI, +ve): 435, $[HgBr(SCH_2CH_2NH_3)_3 - 1]^+$; 356, $[HgBr(SCH_2CH_2NH_3)]^+$; 355, $[Hg(SCH_2CH_2NH_3)_2 + 2]^+$. Anal. calcd for $[Hg_9Br_{15}(SCH_2CH_2NH_3)_9](Cl_{0.8}{\cdot}Br_{0.2})_3$: C, 5.68; H, 1.66; N, 3.31. Found: C, 5.49; H, 1.58; N, 3.24.

Synthesis of $\{[HgBr_4][(NH_3CH_2CH_2S\text{-})_2]\}$ (95): To a stirring solution of AET (0.770 g, 10.0 mmol) in DI water (60 mL), mercury(II) bromide (1.80 g, 5.00 mmol) dissolved in methanol (20 mL) was added and stirred at room temperature for 2 days. The white precipitate was removed and dried and the filtrate was slowly evaporated to obtain colorless crystals. Yield (precipitate + crystals): 1.74 gm (52.0 %). Mp: 220 - 222 ºC (dec without melting). ^{1}H NMR (DMSO, 200 MHz, ppm): δ 3.02 (b, 4H, NCH_2CH_2S), δ 6.04 (b, 3H, NH_3). ^{13}C NMR (DMSO, 200 MHz, ppm): δ 29.4 (CH_2S), δ 41.9 (CH_2N).

IR/Raman (KBr, ν/cm^{-1}): 3430,3257, 2973, 2869, 1557, 1458, 1372, 1264, 1065, 1001, 936, 720, 647, 457, 336, 305, 157. MS (EI, +ve): 680, $[M - 6]^+$; 594, $[M - Br]^+$, 512, $[M - 2Br]^+$; 480, $[(HgBr_2)(CH_2CH_2SSCH_2CH_2)]^+$; 452, $[(HgBr_2)(CH_2SSCH_2)]^+$; 293, $[(Hg)(CH_2SSCH_2)]^+$; 281, $[(Hg)(CH_2SS)]^+$; 200, $[Hg]^+$. Anal. calcd for $\{[HgBr_4][(NH_3CH_2CH_2S\text{-})_2]\}$: C, 7.12; H, 2.09; N, 4.15. Found: C, 7.01; H, 2.15; N, 4.09.

Synthesis of $[Hg(SCH_2CH_2NH3)_2](Cl/Br)_2$ (96): To a stirring solution of AET·HCl (1.14 g, 10.0 mmol) in DI water (15 mL) was added mercury(II) bromide (1.80 g, 5.00 mmol) and stirred overnight at room temperature. The resulting solution was evaporated at room temperature to yield crystalline white precipitate of **96** in quantitative yield. The characterization data are similar to that of **88**.

Synthesis of $[Hg(SCH_2CH_2NH_3)]I_2$ (97): To a stirring solution of AET·HCl (1.14 g, 10.0 mmol) in DI water (15 mL) was added mercury(II) Iodide (2.27 g, 5.00 mmol) dissolved in minimum amount of methanol and stirred overnight at room temperature. The resulting solution was evaporated at room temperature to yield crystalline white precipitate of **97**. The characterization data are similar to that of **88**.

Synthesis of $[Hg_4I_8(SCH_2CH_2NH_3)_2]_n \cdot nH_2O$ (98): To a stirring solution of AET·HCl (10.0 mmol, 1.14 g) in a mixture of DI water (90.0 mL) and methanol (10.0 mL) was added mercury(II) Iodide (5.00 mmol, 2.27 g) dissolved in minimum amount of methanol and stirred at room temperature for three days. The precipitate was removed, washed with

methanol followed by cold water and vacuum dried. Evaporation of the filtrate at room temperature yielded x-ray quality crystals. Crystals could also be obtained by recrystallization of precipitate from DI water. Yield (crystals + precipitate): 4.03 g (80.0 %). Mp: 110 - 112º. ^{1}H NMR (d_6-DMSO, 200 MHz, ppm): δ 3.04 (m, 4H, SCH_2 and NCH_2), δ 7.68 (br, 3H, NH_3). ^{13}C NMR (d_6-DMSO, 200 MHz, ppm): δ 27.3 (CH_2S), δ 42.5 (CH_2N). IR (KBr, ν/cm^{-1}): 3720, 3448, 3164, 2962, 2831, 1594, 1468, 1407, 1364, 1260, 1086, 804, 675. MS (MALDI, m/z): 172, $[CH_2CH_2NH_3I]^+$; 144, $[NH_4I]^+$. Anal. calcd for $[Hg_4I_8(SCH_2CH_2NH_3)_2]\cdot 2H_2O$: C, 2.39; H, 0.903; N, 1.39. Found: C, 2.39; H, 0.903; N, 1.39.

Synthesis of $[Hg_4I_4(SCH_2CH_2NH_2)_4]$ (**99**): To a stirring solution of AET·HCl (10.0 mmol, 1.14 g) and sodium hydroxide (10.0 mmol, 0.400 g) in a mixture of DI water (90.0 mL) and methanol (10.0 mL) was added mercury(II) iodide (5.00 mmol, 2.27 g) dissolved in minimum amount of methanol and stirred at room temperature for three days. The precipitate was removed, washed with methanol followed by cold water and vacuum dried. Evaporation of the filtrate at room temperature yielded x-ray quality crystals. Yield (crystals + precipitate): 2.50 g (62.0 %). Mp: 175 - 177º. ^{1}H NMR (d_6-DMSO, 200 MHz, ppm): δ 2.84 (t, 2H, SCH_2), δ 2.96 (t, 2H, NCH_2), δ 6.06 (br, 2H, NH_2). ^{13}C NMR (d_6-DMSO, 200 MHz, ppm): δ 29.1 (CH_2S), δ 42.7 (CH_2N). IR (KBr, ν/cm^{-1}): 3445, 3164, 2831, 1601, 1555, 1364, 1266, 1153, 1018, 935, 630. MS (MALDI, m/z): 356, $[Hg(SCH_2CH_2NH_2)_2]^+$; 401, $[HgI(SCH_2CH_2NH_2)]^+$; 146, $[NH_4I]^+$; 172, $[CH_2CH_2NH_3I]^+$; 78, $[SCH_2CH_2NH_2)]^+$. Anal. calcd for $[Hg_4I_4(SCH_2CH_2NH_2)_4)]$: C, 5.95; H, 1.49; N, 3.47. Found: C, 5.94; H, 1.48; N, 3.48.

Synthesis of $[Hg_4I_6(SCH_2CH_2NH_2)_2(SCH_2CH_2NH_3)_2](H_2O)(EtOH)$ (100): To a stirring solution of AET (10.0 mmol, 0.770 g) in DI water (30.0 mL), mercury(II) iodide (5.00 mmol, 2.27 g) dissolved in ethanol (20.0 mL) was added and stirred at room temperature for three days. The light yellow precipitate was removed, washed with methanol followed by cold water and vacuum dried. Supernatant at 4 ºC yielded light yellow crystals. Yield (crystals + precipitate): 3.20 g (68.0 %). Mp: 188 - 190º (dec). ^{1}H NMR (d_6-DMSO, 200 MHz, ppm): δ 2.94 (b, 4H, NCH_2CH_2S), δ 3.58 (b, 2H, NH_2). ^{13}C NMR (d_6-DMSO, 200 MHz, ppm): δ 32.4 (CH_2S), δ 41.4 (CH_2N). IR (KBr, ν/cm^{-1}): 3445, 3164, 2831, 1601, 1555, 1364, 1266, 1153, 1018, 935, 630. MS (EI, +ve): 679, $[Hg_2C_4H_{13}N_2S_2I_2]^+$; 351, $[HgC_4H_{13}N_2S_2]^+$; 336, $[351 - CH_2]^+$; 326, $[336 - CH_2]^+$; 278, $[Hg(SCH_2CH_2NH_2)]^+$; 202, $[Hg]^+$; 77, $[SCH_2CH_2NH_3]^+$. Anal. calcd for $[Hg_4I_6S_4C_{10}H_{31}N_4O_2]$: C, 6.21; H, 1.61; N, 2.90. Found: C, 6.19; H, 1.59; N, 3.00.

4.6 Conclusion

Novel Hg(II)-2-aminoethanethiolates have been synthesized and characterized. In aqueous media the halide seems to be responsible for the formation of clusters rather than a two-coordinate compound with weak interactions. These results are in contrast to the reported Hg(II)-thiolates, where Cl, Br and sometime I derivatives are isostructural. The coordination around tetrahedral Hg in the clusters (**89**, **90**, **93**, and **94**) is more inclined toward a linear geometry. This may be related to the metal sites in metallothioneins, where incorporation of more than four Hg ions leads to a progressive change from tetrahedral to an essentially linear geometry.[182] The Hg---Hg contact observed in **90** are the shortest mercurophilic interaction reported for Hg(II)-thiolates for far. In the I derivatives, it is observed that the stronger Hg-I contacts (**98** - **100**) lead to the formation of low (two- or three-) coordination compounds, which then serve as precursors for the resulting thiolate clusters. On the other hand, Cl and Br derivatives along with additional secondary contacts to Hg are more prone to undergo rearrangement in solution due to a weak Hg-Cl/Br bond. This variation in geometries is due to the labile nature of low-coordinate Hg(II)-thiolates in solution, which is even more interesting in aqueous media.

The Hg-S distances in two-coordinate compounds (**88**, **96** and **97**) are in accordance to those observed for two-coordinate Hg(II)-thiolates (**44**, **45**). The distortion observed in S-Hg-S is related to weak interactions with counter anions. However in **97** despite the presence of I in close proximity, the S-Hg-S angle is essentially linear (180º). This linearity is not observed in two-coordinate compounds unless the ligand contains a bulky group. The Hg-S distances associated with four-coordinate Hg in **89** - **94** are much shorter comparable to those reported for four-coordinate Hg(II)-thiolates (**48** - **57**). The

Hg-N distances in **91** are shorter compared to those observed in **92** despite having a similar five-membered chelate around Hg as well as those observed in **66** - **68** and **73**. The strong Hg-N bond in **91** might be responsible for the distorted environment around Hg. The bridging Hg-S distances are **94** are much longer than those observed in similar Hg(II)-thiolates (**63** - **67**, **69**, **70** - **74**). However the bridging Hg-Br distances are within the limit reported in the literature. This implies the stronger influence of Br compared to thiolate for the formation of clusters. The symmetrical Br-Hg-Br distances in **94** are in contrast to unsymmetrical Br-Hg-Br distances usually reported for Hg(II)-thiolates. In **98** - **100**, despite similar reaction conditions variable coordination environments around Hg are observed. The geometry around the Hg atoms are distorted tetrahedral with increasing deviation in the order S-Hg-S < S-Hg-I< I-Hg-I. This implies the tendency of Hg to maximize bonding with S atoms. The Hg-S distances in **99** and **100** are variable despite similar Hg environments. However, the Hg-N distance in **100** is intermediate to those observed in **99**. The Hg-I distance in **99** is shorter compared to that observed in **100** despite similar coordination environments around Hg.

Chapter 5

Conclusion and future research

Direct addition of MX_2 (M = Cd(II), Pb(II), Hg(II) and X = Cl, Br, I, nitrate, acetate) with AET.HCl in aqueous media yielded molecular as well as nonmolecular compounds. The coordination environment around Cd in **75** - **84** consist of S, N or X (X = halides). A regular hexa-coordinate Cd in **76**, consisting of S and Cl in the coordination environment is in contrast to the polymeric Cd(II)-thiolates (**20** - **23**), where coordination around Cd consists of S and N atoms. The polymeric **76** consists of bridging Cl as well as S atoms, which is unusual as for polymeric Cd(II)-thiolates bridging S is usually responsible for polymerization. The Cd_2S_2 core observed in **81** is similar to polynuclear Cd(II)-thiolates containing bridging thiolate S atoms (**13**).

In Pb(II)-AET adducts, isostructural **85** and **86** contains two independent Pb centers consisting of S and N and weak interaction with counter anions. A similar reaction with an equivalent amount of base yielded a polymeric structure (**87**) with $[PbCl(SCH_2CH_2NH_3)]$ as the repeating unit. The Pb is either four- or five-coordinate (**85**, **86, 87**), however with weak interactions with counter anions the CN around Pb in **87** increases to 7. Despite similar reactions a Pb-N bond is not observed in **87**, which is due to the presence of an ammonium group. The repeating units in **87** can be considered to link through bridging Cl and S to yield an overall two-dimensional network. This is in contrast to polynuclear Pb(II)-thiolates, which involve bridging S atoms as well as weak Pb---S and Pb---N interactions (**42**, **43**). A central Pb_2S_2 core is observed in **85**, **86** and **87** similar to that in **81**. The unsymmetrical M-S distances in the M_2S_2 (M = Cd, Pb) core are most probably due to the strain associated with the four-membered ring. In **85** - **87**, the

unsymmetrical Pb-S distances as well an open coordination site indicates presence of stereochemically active lone pair on Pb. In **87** short Cl---Cl distance indicate presence of homonuclear interactions.

Similar reactions with HgX_2 (X = Cl, Br, I) yielded complicated structures of various nuclearities. In the polynuclear compounds (**89**, **90**, **93**, **94**, **98, 100**) two or three independent Hg centers are observed. The coordination environment around Hg consists of S, N as well as halides. The geometry around Hg is mostly distorted tetrahedral in the solid- as well as in solution-state. In **89** and **94**, the halides are responsible for the formation of oligomers. In **89**, the three-coordinate Cl as well as bridging S atoms are responsible for the hexanuclear cluster. In **94**, bridging Hg-S distances are longer and bridging the Hg-Br distances are comparable to the distances reported for similar compounds, indicating the influence of Br in the formation of the nonanuclear cluster. The mercurophilic Hg---Hg interactions observed in **90** are the shortest compared to such interaction reported for homo- and heteroleptic Hg(II)-thiolates. This could be attributed to the strain associated with the Hg-S-Hg angle as well as smaller size of Cl. In **91** strong Hg-N bonds are observed compared to Hg(II)-thiolates containing S/N chelate (**66** - **69**, **92**). Such strong Hg-N bonds in **91** might be responsible for the highly distorted geometry around Hg. Compounds **99** and **100** are similar except for the presence of a non-chelated Hg center in the latter one. The kinetically stable products (two-coordinate) for X = Cl, Br and I were isolated in the solid-state. However solution studies (Uv-Vis, ^{199}Hg NMR) indicated the presence of a four-coordinate Hg in solution with effective coordination number of 4 [2 + 2].

Systematic pathways presented for the formation of the complicate structures observed employ mononuclear two-, three- and four-coordinate compounds. It is well known that complicate structures are formed of simple two-coordinate compounds, however such mechanistic studies have not been explored in detail. The reported molecular structures (**88**, **96**, **97**) are in contrast to the fact that simple thiols usually form polymeric structures with bridging thiolate S atoms.

In Cd(II), Pb(II) and Hg(II)-aminoethanethiolates the halides are an integral part of the structure. In non-aqueous media homoleptic thiolates are usually obtained. The absence of M--S as well as M---N interactions in these compounds can be attributed to the presence of halide in the coordination environment. Weak intermolecular hydrogen bonding involving N, S and counter anions are observed in most cases, which is responsible for the three-dimensional framework.

2-Aminoethanethiol provided the oppurtanity to study the advantage to study the aqueous chemistry of d^{10} metal ions. These metal ions usually form insoluble compounds, which makes a determination of their structural chemistry difficult. The study of S/N coordination around the Cd(II) center could make it suitable for studying Cd(II) and Zn(II) containing metallothioneins. Part of the toxicity of Cd(II) and Pb(II) is due to their competition with Zn(II) in zinc-finger proteins and liver alcohol dehydrogenase.[8,163] The ratio of Pb(II) and Zn(II) bound to a particular site in a metalloenzyme was determined by the relative affinities of the two metals for the site.[152] The Cd(II) and Pb(II) compounds reported here with S_2N_2 coordination around the metal center might be useful as a biological model for Zn(II) containing metalloenzymes.

A study of the structural chemistry and reactivity of Hg(II)-thiolates is important, as it is one of the most toxic elements. In heteroleptic Hg(II)-thiolates, the halide seems to be an integral part of the overall structure with profound influence on the geometry around Hg. This is the first study to note this effect. This had not been found in previous work as Hg(II)-thiolates as most of the compounds reported are obtained in less polar solvents such as alcohol, acetonitrile and DMSO. From this work, it is evident that the coordination chemistry of Hg is affected by the nature of the halide as well as reaction condition. The involvement of the halide with the Hg center might be useful to explain the significant distribution of inorganic and organic mercury between red blood cells and plasma.[220] The systematic pathways for the formation of the Hg(II)-thiolate clusters described here might be useful in understanding the behavior of low-coordinate Hg(II)-thiolates in solution, which eventually would help to understand Hg chemistry in biological systems. Such mechanisms might also be useful to understand the chemistry involving conversion of heteroleptic-thiolates to homoleptic-thiolates in biological systems.

There appears to be no systematic structural motif that can be viewed as having relevance to living systems. The structures obtained in this study indicate that the coordination environment around Cd, Pb and Hg is highly variable, with significantly different structures obtained under very similar conditions. Thus, in the presence of free cysteine, or other sulfur containing biomolecules, a wide range of compounds are likely to be observed, and in equilibrium with one another.

Future research regarding aqueous chemistry of Hg(II), Cd(II), Pb(II), and Zn(II) metal ions with S/N ligands should be conducted with L - cysteine under slightly varying

reaction conditions. Similar studies can be pursued with organic ligands, which resemble the active sites of soft metal ions containing metalloproteins. One important study that should be conducted is to combine two-coordinate Hg(II)-AET (**88**, **96**, **97**) with stoichiometric exces of AET to determine the resulting structure. Similar studies should also be conducted with Hg(II)-cysteine compounds.

Appendix

Table A1. Selected bond distances (Å) and angle (º) for mononuclear Cd(II)-thiolates.

Compound	Coordination	Cd-S	Cd-N	S-Cd-S	Ref
1	CdS_2N_2	2.425, 2.457	2.314, 2.330	134.8	[29]
2	$CdSN_2Cl_2$	2.588	2.388, 2.341	-	[30]
3	$CdSN_2Br_2$	2.584	2.336, 2.392	-	[30]
4	$CdSN_2I_2$	2.603	2.306, 2.424	-	[30]
5	$CdSN_2Cl_2$	2.574	2.327,2.356	-	[31]
6	$CdSN_2Br_2$	2.561	2.351, 2.356	-	[31]
7	$CdSN_2I_2$	2.556	2.366, 2.379	-	[31]
8	CdS_2N_4	2.560, 2.602	2.442, 2.469 and 2.291, 2.305	104.6	[30]
9	CdS_2N_4	2.588, 2.549	2.420, 2.530	116.2	[34]
10	CdS_3N_3	2.667	2.474	102.4	[40]
11	$CdS_2N_2O_2$	2.613, 2.706	2.353, 2.428	104.2	[41]
12	$CdS_2N_2Cl_2$	2.622	2.366	104.2	[42]
$[Cd(SR\text{-}Ph)_2(1\text{-}Meimid)_2]$	CdS_2N_2	2.474, 2.451	2.270, 2.291	126.3	[221]
$[Cd(S_2COC_2H_5)_2(phen)]$	CdS_4N_2	2.647 - 2.727	2.386	160.5	[39]
$[Cd(S_2CSC_4H_9\text{-})(bipy)]$	CdS_4N_2	2.66, 2.70	2.363	153.7	[222]

meimid = 1-methylimidazole pyridine, R = 2,4,6-$Pr^i_3C_6H_2$.

Table A2. Geometry around Cd (Å and º) in **13** and similar Cd(II)-thiolates.

Compounds	Geometry	Coordination	Distance	Ref
13	tbp	CdS_3N_2	Cd-S_{ter} = 2.495, Cd-S_{br} = 2.632, Cd-N_{py} = 2.381	[43]
$[Cd_2(S_2CN(C_2H_5)_4]$	tbp	CdS_5	Cd-S_{ter} = 2.536 - 2.594, Cd-S_{br} = 2.644, 2.800	[37]
$[Cd_2(S_2CN(CH_2)_6)_4]$	tbp	CdS_5	Cd-S_{ter} = 2.539 - 2.631, Cd-S_{br} = 2.87	[38]
$[Cd(C_6H_4NO_2)(H_2O)_4]$	oct	CdN_2O_4	Cd-N = 2.310	[223]
$[Cd(HCOO)_2(C_6H_4NCONH_2)(H_2O)_2]$	oct	CdN_2O_4	Cd-N = 2.336	[224]
$[CdCl_2(py)_2]$	oct	$CdCl_4N_2$	Cd-N = 2.35	[52]
$[Cd(C_2H_4NCOO)_2]$	oct	CdN_2O_4	Cd-N = 2.23	[225]

tbp = trigonal bipyramidal, oct = octahedral and, ter = terminal and br = bridging.

Table A3. Selected distances (Å) and angles (º) for **16** - **18**.

Compound	Cd-S	Cd-N	Cd-X	S-Cd-S	S-Cd-N	Ref
16	2.558 (Cd); 2.520, 2.506 (Cd')	2.36 (Cd)	2.946 (Cd); 2.413 (Cd')	172.3 (Cd); 113 (Cd')	80.9 (Cd)	[48]
17	2.518, 2.514 (Cd); 2.501, 2.494 (Cd')	2.366, 2.375 (Cd')	2.681, 2.572 (Cd)	126.3 (Cd); 161.0 (Cd')	83.5 (Cd')	[49]
18	2.464, 2.543, 2.532 (Cd); 2.554, 2.559 (Cd')	2.507 (Cd); 2.558, 2.516 (Cd')	2.733, 2.735 (Cd')	118.4, 121.7, 119.1 (Cd)	83.4, 99.1, 96.6 (Cd); 79.4 (Cd')	[49]

Cd and Cd' represent two different types of Cd atoms within the compound.

Table A4. Selected bond distances (Å) and angles (º) for **20** - **23**.

Compound	Cd-S	Cd-N	S-Cd-N(*trans*)	S-Cd-N(chelate)	S-Cd-S	Ref
20	2.689, 2.868	2.283	90.2	80.8	89.6	[42]
21	2.547, 2.606; 3.061, 3.129	2.283 - 2.328	98.2	57.7	102.3	[53]
22	2.543 - 2.649; 2.809 - 3.083	2.342 - 2.343	101.6	57.2	103.4	[53]
23	2.668 - 2.750	2.398 - 2.479	151.6 - 167.1	61.3 - 61.3	154.7	[54]

Table A5. Selected bond distances (Å) and angles (º) for **27** - **43**.

Compound	Pb-S	Pb-N	S-Pb-S	S-Pb-N	Ref
27	2.709	2.362	-	74.3	[59]
28	2.715	2.295	-	77.2	[59]
29	2.636(avg)	2.550, 2.626	99.2	83.8	[60]
30	2.882, 2.707	2.59, 2.79	86.4	55.8 - 125.0	[61]
31	2.685, 2.727	2.602, 2.654	89.7	67.5, 84.5	[63]
32	2.755, 2.784	2.625, 2.644	74.19	64.9	[64]
33	2.819	-	179.9	88.1	[67]
34	2.582	2.494, 2.759	-	72.3, 134.2	[67]
35	2.734	2.585, 2.486	61.4	67.3 - 167.2	[67]
36	2.716, 3.160	2.444	-	-	[68]
37	3.416, 3.192	2.565, 2.692	107.0	58.6 - 156.7	[69]
38	3.193, 3.251	2.607, 2.695	72.9 - 177.4	62.4, 105.2	[70]
39	2.981, 2.955	2.543 (avg)	128.5	68.2 - 129.8	[70]
40	3.005	2.577	69.3, 130.6	67.2 - 126.7	[70]
41	2.789	2.606, 2.684	-	68.6 - 129.6	[67]
42	2.665, 3.160	2.409, 2.592	69.4 - 93.5	76.3 - 145.7	[60]
43	2.742, 3.237	2.850, 2.510	77.0 - 94.8	56.2	[79]

Table A6. Selected bond distances (Å) and angles (º) for **44 - 62**.

Compound	Geometry	Hg-S	Hg-X	S-Hg-S	S-Hg-X	Ref
44	Essentially Linear	2.342 (avg)	3.232 (Cl)	169.8	-	[92]
45	Essentially Linear	2.329	-	176.9	-	[93]
46	Sq py	2.361, 2.352	-	175.7	--	[94]
47	Essentially Linear	2.346 (avg)	-	178.2	-	[95]
48	dis tg	2.467	2.676, 2.816 (I)	-	119.7, 127.3	[98]
49	dis tg	2.460	2.818, 2.651 (I)	-	108.9, 134.6	[99]
50	dis td	2.452	2.781 (Br)	134.8	98.8 - 134.8	[99]
51	dis td	2.453	2.642 (Cl)	130.8	104.3 - 108.7	[189]
52	dis td	2.494, 2.526	2.647 (Br)	122.6	101.6 - 112.7	[95]
53	dis td	2.6716	2.687 (I)	102.7	97.1 - 112.0	[114]
54	pseudo td	2.451	2.598 (Br)	127.7	105.1, 109.9	[101]
55	pseudo td	2.507	2.644 (Br)	110.3	109.9 - 118.5	[101]
56	pseudo td	2.548	2.795 (I)	109.0	103.1 - 115.2	[101]
57	dis td	2.626	2.708 (I)	88.3	112.9 - 127.3	[98]

58	tri by - td	2.512	2.626 (N)	105.5 - 129.0	75.4 - 78.2	[102]
59	dis by	2.801	2.633, 2.104 (N)	-	60.0 - 99.2	[106]
60	sq py	2.583	2.554, 2.414 (N)	116.0	72.0 - 128.5	[111]
61	dis tet py	2.522	2.402, 2.410 (N)	-	65.1 - 135.3	[30]
62	dis tet py	2.506	2.463 (N)	-	72.7, 135.4	[31]

X = halide, N, dis = distorted, sq = square, tg = trigonal, td = tetrahedral, by = bipyramidal, tet = tetragonal, pyr = pyramidal

Table A7. Selected bond distances (Å) and angles (º) for **63** - **68**.

Compound	Geometry	Hg-S	Hg-X	S-Hg-S	S-Hg-X	Ref
63	dis td	2.435	2.514, 2.756 (Br)	-	108.0 - 138.2	[114]
64	dis td	2.510	2.669, 3.058 (I)	-	101.2 - 123.4	[114]
65	dis tg by	2.406, 2.419	2.490, 2.826 (Br)	-	103.1 - 139.4	[115]
66	sq py	2.694	2.303, 2.464 (N)	92.15	73.6, 141.9	[111]
67	sq py	2.689	2.331, 2.474 (N)	92.58	73.9, 141.5	[111]
68	dis td	2.358	2.856 (N)	174.25	-	[117]

X = halide, N, dis = distorted, sq = square, tg = trigonal, td = tetrahedral, by = bipyramidal, py = pyramidal

Table A8. Selected bond distances (Å) and angles (º) for **70** - **74**.

Compound	Geometry	Hg-S	Hg-X	S-Hg-S	S-Hg-X	Ref
70	dis td	2.453, 2.490	2.582, 2.645 (Cl)	136.0	96.3 - 111.9	[92]
71	dis td	2.320	2.37 (Cl)	-	167.2	[119]
72	dis td	2.464	2.513, 2.634 (Cl)		102.3, 112.5	[88]
73	dis td	2.430	2.451 (N)	143.1	95.0, 110.3	[99]
74	linear	2.339	-	169.7	-	[120]

X = halide, N, dis = distorted, td = tetrahedral.

Table A9. Selected bond lengths (Å) and bond angles (º) for **76**.

Cd(1)-S(1)	2.4825 (14)	Cd(2)-S(2)'	2.6018 (14)
Cd(1)-S(2)	2.4995 (14)	Cd(2)-Cl(2)	2.6679 (14)
Cd(1)-Cl(1)	2.8875 (15)	Cd(2)-Cl(3)	2.6968 (14)
Cd(1)-Cl(2)	2.8276 (14)	Cd(2)-Cl(4)	2.6372 (13)
Cd(1)-Cl(3)	2.7895 (14)	Cd(2)-Cl(5)	2.6060 (14)
Cd(3)-S(1)	2.5417 (14)	Cd(3)-Cl(2)	2.8159 (13)
Cd(3)-Cl(4)	2.7306 (13)		

S(2)-Cd(1)-S(1)	178.22 (5)	S(2)-Cd(1)-Cl(3)	84.70 (4)
S(1)-Cd(1)-Cl(3)	95.85 (4)	S(2)-Cd(1)-Cl(2)	96.23 (5)
S(1)-Cd(1)-Cl(2)	85.52 (5)	Cl(3)-Cd(1)-Cl(2)	82.67 (4)
S(2)-Cd(1)-Cl(1)	91.66 (5)	S(1)-Cd(1)-Cl(1)	86.68 (5)
Cl(3)-Cd(1)-Cl(1)	87.82 (4)	Cl(2)-Cd(1)-Cl(1)	167.01 (4)
S(2)-Cd(1)-Cl(1)'	84.86 (4)	S(1)-Cd(1)-Cl(1)'	94.80 (4)
Cl(3)-Cd(1)-Cl(1)'	167.25 (4)	Cl(2)-Cd(1)-Cl(1)'	91.20 (4)
Cl(1)-Cd(1)-Cl(1)'	99.79 (2)	S(2)'-Cd(2)-Cl(5)	90.65 (4)
Cl(5)-Cd(2)-Cl(4)	90.22 (4)	Cl(5)-Cd(2)-Cl(2)	88.05 (4)
Cd(1)-Cl(1)-Cd(1)'	142.52 (5)	Cd(2)-Cl(2)-Cd(1)	94.74 (4)
Cd(2)'-Cl(3)-Cd(1)	90.50 (4)	Cd(1)-S(2)-Cd(2)'	101.90 (5)

Table A10. Selected bond lengths (Å) and bond angles (º) for **81**.

Cd-N(1)	2.3087 (18)	Cd-N(2)	2.436 (2)
Cd-S(1)	2.7359 (7)	Cd-S(1)'	2.5813 (7)
Cd-S(2)	2.4920 (7)	S(1)-Cd'	2.5843 (7)

N(1)-Cd-N(2)	85.54 (7)	N(1)-Cd-S(2)	137.38 (5)
N(2)-Cd-S(2)	81.66 (5)	N(1)-Cd-S(1)	78.22 (5)
N(2)-Cd-S(1)	161.82 (6)	S(2)-Cd-S(1)	104.85 (2)
S(1)'-Cd-S(1)	93.54 (2)	Cd'-S(1)-Cd	86.46 (2)
N(1)-Cd-S(1)'	101.85 (5)	N(2)-Cd-S(1)'	97.79 (6)

Table A11. Stoichiometric amount of the reactants (Pb(II), AET·HCl and NaOH) used for the formation of Pb(II)-2-aminoethanethiolates.

Product	Reactants	Ref
$[Pb_2Cl(SCH_2CH_2NH_2)_3]$ (**85**)	1:2:4	150
$[Pb_2(SCH_2CH_2NH_2)_3]^+$ (**86**)	1:2:4	150
$[PbCl(SCH_2CH_2NH_3)]^+$ (**87**)	1:1:1	151
$[PbCl_2(SCH_2CH_2NH_3)]$ (**88**)	1:2:2	60
$[\{Pb(SCH_2CH_2NH_2)_2\}\cdot 2\{PbCl(SCH_2CH_2NH_2)\}]$ (**89**)	1:2:5 or 1:2:7	60

Table A12. NMR data (ppm) for AET·HCl and **85 - 87** in D_2O and d_6-DMSO.

^{1}H and ^{13}C NMR	2-aminoethanethiol hydrochloride	**85**	**86**	**87**
^{1}H NCH_2	2.69	2.85	2.74	2.89
^{1}H SCH_2	2.99	3.02	3.20	3.06
^{13}C CN	42.83	48.5	49.3	44.6
^{13}C CS	22.22	29.1	30.0	25.1

Table A13. Selected bond distances (Å) and angles (º) for **85**.

Pb(1)-N(1)	2.629 (6)	Pb(1)-N(2)	2.613 (7)
Pb(1)-S(1)	2.713 (2)	Pb(1)-S(2)	2.673 (2)
Pb(2)-S(2)	2.897 (2)	Pb(2)-N(3)	2.394 (7)
Pb(2)-S(3)	2.7377 (1)	Pb(2)-S(3)'	3.053 (2)
Pb(2)-Cl(1)	3.082 (2)		

N(1)-Pb(1)-S(1)	73.17 (1)	N(1)-Pb(1)-S(2)	86.41 (1)
N(2)-Pb(1)-S(1)	81.08 (1)	N(2)-Pb(1)-S(2)	73.51 (1)
N(3)-Pb(2)-S(2)	83.89 (1)	N(3)-Pb(2)-S(3)	73.61 (1)
S(2)-Pb(1)-S(1)	99.56 (6)	S(3)-Pb(2)-S(2)	83.81 (6)
S(2)-Pb(2)-S(3)'	165.09 (5)	S(3)-Pb(2)-S(3)'	84.35 (6)

Table A14. Selected bond distances (Å) and angles (º) for **86**.

Pb(1)-N(1)	2.604 (7)	Pb(1)-N(2)	2.575 (7)
Pb(1)-S(1)	2.7138 (1)	Pb(1)-S(2)	2.6806 (1)
Pb(2)-S(2)	2.893 (2)	Pb(2)-N(3)	2.411 (7)
Pb(2)-S(3)	2.704 (2)	Pb(2)-S(3)'	3.0857 (1)
N(1)-Pb(1)-S(1)	72.39 (1)	N(1)-Pb(1)-S(2)	84.28 (1)
N(2)-Pb(1)-S(1)	83.32 (1)	N(2)-Pb(1)-S(2)	73.54 (1)
N(3)-Pb(2)-S(2)	84.43 (1)	N(3)-Pb(2)-S(3)	74.15 (1)
S(2)-Pb(1)-S(1)	100.78 (6)	S(2)-Pb(2)-S(3)'	168.83 (6)
S(3)-Pb(2)-S(2)	86.00 (6)	S(3)-Pb(2)-S(3)'	87.00 (6)
Pb(1)-S(2)-Pb(2)	96.11 (6)	Pb(2)-S(3)-Pb(2)'	95.65 (6)

Table A15. Selected bond distances (Å) and angles (º) for **87**.

Pb1-S1	2.7383(1)	Pb1-Cl1	2.8031(1)
Pb1-S2'	2.8399(1)	Pb1-Cl2'	2.9879(1)
Cl1-Pb2	3.0788(1)	S1-Pb2'	2.8458(1)
Pb2-S2	2.7275(1)	Pb2-Cl2	2.7694(1)
Pb2-S1'	2.8458(1)	S2-Pb1'	2.8399(1)
S1-Pb1-Cl1	84.53(5)	S1-Pb1-S2'	83.92(5)
Cl1-Pb1-S2'	89.19(4)	S1-Pb1-Cl2'	96.11(4)
Cl1-Pb1-Cl2'	170.48(3)	S2-Pb1-Cl2	81.44(3)
S2-Pb2-Cl2	86.71(5)	S2-Pb2-S1'	84.01(5)
S2-Pb2-Cl1	96.20(4)	Cl2-Pb2-Cl1	172.96(3)
Pb1-Cl1-Pb2	130.38(7)	Pb2-Cl2-Pb1'	132.82(7)

Table A16. Reaction conditions for the formation of $[Hg(SR)_xCl_y]$ type complexes from $HgCl_2$ and AET·HCl.

Compounds	Hg(II):RSH, Conditions	Crystalliz	Coord	Ref
88	1:2; RT, DI H_2O	R T Evap	2S	[174]
89	1:2; RT, DI H_2O	4 ºC	2S2Cl, 3S2Cl	[175]
90*	1:2; RT, DI H_2O	R T Evap	2S2Cl, 2SCl	[176]
91*	1:2; RT, DI H_2O	R T Evap	2SNCl	[176]
92	1:2; RT, MeOH	- 20 ºC	2S2N	[126]
93	1:2; 0ºC, DI H_2O	4 ºC	2S2Cl	[177]

* $Hg_2Cl_2 \rightarrow$ Hg(0) (50%) + Hg(II)(50%).

Table A17. Chemical shifts (ppm) observed for ^{1}H and ^{13}C in **88** - **92**.

Compound/ Solvent	^{1}H (SCH_2)	^{1}H (NCH_2)	^{1}H (NH_2/NH_3^+)	^{13}C (CS)	^{13}C (CN)	Ref
88 (D_2O)	3.27	3.23		25.2	43.3	[174]
89 (d_6-DMSO)	3.14	3.00	7.91	25.9	43.0	[175]
90 (d_6-DMSO)	3.08	2.94	6.33	26.7	42.8	[176]
91 (d_6-DMSO)	2.97	3.09	8.13	25.6	42.9	[176]
92 (Cd_3OD)	2.83	2.92	-	33.0	46.1	[126]

Table A18. Selected vibrational frequencies (cm^{-1}) for **88** - **92**.

Compound	Geometry	ν(Hg-S)	ν(Hg-Cl)	References
88	Essentially linear	361 (as)		[226]
89	Distorted td	272 (s), 340 (as)	234 (t)	[175]
90	Distorted td	269 (s) 351 (as)	225 (t)	[176]
91	Distorted td	299 (s), 345 (as)	226 (t)	[176]
92	Distorted td	362 (as)	-	[126]
$[HgCl_2\{\mu\text{-}S(CH_2)_3NH(CH_3)_2\}]$	Distorted td	272 (s), 308 (as)	232 (t)	[88]
$[HgCl_2(SCHN(CH_3)_2)_2]$	Pseudo td	270 (s), 308 (as)	225 (t)	[116]

td = tetrahedral, s = symmetric, as = asymmetric, t = terminal

Table A19. Selected bond distances (Å) and angles (º) for **89**.

Hg(1)---Hg(2)	4.927(4)	Hg(1)---Hg(3)	3.797(4)
Hg(2)---Hg(3)	3.776(4)	Hg(1)---Hg(1)'	4.379(4)
Hg(1)---Hg(2)'	4.927(4)	Hg(1)---Hg(3)'	3.898(4)
Hg(2)---Hg(1)'	4.927(4)	Hg(2)---Hg(2)'	9.819(4)
Hg(3)---Hg(1)'	3.898(4)	Hg(3)---Hg(2)'	7.347(4)
Hg(3)---Hg(3)'	6.329(4)		
Hg(1)-S(1)	2.410(14)	Hg(2)-S(2)	2.397(13)
Hg(1)-S(3)	2.394(14)	Hg(2)-S(4)	2.339(14)
Hg(1)-Cl(1)	2.732(15)	Hg(2)-Cl(2)	3.106(14)
Hg(1)-Cl(3)	2.895(13)	Hg(2)-Cl(3)	2.983(13)
Hg(3)-S(1)	2.501(14)	Hg(3)-S(3)'	2.631(15)
Hg(3)-S(2)	2.518(14)	Hg(3)-S(3)	2.631(15)
Hg(3)-Cl(3)	2.894(13)	Hg(3)-Cl(4)	2.831(15)

Hg(3)-Hg(1)-Hg(3)	48.97	Hg(1)-Hg(3)-Hg(2)	79.87
Hg(1)-Hg(2)-Hg(3)	51.16	Hg(1)-S(1)-Hg(3)	101.24(5)
Hg(2)-S(2)-Hg(3)	100.34(5)	Hg(1)-Cl(3)-Hg(2)	159.97(5)
Hg(1)-Cl(3)-Hg(3)	81.94(3)	Hg(2)-Cl(3)-Hg(3)	79.91(3)
S(1)-Hg(1)-S(3)	158.06(5)	S(2)-Hg(2)-S(4)	171.87
S(1)-Hg(1)-Cl(1)	105.34(5)	S(2)-Hg(2)-Cl(2)	94.96
S(1)-Hg(1)-Cl(3)	89.26(4)	S(2)-Hg(2)-Cl(3)	89.15(4)
S(3)-Hg(1)-Cl(1)	95.03(5)	S(4)-Hg(2)-Cl2)	89.06
S(3)-Hg(1)-Cl(3)	98.37(4)	S(4)-Hg(2)-Cl(3)	98.37(4)
S(1)-Hg(3)-S(2)	162.64(5)	S(1)-Hg(3)-S(1)'	100.70(4)
S(2)-Hg(3)-S(3)"	96.54(4)	(S1)-Hg(3)-Cl(3)	87.55(4)
S(1)-Hg(3)-Cl(4)	85.72(4)	S(2)-Hg(3)-Cl(3)	88.87(4)
S(2)-Hg(3)-Cl(4)	93.96(4)	S(3)'-Hg(3)Cl(3)	95.23(4)
S(3)'-Hg(3)Cl(4)	97.95(4)		

Table A20 Selected bond distances (Å) and angles (º) for **90**.

Hg(1)-Hg(2)	3.5644(3)	Hg(1)-Hg(2)'	3.8345(3)
Hg(1)-S(1)	2.3723(1)	Hg(2)-S(2)	2.4795(1)
Hg(1)-S(2)	2.4086(1)	Hg(2)-S(3)	2.5076(1)
Hg(1)-Cl(1)	2.7635(1)	Hg(2)-S(1)'	2.7249(1)
Hg(2)-Cl(2)	2.7225(1)	Hg(3)-Cl(3)	2.4346(1)
Hg(3)-S(3)	2.4504(1)	Hg(3)-Cl(4)	2.5418(1)
Hg(3)-Cl(5)	2.7070(1)	S(1)-Hg(2)'	2.7248(1)

Hg(2)-Hg(1)-Hg(2)'	102.341(7)		
S(1)-Hg(1)-S(2)	167.98(5)	S(1)-Hg(1)-Cl(1)	106.61(4)
S(2)-Hg(1)-Cl(1)	85.35(4)	S(1)-Hg(1)-Hg(2)	143.33(3)
S(2)-Hg(1)-Hg(2)	43.97(3)	Cl(1)-Hg(1)-Hg(2)	54.83(3)
S(1)-Hg(1)-Hg(2)'	44.81(3)	S(2)-Hg(1)-Hg(2)'	133.71(3)
Cl(1)-Hg(1)-Hg(2)'	98.39(3)	S(2)-Hg(2)-S(3)	149.37(5)
S(2)-Hg(2)-Cl(2)	94.81(4)	S(3)-Hg(2)-Cl(2)	90.90(4)
S(2)-Hg(2)-S(1)'	116.95(4)	S(3)-Hg(2)-S(1)'	91.85(4)
Cl(2)-Hg(2)-S(1)'	98.14(4)	S(2)-Hg(2)-Hg(1)	42.41(3)
S(3)-Hg(2)-Hg(1)	111.44(3)	Cl(2)-Hg(2)-Hg(1)	124.27(3)
S(1)'-Hg(2)-Hg(1)	129.50(3)	Cl(3)-Hg(3)-S(3)	142.33(5)
Cl(3)-Hg(3)-Cl(4)	98.00(5)	S(3)-Hg(3)-Cl(4)	112.66(5)
Cl(3)-Hg(3)-Cl(5)	93.15(5)	S(3)-Hg(3)-Cl(5)	102.61(4)
Cl(4)-Hg(3)-Cl(5)	99.09(4)	C(1)-S(1)-Hg(1)	105.93(1)
C(1)-S(1)-Hg(2)'	107.61(1)	Hg(1)-S(1)-Hg(2)'	97.33(4)
Hg(1)-S(2)-Hg(2)	93.62(5)	C(5)-S(3)-Hg(3)	104.41(1)
C(5)-S(3)-Hg(2)	100.55(1)	Hg(3)-S(3)-Hg(2)	94.39(5)

Table A21. Selected bond distances (Å) and angles (º) for **91**.

Hg(1)-S(1)	2.3932(1)	Hg(1)-N(1)'	2.236(4)
Hg(1)-S(1)'	2.6928(1)	Hg(1)-Cl(1)	2.7199(1)
S(1)-Hg(1)'	2.6927(1)	N(1)-Hg(1)'	2.236(4)
Hg(2)-N(3)'	2.277(4)	Hg(2)-S(2)	2.4001(1)
Hg(2)-S(3)'	2.5803(1)	Hg(2)-Cl(2)	2.7171(1)
S(2)-Hg(3)	2.6520(1)	N(2)-Hg(3)	2.268(4)
Hg(3)-S(3)	2.4239(1)	Hg(3)-Cl(3)	2.6306(1)
S(3)-Hg(2)'	2.5802(1)	N(3)-Hg(2)'	2.277(4)

S(1)-Hg(1)-S(1)'	125.78(5)	N(1)'-Hg(1)-S(1)	147.25(1)
N(1)"-Hg(1)-S(1)'	80.78(1)	N(1)'-Hg(1)-Cl(1)	86.42(1)
S(1)-Hg(1)-Cl(1)	108.72(4)	S(1)'-Hg(1)-Cl(1)	92.16(4)
C(1)-S(1)-Hg(1)	101.54(1)	C(1)-S(1)-Hg(1)'	92.44(1)
Hg(1)-S(1)-Hg(1)'	104.03(5)	N(3)'-Hg(2)-S(2)	135.25(1)
N(3)"-Hg(2)-S(3)'	82.11(1)	S(2)-Hg(2)-S(3)'	137.13(4)
N(3)"-Hg(2)-Cl(2)	87.80(1)	S(2)-Hg(2)-Cl(2)	103.18(4)
S(3)"-Hg(2)-Cl(2)	97.38(4)	Hg(2)-S(2)-Hg(3)	105.21(5)
N(2)-Hg(3)-S(3)	140.82(1)	N(2)-Hg(3)-Cl(3)	97.14(1)
S(3)-Hg(3)-Cl(3)	101.58(4)	N(2)-Hg(3)-S(2)	80.61(1)
S(3)-Hg(3)-S(2)	128.11(4)	Cl(3)-Hg(3)-S(2)	100.76(4)
Hg(3)-S(3)-Hg(2)'	104.75(5)		

Table A22. Selected bond distances (Å) and angles (º) for **94**.

Hg(1)---Hg(2)	3.605(9)	Hg(2)---Hg(3)	3.750(11)
Hg(1)---Hg(3)	7.169(17)	Hg(1)---Hg(2)'	3.980(11)
Hg1---Hg(1)'	5.472(9)	Hg(2)---Hg(1)'	3.980(17)
Hg(1)-S(1)	2.375(2)	Hg(2)-S(2)	2.487(2)
Hg(1)-S(2)	2.424(2)	Hg(2)-S(3)	2.482(2)
Hg(1)-Br(2)	2.935(1)	Hg(2)-S(1)'	2.811(2)
Hg(1)-Br(2)'	3.073(1)	Hg(2)'-S(1)	2.811(2)
Hg(1)1A-Br(2)	3.073(1)	Hg(2)-Br(1)	2.7903(1)
Hg(3)-S(3)	2.482(2)	Hg(3)-Br(3)	2.555(1)
Hg(3)-Br(4)	2.688(1)	Hg(3)-Br(5)	2.784(1)

Hg(1)-S(2)-Hg(2)	94.43(8)	Hg(1)-S(1)-Hg(2)'	99.91(8)
Hg(1)-Br(2)-Hg(1)'	131.17(4)	Hg(2)-S(3)-Hg(3)	97.96(9)
S(1)-Hg(1)-S(2)	172.06(8)	S(2)-Hg(2)-S(3)	153.74(8)
S(1)-Hg(1)-Br(2)	105.01(5)	(S2)-Hg(2)-S(1)'	110.00(7)
S(1)-Hg(1)-Br(2)'	94.55(6)	S(3)-Hg(2)-S(1)'	92.94(7)
S(2)-Hg(1)-Br(2)	82.15(6)	S(2)-Hg(2)-Br(1)	98.54(6)
S(2)-Hg(1)-Br(2)'	85.82(6)	S(3)-Hg(2)-Br(1)	90.41(6)
S(3)-Hg(3)-Br(3)	141.34(6)	S(3)-Hg(3)-Br(4)	108.18(6)
S(3)-Hg(3)-Br(5)	99.69(7)	Br(3)-Hg(3)-Br(4)	99.25(4)
Br(3)-Hg(3)-Br(5)	98.40(4)	Br(4)-Hg(3)-Br(5)	105.75(4)

Table A23. Selected bond distances (Å) and angles (º) for **95**.

Hg1-Br2	2.5551(10)	Hg1-Br3	2.5640(11)
Hg1-Br4	2.5914(12)	Hg1-Br1	2.7616(11)
Br2-Hg1-Br3	126.09(4)	Br2-Hg1-Br4	112.46(4)
Br3-Hg1-Br4	112.75(3)	Br2-Hg1-Br1	101.73(4)
Br3-Hg1-Br1	98.00(4)	Br4-Hg1-Br1	99.78(4)

Table A24. Chemical shifts (ppm, d_6-DMSO) observed for ^{1}H and ^{13}C in **98 - 100**.

Compound/ Solvent	^{1}H (SCH_2)	^{1}H (NCH_2)	^{1}H (NH_2/NH_3^+)	^{13}C (CS)	^{13}C (CN)	Ref
97	3.27	3.23		25.2	43.3	[177]
98	3.10	3.04	7.68	27.3	42.5	[206]
99	2.96	2.84	6.06	29.1	42.7	[206]
100*	2.94	-	-	32.4	41.4	[198]

* A single broad peak at 2.94 ppm integrates to the four protons for the SCH_2CH_2N group.

Table A25. Selected bond distances (Å) and angles (º) for **98**.

Hg(1)-S(1)	2.464(3)	Hg(2)-S(2)	2.463(3)
Hg(3)-S(1)'	2.491(3)	Hg(3)-S(2)	2.482(3)
Hg(3)'-S(1)	2.491(3)	Hg(1)-I(1)	2.936(9)
Hg(2)-I(1)	2.989(1)	Hg(1)-I(2)	3.046(1)
Hg(2)-I(2)	2.932(1)	Hg(1)-I(3)	2.668(1)
Hg(2)-I(4)	2.932(1)	Hg(3)-I(5)	2.965(1)
Hg(4)-I(5)	2.797(1)	Hg(4)-I(6)	3.129(1)
Hg(4)-I(7)	2.704(1)	Hg(4)-I(8)	2.697(1)

S(1)-Hg(1)-I(1)	106.21(8)	S(2)-Hg(2)-I(1)	104.09(3)
S(1)-Hg(1)-I(2)	99.50(8)	S(2)-Hg(2)-I(2)	106.77(8)
S(1)-Hg(1)-I(3)	141.62(8)	S(2)-Hg(2)-I(4)	139.56(8)
I(1)-Hg(1)-I(2)	91.19(3)	I(1)-Hg(2)-I(2)	92.42(3)
I(1)-Hg(1)-I(3)	105.26(3)	I(1)-Hg(2)-I(4)	102.38(3)
I(2)-Hg(1)-I(3)	101.26(3)	I(2)-Hg(2)-I(4)	104.09(3)
S(2)-Hg(3)-S(1)'	133.59(9)	I(5)-Hg(4)-I(6)	89.96(3)
S(2)-Hg(3)-I(5)	107.56(8)	I(5)-Hg(4)-I(7)	119.61(3)
S(2)-Hg(3)-I(6)	110.62(8)	I(5)-Hg(4)-I(8)	111.07(3)
S(1)'-Hg(3)-I(5)	98.09(8)	I(6)-Hg(4)-I(7)	95.09(3)
S(1)'-Hg(3)-I(6)	110.60(8)	I(6)-Hg(4)-I(8)	103.42(3)
I(5)-Hg(3)-I(6)	92.79(3)	I(7)-Hg(4)-I(8)	125.71(3)
Hg(2)-S(2)-Hg(3)	106.65(1)	Hg(1)-S(1)-Hg(3)'	105.28(1)
Hg(1)-I(1)-Hg(2)	86.21(3)	Hg(1)-I(2)-Hg(2)	85.26(3)
Hg(3)-I(5)-Hg(4)	90.53(3)	Hg(3)-I(6)-Hg(4)	86.70(3)

Table A26. Selected bond distances (Å) and angles (º) for **99**.

Hg(1)-S(1)	2.518(1)	Hg(2)-S(1)'	2.473(1)
Hg(1)-S(2)	2.476(1)	Hg(2)-S(2)	2.530(1)
Hg(1)-N(1)	2.404(4)	Hg(2)-N(2)	2.371(4)
Hg(1)-I(1)	2.762(4)	Hg(2)-I(2)	2.755(4)
S(2)-Hg(1)-S(1)	123.47(5)	S(2)-Hg(2)-S(1)'	124.18(5)
N(1)-Hg(1)-S(1)	81.53(1)	N(2)-Hg(2)-S(1)'	108.94(1)
N(1)-Hg(1)-S(2)	109.45(1)	N(2)-Hg(2)-S(2)	82.00(1)
S(1)-Hg(1)-I(1)	112.34(4)	S(1)'-Hg(2)-I(2)	112.35(3)
S(2)-Hg(1)-I(1)	115.81(3)	S(2)-Hg(2)-I(2)	112.65(3)
Hg(1)-S(2)-Hg(2)	104.62(5)	Hg(1)-S(1)-Hg(2)'	100.62(5)

Table A27. Selected bond distances (Å) and angles (º) for **100**.

Hg1-S2	2.498(2)	Hg1-S1	2.519(2)
Hg1-I1	2.8130(7)	Hg1-I	2 2.8613(7)
Hg2-N2	2.391(8)	Hg2-S1	2.468(2)
Hg2-S2	2.486(2)	Hg2-I3	2.8078(7)
S2'-Hg2	2.486(2)	N2"-Hg2	2.391(8)

S2-Hg1-S1	117.34(7)	S2-Hg1-I1	110.89(5)
S1-Hg1-I1	110.51(5)	S2-Hg1-I2	107.89(5)
S1-Hg1-I2	108.09(5)	I1-Hg1-I2	100.74(2)
N2-Hg2-S1	113.5(2)	N2-Hg2-S2	82.37(19)
S1-Hg2-S2	135.91(7)	N2-Hg2-I3	102.7(2)
S1-Hg2-I3	108.71(5)	S2-Hg2-I3	106.96(5)
Hg2-S1-Hg1	103.12(8)	Hg2-S2-Hg1	104.58(7)

Table A29. Crystal data for **85**, **86** and **87**.

Data/ Compound	**85**	**86**	**87**
Empirical formula	$C_6H_{18}N_3S_3Pb_2Cl$	$C_6H_{18}N_{3.67}O_{2.02}S_3Pb_2$ $C1_{0.33}$	$C_4H_{14}ClN_2S_2O_2$ Pb
Molecular weight	678.24	696.15	428.93
Temperature (ºK)	145 (2)	206 (2)	90.0(2)
Wavelength (Å)	0.71073	0.71073	0.71073
Crystal system	Monoclinic	Monoclinic	Monoclinic
Space group	P 21/n	P 21/n	P 21
Unit cell dimensions in (Å) and (^{0})	a = 9.1680 (10) b = 9.5880 (10) c = 16.707 (2) α = 90 β = 95.410 (10) γ = 90	a = 9.3600 (10) b = 9.5300 (10) c = 17.057 (10) α = 90 β = 95.860 (10) γ = 90	a = 10.614(2) b = 6.7150(1) c = 11.501(2) α = 90.0 β = 108.260(8) γ = 90.0
V (Å^3)	1462.1 (3)	1513.5 (3)	778.47(2)
Z	4	4	4
Absorption coefficient (mm^{-1})	23.58	22.68	22.24
F(0 0 0)	1216	1254	688
Goodness-of-fit on F^2	0.492	1.049	1.067
R_1 (on F, I>2σ(I))	0.0249	0.0327	0.0147
R_1 (all data)	0.0359	0.0453	0.0190
wR_2 (on F^2,	0.0625	0.0582	0.0393

$I>2\sigma(I)$)			
wR_2 (all data)	0.0686	0.0619	0.0400
Refinement Method	Full-matrix least-square on F^2	Full-matrix least-square on F^2	Full-matrix least-square on F^2

Table A30. Crystallographic data for **76** and **81**.

Data/ Compound	**76**	**81**
Empirical formula	$C_4H_{14}N_2S_2Cd_{2.5}Cl_5$	$C_4H_{12}N_2S_2Cd$
Molecular weight	612.54	264.68
Temperature (ºK)	173 (1)	145(2)
Wavelength (Å)	0.71073	0.71073
Crystal system	Monoclinic	Triclinic
Space group	P 21/n	P –1
Unit cell dimensions in (Å) and (^{0})	a = 10.4530 (6) b = 8.1430 (5) c = 17.5180 (8) α = 90 β = 90.426 (3) γ = 90	a = 6.2800 (10) b = 8.2360 (10) c = 8.5420 (10) α = 92.270 (10) β = 99.566 (10) γ = 102.563 (10)
V (Å^3)	1491.07 (14)	423.92 (10)
Z	4	2
Absorption coefficient (mm^{-1})	4.694	2.990
Goodness-of-fit on F^2	1.050	1.081
R_1 (on F, I>2σ(I))	0.0354	0.0154
R_1 (all data)	0.0513	0.0176
wR_2 (on F^2, I>2σ(I))	0.0737	0.0350
wR_2 (all data)	0.0787	0.0355

Table A31**.** Crystal Data for **88 - 89**.

Data	**88**	**89**
Empirical Formula	$C_4H_{14}Cl_2HgN_2S_2$	$C_4H_{16}C1_3Hg_{1.5}N_2OS_2$
Formula Weight	425.78	1276.99
Temperature (K)	145(1)	173(1)
Crystal System	Monoclinic	Monoclinic
Space Group	P 21/c	P 21/n
Unit Cell Dimensions (Å and º)	a = 7.746(1) b = 12.138(1) c = 12.023(1) α = 90 β = 103.61 γ = 90	a = 14.162(3) b = 8.0090(16) c = 19.604(4) α = 90.000 β = 92.79(3) γ = 90.00
Volume ($Å^3$)	1098.7(2)	2220.9(8)
Z	4	4
Density Calculated (mg/m^3)	2.578	3.819
Absorption Coefficient (mm^{-1})	14.823	30.412
Reflection Collected	4925	13479
Independent Reflections	2528 (R(int) = 0.0295)	3911 (R(int) = 0.0799)
Refinement Method	Full-matrix least-square on F^2	Full-matrix least-square on F^2
Final R indices [I>2sigma(I)]	R_1 = 0.0240 wR_2 = 0.0444	R_1 = 0.0357 wR_2 = 0.0562
R indices (all data)	R_1 = 0.0194 wR_2 = 0.0431	R_1 = 0.0587 wR_2 = 0.0619

Table A32**.** Crystal Data for **90** and **91**.

Data	**90**	**91**
Empirical Formula	$C_6H_{21}C1_6Hg_3N_3S_3$	$C_6H_{22}Cl_{13}Hg_3N_3S_3O_3$
Formula Weight	1045.91	972.51
Temperature (K)	90.0(2)	90.0(2)
Crystal System	Monoclinic	Orthorhombic
Space Group	P 21/n	P b c a
Unit Cell Dimensions (Å and º)	a = 13.7992(3) b = 7.7167(2) c = 19.6891(4) α = 90.0 β = 93.4(11) γ = 90.0	a = 21.1255(10) b = 7.9607(2) c = 22.6473(3) α = 90.0 β = 90.0 γ = 90.0
Volume ($Å^3$)	2092.76(8)	3808.68(11)
Z	4	8
Density Calculated (mg/m^3)	3.320	3.392
Absorption Coefficient (mm^{-1})	23.014	24.877
Reflection Collected	21724	8215
Independent Reflections	4789 (R(int) = 0.0498)	4375 (R(int) = 0.0289)
Refinement Method	Full-matrix least-square on F^2	Full-matrix least-square on F^2
Final R indices [I>2sigma(I)]	R_1 = 0.0272 wR_2 = 0.0508	R_1 = 0.0247 wR_2 = 0.0542
R indices (all data)	R_1 = 0.0404 wR_2 = 0.0542	R_1 = 0.0359 wR_2 = 0.0573

Table A33**.** Crystal Data for **94** and **95**.

Data	**94**	**95**
Empirical Formula	$C_6H_{21}Br_{5.2}Cl_{0.8}Hg_3N_3S_3$	$C_{2.67}H_{10.67}Hg_{0.67}Br_{2.67}N_{1.33}O_{0.67}S_{1.33}$
Formula Weight	1276.99	461.69
Temperature (K)	173 (1)	90.0(2)
Wavelength Å	0.71073	0.71073
Crystal System	Monoclinic	Monoclinic
Space Group	P 21/n	P 21/c
Unit Cell Dimensions (Å and º)	a = 14.162(3) b = 8.0090(16) c = 19.604(4) α = 90.0 β = 92.79(3) γ = 90.0	a = 6.3250(13) b = 12.381(3) c = 10.112(2) α = 90.0 β = 101.16(3) γ = 90.0
Volume ($Å^3$)	2220.9(8)	776.9(3)
Z	4	3
Density Calculated (mg/m^3)	3.819	2.961
Absorption Coefficient (mm^{-1})	30.412	20.439
F(000)	2246	628
Reflection Collected	13479	9830
Independent Reflections	3911 (R(int) = 0.0799)	17635 (R(int) = 0.0605)
Refinement Method	Full-matrix least-square on F^2	Full-matrix least-square on F^2
Goodness of fit on F^2	0.950	1.055
Final R indices [I>2sigma(I)]	R_1 = 0.0357 wR_2 = 0.0562	R_1 = 0.0345 wR_2 = 0.0660
R indices (all data)	R_1 = 0.0587 wR_2 = 0.0619	R_1 = 0.0463 wR_2 = 0.0697

Table A34**.** Crystal Data for **98 - 100**.

Data	**98**	**99**	**100**
Empirical Formula	$C_2H_9Hg_2I_4NOS$	$C_4H_{12}Hg_2I_2N_2S_2$	$C_{5.28}H_{16.2}Hg_2I_3N_2OS_2$
Formula Weight	1003.94	807.26	969.76
Temperature (K)	90.0(2)	90.0(2)	90.0(2)
Wavelength Å	0.71073	0.71073	1.54178
Crystal System	Orthorhombic	Monoclinic	Monoclinic
Space Group	P c a 21	P 21/c	P 21/c
Unit Cell Dimensions (Å and º)	a = 29.6018(3) b = 7.25240(10) c = 13.3459(2) α = 90.000 β = 90.0 γ = 90.00	a = 9.2107(2) b = 8.1173(2) c = 18.1332(4) α = 90.0 β = 100.5020(10) γ = 90.0	a = 12.3749(2) b = 8.1190(2) c = 17.9245(4) α = 90.0 β = 105.5780(10) γ = 90.0
Volume ($Å^3$)	2865.15(7)	1333.04(5)	1737.42(6)
Z	8	4	4
Density (mg/m^3)	4.655	4.022	3.705
Absorption Coefficient (mm^{-1})	30.137	27.911	75.182
F(000)	3392	1392	1684
Reflection Collected	6261	20973	22510
Independent Reflections	6261 (R(int) = 0.00)	3054 (R(int) = 0.0540)	3128 (R(int) = 0.0638)
Refinement Method	Full-matrix least-square on F^2	Full-matrix least-square on F^2	Full-matrix least-square on F^2
Goodness of fit on F^2	1.044	1.086	1.059
Final R indices [I>2sigma(I)]	R_1 = 0.0345 wR_2 = 0.0740	R_1 = 0.0248 wR_2 = 0.0427	R_1 = 0.0366 wR_2 = 0.0912

R indices (all data)	$R_1 = 0.0429$ $wR_2 = 0.0776$	$R_1 = 0.0366$ $wR_2 = 0.0455$	$R_1 = 0.0397$ $wR_2 = 0.0933$

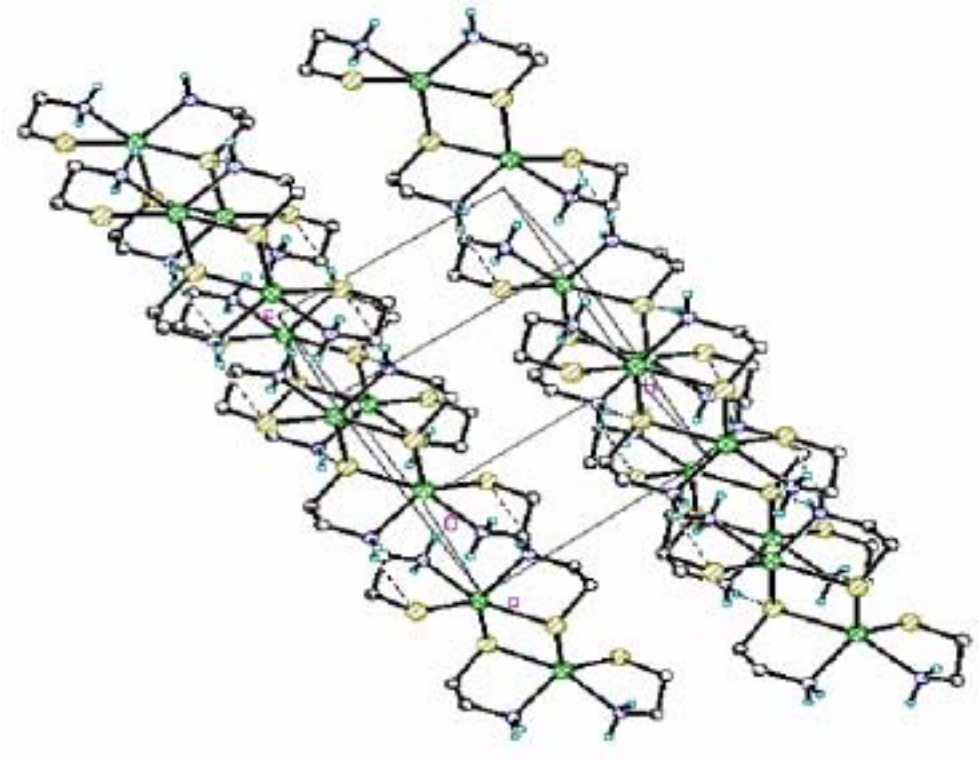

Figure A1. View of the unit cell of **81** emphasizing the intermolecular hydrogen bonding. A simplified figure showing this bonding is shown in the inset.

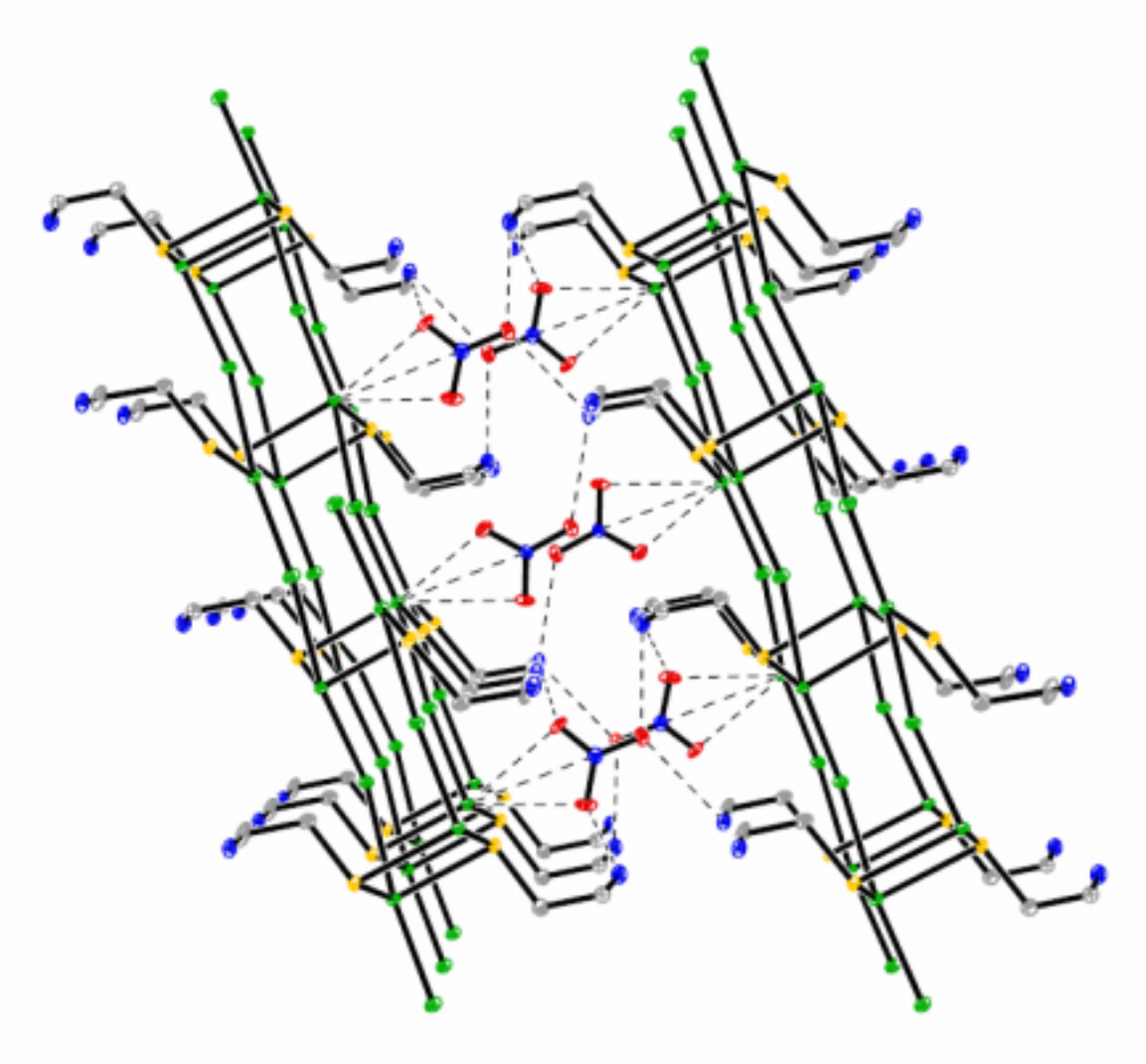

Figure A2. Intermolecular hydrogen bonding observed in **87** along the 'b' axis shown with dotted lines.

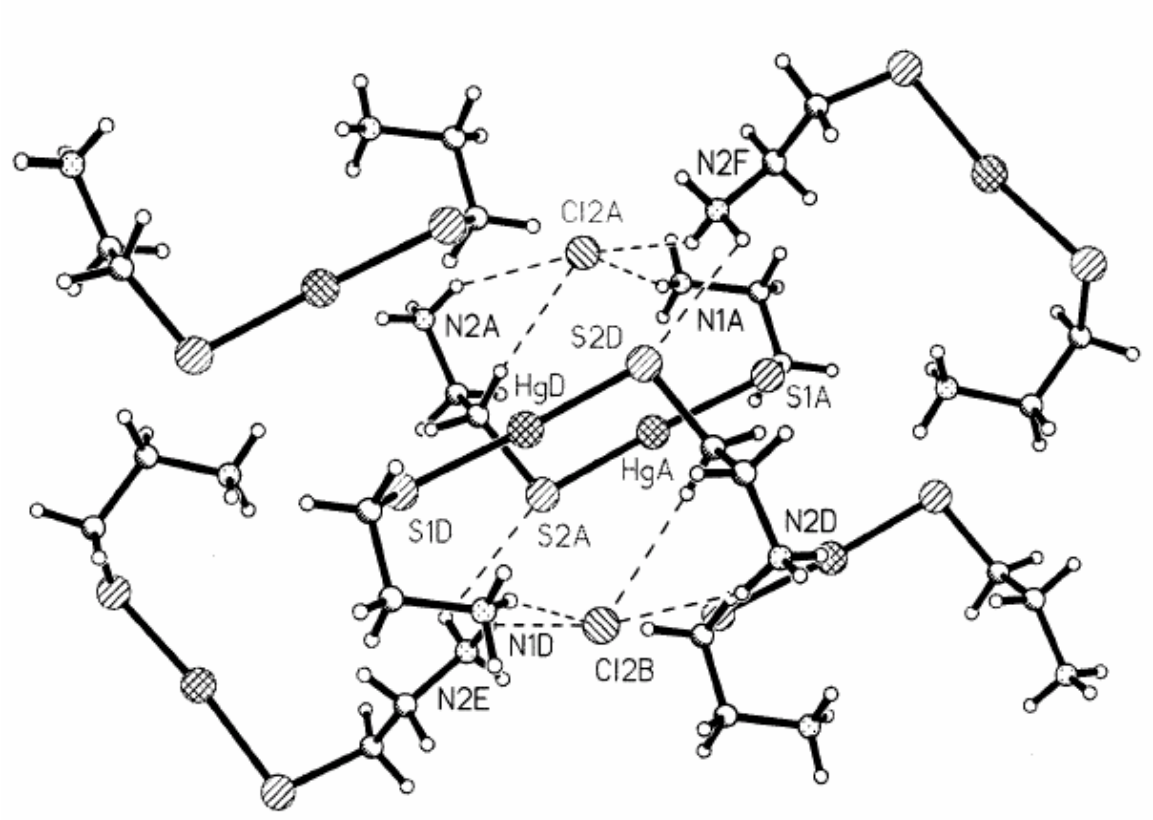

Figure A3. Packing diagram of **88** showing hydrogen bonding.

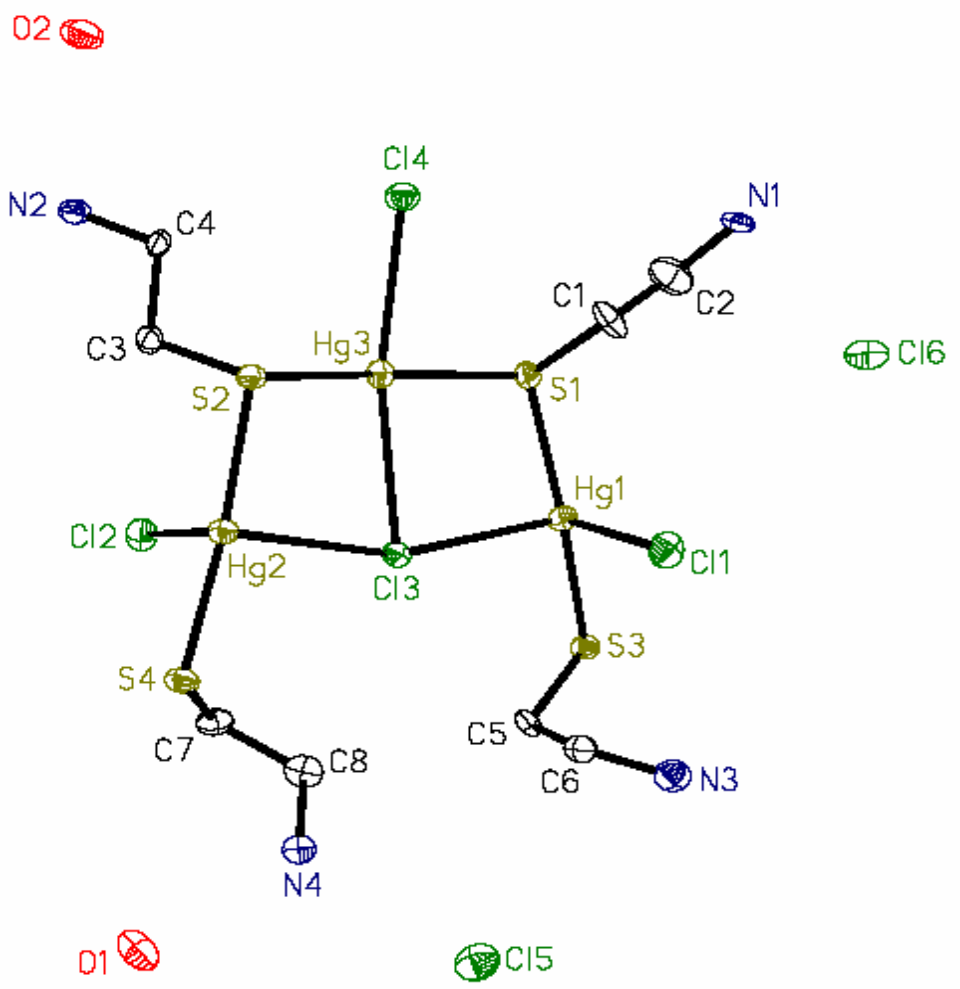

Figure A4. The trinuclear moiety of **89** showing triply bridged Cl atoms. The bridging Hg3-S" and S3-Hg3" bonds are not shown.

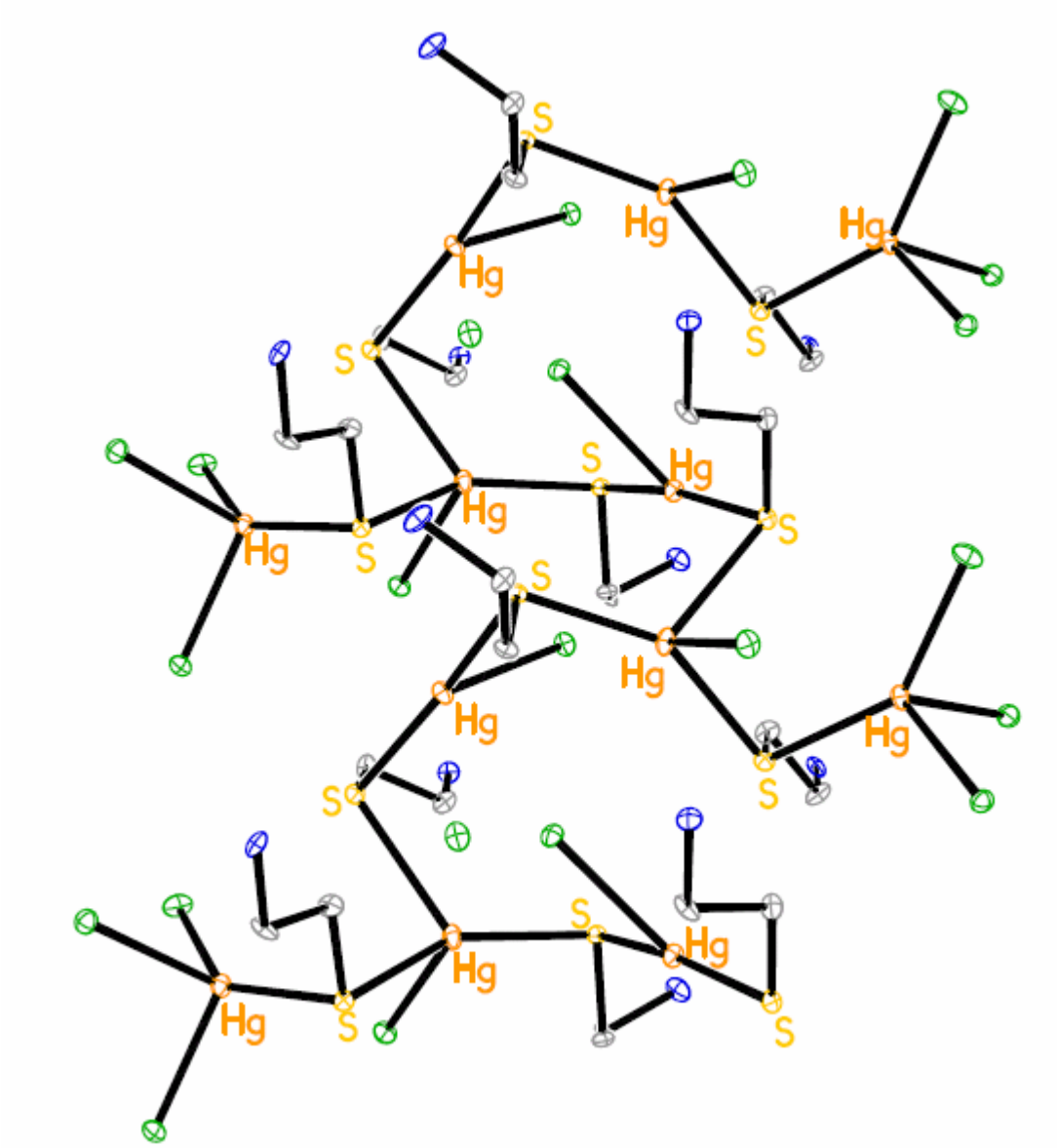

Figure A5. The polymeric unit of **90**.

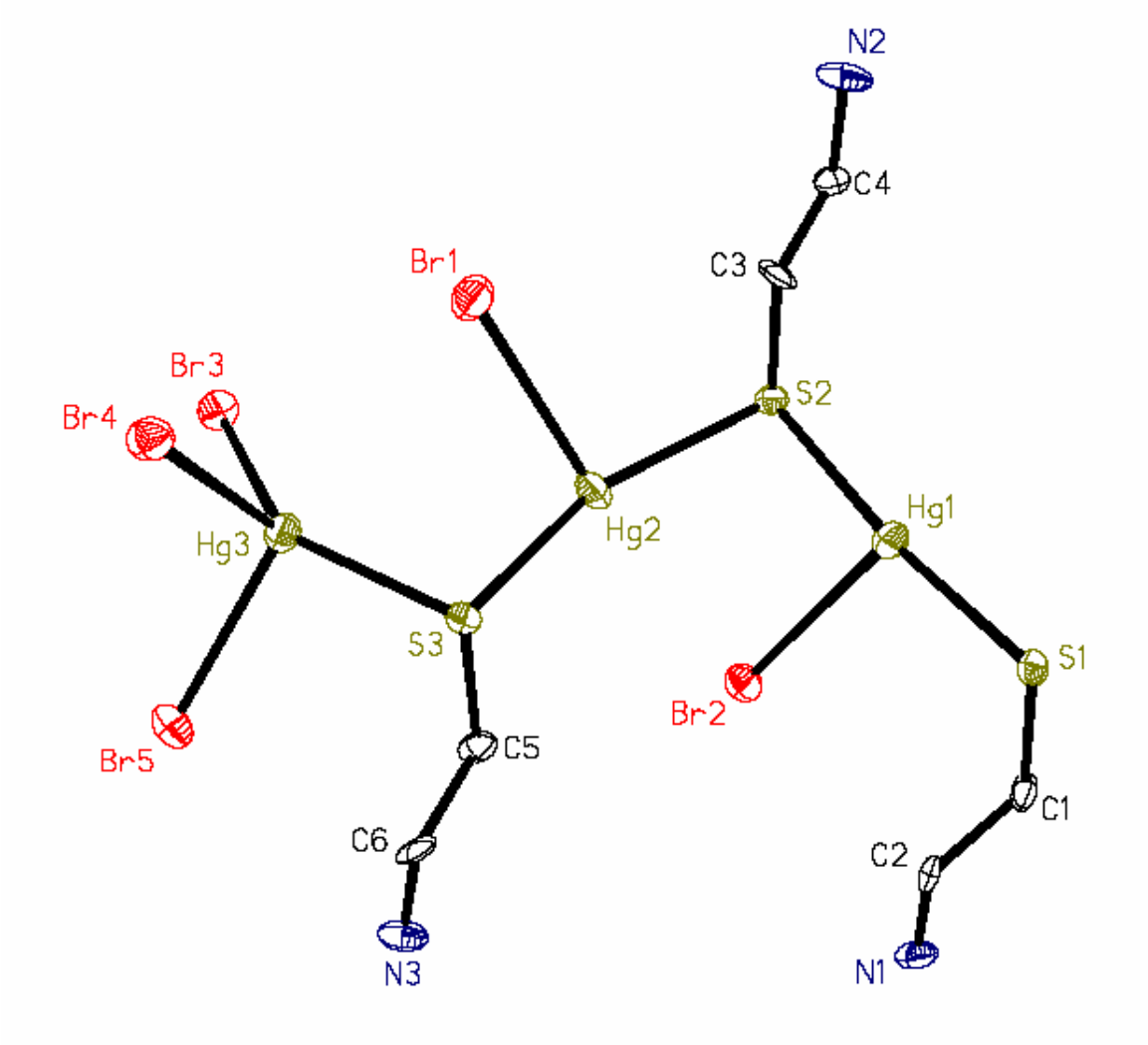

Figure A6. Asymmetric unit in the structure of **94** (without counter anions) with 50 % thermal ellipsoids.

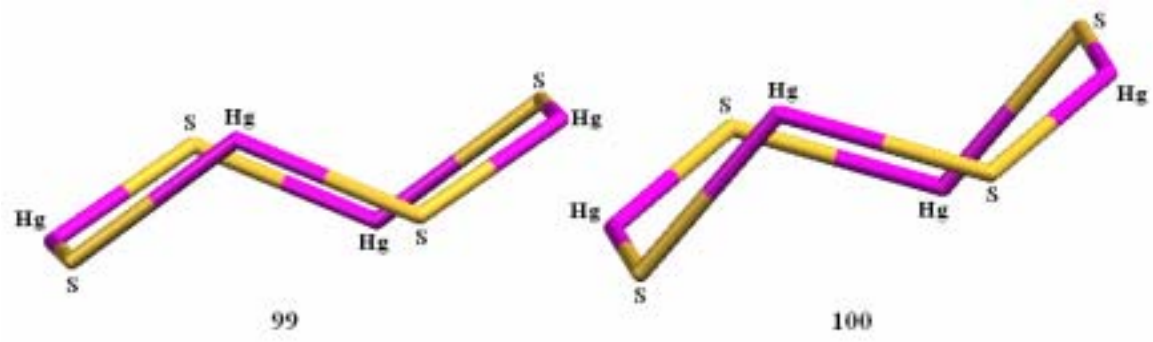

Figure A7. The chair configuration acquired by the core of **99** and **100**.

References

(1) Raper, E. S. *Coord. Chem. Rev.* **1985**, *61*, 115.

(2) Dance, I. G. *Polyhedron* **1986**, *5*, 1037.

(3) Blower, P. G.; Dilworth, J. R. *Coord. Chem. Rev.* **1987**, *76*, 121.

(4) Krebs, B.; Henkel, G. *Angew. Chem. Int. Ed. Engl.* **1991**, *30*, 769.

(5) Dilworth, J. R.; Hu, J. *Adv. Inorg. Chem.* **1993**, *40*, 411.

(6) Raper, E. S. *Coord. Chem. Rev.* **1996**, *153*, 199.

(7) Raper, E. S. *Coord. Chem. Rev.* **1997**, *165*, 475.

(8) Holm, R. H.; Solomon, E. I. *Chem. Rev.* **1996**, *96*, 2239.

(9) Rajagopalan, P. T. R.; Datta, A.; Pei, D. *Biochemistry* **1977**, *36*, 13910.

(10) Grapperhaus, C. A.; Mullins, C. S.; Kozlowski, P. M.; Mashuta, M. S. *Inorg. Chem.* **2004**, *43*, 2859 and refs therein.

(11) Kruger, H. J.; Peng, G.; Holm, R. H. *Inorg. Chem.* **1991**, *30*, 734.

(12) Henkel, G.; Krebs, B. *Chem. Rev.* **2004**, *104*, 801.

(13) Shaw, C. F. *Chem. Rev.* **1999**, *99*, 2589.

(14) Markello, T. C.; Bernardeni, I. M.; Gahl, W. A. *N. Eng. J. Med.* **1993**, *328*, 1157.

(15) Alexander, P.; Bacq, Z.; Cousens, S.; Fox, M.; Herve, A.; Lazar, J. *Radiat. Res.,* **1955**, *2*, 392.

(16) Aposhian, H. V. *Metal Ions in Biology.* Lippincoat, 1960.

(17) Barone, G.; Chaplin, R.; Hibbert, T. G.; Kana, A. T.; Mahon, M. F.; Molloy, K. C.; Worsely, I. D.; Parkin, I. P.; Price, L. S. *J. Chem. Soc., Dalton Trans.* **2002**, 1085.

(18) Osakada, K.; Yamamoto, T. *Inorg. Chem.* **1991**, *30*, 2328.

(19) Cheon, J.; Talaga, D. S.; Zink, J. I. *J. Am. Chem. Soc.* **1997**, *119*, 163.

(20) Konno, T.; Chikamoto, Y.; Okamoto, K.; Yamaguchi, T.; Ito, T.; Hirotsu, M. *Angew. Chem., Int. Ed.,* **2001**, *39*, 4098.

(21) Morrow, H. *Cadmium(Cd), Metals Handbook*; ASM International: Metal Park, Ohio, 1990.

(22) Nriage, J. M.; Pacyna, J. M. *Nature* **1988**, *333*, 134.

(23) Goyer, R. *Toxic Effects of Metal*; Pergamon: New York, 1991.

(24) Friberg, L.; Piscator, M.; Norrdberg, G. F.; Kjellstrom, T. *Cadmium in the Environment.*; CRC Press: Cleveland, 1974.

(25) Klaaseen, C. D.; J, L. *Drug Metab Rev.* **1977**, *29*, 79.

(26) Bottari, E.; Festa, M. R.; R, J. *J. Coor. Chem.* **1988**, *17*, 245.

(27) Vecchio-Sadus *J. Appl. Electrochem.* **1993**, *23*, 401.

(28) Fleischer, H. *Coor. Chem. Rev.* **2004**, *249*, 799.

(29) Pecs, L.; Ozols, J.; Kemme, A.; Bliedelis, J.; Sturis, A. *Latv. PSR Zinat. Akad, Vestis, Khim. Ser.* **1979**, *3*, 259.

(30) Bermejo, E.; Castineiras, A.; Garcia-Santos, I.; West, D. X. *Z. Anorg. Allg. Chem.* **2004**, *630*, 1096.

(31) Castineiras, A.; Garcia, I.; Bermejo, E.; Ketcham, K. A.; West, D. X.; El-Sawaf, A. K. *Z. Anorg. Allg. Chem.* **2002**, *628*, 492.

(32) West, D. X.; Ives, J. S.; Krejci, J.; Salberg, M. M.; Zumbahlen, T. L.; Bain, G. A.; Liberta, A. E.; Valdes-Martinez, J.; Hernandez-Ortega, S.; Toscano, R. A. *Polyhedron* **1995**, *14*, 2189.

(33) Ketcham, K. A.; Swearingen, J. K.; Castineiras, A.; Garcia, I.; Bermejo, E.; West, D. X. *Polyhedron* **2001**, *20*, 3265.

(34) Castro, R.; Duran, M. L.; Garcia-Vazquez, J. A.; Romero, J.; Sousa, A.; Castineiras, A.; Hiller, W.; Strahle, J. *Z. Naturforsch.* **1992**, *47B*, 1067.

(35) Fletcher, S. R.; Scapski, A. C. *J. Chem. Soc.* **1972**, 635.

(36) Deeming, A. J.; Meah, M. N.; Randle, N. P. *J. Chem. Soc., Dalton Trans.* **1989**, 2211.

(37) Domenicano, A.; Torelli, L.; Vaciago, A.; Zambonelli, L. *J. Chem. Soc. A.* **1968**, 1351.

(38) Agre, V. M.; Shugam, E. A. *Kristallografiya* **1972**, *17*, 303.

(39) Raston, C. L.; White, A. H. *Aust. J. Chem.* **1976**, *29*, 739.

(40) McCleverty, J. A.; Gill, S.; Kowalski, R. S. Z.; Bailey, N. A.; Adams, H.; Lumbard, K. W.; Murphy, M. A. *J. Chem. Soc., Dalton Trans.* **1982**, 493.

(41) Berreau, L. M.; Mkowska-Grzyska, M. M.; Arif, A. M. *Inorg. Chem.* **2000**, *39*, 4390.

(42) Dubler, E.; Gyr, E. *Inorg. Chem.* **1988**, *27*, 1466.

(43) Castro, R.; Garcia-Vazquez, J. A.; Romero, J.; Sousa, A.; Chang, Y. D.; Zubieta, J. *Inorg. Chim. Acta* **1993**, *211*, 47.

(44) Mikyriya, M.; Jian, X.; Ikemi, S.; Kawasashi, T.; Tsutsumi, H.; Nakasone, A.; Lim, J. *Inorg. Chim. Acta* **2001**, *312*, 183.

(45) Vossmeyer, T.; Reck, G.; Katsikas, L.; Haupt, E. T. K.; Schulz, B.; Weller, H. *Inorg. Chem.* **1995**, *34*, 4926.

(46) Vossmeyer, T.; Reck, G.; Schulz, B.; Katsikas, L.; Weller, H. *J. Am. Chem. Soc.* **1995**, *117*, 12881.

(47) Dance, I. G.; Garbutt, R. G.; Craig, D. C. *Aust. J. Chem.* **1986**, *39*, 1449.

(48) Fawcett, T. G.; Ou, C. C.; Potenza, J. A.; Schugar, H. J. *J. Am. Chem. Soc.* **1978**, *100*, 2058.

(49) Casals, I.; Gonzalez-Duarte, P.; Clegg, W.; Foces-Foces, C.; Cano, F. H.; Martinez-Ripoll, M.; Gomez, M.; Solans, X. *J. Chem. Soc., Dalton Trans.* **1991**, 2511.

(50) Castro, R.; Garcia-Vazquez, J. A.; Romero, J.; Sousa, A.; Pritchard, R.; McAuliffe, C. A. *J. Chem. Soc., Dalton Trans.* **1994**, 1115.

(51) Habeeb, J. J.; Tuck, D. G.; Walters, F. H. *J. Coor. Chem.* **1978**, *8*, 27.

(52) Paulus, H. *Z. Anorg. Allg. Chem.* **1969**, *369*, 38.

(53) Hursthouse, M. B.; Khan, O. F. Z.; Mazid, M.; Motevalli, M.; O'Brien, P. *Polyhedron* **1990**, *9*, 544.

(54) Castro, R.; Romero, J.; Garcia-Vazquez, J. A.; Sousa, A.; Zubieta, J.; Chang, L. W. *Polyhedron* **1996**, *15*, 2741.

(55) Freeman, H. C.; Huq, F.; Stevens, G. N. *J. Chem. Soc., Chem. Commun.* **1976**, 90.

(56) Meester, P.; Hodgson, D. J. *J. Am. Chem. Soc.* **1977**, *99*, 6884.

(57) Barrie, P. J.; Gayani, A.; Motevalli, M.; O'Brien, P. *Inorg. Chem.* **1993**, *32*, 3862.

(58) Erskine, P. T.; Senior, N.; Awan, S.; Lambart, R.; Lewis, G.; Tickle, U.; M., S.; Sencer, P.; Thomas, P.; Warren, M. J. *Nat. Structure. Biol.* **1997**, *4*, 1025.

(59) Martan, H.; Weiss, J. *Z. Anorg. Allg. Chem.* **1984**, *514*, 107.

(60) Fleischer, H.; Schollmeyer, D. *Inorg. Chem.* **2004**, *43*, 5529.

(61) Sousa-Pedrares, A.; Casanova, M. I.; Garcia-Vazquez, J. A.; Duran, M. L.; Romero, J.; Sousa, A.; Silver, J.; Titler, P. J. *Eur. J. Inorg. Chem.* **2003**, 678.

(62) Bailey, N. A.; Fenton, D. E.; Jackson, I. T.; Moody, R.; Barbarian, C. R. *J. Chem. Soc., Chem. Commun.* **1983**, 1463.

(63) Labisbal, E.; Sousa, A.; Castineiras, A.; Garcia-Vazquez, J. A.; Romero, J.; West, D. X. *Polyhedron* **2000**, *19*, 1255.

(64) Pedrido, R.; Bermejo, M. R.; Romero, J. M.; Vazquez, M.; Gonzalez-Noya, A. M.; Manerio, M.; Rodriguez, M. J.; Fernandez, M. I. *J. Chem. Soc., Dalton Trans.* **2005**, 572.

(65) Shimoni-Livny, L.; Glusker, J. P.; Brock, C. W. *Inorg. Chem.* **1998**, *37*, 1853.

(66) Hancock, R. D.; Shaikfee, M. S.; Dobson, S. M.; Boeyens, J. C. A. *Inorg. Chim. Acta* **1988**, *154*, 229.

(67) Casas, J. S.; Castellano, E. E.; Ellena, J.; Garcia, T.; Sanchez, A.; Sordo, J.; Viddarate, M. J. *Inorg. Chem.* **2003**, *42*, 2584.

(68) Freeman, H. C.; Stevens, G. N.; Taylor, I. F. *J. Chem. Soc., Chem. Commun.* **1974**, 366.

(69) Bashall, A.; Mcpartlin, M.; Murphy, B. P.; Powell, H. R.; Waiker, S. *J. Chem. Soc., Dalton Trans.* **1994**, 1383.

(70) Aragoni, M. C.; Arca, M.; Demartin, F.; Devillanova, F. A.; Isaia, F.; Garau, A.; Lippolis, V.; Jalali, F.; Papke, U.; Shamsipur, M.; Tei, L.; Yari, A.; Verani, G. *Inorg. Chem.* **2002**, *41*, 6623.

(71) Constable, E. C.; Sacht, C.; Palo, G.; Tocher, D. A.; Truter, M. *J. Chem. Soc., Dalton Trans.* **1993**, 1307 and references therein.

(72) Pauling, L. *The Nature of Chemical Bond, 3rd Ed.*; Cornell University Press: Ithaca, 1960.

(73) Kupper, H. J.; Weighardt, K.; BNuber, B.; Weiss, J. *Z. Anorg. Allg. Chem.* **1989**, *577*, 155.

(74) Blake, A. J.; Fenske, D.; Li, W. S.; Lippolis, V.; Schroder, M. *J. Chem. Soc., Dalton Trans.* **1998**, 3961.

(75) Alcock, N. W.; Curzon, E. H.; Moore, P. *J. Chem. Soc., Dalton Trans.* **1984**, 2813.

(76) Bashall, A.; McPartlin, M.; Murphy, B. P.; Fenton, D. E.; Kitchen, S. J.; Tasker, P. A. *J. Chem. Soc., Dalton Trans.* **1990**, 505.

(77) Shannon, R. D. *Acta. Crystallogr., Sect. A.* **1976**, *32*, 751.

(78) Bazzicalupi, C.; Bencini, A.; Fusi, V.; Giorgi, C.; Paoletti, P.; Valtanocli, B. *J. Chem. Soc., Dalton Trans.* **1999**, 393 and ref therein.

(79) Block, E.; Ofori-Okai, G.; Kang, H.; Wu, J.; Zubieta, J. *Inorg Chim Acta.* **1991**, *190*, 5.

(80) Jurkschat, K.; Peveling, K.; Schurmann, M. *Eur. J. Inorg. Chem.* **2003**, 3563.

(81) Falconer, M.; Vaillant, A.; Rehul, K. R. *Neurotoxicology* **1994**, *145*, 109.

(82) Penddergrass, J. C.; Haely, B. E.; Vimy, M. *Neurotoxicology* **1997**, *18*, 315.

(83) Govindaswamy, N.; Moy, J.; Millar, M.; Koch, S. A. *Inorg. Chem.* **1992**, *31*, 5343.

(84) Bowmaker, G. A.; Dance, I. G.; Dobson, B. C.; Roger, D. A. *Aust. J. Chem.* **1984**, *37*, 1607.

(85) Henkel, G.; Betz, P.; Krebs, B. *J. Chem. Soc., Chem. Commun.* **1985**, *21*, 1498.

(86) Henkel, G.; Betz, P.; Krebs, B. *Inorg. Chim. Acta* **1987**, *134*, 195.

(87) Krauter, G.; Neumuller, B.; Goedken, V. L.; Rees, W. S. *Chem. Mater.* **1996**, *8*, 360.

(88) Casals, I.; Gonzalez-Duarte, P.; Sola, J.; Miravitlles, C.; Molins, E. *Polyhedron* **1988**, *44*, 2509.

(89) Canty, A. J.; Raston, C. L.; White, A. H. *Aust. J. Chem.* **1979**, *32*, 311.

(90) Biscarini, P.; Foresti, E.; Paradella, G. *J. Chem. Soc., Dalton Trans.* **1984**, 953.

(91) Alsina, T.; Clegg, W.; Fraser, K. A.; Sola, J. *J. Chem. Soc., Chem. Commun.* **1992**, *14*, 1010.

(92) Taylor, N. J.; Carty, A. J. *J. Am. Chem. Soc.* **1977**, *99*, 6143.

(93) Barrera, H.; Bayon, J. C.; Gonzalez-Duarte, P.; Sola, J.; Vinas, J. M. *Polyhedron* **1982**, *1*, 647.

(94) Almagro, X.; Clegg, W.; Cucurull-Sanchez, L.; Gonzalez-Duarte, P.; Traveria, M. *J. Organomet. Chem.* **2001**, *623*, 137.

(95) Bell, N. A.; Coles, S. J.; Constable, C. P.; Hibbs, D. E.; Hursthouse, M. B.; Mansor, R.; Raper, E. S.; Sammon, C. *Inorg. Chim. Acta* **2001**, *323*, 69.

(96) Bradely, D. C.; Kunchur, N. R. *J. Chem. Phys.* **1964**, *40*, 2258.

(97) Christou, G.; Folting, K.; Huffman, J. C. *Polyhedron* **1984**, *3*, 1247.

(98) Popovic, Z.; Soldin, Z.; Matkovic-Calogovic, D.; Pavlovic, G.; Rajic, M.; Giester, G. *Eur. J. Inorg. Chem.* **2002**, 171.

(99) Popovic, Z.; Matkovic-Calogovic, D.; Soldin, Z.; Pavlovic, G.; Davidovic, N.; Vikic-Topic, D. *Inorg. Chim. Acta* **1999**, *294*, 35.

(100) Nyburg, S. C.; Faerman, C. H. *Acta. Crystallogr., Sect. B.* **1985**, *41*, 274.

(101) Bell, N. A.; Branston, T. N.; Clegg, W.; Creighton, J. R.; Cucurull-Sanchez, L.; Elsegood, M. R. J.; Raper, E. S. *Inorg. Chim. Acta* **2000**, *303*, 220.

(102) Cecconi, F.; Ghilardi, C. A.; Midollini, S.; Orlandini, A. *Inorg. Chim. Acta* **1998**, *269*, 274.

(103) Chessa, G.; Marangoni, G.; Pitteri, B.; Bertolasi, V.; Ferretti, V.; Gilli, G. *J. Chem. Soc. Dalton Trans.* **1990**, 915 and references therein.

(104) Ghilardi, C. A.; Innocenti, P.; Midollini, S.; Orlandini, A.; Vacca, A. *J. Chem. Soc., Chem. Commun.* **1992**, 1691.

(105) Ghilardi, C. A.; Midollini, S.; Orlandini, A.; Vacca, A. *J. Organomet. Chem.* **1994**, *471*, 29.

(106) Tung, J.; Liau, B.; Elango, S.; Chen, J.; Hsiesh, H.; Liao, F.; Wang, S.; Hwang, L. *Inorg. Chem. Commun.* **2002**, *5*, 150.

(107) Latos-Grazynski, L.; Lisowski, J.; Olmstead, M. M.; Balch, A. L. *Inorg. Chem.* **1989**, *28*, 1183.

(108) Bond, A. M.; Cotton, R.; Hollenkamp, A. F.; Hoskin, B. F.; McGregor, K. *J. Am. Chem. Soc.* **1987**, *109*, 1969.

(109) Iwasaki, H. *Acta. Crystallogr.* **1973**, *B29*, 2115.

(110) Lawton, S. L. *Inorg. Chem.* **1971**, *10*, 2115.

(111) Bermejo, E.; Castineiras, A.; Garcia, I.; West, D. X. *Polyhedron* **2003**, *22*, 1147.

(112) Bu, X.; Coppen, P.; Naughton, M. J. *Acta. Crystallogr. Sect. C: Cryst. Struct. Commun.* **1990**, *C46*, 1609.

(113) Pbast, I.; Bats, J. W.; Fuess, H. *Acta. Crystallogr. Sect. B* **1990**, *B46*, 503.

(114) Popovic, Z.; Pavlovic, G.; Soldin, Z.; Popovic, J.; Matkovic-Calogovic, D.; Rajic, M. *Struct. Chem.* **2002**, *13*, 415.

(115) Raper, E. S.; Creighton, J. R.; Bell, N. A.; Clegg, W.; Cucurull-Sanchez, L. *Inorg. Chim. Acta* **1988**, *277*, 14.

(116) Stalhandske, C. M. V.; Persson, I.; Sandstrom, M.; Aberg, M. *Inorg. Chem.* **1997**, *36*, 4945.

(117) Matkovic-Calogovic, D.; Mrvos-Sermek, D.; Popovic, Z.; Soldin, Z. *Acta. Crystallogr. Sect. C: Cryst. Struct. Commun.* **2004**, *C60*, m44.

(118) Canty, A. J.; Raston, C. L.; White, A. H. *Aust. J. Chem.* **1978**, *31*, 677.

(119) Book, L.; Mak, T. C. W. *Inorg. Chim. Acta* **1978**, *92*, 265.

(120) Das, A. K.; Seth, S. *J. Inorg. Biochem.* **1997**, *65*, 207.

(121) Matkovic-Calogovic, D.; Popovic, Z.; Korpar-Colig, B. *J. Chem. Crystallogr., Sect. B.* **1995**, *25*, 453.

(122) Vallee, B. L. *Zinc Proteins*; Wiley: New York, 1983.

(123) Miller, J.; McLachlan, A. D.; Klug, A. *EMBO J.* **1985**, *4*, 1609.

(124) Lover, T.; Bowmaker, G. A.; Seakins, J. M.; Cooney, R. P. *Chem. Mater.* **1997**, *9*, 967.

(125) Inomata, Y.; Arai, Y.; Yamakoshi, T.; Howell, F. S. *J. Inorg. Biochem.* **2004**, *98*, 2149.

(126) Fleischer, H.; Dienes, Y.; Mathiasch, B.; Schmitt, V.; Schollmeyer, D. *Inorg. Chem.* **2005**, *44*, 8087.

(127) Masciocchi, N.; Moret, M.; Sironi, A.; Bruni, S.; Cariati, F.; Pozzi, A.; Manfredini, T.; Menabue, L.; Pellacani, G. C. *Inorg. Chem.* **1992**, *31*, 1401.

(128) Dance, I. G.; Garbutt, R. G.; Bailey, T. D. *Inorg. Chem.* **1990**, *29*, 603.

(129) Santos, R. A.; Gruff, E. S.; Koch, S. A.; Harbison, G. S. *J. Am. Chem. Soc.* **1990**, *112*, 9257 and refs therein.

(130) Jicha, D. C.; Busch, D. H. *Inorg. Chem.* **1962**, *1*, 872.

(131) Roesky, H. W. *Solid State Science* **2001**, *3*, 777.

(132) Sousa-Pedrares, A.; Romero, J.; Garcia-Vazquez, J. A.; Duran, I.; Casanova, A. S. *J. Chem. Soc., Dalton Trans.* **2003**, 1379.

(133) Clegg, W.; Casals, I.; Gonzalez-Duarte, P. *Acta Cryst.* **1993**, *C49*, 129.

(134) Renz-Kreikebhom, V. C.; Stromburg, B.; Engelhardt, U. *Acta Cryst.* **1991**, *C47*, 1403.

(135) Tarafdar, M. T. F.; Khoo-Teng, J.; Crouse, K. A.; Ali, A. M.; Yamin, B. M.; Fun, H. K. *Polyhedron* **2002**, *21*, 2547.

(136) Castineiras, A.; Bermejo, E.; West, D. X.; Ackerman, L. J.; Valdes-Martinez, J.; Hernandez-Ortega, S. *Polyhedron* **1999**, *18*, 1463.

(137) Engelhardt, L. M.; Renz-Kreikebhom, V. C. *Acta Cryst.* **1989**, *C45*, 1679.

(138) Ogawa, E.; Suzuki, S.; Tsuzuki, H. *Japan J. Pharmacol.* **1972**, *22*, 275.

(139) Eddaoudi, M.; Kim, J.; Rosi, N.; Vodak, D.; Wachter, J.; O'Keeffe, M.; Yaghi, O. M. *Science* **2002**, *295*, 469.

(140) Leininger, S.; Olenyuk, B.; Stang, P. J. *Chem. Rev.* **2000**, *100*, 853.

(141) Cote, A. P.; Shimizu, G. K. H. *Coor. Chem. Rev.* **2003**, *245*, 49.

(142) Moulton, B.; Zawarotko, M. J. *Chem. Rev.* **2001**, *101*, 1629.

(143) Bharara, M. S.; Atwood, D. A. *Encyclopedia of Inorganic Chemistry*; Wiley: Chichester, England., 2005.

(144) Cramer, R. E.; Waddling, C. A.; Fujimoto, C. H.; Smith, D. W.; Kim, K. E. *J. Chem. Soc., Dalton Trans.* **1997**, 1675.

(145) Appleton, S. E.; Briand, G. G.; Decken, A.; Smith, A. S. *J. Chem. Soc., Dalton Trans.* **2004**, 3515.

(146) Agre, V. M.; Shugam, E. A. *Russ. J. Struct. Chem.* **1971**, *12*, 102.

(147) Pech, L. Y.; Ozols, Y. K.; Apinitis, S. K.; Sturis, A. P. *Latv. PSR Zinat. Akad, Vestis, Khim. Ser* **1982**, 26.

(148) Pech, L. Y.; Bankovsky, Y.; Fundamensky, V.; Sturis, A. P.; Bruvere, A. *Latvian J. Chem.* **1992**, 488.

(149) Anjali, K. S.; Jeyagowry, T. S.; Vittal, J. J. *Inorg. Chim Acta* **1999**, *295*, 9.

(150) Bharara, M. S.; Kim, C. H.; Parkin, S.; Atwood, D. A. *Polyhedron* **2005**, *24*, 865.

(151) Bharara, M. S.; Parkin, S.; Atwood, D. A. *Inorg. Chim. Acta* **2006**, Submitted.

(152) Payne, J. C.; Horst, M. A.; Godwin, H. A. *J. Am. Chem. Soc.* **1999**, *121*, 6850.

(153) Bharadwaj, P. K.; Arbuckle, B. W.; Musker, W. K. *Inorg. Chim. Acta* **1988**, *142*, 243.

(154) Rae, D. A.; Craig, D. C.; Dance, I. G.; Scudder, M. L.; Dean, P. A.; Kmetic, M. A.; Payne, N. C.; Vittal, J. J. *Acta Cryst.* **1997**, *B53*, 457.

(155) Clegg, W.; Abrahams, I. L.; Garner, C. D. *Acta Cryst.* **1984**, *C40*, 1367.

(156) Brown, I. D. *Chem. Soc. Rev.* **1978**, *7*, 359.

(157) Wojnowski, W.; Wojnowski, M.; Peters, K.; Peters, E. M.; Schnering, H. G. *Z. Anorg. Allg. Chem.* **1986**, *535*, 56.

(158) Glass, R. S.; Andruski, S. W.; Broeker, J. L.; Firouzabadi, H.; Steffen, L. K.; Wilson, G. S. *J. Am. Chem. Soc.* **1989**, *111*, 4036 and refs therein.

(159) Hummel, H. U.; Meske, H. *Z. Naturforsh., B: Chem. Sci.* **1988**, *43*, 389.

(160) Herbstein, F. H.; Reisner, G. M. *Z. Kristallogr.* **1984**, *169*, 83.

(161) Coucouvanis, D.; Lippard, S. J. *Progress in Inorganic Chemistry*; Wiley: New York, 1979.

(162) Reger, D. L.; Wright, T. D.; Smith, M. D.; Rheingold, A. L.; Kassel, S.; Concolino, T.; Rhagitan, B. *Polyhedron* **2002**, *21*, 1795.

(163) Lipscomb, W. N.; Strater, N. *Chem. Rev.* **1996**, *96*, 2375.

(164) Bidstrup, P. L. *Toxicity of Mercury and its Compounds*; Elsevier: Amsterdam, 1964.

(165) Wong, Y. S.; Carty, A. J.; Chieh, P. C.; Chung, C. P. *J. Chem. Soc., Dalton Trans.* **1977**, 1157.

(166) Bach, R. D.; Rajan, S. J.; Vardhan, H. B.; lang, T. J.; Albrecht, N. G. *J. Am. Chem. Soc.* **1981**, *103*, 7727.

(167) Picot, A.; Proust, N.; trace, J. *Microprobe Tech.* **2000**, *18*, 183.

(168) Bramlett, J. M.; Im, H.; Yu, X.; Chen, T.; Cai, H.; Roecker, L. E.; Barnes, C. E.; Dai, S.; Xue, Z. *Polyhedron* **2004**, *357*, 243.

(169) Wright, J. G.; Natan, M. J.; MacDonnell, F. M.; Ralston, D. M.; O'Halloran, T. V. *Prog Inorg Chem.* **1990**, *38*, 323.

(170) Terzis, A.; Faught, J. B.; Pouskoulelis, G. *Inorg. Chem.* **1980**, *19*, 1060.

(171) Philip, A. W. D.; Vittal, J. J.; Wu, Y. *Inorg. Chem.* **1994**, *33*, 2180.

(172) Cheesman, B. V.; Arnold, A. P.; Rabenstien, D. L. *J. Am. Chem. Soc.* **1988**, *110*, 6359.

(173) Cotton, F. A.; Jamerson, J. D. *J. Am. Chem. Soc.* **1976**, *98*, 1273.

(174) Kim, C. H.; Parkin, S.; Bharara, M. S.; Atwood, D. A. *Polyhedron* **2002**, *21*, 225.

(175) Bharara, M. S.; Thanhhoa, H. B.; Parkin, S.; Atwood, D. A. *Inorg. Chem.* **2005**, *44*, 5753.

(176) Bharara, M. S.; Thanhhoa, H. B.; Parkin, S.; Atwood, D. A. *J. Chem. Soc., Dalton Trans.* **2005**, 3874.

(177) Bharara, M. S.; Parkin, S.; Atwood, D. A. **Unpublished Results**.

(178) Watton, S. P.; Wright, J. G.; MacDonnell, F. M.; Bryson, J. W.; O'Halloran, T. V. *J. Am. Chem. Soc.* **1990**, *112*, 2824.

(179) Tamilarasan, R.; McMillin, D. R. *Inorg. Chem.* **1986**, *26*, 3139.

(180) Beltramine, M.; Lerch, K.; Vasak, M. *Biochemistry* **1981**, *23*, 3422.

(181) Vasak, M.; Kagi, J. H.; Hill, H. A. *Biochemistry* **1981**, *20*, 2582.

(182) Johnson, B. A.; Armitage, I. M. *Inorg. Chem.* **1987**, *26*, 3139.

(183) Desiraju, G. R.; Steiner, T. *The Weak Hydrogen Bond*; Oxford University Press: Oxford, 1999.

(184) Adman, E.; Watenpaugh, K. D.; Jensen, L. H. *Proc. Natl. Acad. Sci.* **1975**, *72*, 4854.

(185) Ueyama, N.; Yamada, Y.; Okamura, T.; Kimura, S.; Nakamura, A. *Inorg. Chem.* **1996**, *35*, 6473.

(186) Alsaadi, B. M.; Sandstrom, M. *Acta Chim. Scand. A.* **1982**, *36*, 509.

(187) Stalhandske, C. M. V.; Zintl, F. *Acta Cryst.* **1986**, *C42*, 1731.

(188) Puff, V. H.; Seivers, R.; Elsner, G. *Z. Anorg. Allg. Chem.* **1975**, *413*, 37.

(189) Pavlovic, G.; Popovic, Z.; Soldin, Z.; Matkovic-Calogovic, D. *Acta. Crystallogr., Sect. C.* **2000**, *C56*, 61.

(190) Stalhandske, C. M. V.; Persson, I.; Sandstrom, M.; Kamineska-piotrowicz, E. *Inorg. Chem.* **1997**, *36*, 3174.

(191) Book, L.; Mak, T. C. W. *Inorg. Chim. Acta* **1984**, *92*, 265.

(192) Chung, C. P. *Can. J. Chem.* **1977**, *55*, 65.

(193) Bochmann, M.; Webb, K. J.; Powell, A. K. *Polyhedron* **1992**, *11*, 513.

(194) In;; Distances calculated in Mercury, CCDC, http://www.ccdc.cam.ac.uk/products/csd_system/mercury/.

(195) Berry, S. M.; Bebout, D. C.; Butcher, R. J. *Inorg. Chem.* **2005**, *44*, 27 and ref therein.

(196) Del Hierro, I.; Sierra, I.; Perez-Quintanilla, D.; Carrillo-Hermosilla, F.; Lopez-Solera, I.; Fajardo, M. *Inorg. Chim. Acta* **2003**, *355*, 347.

(197) Akinchan, N. T.; Drozdzewski, P. M.; Akinchan, R. *Pol. J. Chem.* **2000**, *74*, 1221.

(198) Bharara, M. S.; Parkin, S.; Atwood, D. A. *Inorg. Chem.* **2006**, *Submitted.*

(199) Castineiras, A.; Arquero, A.; Masaguer, J. R.; Martinez-Carrera, S.; Garcia-Blanco, S. *Z. Anorg. Allg. Chem.* **1986**, *539*, 219.

(200) Vittal, J. J.; Dean, P. A. W.; Payne, N. C. *Can. J. Chem.* **1993**, *71*, 2043.

(201) Busetto, L.; Bordoni, S.; Zanotti, V.; Albano, V. G.; Braga, D.; Monari, M. J. *Organomet. Chem.* **1990**, *389*, 341.

(202) Khandelwal, B. L.; Singh, A. K.; Srivastava, V.; Povey, D. C.; Smith, G. W. *Polyhedron* **1990**, *9*, 2041.

(203) Chandha, R. K.; Drake, J. E.; McManus, N. T.; Mislankar, A. *Can. J. Chem.* **1987**, *65*, 2305.

(204) Betz, P. In *Chemistry*; Universitat Munster, 1986.

(205) Chen, J.; Zhang, W.; Ren, Z.; Zhang, Y.; Lang, J. *Acta Cryst.* **2005**, *E61*, m60.

(206) Bharara, M. S.; Parkin, S.; Atwood, D. A. *Inorg. Chem.* **2006**, *45*, 2112.

(207) Al-Showiman, S. S. *Inorg. Chim. Acta* **1988**, *141*, 263.

(208) Nakamoto, K. *Infrared Spectra of Inorganic and Coordination Compounds*, 1963.

(209) Bell, N. A.; Branston, T. N.; Clegg, W.; Parker, L.; Raper, E. S.; Constable, C. P.; Sammon, C. *Inorg. Chim. Acta* **2001**, *319*, 130.

(210) Svensson, P. H.; Kloo, L. *Inorg. Chem.* **1999**, *38*, 3390 and refs therein.

(211) Dean, P. A.; Jagadese, J. V.; Wu, Y. *Inorg. Chem.* **1994**, *33*, 2180 and refs therein.

(212) Casals, I.; Gonzalez-Duarte, P.; Sola, J.; Miravitlles, C.; Molins, E. *Polyhedron* **1988**, *7*, 2509.

(213) Grdenic, D. *Q. Rev.* **1965**, *19*, 303.

(214) Gruff, E. S.; Koch, S. A. *J. Am. Chem. Soc.* **1990**, *112*, 1245.

(215) Sens, M. A.; Wilson, N. K.; Ellis, P. D.; Odon, J. D. *J. Magn. Reson.* **1975**, *19*, 323.

(216) Pregosin, P. S. *Transition Metal Nuclear Magnetic Resonances*; Elsevier: New York, 1991.

(217) Otwinowski, Z.; Moinor, W. *Methods Enzymol.* **1997**, *276*, 307.

(218) Sheldrick, G. M. *SADABS-An Empirical Adsorption Correction Program* Madison, WI, 1996.

(219) *International Tables for Crystallography Vol. C*; Kluwer Academic Publishers: Dordrecht, The Netherlands, 1992.

(220) Aberg, B.; Ekman, L.; Falk, R.; Greitz, U.; Persson, G.; Snihs, J. O. *Arch. Environ. Health* **1969**, *10*, 478.

(221) Corwin, D. T.; Gruff, E. S.; Koch, S. A. *J. Chem. Soc., Chem. Commun.* **1987**, 966.

(222) Black, S. J.; Einstein, F. W. B.; Hayes, P. C.; Kumar, R.; Tuck, D. G. *Inorg. Chem.* **1986**, *25*.

(223) Biagini, M.; Gaetani, A.; Guastani, C.; Musatti, A.; Nardelli, M. *Gazz. Chim. Ital.* **1971**, *101*, 815.

(224) Antsyskina, A. S.; Porai-Koshits, M. A.; Khandlovich, M.; Ostrikova, V. N. *Koord. Khim.* **1981**, *7*, 461.

(225) Deloume, J. P.; Loiseleur, H. *Acta. Crystallogr.* **1974**, *B30*, 607.

(226) Fleissner, G.; Kozlowski, P. M.; Vargek, M.; Bryson, J. W.; O'Halloran, T. V.; Spiro, T. G. *Inorg. Chem.* **1999**, *38*, 3523.

Vita

The author was born in Bageshwer, Uttranchal, India on July 11, 1978. He graduated with a Bachelor of Science in Chemistry (1998) from Ahmednagar College, Pune, India in May of 1998. He graduated with a Master of Science in Chemistry from Indian Institute of Technology, Bombay, India, in May 2000. He attended graduate school at University of Kentucky. He is a member of the American Chemical Society and its Inorganic Division.

List of publications

Chong-Hyeak Kim, Sean Parkin, Mohan S. Bharara and David A. Atwood., "Linear Coordination of Hg(II) by Cysteamine " *Polyhedron*, **2002**, 21, 225.

Mohan S. Bharara, Chong-Hyeak Kim, Sean Parkin and David A. Atwood., "Synthesis and X-ray Crystal Structures of Dinuclear Hydrogen-Bonded Cadmium and Lead 2-Aminoethanethiolates " *Polyhedron*, **2005**, 24, 865.

Mohan S. Bharara, Thanhhoa H. Bui, Sean Parkin and David. A. Atwood., "Mercurophilic Interaction in Novel Hg(II)-2-aminoethanethiolates" *J. Chem. Soc., Dalton Trans*., **2005**, 3874.

Mohan S. Bharara, Thanhhoa H. Bui, Sean Parkin and David. A. Atwood., "The Structure Directing Influence of Halide in Hg-thiolate Clusters" *Inorg Chem*., **2005**, 44, 5753.

Mohan S. Bharara, Sean Parkin and David. A. Atwood., "Solution and Solid-state Study of Heteroleptic Hg(II)-thiolates: Crystal Structures of $[Hg_4I_4(SCH_2CH_2NH_2)_4]$ and $[Hg_4I_8(SCH_2CH_2NH_3)_2]_n \cdot nH_2O$ " *Inorg. Chem*. **2006**, 45, 2112.

Mohan S. Bharara, Sean Parkin and David A. Atwood., "Solution behavior of Hg(II)-cystamine by Uv-Vis and 199Hg NMR". *Main Group Chemistry*. **2006**, ***In press***.

Mohan S. Bharara, Sean Parkin and David A. Atwood., "Homonuclear Interactions Observed in Two-dimensional Pb-2-aminoethanethiolate Network" *Inorg Chimi Acta,* **2006***,* **In press.**

Mohan S. Bharara, Sean Parkin and David A. Atwood., "Hg(II)-2-aminoethanethiolateClusters: Intramolecular Transformations and Mechanisms" *Inorg. Chem.* **2006**, **Accepted**.